THE EVOLUTION AND FUNCTION OF MELANOCORTIN

AND

MELANIN-CONCENTRATING HORMONE RECEPTORS

Darren Logan

Submitted for the Degree of

Doctor of Philosophy

at the

University of Edinburgh

2003

Declaration

I declare

a) that this thesis is composed by myself , and
b) that this work is my own, except where otherwise stated.

Darren W Logan

September 2003

Publications

Some of the data described in this thesis has been previously published.

DW Logan, RJ Bryson-Richardson, PD Currie and IJ Jackson. Large scale analysis of genomic structure in rhodopsin-like GPCRs: evidence for ancient introns. Submitted.

DW Logan, RJ Bryson-Richardson, MS Taylor, PD Currie and IJ Jackson. 2003. Sequence characterization of teleost fish melanocortin receptors. *Ann. N. Y. Acad. Sci.* **994**: 319-330.

DW Logan, RJ Bryson-Richardson, KE Pagan, MS Taylor, PD Currie and IJ Jackson. (2003). The structure and evolution of the melanocortin and MCH receptors in fish and mammals. *Genomics*. **81**:184-91.

Acknowledgments

The work described in this thesis would not have been completed without the help and encouragement of many people, to whom I owe many thanks.

I'm very grateful to Ian Jackson, for initially giving me the opportunity to work in his lab and sharing his enthusiasm for the field, then for encouraging me to forge my own path. Thanks are due to all the other members of the melanocyte lab, particularly Siobhan, Alison, Peter and Margaret, who guided me (and always seemed to have the required solutions). I'm also indebted to all of Genecore and Bioinformatics for their help, especially Lisa for looking after my mice (not to mention keeping me up to date on the latest gossip), Ian S and Tom VA for much advice and discussion, and Sally and Kayleene for such excellent work during their time in the lab.

Other members of the HGU, too numerous to mention, have been very gracious with their time. My particular thanks go to the Currie Lab and the other fish users, who were all very patient with my fish questions. I'm especially grateful to Rob Two-Names for making the time to work on the GPCR project with me, and to Paul Perry for his help in with the technical aspects of the melanophore assay. A dubious nod also to Dunc, the students in the old library office and to Sapna, Tom VA, Tom W and Ian S for light relief. Who said the art of polite debate was dead?

Thank you so much to Mum and Dad, for your unwavering support (always kind, often financial) each step of the way. To the rest of my family and adopted family, Claire, Vera, Jean, Papa and Betty, thanks for all your encouragement. Most of all to Rachel, I'm not sure my sanity would have survived these last few months (and years) without your love, support and cooking, a million thanks and a promise to be there next year.

Finally, I'd like to dedicate this thesis to my Gran, Violet Davidson, whom I hope would have been proud.

Abstract

Compared with the genetics of melanogenesis in mammals, the genes regulating pigmentation in lower vertebrates are poorly understood. Mammals undergo morphological colour change under hormonal control, but strikingly, many lower vertebrates display a rapid physiological colour change in response to the same hormones. The recent provision of extensive genome sequencing data from teleost fish provides the opportunity to identify the genes mediating this hormonal response and characterise their function.

This thesis describes the cloning, characterisation, evolution and functional role of potential melanogenic genes in the teleost fish, *Fugu rubripes* and *Danio rerio* (zebrafish). An *in silico* analysis of genome trace sequences was carried out to identify fish orthologues of known mammalian genes. The characterised sequences encode a hormonal regulator of mammalian melanogenesis, pro-opiomelanocortin (POMC), its receptors the melanocortin receptor (MCR) family and their functional antagonists, the melanin-concentrating hormone (MCH) receptor family. These studies revealed that zebrafish has six melanocortin receptors, including two MC5R orthologues, whilst *Fugu*, lacking MC3R, has only four. It is also demonstrated that *Fugu* and zebrafish have two and three MCH receptor encoding genes respectively and that both have a single *POMC* gene that appears to be a marker of pituitary development.

The discovery in *Fugu MC2R* and *MC5R* of an intron located in a uniquely conserved position in both genes, but missing in all other melanocortin receptors genes so far described, provided an opportunity to investigate the evolution of gene structure in the family. Furthermore, the availability of genome sequence data from numerous species meant the analysis could encompass the entire rhodopsin-like G-protein coupled receptor gene family (GPCR-A), of which melanocortin and MCH receptors are members. This investigation revealed that the conserved intron is found within a phylogenetically diverse range of GPCR-As in six vertebrate and invertebrate species, suggesting it is very ancient and has undergone widespread loss. Furthermore, analyses of total intron content in mammalian GPCR-As reveal a large reduction in intron number compared to invertebrate GPCR-A genes. Together, these two lines of investigation provide compelling evidence for the widespread

loss of introns during the evolution of the mammalian GPCR-A family. Thus the melanocortin receptor family, which was previously thought to have emerged from an intronless ancestor, appears to once have had introns.

Having identified teleost orthologues of genes regulating mammalian melanogenesis, a quantitative assay was developed to investigate melanocortin and MCH signalling in zebrafish melanophores. Some initial experiments are described to demonstrate the scope of this assay system; illustrating the bi-humoral control of colour change in zebrafish and showing the potential uses it may have in future. In conclusion, this thesis describes the evolutionary parallels between melanogenic regulation in fish and mammals, both functionally and genetically. However, downstream of melanocortin and MCH signalling, there are clear mechanistic differences mediating morphological and physiological colour change.

Table of Contents

Chapter 2

The Melanocortin and MCH Receptor System in Teleost Fish

Chapter 3

The Evolution of Rhodopsin-like G-protein Coupled Receptor Genes

Chapter 4

Control of Colour Change in the Zebrafish

List of Figures and Tables

Abbreviations

AC	adenylate cyclase
ACTH	adrenocorticotrophic hormone
AGRP	agouti related protein
AP	anterior/posterior (axis)
ASP	agouti signalling protein
BCIP	5-bromo-4-chloro-3-indolyl phosphate
cAMP	cyclic adenosine 3-phosphate
bp	base pairs
contig	contiguous sequence (of DNA or RNA)
DCU	dermal chromatophore unit
DDC	duplication, degeneration and complementation
DEPC	diethyl pyrocarbonate
DIG	digoxygenin
DMF	dimethyl formamide
DNA	deoxyribonucleic acid
dNTP	dinucleotide triphosphates
dpc	days post coitum
dpf	days post fertilization
DV	dorsal/ventral (axis)
EMU	epidermal melanin unit
g	grams
GPCR	G-protein coupled receptor
GPCR-A	rhodopsin-like G-protein couped receptor (Family A)
HCl	hydrogen chloride
hpf	hours post fertilization
ISHH	*in situ* hybridisation histochemistry
Kb	kilobase pairs
KCl	potassium chloride
L	litres
LiCl	lithium chloride
M	molar solution
Mb	million base pairs

MCH	melanin-concentrating hormone
µg	micrograms
mg	milligrams
$MgCl_2$	magnesium chloride
min	minutes
µl	microlitres
ml	millilitres
µm	micrometres
µM	micromolar solution (M^{-6})
mM	millimolar solution (M^{-3})
MSH	melanocye stimulating hormone
Mya	million years ago
NaCl	sodium chloride
NaOH	sodium hydroxide
NBT	nitro blue tetrazolium
ng	nanogram
nM	nanomolar solution (M^{-9})
ORF	open reading frame (of DNA)
PBS	phosphate buffered saline
PCR	polymerase chain reaction
PFA	paraformaldehyde
pg	picograms
pM	picomolar solution (M^{-12})
POMC	pro-opiomelanocortin
PSS	physiological saline solution
RNA	ribonucleic acid
RT-PCR	reverse transcribed polymerase chain reaction
SDS	sodium-dodecyl-sulphate
sec	seconds
u	standard enzyme units
UTR	un-translated region (of RNA)

A Note on Nomenclature

Throughout this thesis, effort has been made to use standard terms as set by international nomenclature committees. However, in the interests of clarity and comprehension, some liberties are taken in naming species. In general, the most commonly used moniker is given. Thus, *Homo sapiens* is simply referred to as 'human', *Mus musculus* as 'mouse' and *Danio rerio* as 'zebrafish'. Other species names are used in the vernacular in an abbreviated form. For example, the pufferfish *Fugu rubripes* (which is alternatively called *Torafugu* or *Takifugu rubripes*) is referred to here as *'Fugu'*; the fruit-fly *Drosophila melanogaster*, as *'Drosophila'* and the malaria mosquito *Anopheles gambiae*, is termed *'Anopheles'*. In the strictest sense, these terms define genera containing multiple species; but it is important to note that, in the following discussion, their use refers only to the single model species. Unsurprisingly, the nematode worm *Caenorhabditis elegans* is universally abbreviated to *'C. elegans'*, and that term is used here.

For each species, approved gene names and abbreviations have been used whenever possible and nomenclature protocols have been followed. Thus human and *Fugu* genes are abbreviated in italicised capitals (e.g. *MC1R*) and proteins in non-italicised capitals (MC1R). Mouse, *Drosophila* and *Anopheles* genes are similarly abbreviated but with a single, leading capital (gene: *Mc1r*; protein: Mc1r) and zebrafish abbreviations have no caps (gene: *mc1r*, protein: mc1r). When a gene or protein is referred to generically, outwith the context of a single species, human nomenclature is used. Finally, with the provision of large scale sequencing data, in some species a nomenclature system has been introduced for genes annotated *in silico*. For example, *Drosophila* genes are prefixed by CG (for 'computed gene') then numbered (e.g. CG1427), and *C. elegans* genes are named according to nature of the clone sequenced (e.g. Y47H9A is the first gene annotated on YAC 47H9). These names are used where appropriate.

Chapter 1

Introduction

I proceed to a logical development of what I see in nature

Paul Cezanne

1.1 Preface

To the human eye, the colour of an organism is one of its most readily apparent features. Numerous species are defined by their colour, many domesticated animals have been bred for colour and the perception of skin colour has a huge impact in human society. Yet, despite many years of keen study, there is relatively little known about how the genes involved in generating pigment evolved. It is known that melanin, the mammalian chromatophore pigment, is found in a vast number of species and there is a large body of work investigating how it is biochemically synthesised (Jimbow *et al.*, 1976; Ito, 2003). Less understood is how this synthesis is controlled and how the pigment is distributed to generate different colours and patterns in diverse species. There are, of course, great physiological and morphological differences between the mammals of today and their non-mammalian ancestors. Not least among these is the appearance of a coat of hair as a protective covering, resulting in the pigmented skin of their non-hairy ancestors being obscured. A new strategy was required for effective colouration in mammals, thus pigment was transferred to the hair shaft (Quevedo, Jr. and Holstein, 1998). This morphological change is but one example of the strong evolutionary pressures on genes that control pigmentation (Quevedo, Jr. and Holstein, 1992). But at the molecular level exactly how different are the mechanisms resulting in melanic stripes on the cuticle of the wasp, the skin of the zebrafish and the hair of tigers?

To study comparative genetics, single species are used as model organisms representing larger classes. Thus the fruit fly, *Drosophila melanogastor*, has been widely used to study insect pigmentation patterns (O'Grady and DeSalle, 2000; Wittkopp *et al.*, 2003) and huge advances have been made in understanding the genetics of mammalian pigmentation using the laboratory mouse, *Mus musculus* (Jackson, 1994). Due to the inherently visual phenotypes, mammalian pigmentation genetics has been practised unwittingly for hundreds of years (Jackson, 1991). As long ago as 300 A.D. abnormally pigmented mice were noted as unusual and, since the 19th century, variant lines have been maintained and intercrossed by mouse fanciers for purely aesthetic appeal. The mouse fancy exists to the present day and has continued to generate and maintain classical mutations that influence coat colour. It is unsurprising, therefore, that when the mouse became the chosen model for experimental genetics at the beginning of the last

century, coat colour genes were some of the first to be cloned (Keller, 1978; Jackson, 1991). Subsequently, lines derived from fancy mice have given us an insight into developmental processes and cellular functions driven by genes involved in, but not limited to, visible phenotypes (Jackson, 1997). Indeed, the knowledge derived from fancy mice has been successfully applied to humans (Barsh, 1996), shedding light on a number of processes including a genetic basis for red hair and pale skin (Rees, 2000) and various types of albinism, piebaldism and vitiligo (Halaban and Moellmann, 1993).

It is perhaps then not surprising that when George Streisinger first proposed the zebrafish as an experimental model, pigment variants were the strains he studied (Streisinger *et al.*, 1981; Stahl, 1985). Moreover, as the field of zebrafish genetics grew and a large-scale mutagenesis project was carried out (Haffter *et al.*, 1996), over 100 pigment mutants were generated (Kelsh *et al.*, 1996; Odenthal *et al.*, 1996); more than in any other class and comparable to the number of mouse pigment loci (Bennett and Lamoreux, 2003). Yet currently only a handful of these fish mutants have been thoroughly characterised and in even fewer has the genetic lesion been identified (Lister *et al.*, 1999; Kelsh *et al.*, 2000; Parichy *et al.*, 2000; Dutton *et al.*, 2001; Parichy and Turner, 2003). Now, with its large catalogue of mutants, rapid development, optically accessible embryos and with its genome being sequenced, the zebrafish is established as the prime lower vertebrate model for studying development and genetics (Grunwald and Eisen, 2002). This thesis aims to show how zebrafish can be used to study the genetics of lower vertebrate pigment regulation in comparison with the mammalian system. Furthermore, it describes how the study of sequenced genomes from more primitive organisms, combined with appropriate experimental systems, can shed light on the evolution and function of mammalian genes. To begin, however, a review of the literature is presented as an introduction to the field of pigmentation genetics.

1.2 Lower vertebrate pigment cells

The colours displayed by animal species are a result of the interaction of light and pigments within specialised cells. First used as *chromforo* to describe invertebrate pigment cells by Sangiovanni in 1819, the term 'chromatophore' was adopted as a description for the pigment bearing cells of lower vertebrates (Parker, 1948). By the

1960s, enough information about the structure and colour of chromatophores was available to sub classify them according to appearance (Bagnara, 1966) and, despite studies revealing the biochemical nature of the pigments within chromatophore types (Bagnara, 1961; Matsumoto, 1965; Taylor, 1969), this classification system persisted (Fig. 1.2.1a). With the discovery of some mosaic pigment cells containing more than one type of organelle and mosaic organelles containing more than one type of pigment, the distinction between chromatophore type became less clear (Bagnara *et al.*, 1979). However, it has subsequently been demonstrated that pigment vesicles in most species are relatively homogenous so, in the interest of clarity, the chromatic nomenclature remained (Bagnara, 1998).

1.2.1 Xanthophores and Erythrophores

Originally termed 'lipophores' due to their fat-soluble content, chromatophores that contain large amounts of yellow pteridine pigments were renamed xanthophores and those with an excess of red/orange carotinoids termed erythrophores (Bagnara, 1966). Soon after, Matsumoto discovered that pterinosomes and carotinoid vesicles are found within the same cell, and demonstrated that the manifest colour depends on the ratio of red and yellow pigments (Matsumoto, 1965) (compare Figure 1.2.1b and c). Thus the distinction between these cell types, which are found in fish, amhibians and reptiles, is essentially arbitrary. The capacity to biosynthesise pteridines from GTP *de novo* is a feature common to most chromatophores, but xanthophores appear to have supplemental pathways that result in an excess accumulation of yellow pigment (Ziegler, 2003). In contrast, carotinoids are metabolised from the diet and transported to erythrophores. Thus frogs reared on a carotene-restricted diet display an erythrophore specific pigment phenotype (Bagnara, 1998).

1.2.2 Iridophores and leucophores

Biochromes, such as pteridines and carotinoids, selectively absorb a part of the visual spectrum that makes up white incident light, while they let the other wavelengths pass and reach the eye of the observer. Not all colours are generated in this manner, however. Some, most notably animal blues and greens, are generated by the scattering, interference and diffusion of light by crystalline structures called schemochromes.

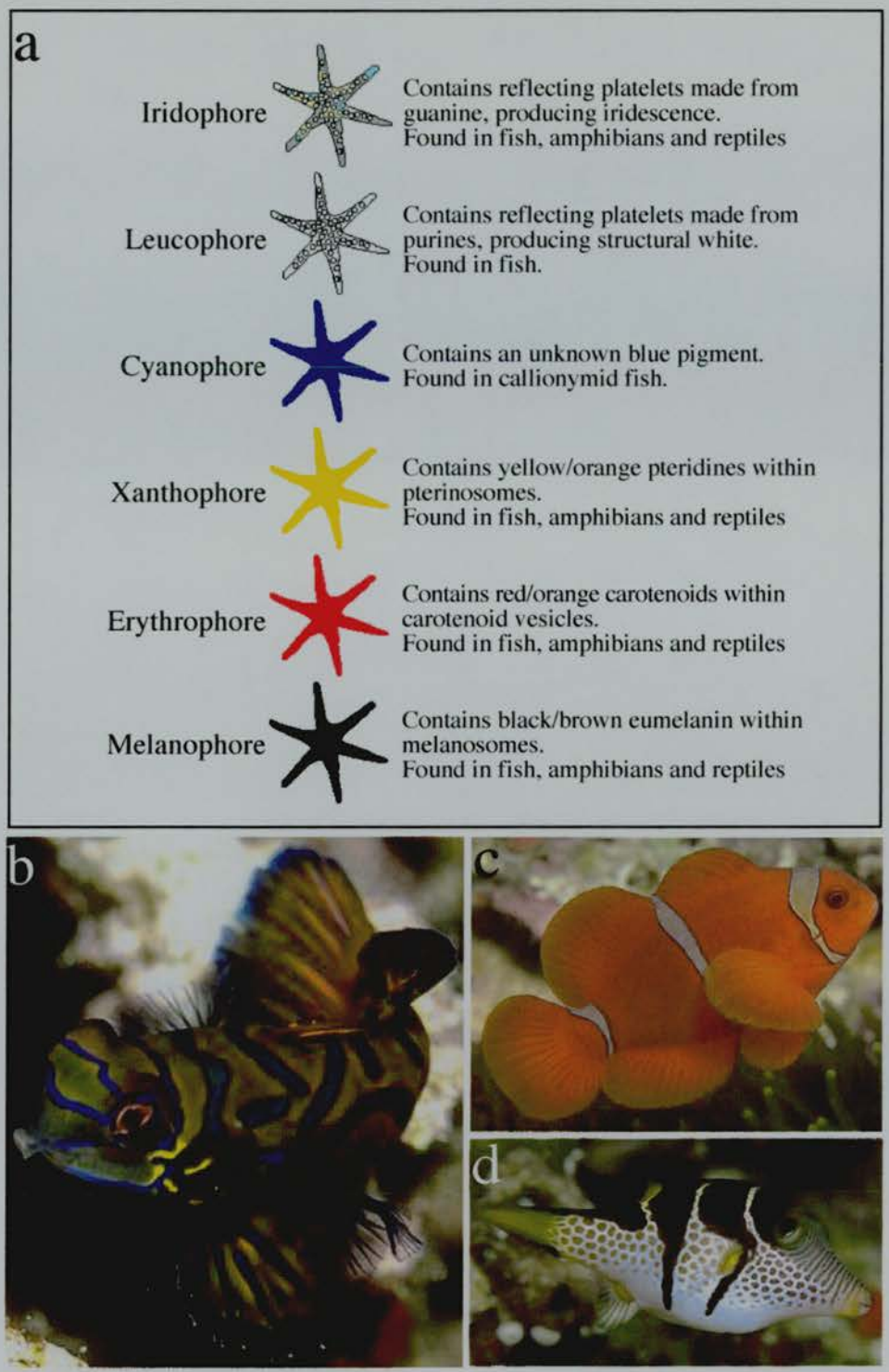

Figure 1.2.1. The chromatophores of lower vertebrates. **a**, a summary of the chromatophore types, their biochromes or schemochromes and taxonomic distribution. **b**, a mandarin fish (*Synchiropus splendidus*) displaying blue cyanophores and xanthophores overlying iridophores. **c**, an anenome fish (*Premnas biaculeatus*) displaying erythrophores and iridophores. **d**, a sharp-nose puffer (*Canthigasler valentini*) displaying xanthophores, leucophores and melanophores. All photos courtesy of Dick Ballendux and used with permission.

Iridophores are lower vertebrate pigment cells that reflect light using plates of crystalline guanine shemochromes (Bagnara, 1966; Taylor, 1969). When illuminated they generate iridescent colours due to the diffraction of light within the stacked plates. It appears that orientation of the schemochrome determines the nature of the structural colour, as illustrated in spiny lizards (Morrison, 1995) and tree frogs (Nielsen, 1978). Furthermore, by using biochromes as filters, iridophores mediate an optical effect known as Tyndall scattering, producing bright blue or green colours that are not modified by the angle of vision (Fujii, 2000).

A related type of chromatophore, the leucophore, is found in some fish species (Menter *et al.*, 1979). Like iridophores, they utilize crystalline purines to reflect light, providing the bright white colour seen in some fish (Fujii, 2000) (Fig 1.2.1d). As with xanthophores and erythrophores, the distinction between iridophores and leucophores in fish is not always obvious, but generally iridophores generate iridescent or metallic colours while leucophores produce structural white hues (Bagnara, 1998).

1.2.3. Cyanophores

In 1995 Goda and Fujii demonstrated that the spectacular blue colours of mandarin fish are not structural in nature. Instead, a blue biochrome of unknown chemical nature is responsible (Goda and Fujii, 1995). This pigment, found within fibrous vesicles in dermal chromatophores in at least two species callionymid fish (see Figure 1.2.1b), is highly unusual in the animal kingdom, as all other blue colourings thus far investigated are schemochromatic. Therefore a novel chromatophore type, the cyanophore, is recognised. Although cyanophores are unusual in their taxonomic restriction, there may be other unusual chromatophore types in lesser-studied fish and amphibians. Indeed, bright coloured chromatophores with undefined pigments have been observed in both poison arrow frogs (Bagnara, 1998) and glass frogs (Schwalm *et al.*, 1977).

1.2.4 Dermal melanophores

The most widely studied chromatophore, due both to its extensive taxonomic distribution and apparent colour, is the melanophore. Melanin, the biochrome found in

melanophores, is generated from tyrosine in a series of catalysed chemical reactions (See Figure 1.3.6). The end melanin product in lower vertebrates is eumelanin, a complex biopolymer containing units of dihydroxyindole and dihydroxyindole-2- carboxylic acid with some pyrrole rings (Ito and Wakamatsu, 2003). This type of melanin, when packaged in vesicles and distributed throughout the cell, appears black or dark brown, due to its light absorbing qualities (Fig. 1.2.1d). In some amphibian species, however, there are other pigments packaged alongside eumelanin. For example, a novel deep red-coloured pigment called rhodomelanochrome was identified in the melanophores of phyllomedusine frogs (Bagnara *et al.*, 1973). This was subsequently identified as pterorhodin, a pterodine dimer that accumulates around eumelanin (Misuraca *et al.*, 1977). While it is likely that other species have also evolved multiple melanophore pigments (Bagnara *et al.*, 1979), it is nevertheless true that the majority of lower vertebrate melanophores studied to date contain eumelanin exclusively (Bagnara, 1998; Ito and Wakamatsu, 2003).

Dermal melanophores are large, dendritic cells mainly found below the basal lamina in the upper portion of the dermis. However they are also present outside the dermis in some species. Indeed, they have been observed on the liver, spleen, kidney, meninges and gonads in fish and frogs (Zuasti *et al.*, 1989; Zuasti *et al.*, 1990), although their function in these organs is currently unknown. In most larvae and adult species with a relatively thin dermis, the dermal melanophores tend to be flat and cover a large surface area (Taylor and Bagnara, 1972). However, in animals with thick dermal layers, such as adult reptiles, dermal melanophores often form three-dimensional units with other chromatophores. These dermal chromatophore units (DCU) consist of an uppermost xanthophore layer, then an iridophore layer, and finally a basket like melanophore layer with processes covering the iridophores (Fig 1.2.2a) (Bagnara *et al.*, 1968).

Both types of dermal melanophores are extremely important in physiological colour change (the rapid translocation of pigment within chromatophores resulting in an apparent change in colour (Parker, 1948))

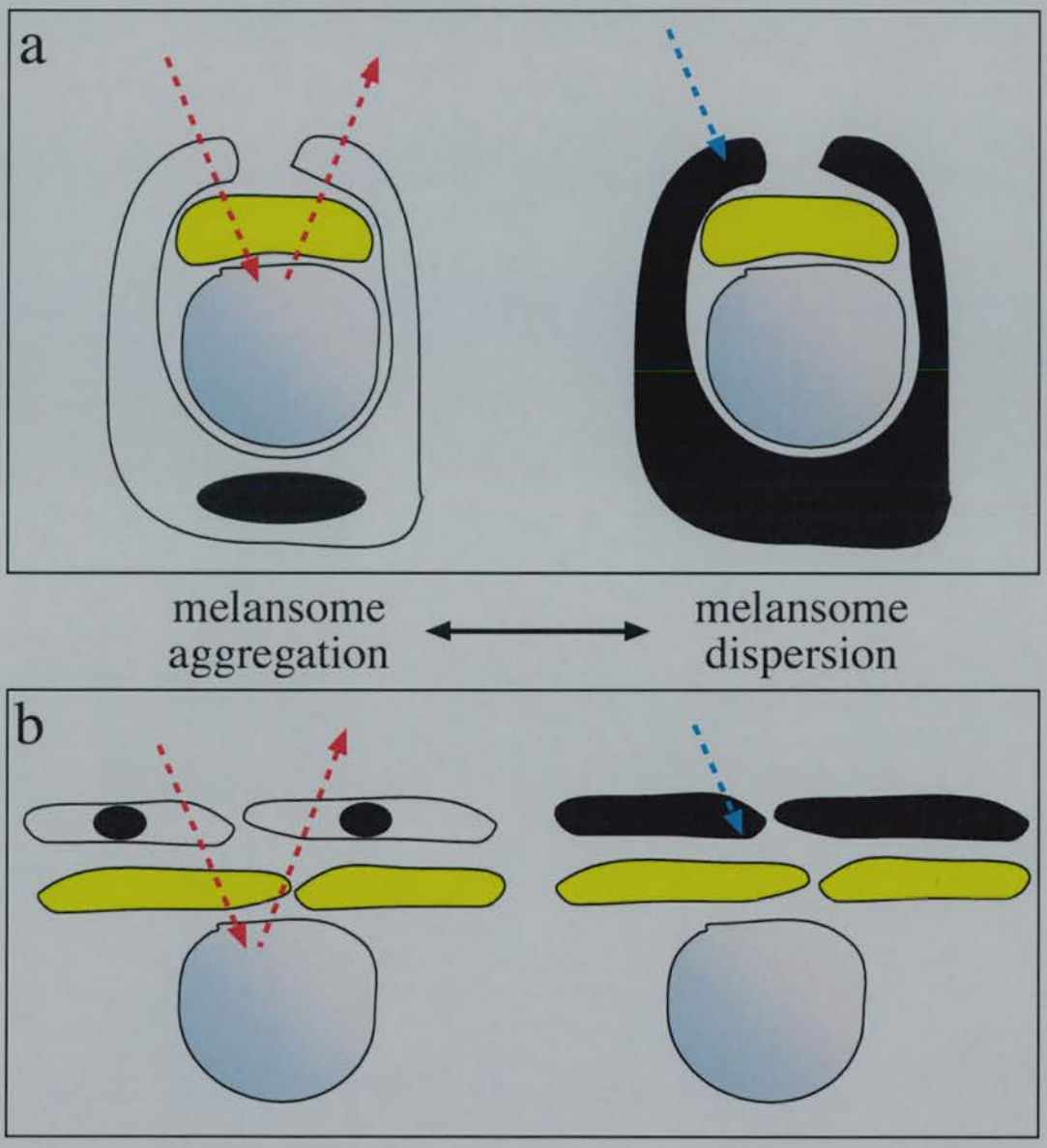

Figure 1.2.2 The structure and organisation of dermal chromatophores. a, in lower vertebrates with thick dermal layers DCUs are formed by melanophores (*black*), xanthophores (*yellow*) and iridophores (*silver*). **b**, larvae and adults species with a thinner dermis do not form DCUs, but instead arrange chromatophores into layers in the dermis. The rapid and repeatable dispersion or aggregation of melanosomes can result in an observed colour change. Melanosome aggregation results in light being reflected from iridophores through a xanthophore layer (*red* arrow), producing a golden colour. Dispersion results in light being absorbed by melanin (*blue* arrow), producing a black colour.

Flat dermal melanophores will often overlay other chromatophores so when the pigment is dispersed throughout the cell the skin appears dark. When the melanosomes are aggregated towards the centre of the cell, the pigments in other chromatophores are exposed to light and thus the skin takes on their hue (Fig. 1.2.2b) (Bagnara and Hadley, 1973). Similarly, after melanin aggregation in DCUs the skin appears green through xanthophore filtering of scattered light from the iridphore layer. On the dispersion of melanin to the processes, the light is no longer scattered and the skin appears dark (Fig. 1.2.2a) (Bagnara *et al.*, 1968; Bagnara and Hadley, 1973). Furthermore, as the other chomatophore types are also capable of pigment translocation (Iga, 1983; Palazzo *et al.*, 1989; Goda and Fujii, 1995), by making good use of the divisional effect lower vertebrates can generate a spectacular array of skin colours.

The control and mechanics of biochrome translocation has been well studied in a multitude of lower vertebrate species, particularly amphibians (Bagnara, 1998) and teleosts (Fujii, 1993; Fujii, 2000). It is thought that both microtubules and microfilaments are involved in the rapid translocation of pigments across the cytoskeleton (Rodionov *et al.*, 1991; Nilsson *et al.*, 1996; Nilsson and Wallin, 1997; Rodionov *et al.*, 1998). It has also been demonstrated that the process can be under hormonal, neuronal control or both (Abe *et al.*, 1969; Baker, 1988; Green and Baker, 1989; Aspengren *et al.*, 2003). Some of these studies are discussed in more detail in Chapter 4.

1.2.5 Epidermal melanophores

As well as those in the dermis and other tissues, there are melanophores found in the epidermis of lower vertebrates (Hadley and Quevedo, Jr., 1967). In amphibia, these tend to be more spindle-like in shape and, together with their neighbouring keratinocytes form an epidermal melanin unit (EMU). The EMU functions by generating melanin in the melanophore that is then deposited into the adjacent cells (Hadley and Quevedo, Jr., 1967; Bagnara and Hadley, 1973). Although the melanophore itself can undergo translocation, the melanin in the adjacent cell is not motile. Thus the EMU is more likely to play a role in morphological colour change than physiological colour change. The molecular basis of EMU function in lower vertebrates is not well studied, however it is thought that they undergo similar processes as mammalian EMUs (see Chapter 1.3.1)

(Bagnara, 1998). In teleosts, epidermal melanophores tend not to function in EMUs, instead keeping their melanophores and undergoing physiological colour change (Fujii, 1993). Other than from location, the only distinction between teleost melanophore types is in their response to melatonin: epidermal melanophores do not respond to melatonin in any vertebrate studied thus far (Bagnara and Hadley, 1970; Bagnara, 1998).

1.3 The mammalian pigment cell

Melanin is the only biochromatic pigment found in mammals, but is one of a number found in lower vertebrates. Thus there was originally some uncertainty over whether the mammalian and lower vertebrate melanin bearing cells should be classified together. The confusion was exacerbated by the differences in melanic pigmentation between higher vertebrates, where the melanin bearing cells appear to be static and uniform (Klaus and Snell, 1967), and lower vertebrates, where they appear to be dynamic and patterned (Parker, 1948; Bagnara and Hadley, 1973). This debate was resolved with the proposition that lower vertebrate melanin-bearing cells are termed 'melanophores' and those from mammals and birds called 'melanocytes' (Fitzpatrick *et al.*, 1966). This nomenclature system is used in the pigment cell community to the present day.

As is the case in melanophores, melanocytes generate melanin from tyrosine in a series of enzymatic reactions within modified lysosome vesicles called melanosomes. The compartmentalization of melanogenesis is ubiquitous because melanin precursors, such as phenols and quinines, would oxidize lipid membranes if released into the cytosol (Orlow, 1995). Melanosomes contain matrix proteins (on which the melanin forms) and enzymes that regulate its biosynthesis (see Chapter 1.3.4). After post-translational modification in the endoplasmic reticulum and Golgi apparatus, the proteins are packaged into melanosomes and readied for transport throughout the cytoplasm (Jimbow and Sugiyama, 1998). As in lower vertebrates, mammalian melanosomes appear to be attached to microtubules in the centre of the cell before being transferred to microfilaments in the dendrites (Hara *et al.*, 2000). The importance of actin filaments became clear when the genetic lesion in *dilute* mice was characterised in the gene encoding Myosin Va. *Myo5a* is required to transfer melanosomes to actin filaments in the periphery of melanocytes. When the protein malfunctions, the melanosomes cannot

be transferred and the melanosomes appear to slip back towards the centre of the melanocyte, resulting in hypopigmentation (Jenkins *et al.*, 1981; Mercer *et al.*, 1991). Humans with mutations in *MYO5A* suffer from Griscelli sydrome, a disease characterised by diffuse skin pigmentation, silvery hair and an accumulation of melanosomes in melanocytes (Pastural *et al.*, 1997). Despite the similarities between melanosome transport in melanophores and melanocytes, there are also important differences. Normally functioning melanocytes do not rapidly translocate melanosomes bi-directionally, like those observed in melanophores. Instead mammalian melanosomes are slowly but continuously dispersed towards the cell periphery. Once in the dendrites, the melanosomes will either be donated to neighbouring cells (see Chapter 1.3.1) or be degraded (Jimbow and Sugiyama, 1998).

The majority of mammalian melanocytes reside in the hair follicles and, in non-hairy skin, the epidermis. But they are also found at other sites including the dermis, the Harderian gland of the mouse, leptomeninges and the stria vascularis of the inner ear (Goldgeier *et al.*, 1984; Johnston *et al.*, 1987; Steel and Barkway, 1989) (see Figure 1.3.3). Dermal melanocytes are found in non-hairy skin of mice and hamsters (Quevedo, Jr., 1981) as well as some monkeys where they generate a spectacular structural blue colour (Price *et al.*, 1976), but they are rarely seen in humans. Specialised melanocytes are also found in the choroid, iris and retinal pigment epithelium (RPE) of the mammalian eye, where they have a photo-protective function. The melanin in these cells has also been demonstrated to protect against oxidative stress, detoxify peroxides and bind zinc (Schraermeyer and Heimann, 1999).

1.3.1 Epidermal melanocytes

As in amphibians, mammalian epidermal melanocytes function as part of an EMU to mediate morphological colour change. In fact it has been estimated that as many as 36 keratinocytes are associated with each melanocyte at the basal layer of the epidermis to form a single unit (Quevedo, Jr. and Holstein, 1998). There is, however, some confusion over the mechanism through which melanosomes are transferred from the melanocyte to neighbouring keratinocytes. Three distinct processes were originally proposed: that melanosomes are released into the intercellular space then endocytosed, that keratinocyes phagocytose the melanocytic dendrites or that there is fusion between

melanocyte and keratinocyte. It is now thought that the latter two modes of transfer do occur in the epidermis (Fig. 1.3.1) (Cohen and Szabo, 1968; Yamamoto and Bhawan, 1994). Irrespective of transfer mechanism, it is the melanin within epidermal keratinocyes that generates the skin colours seen in non-hairy skin, not the melanocytes themselves. Melanosomes are arbitrarily classified based on shape, melanin content and melanogenic enzymatic activity and it appears that the classification type, number, distribution and size of melanosomes in keratinocytes are the major differences between human skin tones (Toda *et al.*, 1972; Konrad and Wolff, 1973). Furthermore, in Caucasians, keratinocyte melanosomes tend to group into complexes. As these keratinocytes ascend to the skin surface to be exfoliated, the complexes are quickly degraded resulting in paler skin tone. In darker skin types, the melanosomes remain distributed as single vesicles (Szabo *et al.*, 1969; Wolff and Konrad, 1971). These melanosomes appear to be more resistant to degradation thus giving the skin a darker appearance (Hori *et al.*, 1968).

1.3.2 Follicular melanocytes

In hairy skin, epidermally derived melanocytes are found mainly in the epidermally derived tissues in the upper hair bulb of the follicle (Fig. 1.3.2a). During anagen (the growth stage of hair shaft formation) the melanocytes discharge melanosomes into keratinocytes that are streaming upwards from the lower hair bulb (Fig. 1.3.2b). These pigmented keratinocytes then undergo complete cornification before forming the cortex and medulla of the hair shaft. The melansomes are arranged singly in the keratinocytes and appear to be resistant to degradation, thus providing the hair shaft with colour (Silvers, 1979; Quevedo, Jr. and Holstein, 1998). By examining *light-silver* mutant mice, Quevedo and colleagues observed that follicular melanocytes are replenished after each hair cycle (Quevedo, Jr. *et al.*, 1994). It is now thought that the source of replacement follicular melanocytes is a stem cell niche in the hair bulge (Akiyama *et al.*, 1995; Nishimura *et al.*, 2002) (Fig. 1.3.2a).

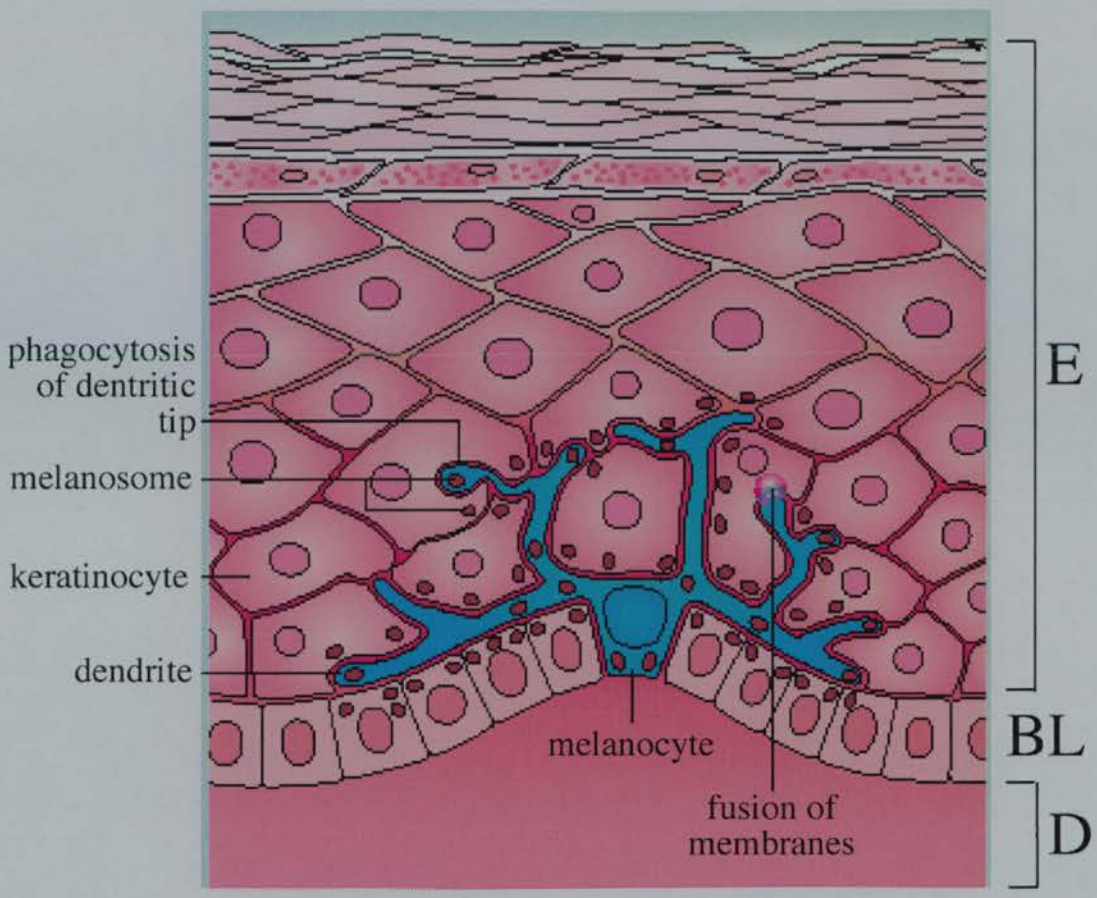

Figure 1.3.1. The mammalian epidermal melanin unit. The melanocyte (*blue* cell) in each EMU is found in the basal layer (BL) of the epidermis (E), directly above the dermis (D). The melanosomes (*brown*) are dispersed along the melanocytic dendrites then transferred into neighbouring keratinocytes (*pink*), via one of two mechanisms. The pigmented keratinocytes then migrate upwards to the epidermal surface where they become cornified before being sloughed off. Figure modified from (Bolognia and Orlow, 2003).

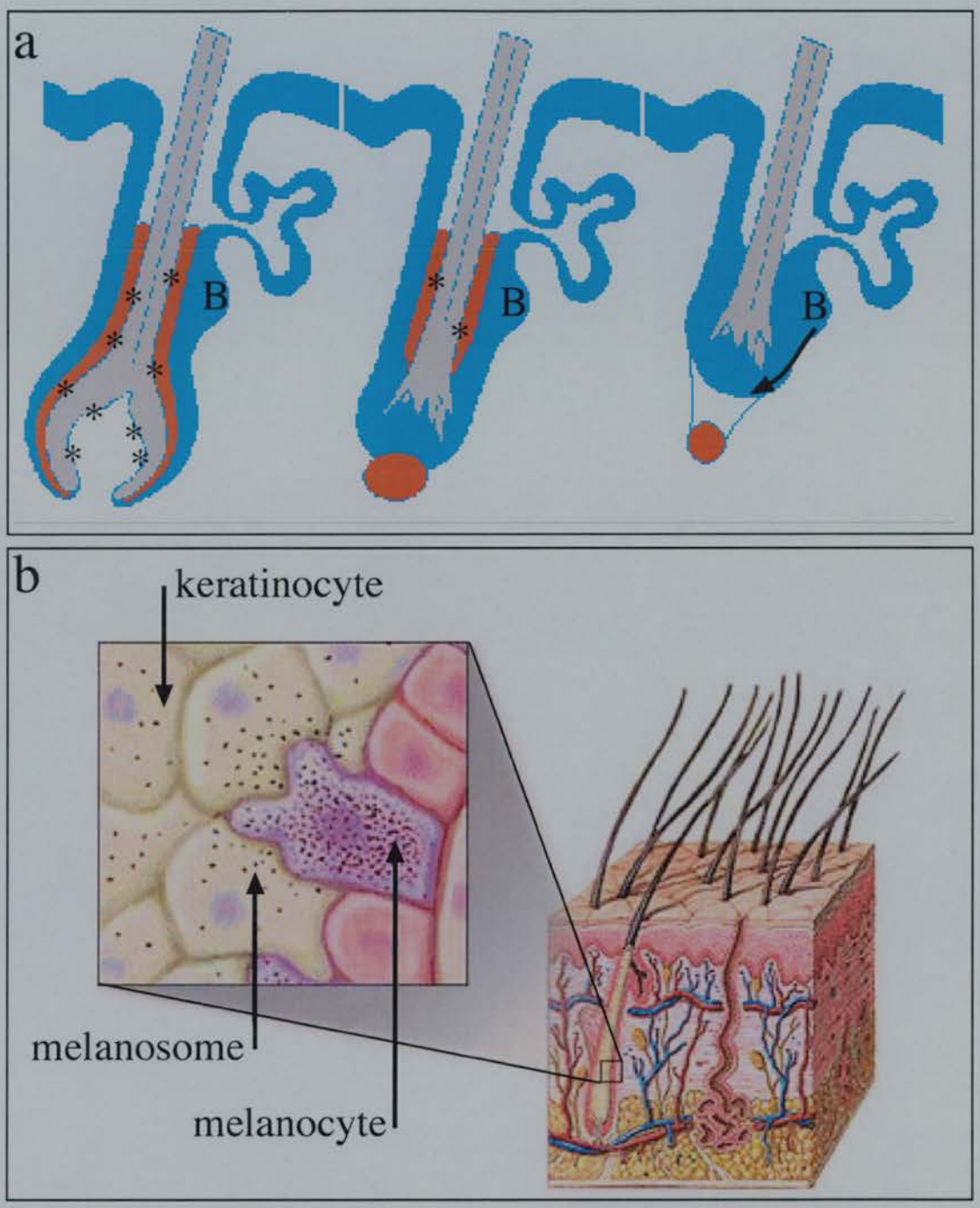

Figure 1.3.2. Melanocytes in the mammalian hair follicle. **a**, the three major stages of follicle development (from left), anagen, catagen and telogen. During anagen, functioning melanocytes (*) are found in the epidermally derived tissue (*blue*). As the follicle cycles through catagen and telogen the melanocytes are destroyed and new cells from the stem cell niche in the bulge (B) take their place, ready for the dermal papilla (*red*) to induce growth of another shaft. **b**, during the growth phase (anagen) melanocytes dispense melanosomes into keratinocytes as they stream upwards, become cornified then form the hair shaft.

1.3.3 Melanoblast development

All melanocytes found in the ear, meninges, uveal tract, dermis and epidermis are derived from the neural crest: a bilaterally paired strip of cells arising in the ectoderm at the margins of the neural tube (Fig. 1.3.3). During embryonic development non-differentiated melanocyte precursors, termed melanoblasts, migrate from the neural crest along a dorsolateral path, between the somites and the overlying epidermis. Neural crest cells that migrate through other pathways go on to differentiate into cell types, such as glial cells and neurons (Fig.1.3.4). Between 11 and 13 dpc in the mouse, the melanoblasts enter the epidermis where they remain in non-hairy skin (Mayer, 1973). In hairy skin the majority of the melanoblasts localise with developing hair follicles, though how this occurs is not yet fully understood (Jordan and Jackson, 2000).

The melanoblast lineage is an excellent model for studying development processes as surviving cells have an inherent reporter system. Furthermore, mice lacking melanocytes are viable and display a white coat colour, therefore genes involved in all stages of mammalian melanocyte development have been identified, ranging from before lineage commitment to the migration into hair follicles. For example, the paired box transcription factor *Pax3* is required early in neural crest cell differentiation. *Pax3* is mutated in *splotch* mice, which display a melanocyte deficiency and neural defects (Epstein *et al.*, 1991; Goulding *et al.*, 1993). Other spotting mutants were shown to result from the disruption of key signalling molecules or transcription factors involved in neural crest differentiation. These include *piebald-lethal (Endothelin receptor b), lethal spotting (Endothelin3)* and *dominant megacolon (Sox10)* (Baynash *et al.*, 1994; Hosoda *et al.*, 1994). Mutations in the tyrosine receptor kinase *Kit* and its ligand, stem cell growth factor (now called kit-ligand (*Kitl*)) have been shown to be responsible for the phenotypically similar *dominant spotting* and *steel* mice (Nocka *et al.*, 1990; Reith *et al.*, 1990; Huang *et al.*, 1990; Copeland *et al.*, 1990; Zsebo *et al.*, 1990). These proteins are necessary later in melanoblast development during migration from the dermis, via the epidermis, to the follicle (Nishikawa *et al.*, 1991; Jordan and Jackson, 2000).

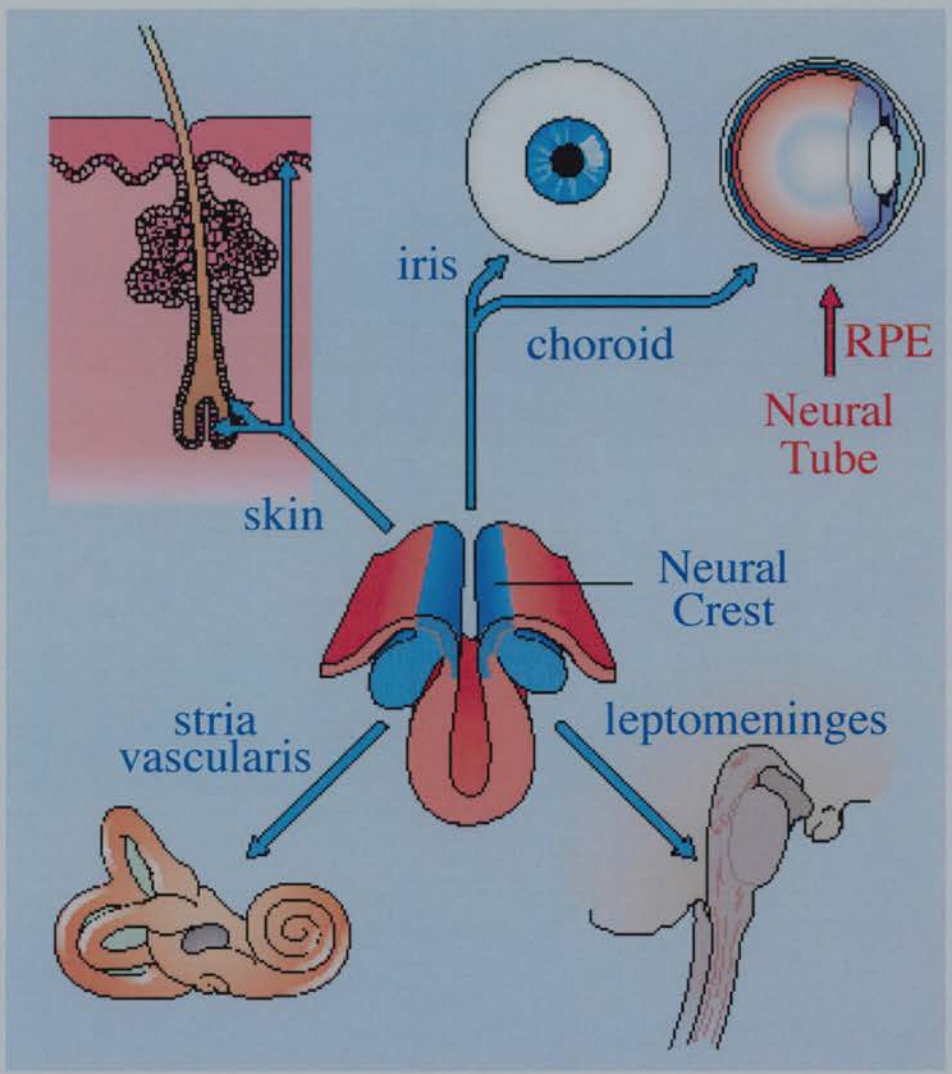

Figure 1.3.3 Melanocytes are derived from the neural crest. Undifferentiated cells from the neural crest (*blue*) destined to become melanocytes migrate through the mesenchyme via a dorsolateral pathway, eventually populating a range of organs.The melanocytes of the RPE are not from the neural crest, instead an outpouching of the neural tube (*red*) generates the optic cup which, in turn, forms the retina. Figure modified from (Bolognia and Orlow, 2003).

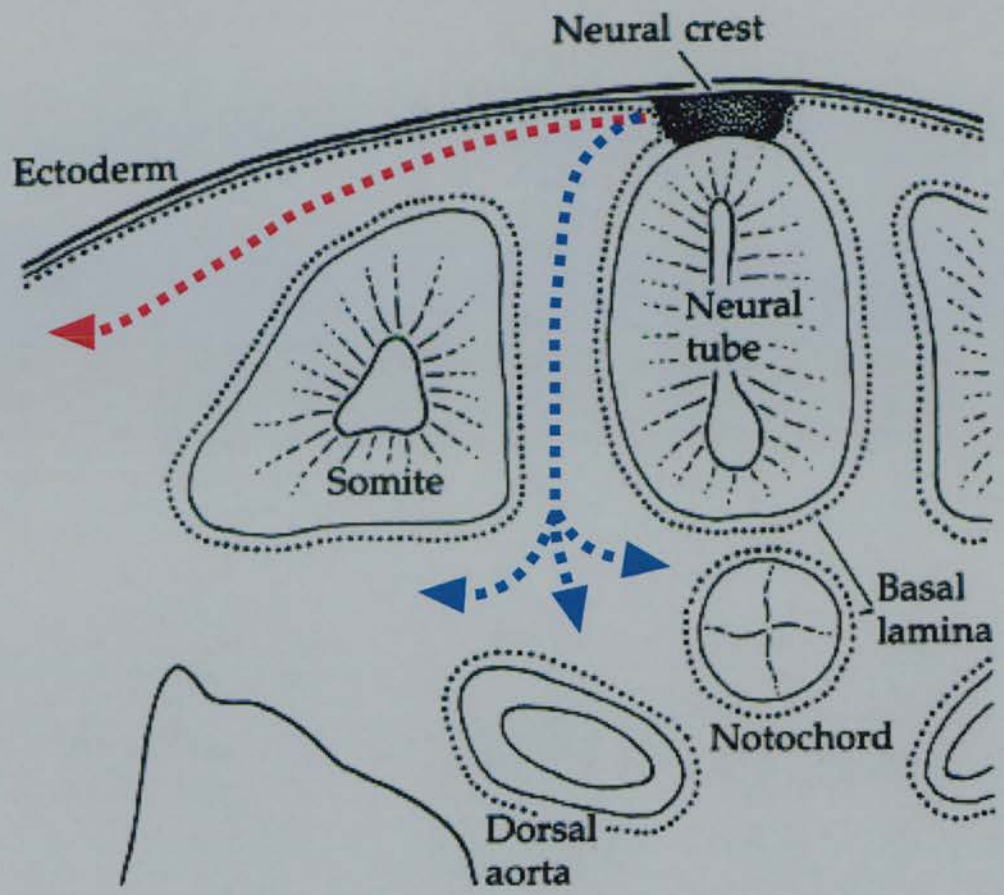

Figure 1.3.4. Trunk melanoblast migration pathways. A schematic representation of a transverse section through the vertebrate trunk demonstrates that neural crest derived cells migrate along steroetyped routes. In mammals, all trunk melanoblasts take dorsolateral route (*red* arrow), whereas glial and neurogenic percursors are specified along the ventromedial route (*blue* arrow). In fish, chromatoblasts migrate along both routes. Figure modified from (www.students.biology.Isa.umich.edu/).

As the neural crest is a defining feature of all vertebrates, chromatophore differentiation and development in lower vertebrate species has also been widely studied. Unlike mammalian melanocytes, teleost chromatoblasts migrate along two pathways: the dorsolateral pathway previously described, and a ventromedial pathway between the somites and the neural tube (Raible and Eisen, 1994)(Fig 1.3.4). It appears that the early chromatoblasts have the potential to differentiate into any chromatophore type, with a combination of intrinsic cues such as differential expression of transcription factors influencing fate specification (Kelsh and Raible, 2002). The generation of many pigment mutants in the zebrafish, *Danio rerio*, facilitated the identification of genes regulating chromatoblast development and migration (Kelsh *et al.*, 1996). Currently, only zebrafish orthologues of genes previously implicated in mammalian melanoblast development have been cloned, including *sparse* (*kit*), *rose* (*endothelin receptor b1*), *nacre* (*mitfa*) and *fms* (a homologue of *Kit*) (Fig. 1.3.5) (Lister *et al.*, 1999; Parichy *et al.*, 2000; Dutton *et al.*, 2001; Parichy and Turner, 2003). But there are many mutant strains with potential neural crest specification and migration phenotypes. The identification of the mutated genes in these fish may further the understanding of both lower vertebrate and mammalian chromatophore development.

1.3.4 Melanogenesis

In skin pigmentation, the range of observed colour is largely due to the variable distribution of melanosomes in epidermal keratinocytes (Hunt *et al.*, 1995). Due to the structure of the keratinised hair shaft, melansomes can only be arranged in columns yet a range of natural hair colours is generated. This is because, unlike lower vertebrate melanophores that produce only black eumelanin, mammalian melanocytes produce a second melanin biopolymer (phaeomelanin) which is yellow or red in colour. The biochemistry of melanogenesis has been widely studied and it is now known that melanin production involves three melanosomal enzymes (Ito, 2003). The key enzyme is tyrosinase (TYR), which catalyses the first reaction in the synthesis of both melanin subtypes, tyrosine to DOPA to DOPA-quinone (Fig. 1.3.6a).

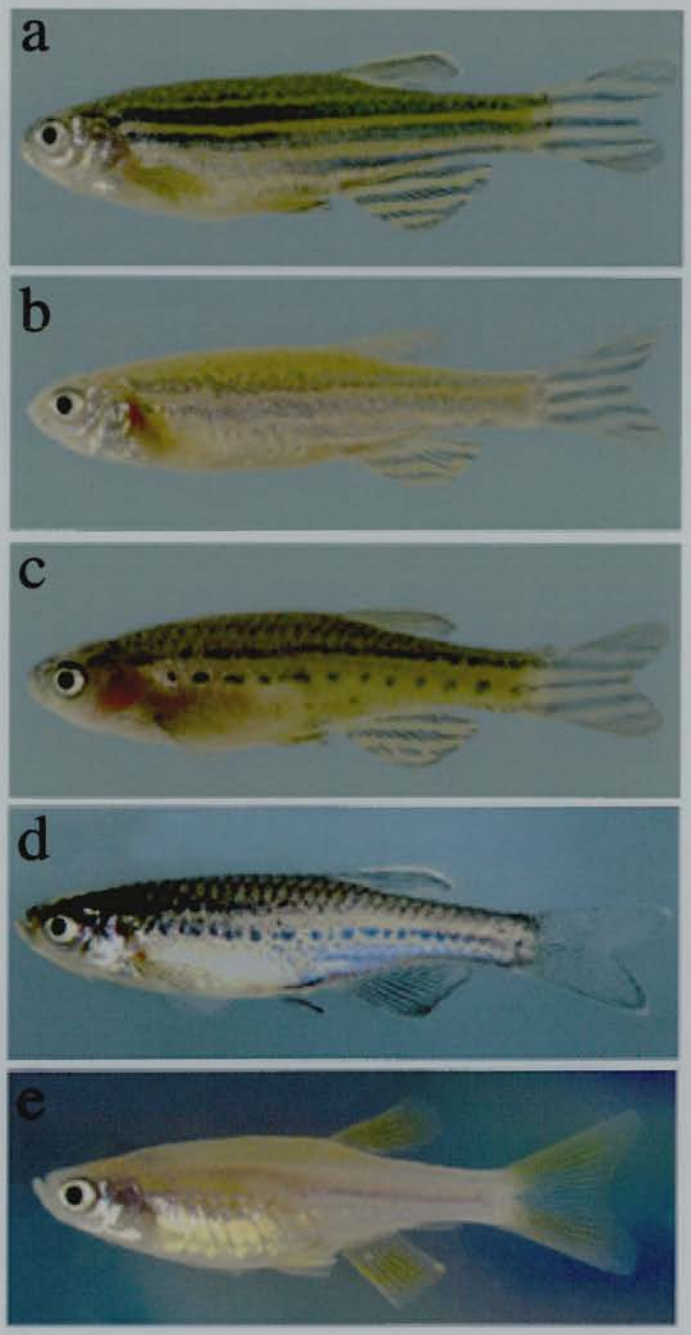

Figure 1.3.5. Zebrafish mutants effecting chromatoblast development. a, a wild-type fish demonstrating the characteristic melanic stripes. **b**, a *sparse* mutant deficient in the tyrosine receptor kinase *kit* and lacking early stripe melanophores. **c**, a *rose* mutant deficient in *endothelin receptor b1* and **d**, a *panther* mutant deficient in *fms* (a *kit* homologue). Both are lacking late stripe melanophores, plus *panther* is also lacking xanthophores. **e**, a *nacre* mutant, deficient in *mitfa* and lacking in all neural crest derived chromatophores. Figure modified from (Rawls *et al.*, 2001).

This is the rate-limiting step of the whole process as TYR appears to be upregulated during eumelanin synthesis, but functions at a basal level during phaeomelanogenesis (Kuzumaki *et al.*, 1993). The pigmentary importance of TYR was demonstrated when it was shown to be defective in the classic mouse mutant, *albino*, which is completely lacking in melanin (Yokoyama *et al.*, 1990; Beermann *et al.*, 1990; Jackson and Bennett, 1990). Subsequent work has shown that loss of function mutations in *TYR* result in albinism in almost every species studied including humans (Kwon *et al.*, 1987) (Fig. 1.3.6b and c).

As TYR is sufficient to generate melanin both *in vitro* and in nonmelanogenic cells *in vivo*, it was originally thought to be the sole melanogenic enzyme (Bouchard *et al.*, 1989; Winder *et al.*, 1993). It soon became clear, however, that other enzymes generated the complex eumelanin biopolymers seen in melanocytes (Hearing and Tsukamoto, 1991). These were subsequently identified as tyrosinase related protein 1 (TRP1), mutated at the *brown* locus and DOPAchrome tautomerase (DCT, also know as TRP2), mutated at the *slaty* locus (Zdarsky *et al.*, 1990; Shibahara *et al.*, 1991; Jackson *et al.*, 1992; Tsukamoto *et al.*, 1992). As both enzymes catalyse the production of eumelanin only (Fig. 1.3.6a), inactivating mutations in their genes results in a lighting of the coat. In contrast, there does not appear to be further enzymes required for phaeomelanin production, instead it forms spontaneously from DOPA-quinone in the presence of cysteine.

Although the full complexity of melanin synthesis within the melanosome has yet to be fully appreciated, the study of mouse pigmentation mutants has identified other key melanosomal proteins. For example, *pink-eye dilution* encodes an integral part of the melanosome membrane that is potentially involved in maintaining the pH of the melanosome, and *silver* encodes a melanosomal matrix protein (Zhou *et al.*, 1994; Lamoreux *et al.*, 1995; Puri *et al.*, 2000). The functions of the proteins encoded by other mutants of this class, such as *beige* and *pale ear*, are not yet known though both are probably localised in the melanosome membrane (Jackson, 1997; Bennett and Lamoreux, 2003).

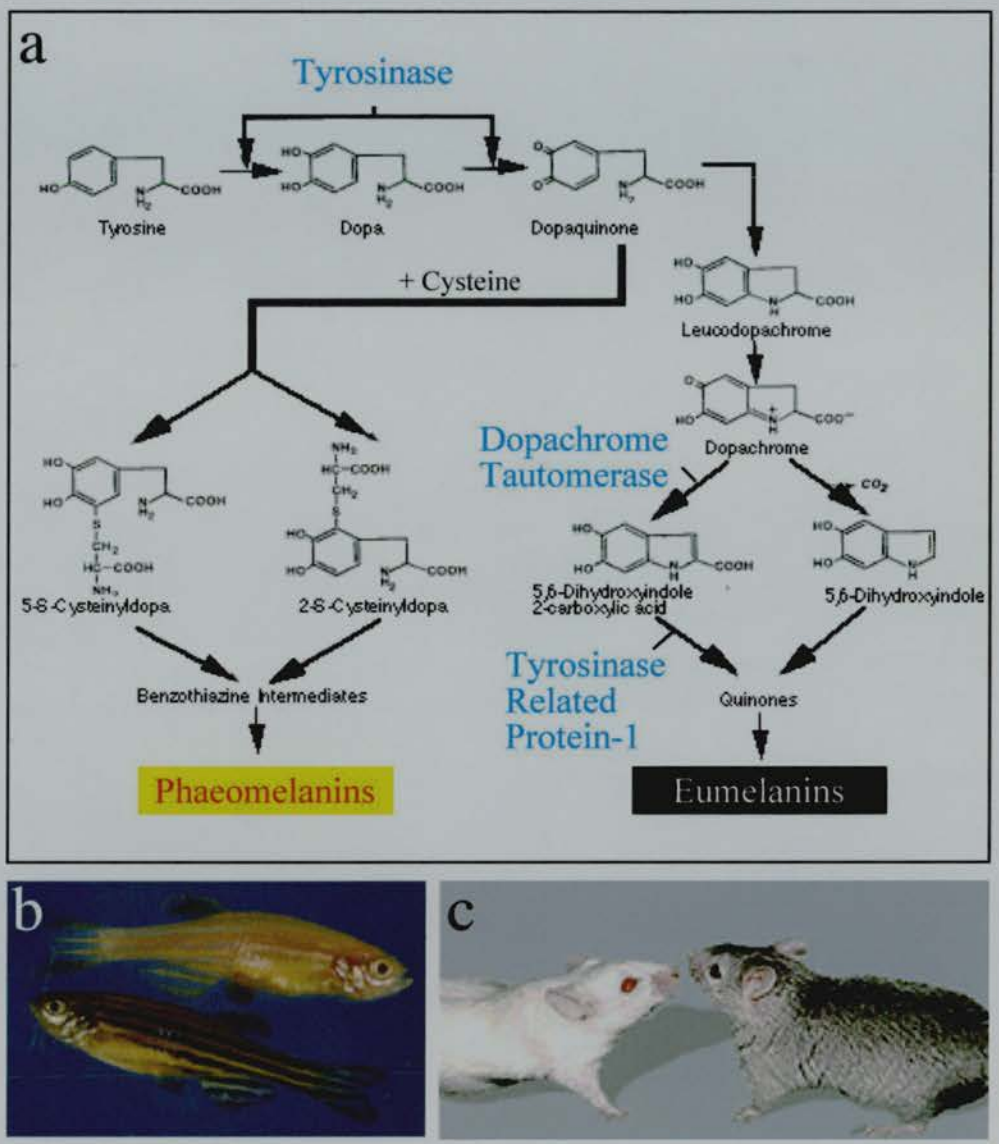

Figure 1.3.6. Enzymatic catalysis of melanogenesis. **a**, melanin is produced from the amino acid tyrosine, but several chemical intermediates (*black* type) are generated in the eventual production of either eumelanin or phaeomelanin. Three melanogenic enzymes (*blue* type) are essential for eumelanin production, however only tyrosinase is required for phaeomelanin production. **b**, *sandy* zebrafish (top) generate no melanin (compare with wildtype (bottom)) even after addition of DOPA. They are therefore probably deficient in a melanogenic enzyme, although which is currently not known. **c**, *albino* mice (left) are tyrosinase deficient and are therefore unpigmented (compare with wildtype (right)). Figure modified from (King *et al.*, 2001)

1.4 Melanocortin signalling

1.4.1 extension and agouti

In humans, phaeomelanin appears red in colour and thus makes up a significant proportion of hair shaft melanosomes in red haired individuals. In comparison, black hair contains only eumelanosomes (Quevedo, Jr. and Holstein, 1998). It appears, however, that different follicular melanocytes produce each melanin type. As keratinocytes migrate upwards from the lower hair bulb (see Fig 1.3.2), they may accept melanosomes from either or both types of melanocyte. The keratinised hair shaft can therefore contain a mixture of both phaeo- and eumelanosomes, the ratio of which depends on the number of each type of melanocyte in the follicle. It is this process that generates the range of hair colours seen in humans, but also limits each hair shaft to a single hue (Jimbow *et al.*, 1984; Quevedo, Jr. and Holstein, 1998). In mice mixed melanogenesis occurs, with both phaeo- and eumelanosomes produced within a single follicular melanocyte. By altering the expression of the melanogenic enzymes, mouse melanocytes can reversibly adjust the type of melanin produced thereby allowing the production of banded hair shafts (Sakurai *et al.*, 1975). Such banding can be observed on the dorsal hair of wild-type mice; two eumelanic bands separated by a single phaeomelanic strip forming a so-called 'agouti' pattern that gives the mouse coat an overall brown appearance (Silvers, 1979). For many years before the molecular basis of melanogenetic switching was elucidated, several mouse lines with apparent deficiencies on phaeo- or eumelanogenesis were investigated. In particular, a series of alleles at both the *extension* (*e*) and *agouti* (*a*) loci were considered candidate genes for regulating melanogenic switching.

The *extension* locus was so named because different alleles seemed to vary the extension of eumelanin along the length of the banded hair shaft. The several mutations in *e* lie in an allelic series with respect to coat colour, the dominant alleles have a eumelanic phenotype, the wild-type allele is intermediate and the recessive alleles result in a yellow colour (Searle, 1968). For example, mice homozygous for the *sombre* allele are almost entirely black, although mature heterozygous mice can be distinguished from homozygotes by the appearance of some yellow hairs on their flanks (Bateman, 1961).

The dominant *tobacco* allele is a naturally present in the tobacco mouse, *Mus poschiavinus*, and causes a darkened dorsum compared to the wild type allele (which has a normal extension of black) (von Lehmann, 1973). The final allele in the series is *recessive yellow*. Mice homozygous for this allele are almost entirely yellow due to the absence of eumelanin production, though they do have black eyes (Hauschka *et al.*, 1968).

The *agouti* locus was named after the eponymous South American rodent (*Dasyprocta aguti*) that best typifies the banded pattern of hair colouration that the wild type gene elicits (Galbraith, 1969). Like *extension* mutants, the *agouti* mouse mutants can be graded with respect to coat colour phenotype. However, the allelic order is diametrically opposite to that of *extension*. Dominant alleles display a yellow coat colour, wild-type have the classic banded pattern and recessive alleles have a darker hue (Dickie, 1969). The *lethal yellow* allele is a semi-dominant mutation initially propagated by mouse fanciers. Heterozygotes are all yellow, but with black eyes, and become obese and sterile after a few months. Other dominant alleles, such as *viable yellow* and *sienna yellow* have a comparable heterozygous phenotype to *lethal yellow* mice, yet are not homozygous lethal. The most common allele found in lab strains is *agouti*, which produces banded phaeomelanic stripes on all hairs. However the true wild-type allele, *light-bellied agouti*, results in a banded hair pattern on the dorsum only, with ventral hairs being fully phaeomelanic (Silvers, 1979). The classic recessive mutant, *nonagouti*, was also isolated and propagated by mouse fanciers. When homozygosed, it results in a mouse with a very dark appearance. Occasional yellow hairs in integumentary regions and the flanks confirm that *nonagouti* is not null unlike the most recessive viable alleles, *extreme nonagouti* and *jet-black* (Dickie, 1969).

It has long been known that α-melanocyte stimulating hormone (αMSH), a peptide produced as a hormone by specialised pituitary cells, stimulates eumelanin production in the mouse (Halaban and Lerner, 1977). Thus it was postulated that the protein products of both the *a* and *e* loci interact with the αMSH signalling pathway in melanocytes (Tamate and Takeuchi, 1984; Takeuchi *et al.*, 1989). However, it was not until after the characterisation of *extension* as an αMSH receptor (Robbins *et al.*, 1993), and *agouti* as a paracrine antagonist of said receptor (Bultman *et al.*, 1992; Miller *et al.*, 1993), that the true ingenuity of melanosome switching was revealed. Furthermore, the study of

extension and *agouti* resulted in cloning of multiple receptors for melanocyte stimulating hormones (melanocortins).

1.4.2 Pro-opiomelanocortin

The term 'melanocortin' refers to the cleavage products of pro-opiomelanocortin (POMC) that possess melanotropic activity (Cone *et al.*, 1996). The existence of such factors was established many years ago when it was demonstrated that ablation of the hypophysis in frogs resulted in a pigmentation phenotype (Allen, 1916; Smith, 1916). The hypophyseal protein responsible for promoting melanogenesis in amphibians was first designated as intermedin then, after it was characterised and demonstrated to have a melanogenic effect in mammals, it was referred to as a melanocyte-stimulating hormone (MSH) (Shizume *et al.*, 1954; Harris and Lerner, 1957). Subsequently, a range of similar hormones, all encoded within the POMC precursor peptide, have been identified in a number of higher and lower vertebrate species (Fig. 1.4.1a). These are processed from three different regions of mammalian POMC, each of which contains a conserved 'pharmacore' sequence (-His-Phe-Arg-Trp-) that is essential for receptor activation (Cone *et al.*, 1996) (Fig. 1.4.1b). The N-terminal melanocortin peptide is designated γMSH, the overlapping middle peptides are called adrenocorticotrophic hormone (ACTH) and αMSH while the C-terminal melanocortin is βMSH (Fig.1.4.1a). The carboxy-terminal portion of POMC also encodes the opioid peptides, β-endorphin and met-enkephalin, and β-lipotropic hormone. The peptides are all post-translationally cleaved from POMC by prohormone convertases, the major products depending on which enzymes are expressed (Marcinkiewicz *et al.*, 1993).

Originally, MSHs were detected in the anterior and intermediate lobes of the pituitary, where they function as circulating hormones (Shizume *et al.*, 1954; Harris and Lerner, 1957). More recently, however, they have been observed in the skin and in various brain nuclei (Dube *et al.*, 1978; Thody *et al.*, 1983). It is now clear that melanocortins are involved in a range of mammalian processes, and have been demonstrated to signal in an endocrine, paracrine, autocrine and neurocrine manner. However, the details of melanocortin signalling were only elucidated after the identification of their high affinity receptors.

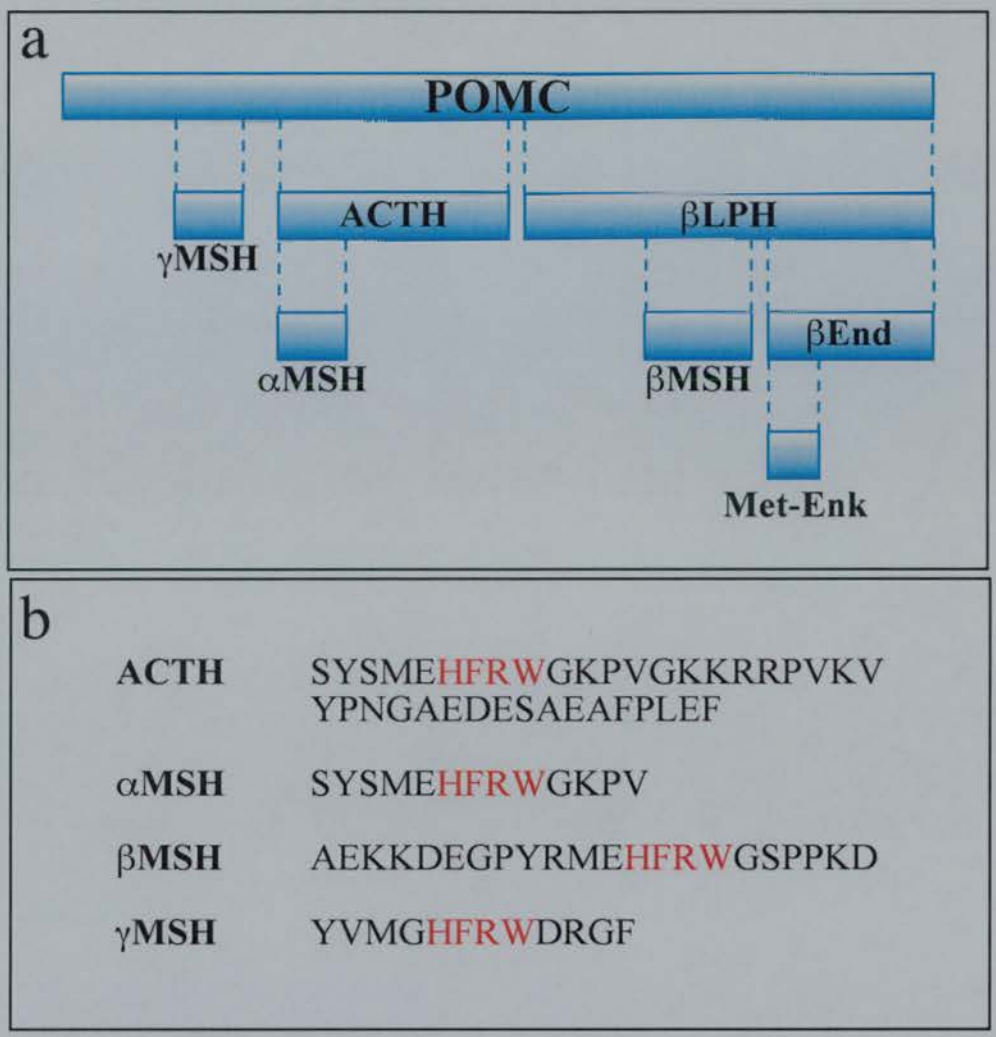

Figure 1.4.1. The structure and sequence of mammalian melanocortins. a, the structure of mammalian pro-opiomelanocortin (POMC). Several peptides are cleaved from the pro-hormone: α, β and γ-melanocyte stimulating hormone (αMSH, βMSH and γMSH), adrenocorticotrophic hormone (ACTH), β-lipotropic hormone (βLPH), β-endorphin (βEnd) and met-enkephalin (Met-Enk). **b,** the peptide sequence of each mammalian melanocortin including the pharmacore (*red*) sequence required to activate melanocortin receptors.

1.4.3 The melanocortin-1-receptor

The mammalian melanocortin receptor family consists of five serpentine G-protein coupled receptors, designated MC1R-MC5R by the order in which they were identified (Chhajlani and Wikberg, 1992; Mountjoy *et al.*, 1992; Gantz *et al.*, 1993a; Gantz *et al.*, 1993b; Labbe *et al.*, 1994). They are all agonised, to a greater or lesser extent, by the melanocortin products of POMC. However, they each have different activation profiles and patterns of tissue expression, reflecting their roles in a multitude of physiological processes (Schioth *et al.*, 1996). The five receptors display 39-61% identity at the amino acid level with MC3, MC4 and MC5 receptors being the most closely related and MC1R and MC2R the most distantly related. The genes encoding the receptor family are not clustered (Table 1.4.1), but they do all share a simple genomic structure consisting of a single coding exon of around 1kb in length (Cone *et al.*, 1996).

Table 1.4.1 Chromosomal positions of melanocortin receptor genes. Human cytogenetic locations are shown for each gene followed by position on the Ensembl genomic assembly. Mouse gene locations are shown as chromosome number followed by position.

Gene	Mouse Map	Human Map
MC1R	8, 123.5 Mb	16q24.3, 91.8 Mb
MC2R	18, 68.7 Mb	18p11.2, 14.0 Mb
MC3R	2, 173.5 Mb	20q13.2, 54.6 Mb
MC4R	18, 67.2 Mb	18q22, 57.9 Mb
MC5R	18, 68.7 Mb	18p11.2, 13.9 Mb

MC1R was cloned after being demonstrated to be expressed in melanocytes and melanomas (Chhajlani and Wikberg, 1992; Mountjoy *et al.*, 1992). Soon after, mouse *Mc1r* was identified as the gene encoded by the *extension* locus and thus as the mediator of αMSH action on melanocytes (Robbins *et al.*, 1993). Binding studies have demonstrated that, of all the melanocortins, mouse Mc1r has the highest affinity for

αMSH followed by ACTH, although human MC1R only displays a negligible preference (Abdel-Malek *et al.*, 1995; Tsatmalia *et al.*, 1999). Since the identification of MC1R, many studies have illustrated the mechanism through which it stimulates eumelanogenesis. Together these suggest that POMC is produced by the keratinocytes surrounding epidermal and follicular melanocyte and cleaved into both αMSH and ACTH (Thody *et al.*, 1983; Schauer *et al.*, 1994; Wakamatsu *et al.*, 1997). The peptides are then secreted in a paracrine manner and one or both binds MC1R on the surface of the melanocyte, resulting in activation of intracellular adenylyl cyclase (AC) by its associated G_s-protein (Haskell-Luevano *et al.*, 1994). AC then elevates cytosolic cAMP levels resulting in transcriptional upregulation of the melanogenic enzymes, probably via protein kinase A (Hunt *et al.*, 1994a). There is also evidence that melanogenic enzymes are functionally activated as a result of MC1R signalling, and that both melanosome dispersal and melanocyte proliferation is stimulated (Fig 1.4.2) (Halaban and Lerner, 1977; Hunt *et al.*, 1994b; Abdel-Malek *et al.*, 1995; Suzuki *et al.*, 1996).

When Robbins and co-workers analysed Mc1r sequence and function in the *extension* allelic series, they revealed how differences in receptor activation explain the observed phenotypes (Robbins *et al.*, 1993). The dominant *sombre* (now termed $Mc1r^{E\text{-}so}$) phenotype is due to a leucine to proline change in the *Mc1r* gene, resulting in an increased level of constitutive activation and explaining the uniformly dark phenotype. The *tobbaco* allele ($Mc1r^{E\text{-}tob}$) also has an amino acid substitution in *Mc1r*, this time resulting in a receptor hyperactive to hormone response. The different mechanism of increased activation is responsible for the more spatially restricted eumelanic phenotype. The *Mc1r* gene in *recessive yellow* mice was shown to have a single nucleotide deletion resulting in a premature termination after the fourth transmembrane domain. *In vitro* assays of receptor function confirmed the mutant gene product is unable to stimulate adenylyl cyclase in response to αMSH activation, thus tyrosinase is not upregulated and eumelanogenesis does not proceed (Robbins *et al.*, 1993).

It soon became clear that the phaeomelanic phenotype of *Mc1r* loss-of-function in *recessive yellow* mice is mirrored in other species. As in mice, deficiency in human MC1R signalling results in an increase of phaeomelanogenesis at the expense eumelanogenesis. Accordingly, it was demonstrated that some variant alleles of human MC1R are associated with red hair and pale skin (Fig 1.4.2d) (Valverde *et al.*, 1995).

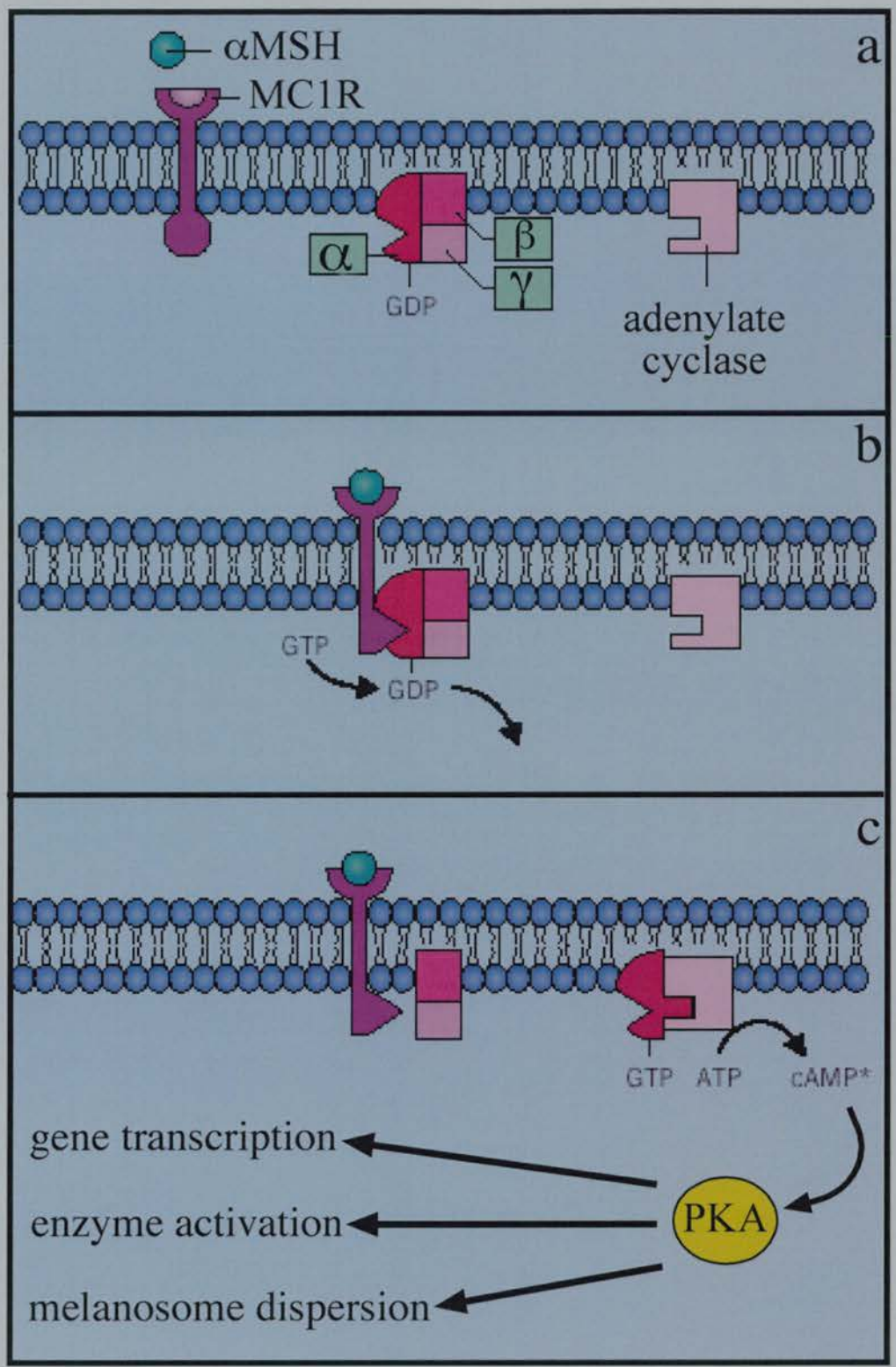

Figure 1.4.2 MC1R mediates the action of αMSH of mammalian melanocytes. Legend overpage.

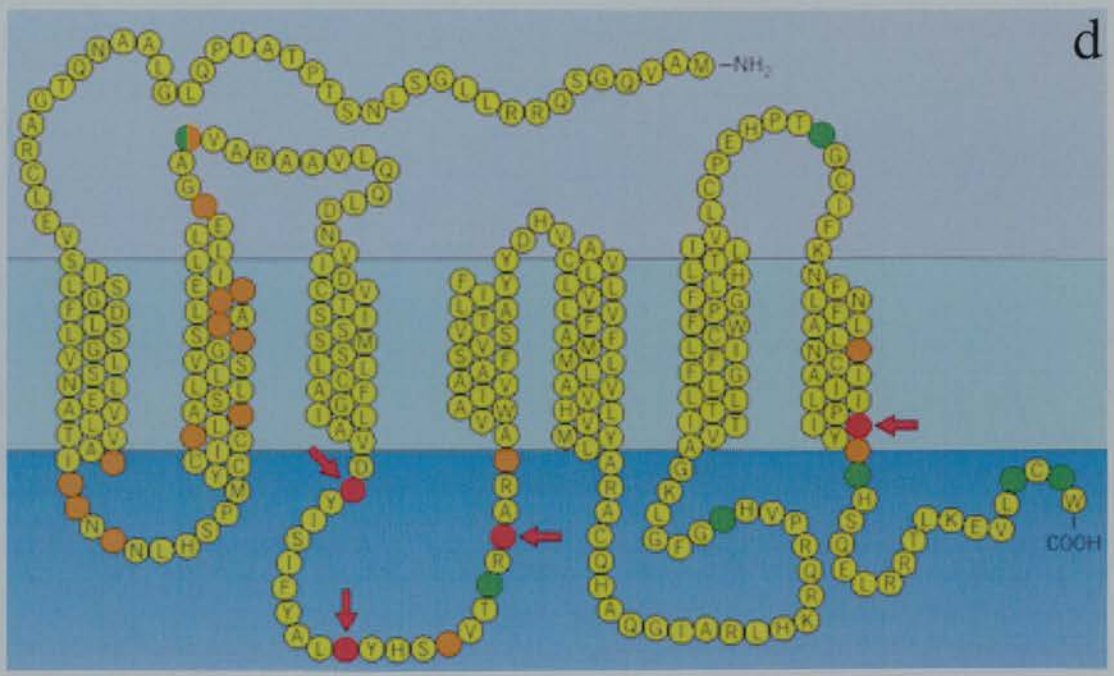

Figure 1.4.2. MC1R mediates the action of αMSH of mammalian melanocytes. a, αMSH (and ACTH) are secreted by keratinocytes in the mammalian epidermis. MC1R, a GDP bound G_s-Protein (consisting of α, β and γ subunits) and adenylate cyclase (AC) are all assocaiated with the plasma membrane of melanocytes. **b**, on stimulation by αMSH, MC1R binds the G_s-Protein resulting in GTP activation of the α-subunit. **c**, $G_{s\alpha}$ activates adenylate cyclase. AC then increases intracellular cAMP levels that, in turn, activate protein kinase A (PKA). This promotes a cascade resulting in gene transcription, melanogenic enzyme activation and increased melanosome dispersion and donation. **d**, schematic of human MC1R sequence and structure illustrating the extracellular N-terminus (top), the 7 transmembrane domains (middle) and the C-terminal intracellular region (bottom). Amino acid residues are indicated (*yellow*). Residues in *green* are varient at the DNA level in the human population, but do not alter the peptide sequence. Residues in *orange* indicate varients that do change the amino acid sequence but are not associated with red hair. Residues in *red* are those variants associated with red hair that have been shown to result in dysfunctional receptors. Figure modified from (Bolognia and Orlow, 2003).

These variants have since been assayed *in vitro* and *in vivo* and in both cases were demonstrated to display a reduced signalling capacity (Schioth *et al.*, 1999; Healy *et al.*, 2001). There is also growing evidence that human MC1R loss-of-function variants are associated with increased risk of cutaneous malignant melanoma (CMM). One study has demonstrated that the tanning ability of white individuals with one variant allele is intermediate to those with two variants and those with none, suggesting that MC1R status influences sun sensitivity in people irrespective of hair colour phenotype (Healy *et al.*, 2000). Furthermore, the ultraviolet protection normally afforded by darker skin colour is negated in people with MC1R variants, increasing their risk of CMM. This demonstrates a strong association between CMM and MC1R genotype, probably a better indicator of risk than skin type, which is normally quoted as a significant factor (Valverde *et al.*, 1996; Palmer *et al.*, 2000).

Since the association between MC1R genotype and pigmentation was discovered, both loss-of-function and gain-of-function alleles have been identified in many more mammalian and avian species (Table 1.4.2), confirming MC1R signalling as an important regulator of higher vertebrate pigmentation (Jackson, 1997). Although αMSH stimulates eumelanogenesis and melanosome dispersion in lower vertebrates (see Chapter 4), at the time this study commenced no melanocortin receptors had been cloned from any poikilothermic species. Therefore a definitive role for MC1R signalling in melanophores is unproven. There are, however, classes of zebrafish mutants that are deficient in melanin synthesis and melanosome aggregation. The melanosome translocation mutants are discussed further in Chapter 4. The melanin deficient lines, including *albino*, *sandy*, *golden* and *pewter*, are good candidates for genes in the melanogenic pathway and at least some will probably encode melanogenic enzymes such as tyrosinase (see Figure 1.3.6b) (Kelsh *et al.*, 1996).

It is unlikely that all fish pigmentation mutations will prove to be orthologous to mammalian genes previously studied. For example, a recent report characterising a fish pigmentation mutant led to the identification of a novel gene. Homozygosity at the classic *b* locus in the freshwater teleost, medaka (*Oryzias latipes*) results in a reduction in melanin, giving the fish a pale orange/white colour (Fig. 1.4.3a). Positional cloning identified the locus as encoding a putative sucrose transporter (AIM1) essential for melanin synthesis and nonfunctional in *b/b* fish (Fukamachi *et al.*, 2001).

Table 1.4.2 MC1R variants associated with pigmentation phenotypes. Loss-of-function (L) or gain-of-function (G) alleles inferred from functional testing or sequence similarity to tested alleles.

Species	Allele	Phenotype	Reference
Dog	L	Phaeomelanic hair colouring of golden retrievers and red setters	(Newton *et al.*, 2000)
Black Bear	L	White phase of Kermode bears	(Ritland *et al.*, 2001)
Big Cats	G	Melanic jaguars and jaguarundis	(Eizirik *et al.*, 2003)
Cattle	L/G	Red hair in Holstein cattle (L) and black hair in eumelanic breeds (G)	(Klungland *et al.*, 1995)
Chicken	L/G	Red (L) and black plumage (G)	(Takeuchi *et al.*, 1996)
Horse	L	Chestnut colouration	(Marklund *et al.*, 1996)
Sheep	G	Black phase of Dala sheep	(Vage *et al.*, 1999)
Bananaquit	G	Melanic morph	(Theron *et al.*, 2001)
Pig	L/G	Multiple red skinned (L) and black skinned strains (G).	(Kijas *et al.*, 1998)
Fox	G	Darkly pigmented Alaskan silver fox	(Vage *et al.*, 1997)
Pocketmice	G	Melanic morphs	(Nachman *et al.*, 2003)

Interestingly, the orthologous gene in mouse colocalises with the classic *underwhite* locus, which confers a light coloured coat when homozygosed (Fig.1.4.3b) (Sweet *et al.*, 1998; Du and Fisher, 2002). This work not only suggests a previously unknown relevance of sucrose in melanogenesis, but also highlights the strength of cross species comparisons when elucidating melanogenic genes.

In addition to its role in mammalian melanogenesis, MC1R is also found in Leydig cells of the testis, macrophages, monocytes, neutrophils, fibroblasts, endothelial cells, astrocytes and in some neurons in the grey matter of the brain. This has led to suggestions that the receptor is also involved in immunomodulation, anti-inflammatory responses and nociception (Star *et al.*, 1995; Catania *et al.*, 1996; Starowicz and Przewlocka, 2003; Mogil *et al.*, 2003).

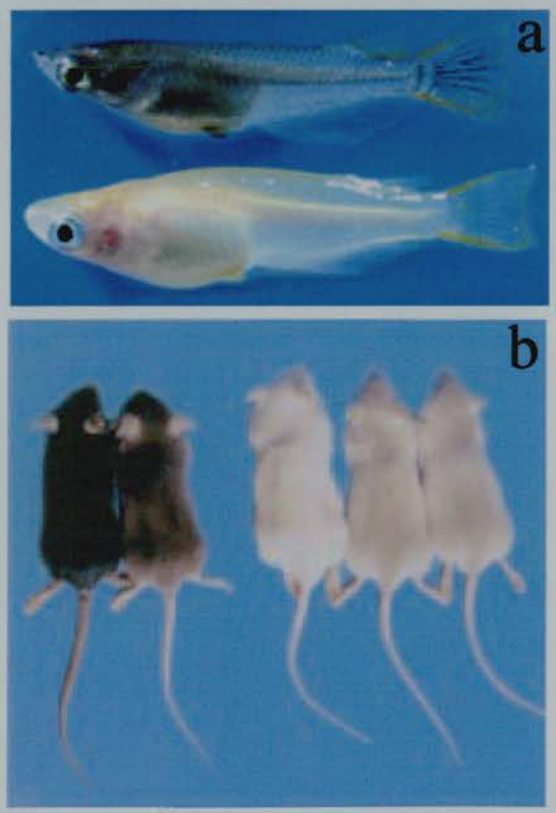

Figure 1.4.3. The medaka *b* locus is orthologous to mouse *underwhite*. **a**, normally pigmented medakafish (top) appear black due to the melanin synthesised in melanophores, however mutants at the *b* locus display a reduction in melanin. A fish homozygous for the most severe allele, b^{s8} is shown (bottom). Figure modified from (Fukamachi *et al.*, 2001). **b**, After characterisation of the medakafish *b* locus as a sucrose synporter (callled AIM1), the classic recessive mouse locus, *underwhite (uw)*, was demonstrated to map to the orthologous gene. Shown from left: a mouse heterozygous for *underwhite dense* (a mild allele), an *underwhite dense* homozygote showing reduced pigmentation, an *underwhite* homozygote with the least pigmentation, two *underwhite intense* homozygotes showing an intermediate phenotype. All mice are on a *nonagouti* background. Figure modified from (Sweet *et al.*, 1998).

1.4.4 Agouti signalling protein

The majority of research into MC1R function has focussed on its role in pigmentation and, soon after its identification, the mouse *agouti* locus was characterised by positional cloning (Bultman *et al.*, 1991; Bultman *et al.*, 1992). The *Agouti* gene has a complex genomic structure and encodes a 131 amino acid peptide termed agouti signalling protein (ASP)(Miller *et al.*, 1993). Unlike *extension*, skin grafting studies had previously indicated that *agouti* alleles are not expressed autonomously by the melanocyte, but by other cells in the follicle microenvironment (Silvers, 1979). This concurs with the observation that ASP is a secreted peptide that blocks αMSH stimulation of Mc1r (Lu *et al.*, 1994). Such inhibition leads to a reduction of cAMP dependent kinase activity, the downregulation of melanogenic enzymes and a switch from production of eumelanin to phaeomelanin (Fig. 1.4.4) (Yang *et al.*, 1997; Sakai *et al.*, 1997). Currently, the downstream consequences of ASP binding to Mc1r are not fully understood and there has been debate over whether an alternative ASP receptor exists in the melanocyte (Conklin and Bourne, 1993). However, recent reports indicate that Mc1r mediation is obligatory for the melanogenic action of ASP *in vivo* and, furthermore, that it functions by inhibiting a constitutive low-level activity of unbound receptor. Therefore ASP is considered an 'inverse' agonist of Mc1r, as opposed to a simple antagonist of αMSH activation (Suzuki *et al.*, 1997; Ollmann *et al.*, 1998; Abdel-Malek *et al.*, 2001).

The banded agouti pattern found on wild-type mouse dorsal hair shafts is produced by the pulsatile expression of ASP. Hair follicle keratinocytes secrete ASP only between days 4-6 of each ~25 day hair cycle, thus transiently switching from eumelanogenesis to phaeomelanogenesis during anagen (Fig. 1.4.5a). However, the complexity of the *Agouti* locus allows for both temporally and spatially regulated expression, providing variable ventral/dorsal phaeomelanin distribution and explaining the range of phenotypes exhibited by *Agouti* alleles (Fig 1.4.5a-e) (Miller *et al.*, 1993; Vrieling *et al.*, 1994; Bultman *et al.*, 1994; Millar *et al.*, 1995).

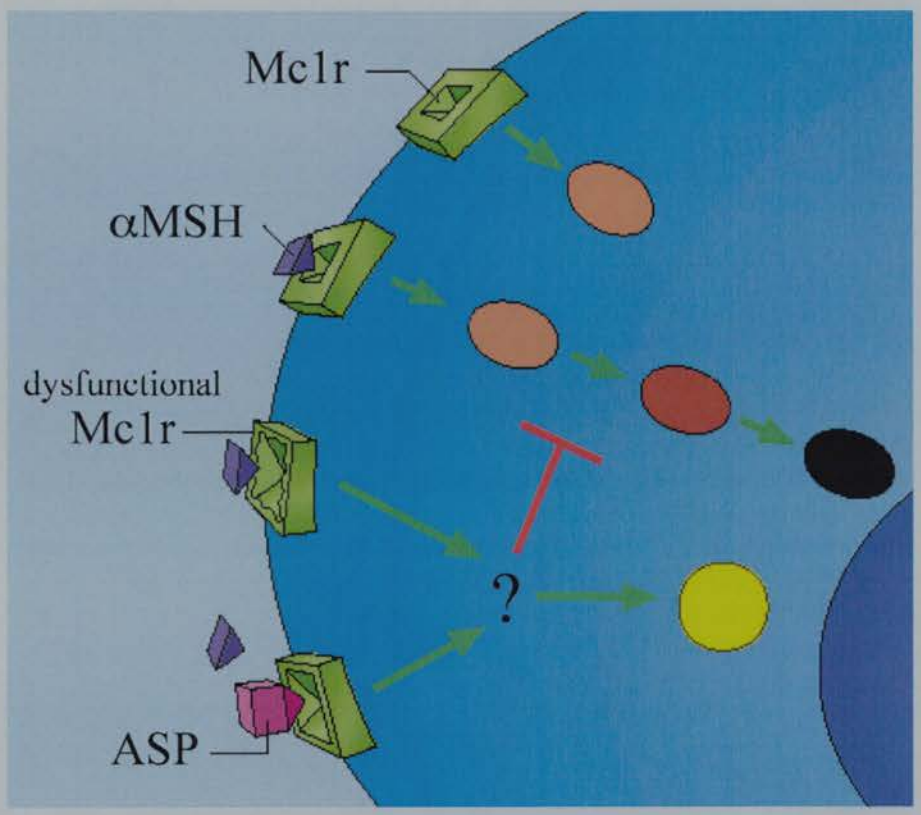

Figure 1.4.4. αMSH, Mc1r and ASP interact to control melanogenesis. Unbound Mc1r signals to produce eumelanin at a basal level (top). On melanocortin activation of Mc1r eulamelanin production is upregulated. A dysfunctional Mc1r cannot activate the eulmelanogenetic pathway, so in default, phaeomelanogenesis occurs through a mechanism not fully understood. When ASP is produced, it competes with αMSH to bind Mc1r (bottom). On binding, it inversely agonises the receptor, resulting in phaeomelanogenesis. Figure modified from (Bolognia and Orlow, 2003).

For example the true wild-type allele, *light-bellied agouti* (A^w), encodes two different hair cycle specific mRNA transcripts responsible for the 'agouti' banded hair pattern, and two ventrum specific transcripts which are responsible for the lighter belly colour (Fig. 1.4.5f) (Bultman *et al.*, 1994). The most common allele, *agouti* (*A*), has a disrupted ventrum specific promoter resulting in a banded hair pattern all over the body (Vrieling *et al.*, 1994) (Fig. 1.4.5a,c,f). Another example is *black and tan* (a^t). It eliminates hair cycle specific transcripts in a recessive manner giving a dark dorsum while allowing ventrum specific transcripts to be expressed normally (Fig. 1.4.5a,d). The recessive mutant *nonagouti* (*a*) is caused by an 11kb insertion between exons D and 2 and results in an extreme reduction in expression of all transcripts giving the mouse a eumelanic appearance (Fig. 1.4.5a,e,f) (Bultman *et al.*, 1994).

It became clear from mRNA analysis that, when compared to the pseudo wild-type *agouti* transcript, the *lethal yellow* (A^y) transcript is both larger and ectopically expressed. This is due to a ~150kb deletion of an upstream gene (*Raly*) which places A^y under its stronger, ubiquitously expressing promotor. Ectopic expression of ASP in A^y mice causes continual phaeomelanin production, thus the yellow hair (Fig. 1.4.5a,b) (Michaud *et al.*, 1993). Interestingly, the lack of a disturbed eye phenotype in both A^y and $Mc1r^e$ homozygous mice confirms that eumelanogenesis in the retinal pigmented epithelium is Mc1r/ASP independent. The prenatal lethality of A^y/A^y mice is probably due to the absence of *Raly*, which encodes a RNA processing protein, as targeted disruption of the gene leads to an embryonic developmental block (Duhl *et al.*, 1994). Moreover, other *Agouti* alleles, such as *viable yellow* and *sienna yellow*, up-regulate ASP expression but do not disrupt another gene. These have a comparable heterozygous phenotype to A^y mice, yet are not homozygous lethal (Siracusa, 1994). The obesity phenotype of mice ectopically expressing *Agouti* is discussed further in Chapter 1.4.6.

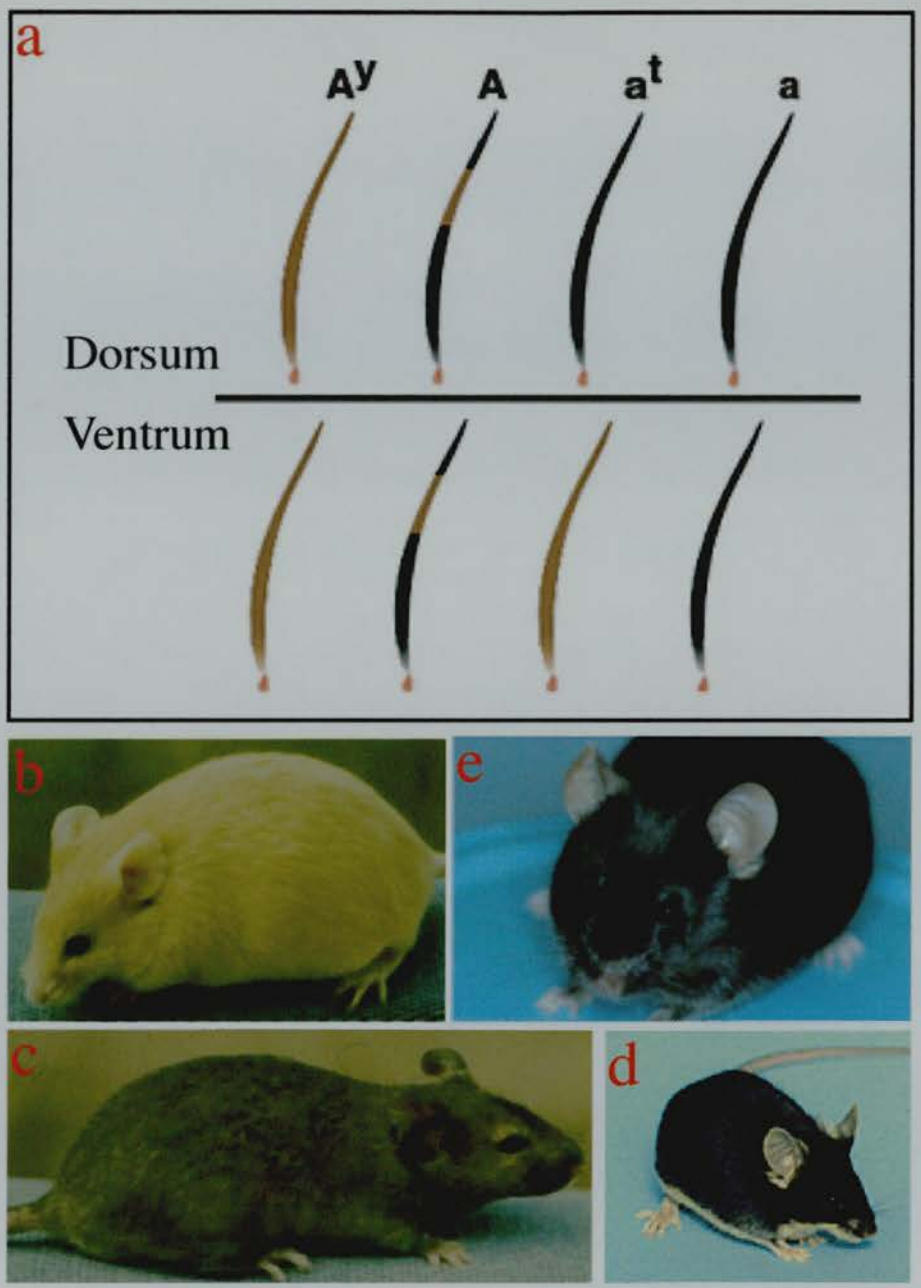

Figure 1.4.5. The phenotype of *Agouti* alleles. Legend overpage.

f

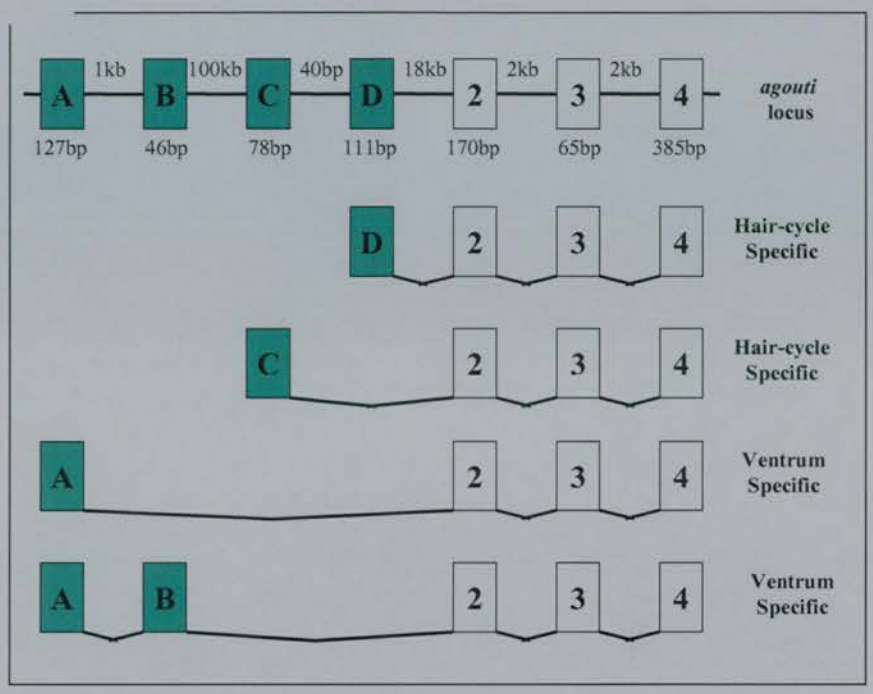

Figure 1.4.5. The phenotype of *Agouti* alleles. a, a schematic representation of the hair shaft phenotype of Agouti alleles *lethal yellow* (A^y), *agouti* (A), *black and tan* (a^t) and *nonagouti* (a). **b,** an A^y/A mouse; **c**, an A/A mouse; **d**, an a^t/a^t mouse; **e**, an a/a mouse. **f**, the structure and multiple transcripts of the mouse *Agouti* gene. The gene is shown from proximal (left) to distal. Non-coding exons are filled boxes lettered A, B, C and D. Exons 2, 3 and 4 are protein coding and in white boxes. The lengths of the exons are indicated, the numbers between exons indicate the intronic sizes. The transcripts are in two sets: hair-cycle specific and ventrum specific. Wild-type *light-bellied agouti* (A^w) mice produce all four transcripts, *agouti* (A) mice produce only hair-cycle specific transcripts and and *black and tan* (a^t) mice produce only ventrum specific transcripts. Figure modified from (www.people.fas.harvard.edu/~brown/dogs/genetics/color-genetics.htm)

There are now more that 20 dominant and recessive *Agouti* alleles identified in other species including fox, cattle and horses (Adalsteinsson *et al.*, 1995; Vage *et al.*, 1997; Rieder *et al.*, 2001). In these species, as in rodents, the primary role of ASP is the regulation of melanogenesis, illustrated by the fact that *Agouti* is expressed exclusively in the skin of mice (Lu *et al.*, 1994). In humans, however, ASP does not appear to have a pigmentary function, instead it has a wide distribution pattern (including testis, ovary, heart, foreskin, kidney and liver) but its biological function in these tissues is unknown (Kwon *et al.*, 1994; Wilson *et al.*, 1995).

1.4.5 The melanocortin-2-receptor

At the same time *MC1R* was cloned, a second melanocortin receptor gene was identified (Mountjoy *et al.*, 1992). The MC2 receptor, probably the most specialised member of its family, is strongly expressed in the adrenal cortex, particularly the zona fasciculata and zona glomerulosa (Xia and Wikberg, 1996). Compared to the other receptors, which are more promiscuous in their melanocortin binding, MC2R is exclusively activated by ACTH. This results in a intracellular increase in cAMP by stimulation of adenylate cyclase (Schioth *et al.*, 1996). This ligand-binding profile is indicative of the physiological role of MC2R in the adrenals where it mediates the action of ACTH on glucocorticoid synthesis. Evidence for this includes familial glucocorticoid deficiency (FGD) syndrome, which can be caused by loss-of-function mutations in the human *MC2R* gene. FGD syndrome is a rare autosomal recessive disorder characterised by degeneration of the zona fasciculata and unresponsiveness to ACTH. Around half of the individuals with FGD have a MC2R dysfunction; the molecular basis of the other half (and the closely related Triple-A syndrome) has yet to be elucidated (Weber and Clark, 1994). *MC2R* activating mutations have never been seen in adrenal tumours despite an extensive search, though loss of heterozygosity for the receptor seems to be associated with an undifferentiated phenotype suggesting a role as a differentiation factor (Allolio and Reincke, 1997). In addition to its role in steroid synthesis, mouse *Mc2r* is expressed in white adipose tissue where it mediates the lipolytic activity of ACTH (Boston and Cone, 1996). This activity appears to be conserved in other mammals, but not humans (Boston, 1999).

1.4.6 The melanocortin-3 and melanocortin-4-receptors

The third and fourth melanocortin receptors cloned are both widely expressed in the central nervous system, MC4R exclusively so, while MC3R is also expressed in other tissues including the placenta, gut and pancreas (Gantz *et al.*, 1993a; Gantz *et al.*, 1993b). They are strongly agonised by ACTH and both forms of αMSH, the peripherally expressed form (monoacetyl-αMSH) and the tissue specific form (desacetyl-αMSH) (Mountjoy *et al.*, 1994). Uniquely, MC3R also binds γMSH and βMSH with high affinity, making it the only receptor that is potently activated by all melanocortins (Gantz *et al.*, 1993a). MC3 and MC4 receptors have recently been shown to have an important role in regulating body weight through separate, but complementary mechanisms. *Mc4r*$^{-/-}$ mice are obese, indicating that the receptor is required to limit food intake (Huszar *et al.*, 1997). In comparison *Mc3r*$^{-/-}$ mice display normal food intake but increased body fat, suggesting this receptor mediates feeding efficiency signalling. Mice lacking both genes show an exacerbated obesity phenotype, confirming the distinct function each receptor has in controlling body weight (See Figure 1.5.2) (Chen *et al.*, 2000). The discovery of melanocortin receptors that are involved in energy metabolism explained the obesity phenotype of ectopically-expressed *Agouti* alleles. Accordingly, it was demonstrated that ASP antagonises Mc4r function in *lethal yellow* heterozygous mice, thus recapitulating the *Mc4r* null obesity phenotype (Michaud *et al.*, 1994; Klebig *et al.*, 1995).

There is evidence that the human orthologues of these genes carry out a similar function. Rare *MC4R* variants have been found at a high frequency in morbidly obese patients, including both dominant and recessive alleles (Yeo *et al.*, 1998; Farooqi *et al.*, 2000; Vaisse *et al.*, 2000). Furthermore, all of these alleles so far tested have been demonstrated to encode malfunctioning proteins (Yeo *et al.*, 2003). There is, however, no association between *MC3R* variants and human obesity or type 2 diabetes mellitus (Hani *et al.*, 2001; Dubern *et al.*, 2001a). More recently, another role for melanocortin signalling in the CNS has been elucidated. Van der Ploeg and co-workers report that MC4R modulates penile erectile function and sexual behaviour in both rats and humans (Van der Ploeg *et al.*, 2002). This has precipitated research efforts to identify specific MC4R agonists for clinical use (Sebhat *et al.*, 2002).

1.4.7 Agouti related protein

Although ASP can strongly antagonise Mc4r, and to a lesser extent Mc3r signalling, *in vitro* and *in vivo*, this interaction does not occur in wild-type mice as ASP is not expressed outside the skin (Klebig *et al.*, 1995; Yang *et al.*, 1997). However, the discovery of an agouti related protein (AGRP) expressed in mouse and human brain, and up-regulated in obese mutant mice, revealed a weight control signalling mechanism parallel to the MC1R mediated melanogenic pathway (Ollmann *et al.*, 1997; Shutter *et al.*, 1997). AGRP was subsequently demonstrated to be a potent antagonist of MC4R and MC3R mediated αMSH signalling *in vitro* (Fong *et al.*, 1997; Rosenfeld *et al.*, 1998). Thus, similar to mice over-expressing ASP, ectopic expression of AGRP results in an obesity phenotype. AGRP does not, however, antagonise Mc1r signalling so these mice are not phaeomelanic (Ollmann *et al.*, 1997).

There is evidence that human AGRP carries out a similar function. The specific brain expression of AGRP, primarily in the hypothalamus, is strikingly alike in mouse and human (Shutter *et al.*, 1997). Moreover, infusion of an αMSH analogue into primates suppresses feeding behaviour while AGRP has the opposite effect (see Figure 1.5.2) (Koegler *et al.*, 2001). Investigations into AGRP in human obesity syndromes consistently reveal a correlation between plasma levels and body mass index (Katsuki *et al.*, 2001), but there are no reports demonstrating a mutation in *AGRP* as a causative factor (Norman *et al.*, 1996; Dubern *et al.*, 2001b). However, there is a suggestion an *AGRP* variant is significantly enriched in individuals with anorexia nervosa (Vink *et al.*, 2001). The role of AGRP in mammalian appetite control and energy metabolism is not yet fully understood, although there is a large body of ongoing research into its actions due to the obvious clinical benefits an AGRP inhibitor may have. However, unlike the action of ASP at MC1R, AGRP suppression is unlikely to be sufficient to discontinue the functional antagonism of melanocortin signalling in the brain. This is due to the complexity of appetite control in mammals, something that was validated by the recent discovery of an antagonistic pathway functioning parallel to MC3R/MC4R signalling in the mouse brain (See Chapter 1.5)

1.4.8 The melanocortin-5-receptor

The final mammalian melanocortin receptor cloned, MC5R, has the widest expression profile, albeit at a low level. It was initially identified in an array of peripheral tissues including muscle, gonads, spleen, brain, skin, liver, lung, pituitary and adrenal tissue (Labbe *et al.*, 1994). MC5R can be potently agonised by αMSH, ACTH and βMSH, and its extensive expression in the organs of the immune system suggested it could have a role in mediating the recognised anti-inflammatory action of melanocortins (Martin *et al.*, 1991). However, *Mc5r*$^{-/-}$ mice have a normal immuno-modulatory phenotype and seem normal in behaviour, mass and appearance. They do, however, have a severe defect in water repulsion and thermoregulation due to a reduction of sebaceous lipid production. Mouse Mc5r was subsequently shown to have high expression levels in multiple exocrine tissues including the Harderian, lacrimal and sebaceous glands, implicating it as a mediator of the exocrine function of melanocortin peptides (Chen *et al.*, 1997). It should be noted, however, that this phenotype has not been recognised in humans. Furthermore, in a study of patients with dermatological conditions there was no evidence of a causative role for MC5R in human sebaceous gland dysfunction, despite being expressed there (Thiboutot *et al.*, 2000). While population studies identified the same five human *MC5R* sequence variants in various ethnic groups (suggesting they are old in evolutionary terms) the dermatological phenotype of each variant was indistinguishable (Hatta *et al.*, 2001).

Since the identification of the first melanocortin receptor 11 years ago, considerable advances have made in understanding the nuances of melanocortin signalling. In some systems with tissue restricted pathways, such as the regulation of melanogenesis or steroidogenesis, the molecular biology of melanocortin signalling is now relatively well understood. Other signalling pathways, such as those mediated by MC5R, may regulate multiple intracellular processes with subtle effects in many different tissues. However, the diverse array of biological systems regulated by melanocortin receptors is perhaps best illustrated by the remarkable phenotype of two individuals with mutations in the *POMC* gene. Both probands suffer from early-onset obesity, adrenal insufficiency and have strikingly red hair due to the disruption of melanocortin signalling via MC4R/MC3R, MC2R and MC1R respectively (Krude *et al.*, 1998). Unfortunately the

exocrine secretions of the two patients were not analysed, so the potential consequences of a disruption in MC5R mediated signalling is unknown.

1.5 Melanin-concentrating hormone signalling

1.5.1 Melanin-concentrating hormone

Melanin-concentrating hormone (MCH), initially designated melanophore-concentrating hormone, was first identified as a brain derived factor mediating colour lightening in catfish (Enami, 1955). This discovery confirmed many years of speculation that such a factor existed, antagonising the action of MSH (Hogben and Slome, 1931; Waring, 1963). The protein was eventually characterised as a cyclic 17 amino acid peptide refined from a prohormone produced in the pituitaries of chum salmon, then released into circulation (Kawauchi *et al.*, 1983). It is now known that MCH lightens the appearance of fish by stimulating the aggregation of melanosomes in both dermal and epidermal melanophores (Baker *et al.*, 1986). Therefore in teleosts at least, melanosome translocation (and subsequently colour change) is under the bihumoral control of MCH and MSH (Baker, 1988).

Several years after its discovery in fish, MCH was isolated from the mammalian brain (Vaughan *et al.*, 1989; Nahon *et al.*, 1989) and the human, rat and salmon proMCH (*PMCH*) genes were cloned (Takayama *et al.*, 1989; Presse *et al.*, 1990; Thompson and Watson, 1990). This revealed that other peptide products are cleaved from the MCH prohormone (Fig 1.5.1), however, the function of these are currently unknown. In addition, two further mRNA products from the mammalian *PMCH* locus have been isolated. One, called *MGOP* (MCH gene overprinted polypeptide), codes in an alternate reading frame and the other, termed *AROM* (antisense RNA overlapping MCH), is in the antisense orientation. Again, these are yet to have a specific function assigned to them (Toumaniantz *et al.*, 1996; Borsu *et al.*, 2000).

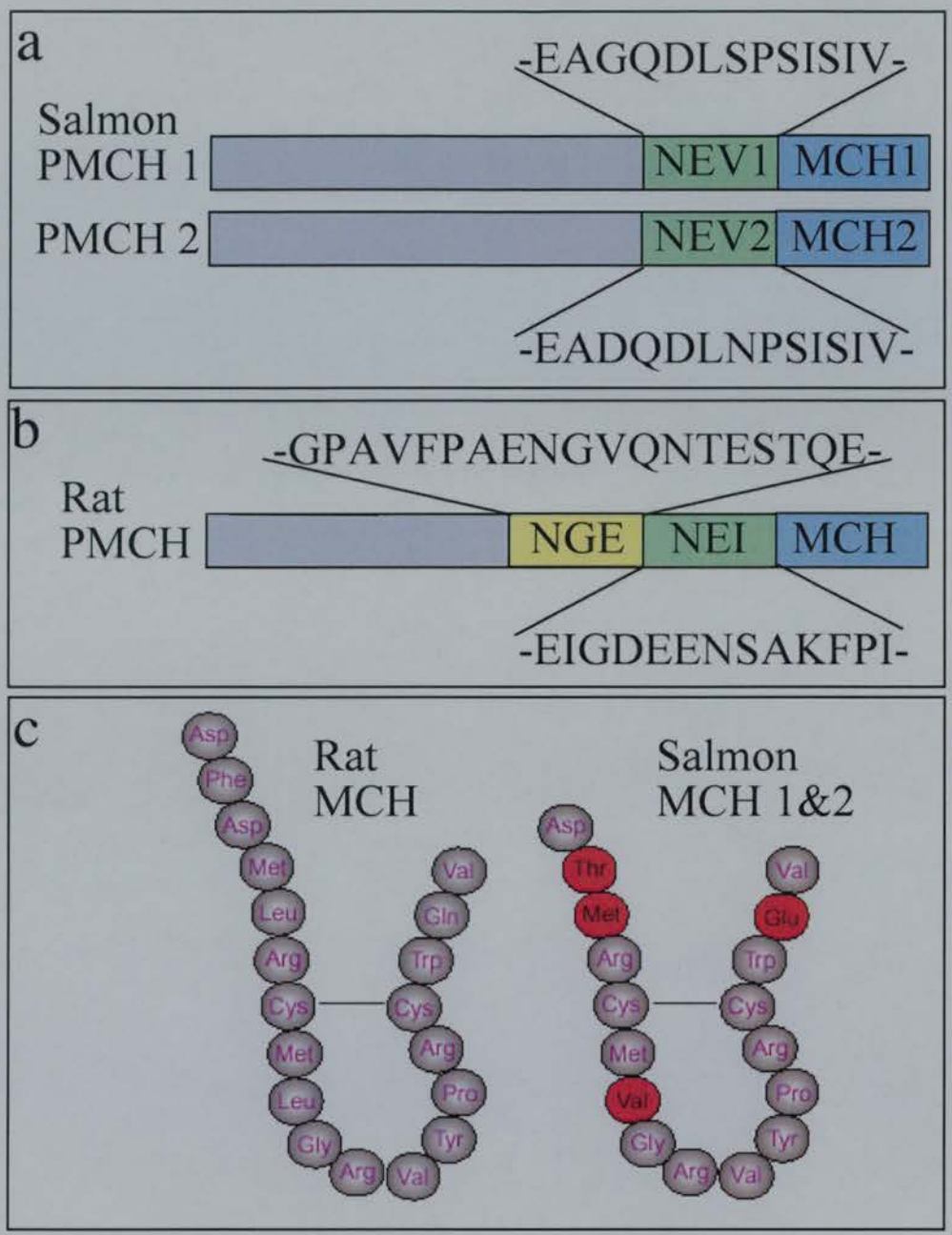

Figure 1.5.1. The structure and sequence of pro melanin-concentrating hormone. a, Salmon has two PMCH genes due to a recent genome duplication. Both contain regions encoding identical MCH peptides and another peptide named NEV after the first and last amino acid in the sequence. **b**, mammals have a single PMCH gene encoding MCH plus two other peptides, NGE and NEI. **c**, a schematic representation of rat and salmon MCH peptides. The residues that differ in salmon MCH are coloured *red*, in addition salmon lack two further amino acids at the N-terminus. The conserved cysteine bond is indicated. Figure modified from (Pissios and Maratos-Flier, 2003).

In contrast to fish, mammalian MCH is not synthesised in the pituitary, instead it is expressed in neurons of the lateral hypothalamus and zona incerta. These areas are thought to control drinking and ingestion in addition to some aspects of emotional arousal. However a specific role for MCH in these behaviours was unclear until *Pmch* was observed to be upregulated in obese leptin deficient (*ob/ob*) mice, suggesting the protein may play a direct role in regulating appetite (Qu *et al.*, 1996). This was later confirmed when direct infusion or over-expression of MCH resulted in hyperphagia in rodents (Rossi *et al.*, 1997; Ludwig *et al.*, 2001) and *Pmch* knockout mice became hypophagic and lean (Shimada *et al.*, 1998). Therefore the orexigenic impact of MCH in the mammalian brain is clearly antagonistic to the effect of melanocortins on MC3R/MC4R (Fig. 1.5.2). *Pmch* expression has recently been reported in some peripheral tissues, including the skin and immune cells (Hoogduijn *et al.*, 2002; Verlaet *et al.*, 2002). Despite this, and in contrast to its function in teleost fish, *in vivo* modulation of mouse MCH appears to have no effect on pigmentation, suggesting that MCH is not a functional antagonist of melanocortin action on melanocytes.

1.5.2 Melanin-concentrating hormone receptors

As the studies described in this thesis commenced, a high affinity receptor for MCH was described in the literature. Several researchers independently reported that SLC-1 (a Class-A orphan G-protein coupled receptor) is activated by sub-nanomolar levels of MCH *in vitro*. Moreover, it was demonstrated that this receptor, since renamed MCHR1, is expressed in the same brain regions (Chambers *et al.*, 1999; Saito *et al.*, 1999; Bachner *et al.*, 1999; Lembo *et al.*, 1999) and peripheral tissues as MCH (Hoogduijn *et al.*, 2002; Verlaet *et al.*, 2002). Later work revealed that activated MCHR1 decreases intracellular cAMP levels by association with a G_i-protein, although when expressed in heterologous cell lines the receptor is also capable of influencing other pathways via G_o and G_q (Hawes *et al.*, 2000).

Recently, *Mchr1* null mice were generated and, as one might expect, they exhibit a decreased fat mass. Somewhat surprisingly, though, they also appear to be hyperphagic, with their leanness due to hyperactivity and altered metabolism (Marsh *et al.*, 2002;

Chen *et al.*, 2002). The discrepancy between the transgenic *Mchr1*$^{-/-}$ and *Pmch*$^{-/-}$ phenotypes is not yet fully understood, however these data do suggest MCHR1 has a role in diet induced obesity and thus makes it an attractive target for drug treatment (Fig. 1.5.2) (Borowsky *et al.*, 2002).

Using the MCHR1 protein sequence as a template for database searches, numerous research groups identified SLT-1, another orphan G-protein coupled receptor, as a second high affinity MCH receptor (now renamed MCHR2). However, unlike MCHR1, this receptor cannot decrease cAMP levels by inhibiting adenylate cyclase, instead it couples with G_q exclusively, resulting in inositol phosphate turnover and the release of intracellular calcium (An *et al.*, 2001; Sailer *et al.*, 2001; Rodriguez *et al.*, 2001; Mori *et al.*, 2001; Wang *et al.*, 2001; Hill *et al.*, 2001). MCHR2 is expressed in the brain in an overlapping pattern to MCHR1, with strong expression reported in the frontal cortex and the amygdala (An *et al.*, 2001; Sailer *et al.*, 2001). It has also been detected in some peripheral tissues namely the intestine, adipocytes and prostate (Hill *et al.*, 2001). Interestingly, a gene encoding MCHR2 is not present in rodents (Tan *et al.*, 2002), therefore this receptor cannot be responsible for the different phenotype observed in *Mchr1* and *Pmch* null mice. Although the distribution of MCHR2 in the human brain suggests it may have a similar physiological role as MCHR1 (Pissios and Maratos-Flier, 2003), without an appropriate animal model a more detailed investigation into its function will be difficult.

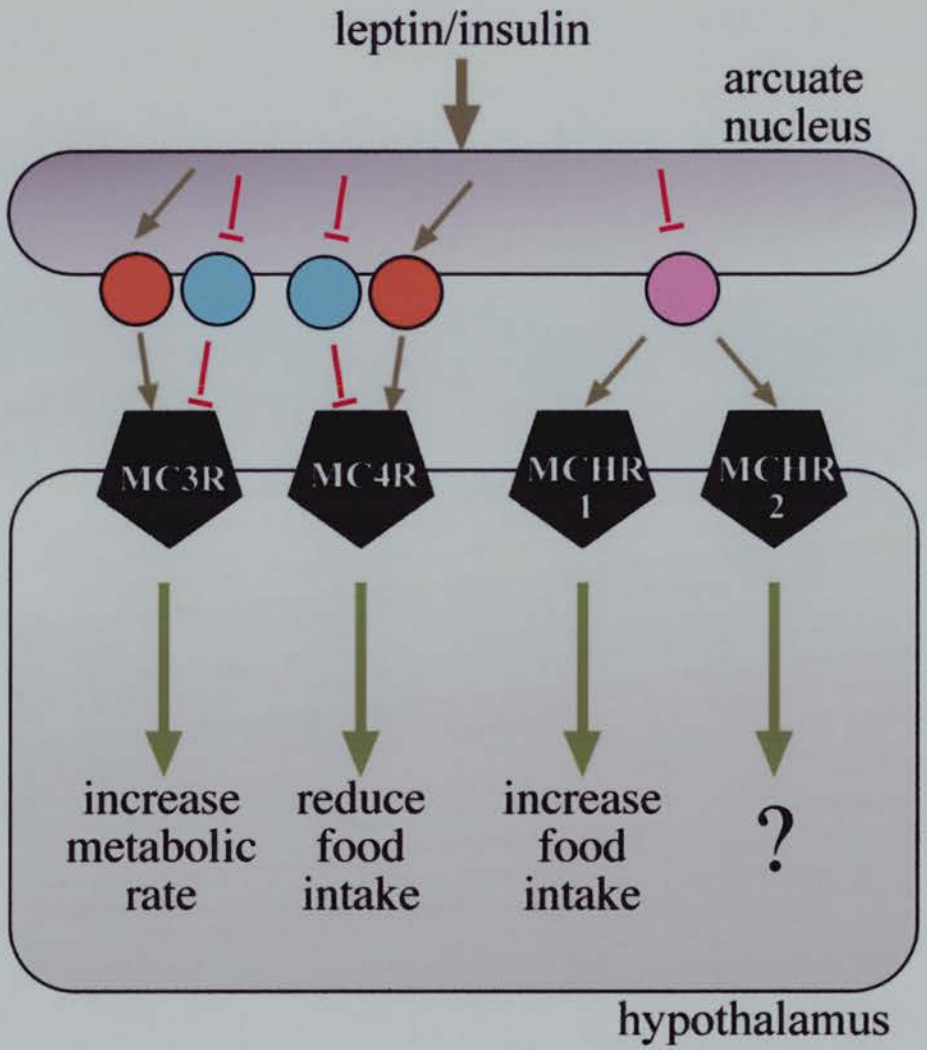

Figure 1.5.2. The antagonistic effects of melanocortins and MCH on appetite regulation. A schematic representation of the melanocortin and MCH signalling system in the human brain. When body fat is at an appropriate level, circulating leptin and insulin are produced. In the brain these activate receptors on neurons in the arcuate nucleus. Through a cascade of intermediate signalling molecules, melanocortin (*orange* circles) production is promoted and AGRP (*blue* circles) production is supressed. Melanocortins then activate MC3R and MC4R on hypothalamic neurons. This stimulates, through an unknown mechanism, a signalling cascade resulting in a reduction in food intake and an increase in metabolism. Furthermore, leptin/insulin also supresses MCH (*pink* circles) expression. When leptin and insulin are reduced in the starved state, melanocortin signalling is inhibited by increased AGRP expression and MCH promotes increased food intake via MCHR1. The downstream effects of MCHR2 are currently unknown.

Chapter 2

The Melanocortin and MCH Receptor System in Teleost Fish

We must however acknowledge, as it seems to me, that man with all his noble qualities, still bears in his bodily frame the indelible stamp of his lowly origin.

Charles Darwin
Closing words, Descent of Man.

2.1 Preface

Although the melanocortin and melanin-concentrating hormones were first identified in cold-blooded vertebrate species (Allen, 1916; Smith, 1916; Enami, 1955), the focus of the resulting body of research has been firmly on their function in a mammalian context. A range of physiological processes mediated by melanocortins, via their high-affinity receptors, was uncovered initially in mouse models (Robbins *et al.*, 1993; Huszar *et al.*, 1997; Chen *et al.*, 1997; Chen *et al.*, 2000). Subsequent analysis identified orthologous genes with comparable functions in humans and, in the case of MC1R, a large number of other mammalian and avian species (Valverde *et al.*, 1995; Jackson, 1997; Yeo *et al.*, 1998; Vaisse *et al.*, 2000). Indeed, the importance of melanocortins in human pigmentation, energy homeostasis and sexual function has very much focussed attention on potential clinical and cosmetic benefits synthetic analogues may have (Dorr *et al.*, 1996; Molinoff *et al.*, 2003). Melanin-concentrating hormone receptors, too, were first identified in mammals (Chambers *et al.*, 1999; Saito *et al.*, 1999; An *et al.*, 2001; Sailer *et al.*, 2001). The discovery that MCH, in comparison to melanocortins, has an antagonistic effect on appetite in animal models (Shimada *et al.*, 1998; Ludwig *et al.*, 1998) and the recent proposal that MCH may play a role in human pigmentation (Hoogduijn *et al.*, 2002) suggests a link between the two signalling systems. Remarkably, a similar mechanism was first proposed to explain colour change in amphibians over 70 years ago (Hogben and Slome, 1931).

Until recently, the popularity of the mouse as a genetic model organism has not been matched by a lower vertebrate equivalent. However, boasting a similar gene repetoire to mammals, the compact nature of the *Fugu rubripes* genome precipitated its role as model organism for studying vertebrate genomics (Brenner *et al.*, 1993). Further fish genome sequencing efforts have focussed on the closely related pufferfish, *Tetraodon nigroviridis* and the more experimentally amenable zebrafish, *Danio rerio*. When the sequencing and annotation of these genomes is complete, a resource of three closely related species (including one excellent model of vertebrate development) will exist to compare and contrast with the genomes of mammals. However, studying teleost genomes not only sheds light on the evolution of mammalian genes (Aparicio, 2000), but

can provide an alternative model for understanding the evolution of gene function in a biological context (Marshall and Singer, 2002; Marshall *et al.*, 2002). In the case of melanocortin and MCH, it will become possible to revisit early experimental discoveries armed with the knowledge of genomic content, thus providing a molecular basis to their function. Furthermore, identification of the teleost melanocortin and MCH signalling genes is a step towards finding the evolutionary origin of their role as antagonistic hormones.

This chapter details the *in silico* identification of genes involved in melanocortin and MCH signalling in teleost fish using raw genome sequencing data. It then describes a comparative analysis of each gene in terms of expression, sequence, structure and evolution.

2.2 Searching for Melanocortin Receptor Genes

2.2.1 Gene identification

In February 2001, the Sanger Centre began to sequence zebrafish DNA using a whole genome shotgun approach (http://www.sanger.ac.uk/Projects/D_rerio/). These data were regularly deposited in a trace repository (http://trace.ensembl.org/) as single pass DNA sequencing reads, associated traces and quality values. Similar sequencing efforts were underway to sequence the pufferfish *Fugu rubripes* and *Tetraodon nigroviridis*. The DNA sequence reads at the repository were in a format allowing searches by SSAHA (Sequence Search and Alignment by Hashing Algorithm) (Ning *et al.*, 2001), however this could only be carried out at the DNA level. Attempts to align mammalian and avian melanocortin and DNA sequences with trace reads proved unsuccessful, this was because the orthologous sequences are too diverse at the DNA level for alignment to occur. However, it was possible that there may simply have been no melanocortin receptor genes sequenced at that time.

An alignment of the DNA sequence from all cloned mammalian and avian melanocortin receptors revealed short regions of conservation in the transmembrane domains, therefore PCR primers based on these sequences were designed and PCR reactions on

zebrafish and *Fugu* DNA carried out. These failed to amplify fragments of melanocortin receptors despite modulation of PCR conditions. An amplified fragment of chicken MC1R DNA (equivalent to nucleotides 365-573 of Genbank accession: AY220303) was then used to probe a zebrafish late somitogenesis cDNA library (cDNA filters: 39.1.230, 39.2.135 and 39.3.128 from RZPD, Berlin, Germany). The probe showed weak hybridisation to a single, correctly duplicated colony pattern (clone ICRF p524E1213Q10, filter: 39.1.230). This clone was sequenced and contained a 489bp insert that was identical to the zebrafish stem cell leukemia gene (*scl*). On analysis, this sequence showed 92% identity to a short stretch of probe DNA sequence, which may explain the weak hybridisation.

At this point, Dr. Martin Taylor generated indexed databases containing all the sequences generated from genome trace reads found at the trace repository (Project-BLAST). The databases are actively curated, regularly updated and are built in a manner that allows sequences to be rapidly retrieved (Table 2.2.1). Furthermore, the format of the databases means that they are accessible to the BLAST suite of programmes; permitting trace sequences to be translated in all frames and compared to any protein sequence (TBLASTN).

Table 2.2.1. Project-BLAST databases used to identify genes *in silico*. "Nightly" indicates new sequences were added each evening, otherwise updates occurred on the occasion of a new release. Modified from Project-Blast web-page, created by Dr. Martin Taylor (http://longrow.hgu.mrc.ac.uk/genecore/res_blast.html)

Database	Description	Version
Cs_wgs	*Ciona savignyi* whole genome shotgun sequences	1.0
Dr_wgs	*Danio rerio* whole genome shotgun sequences	Nightly
Fr_asm	*Fugu rubripes* whole genome shotgun assembly	1.0
Fr_wgs	*Fugu rubripes* whole genome shotgun sequences	1.0
Tn_wgs	*Tetraodon nigroviridis* whole genome shotgun sequences	1.0

This search method identified trace sequences that contained open reading frames with significant stretches of identity to melanocortin receptors at the protein level. When these matching sequences were compared at the DNA level there were few stretches of

significant homology, confirming the need for translation before searching. When the matching translated trace sequences were used to search back against a mammalian protein database they consistently showed the highest match to melanocortin receptors, suggesting the reciprocal best matches in each dataset (at that time) had been identified. It was now possible to search with trace sequence databases at the DNA level, using potential teleost melanocortin receptor fragments identified from the TBLASTN search in an attempt to extend the boundaries of the known sequence. When an overlapping match was identified, it was assembled to make an extended contiguous sequence then translated and compared with its mammalian match (see Chapter 5.4.2 for method). Then the process was repeated to further extend the contiguous sequence. Such iterative BLAST searching was continued until each contiguous sequence identified no more extending matches in each database. Zebedee, a programme by Drs. Colin Semple and Robert Bryson-Richardson, was written to repeat this process on a daily basis as more sequence traces were added to the databases. Once full open reading frames were identified, the assembled DNA sequences were confirmed by PCR and resequencing (see Table 5.1.2 for primers).

2.2.2 The teleost melanocortin receptor gene repertoire

By analysis of sequence traces, six complete melanocortin receptor genes in zebrafish and four each in *Fugu* and *Tetraodon* were identified. Phylogenetic analysis confirms four *Tetraodon* and *Fugu* genes are clearly orthologous and have a very highly conserved amino-acid sequence, as one might expect from pufferfish only 20-30 Mya distant (Crnogorac-Jurcevic *et al.*, 1997). Therefore, in the interest of clarity and because it has been more widely studied, *Fugu* will be the major focus in the following discussion. By direct comparison of the conceptual translations, the high degree of amino acid identity between individual fish and human receptors suggested orthology (Table 2.2.2). However, in order to understand the evolutionary relationship of these genes, the phylogeny of the proteins was examined. A neighbour-joining tree summarising the phylogenetic relationship of zebrafish and *Fugu* receptors along with the five receptors from human, mouse, and chicken was generated (Fig. 2.2.1). There is high bootstrap support for the grouping of fish genes into five separate clades, each containing a single mammalian receptor subtype.

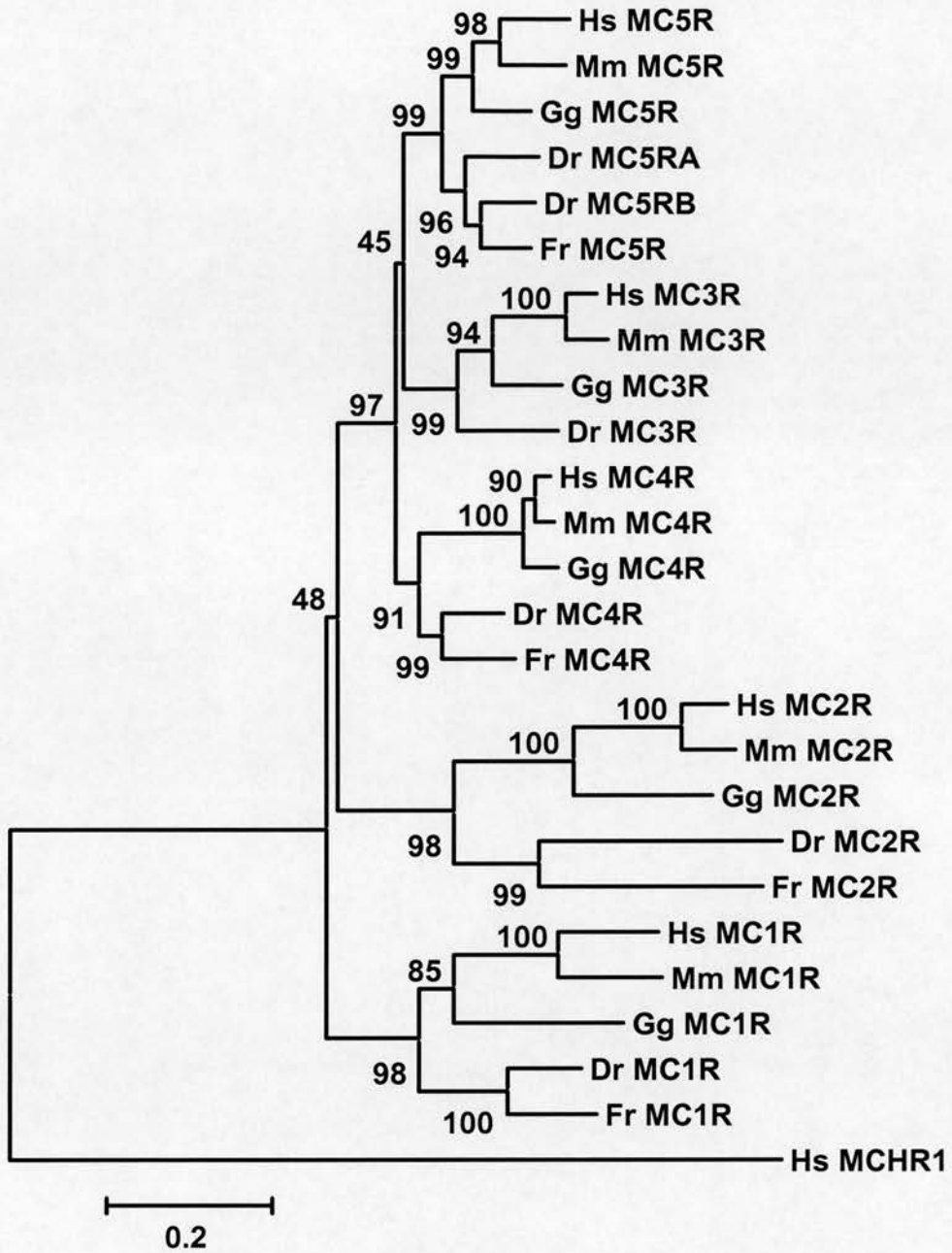

Figure 2.2.1. Phylogeny of melanocortin receptor protein sequences. Proteins from human (Hs), mouse (Mm), chicken (Gg), zebrafish (Dr) and *Fugu* (Fr) are included. The tree uses a Poisson correction distance between the two sequences where the proportion of amino acid sites at which the two differ is corrected for multiple substitutions at the same site. Thus, the distance is equal to –ln(1-p), where p is the proportion of sites that differ. The number at each branch is the percentage of bootstrap replicates of the node from 1000 repetitions. The phylogeny is based on a 360aa alignment with gapped sites removed. The tree is rooted against human melanin-concentrating hormone receptor 1 (Hs MCHR1).

Indeed the only branch points without high statistical support are where MC1R splits from the rest of the gene family and where MC3R and MC5R split after diverging from MC4R. If these nodes are discounted, then it appears that the original melanocortin receptor gene may have split into three members initially, forming the ancestors of MC1R, MC2R and a single ancestor for the rest of the family. This single ancestor may then have split into three, which became MC3R, MC4R and MC5R. However, this phylogeny strongly suggests all five melanocortin receptor genes were established prior to the divergence of tetrapod and teleost lineages, over 450 Mya.

Each mammalian melanocortin receptor subtype has a single orthologue in each teleost with two exceptions. The clade containing MC5R proteins contains two zebrafish sequences (termed mc5ra and mc5rb). These sequences appear to represent a recently duplicated pair of receptors in the fish lineage, yet only one *MC5R* gene in *Fugu* was identified. At the time of analysis the coverage afforded by the available sequence data was estimated to be 5.6x (Aparicio *et al.*, 2002), giving a >95% chance of a read containing the sequence.

Table 2.2.2. Protein sequence identities of melanocortin receptors. Human (Hs) full-length sequences are compared with zebrafish (Dr) and *Fugu* (Fr) sequences. The highest human match to each fish gene, suggesting orthology, is indicated by a shaded box. The values are percent identity of aligned proteins.

	Hs MC1R	Hs MC2R	Hs MC3R	Hs MC4R	Hs MC5R
Dr MC1R	53.7	40.3	43.9	50.4	50.1
Dr MC2R	36.9	45.5	36.9	41.4	39.1
Dr MC3R	48.6	42.5	63.5	58.1	61.8
Dr MC4R	48.2	44.4	55.1	68.7	62.8
Dr MC5RA	45.2	43.3	55.4	62.8	69.0
Dr MC5RB	45.4	44.3	54.1	61.9	69.5
Fr MC1R	53.0	39.9	42.5	47.7	46.5
Fr MC2R	38.0	46.6	35.3	42.0	38.8
Fr MC4R	49.5	46.0	57.7	65.2	62.2
Fr MC5R	44.3	42.4	52.4	62.9	67.7

Furthermore, the dataset consisting of 6x coverage of DNA sequence from *Tetraodon nigroviridis* also contained sequence from only a single *MC5R* gene. Therefore the probability that these combined databases lacked a second pufferfish *MC5R* gene by chance was less than 0.002. The *Fugu* genome sequence has since undergone numerous rounds of assembly and annotation (these are available to view online at www.ensembl.org/Fugu_rubripes/). TBLASTN analysis with both zebrafish mc5r protein sequences continues to identify only one *MC5R* gene in the *Fugu* genome up to, and including, Ensembl release v15.2.1 (2 July 2003). It is highly likely therefore that only one *MC5R* gene is present in the *Fugu* lineage. Both zebrafish and *Fugu* contain single orthologues of *MC1R*, *MC2R* and *MC4R* (Fig. 2.2.1). *MC3R* however, appears to be absent from *Fugu*. Again, consideration was given to the depth of sequence coverage of the *Fugu* data, but combined with the absence of any *MC3R* gene sequences in the *Tetraodon* sequence trace database, it seems likely that pufferfish have lost the *MC3R* gene. This too is confirmed by the absence of an *MC3R* gene in subsequent *Fugu* genome annotated assemblies.

2.2.3 Can melanocortin receptors be identified in more distant species?

The successful identification of melanocortin receptors *in silico* inspired the search for similar genes in organisms even more divergent from mammals. The class chondrichthyes contains cartilaginous fish such as sharks, rays and chimaeras which diverged from the bony vertebrates over 520 Mya. However, these do not make good genomic model organisms, as they have a mean genome size five times larger than teleosts (Gregory, 2001). Subsequently there is very little gene sequence data publicly available from these species and no concerted effort to sequence the entire genome.

More distant to tetrapods are the ascidians, *Ciona savignyi and Ciona intestinalis*. As tunicates they diverged from chordates just before many of the large-scale gene duplications that occurred in the lineage, yet they have a comparable cell fate and body plan (Satoh and Jeffery, 1995). Ascidians are therefore excellent models to use when attempting to identify the expansion of vertebrate specific genes and gene families (Corbo *et al.*, 2001). At the time this work commenced, the Whitehead Institute Centre for Genome Research had generated whole genome shotgun reads totalling

approximately 14x from a single, heterozygous diploid *C. savigny* individual. Dr Martin Taylor indexed a project-BLAST database containing these reads and a TBLASTN search for melanocortin receptors gene was carried out. Despite such extensive genome coverage, no high similarity matches were identified that matched back against melanocortin receptor genes in a reciprocal search. On the release of the first genome assembly (available at http://www-genome.wi.mit.edu/annotation/ciona/index.html), a second search with melanocortin receptors was carried; again no melanocortin receptor genes were identified. It therefore appears the melanocortin receptor subfamily may be vertebrate specific. To investigate whether melanocortin receptors exist in protostome invertebrates, TBLASTN searches were carried out on the completely sequenced genomes of *Drosophila melanogastor* and *Caenorhabditis elegans* (C.elegans Sequencing Consortium, 1998; Adams *et al.*, 2000). Once again, no orthologous melanocortin receptor sequences were identified.

2.3 Characterising teleost melanocortin receptor genes

2.3.1 The melanocortin 1 receptor.

Figure 2.3.1 shows the protein sequences of MC1R from human, mouse, chicken, *Fugu* and zebrafish. The highest level of conservation is in the transmembrane domains with the N-terminus showing the most variation. As the melanocortin receptor responsible for variation in pigmentation, a good deal of information is known about the effects of both natural and site directed mutations in MC1R (Valverde *et al.*, 1995; Frandberg *et al.*, 1998; Healy *et al.*, 2000; Sturm *et al.*, 2001). Almost all the amino acid residues known to be important from these mutations are conserved in the fish MC1R sequences. One major difference is in the third intracellular loop. Replacement of certain residues in this loop, between amino acids 226 and 238, with an alanine residue result in the loss of coupling of the human receptor to G-proteins (Frandberg *et al.*, 1998).

Figure 2.3.1 (overpage). Alignment of MC1R amino acid sequences. Proteins from human (Hs), mouse (Mm), chicken (Gg), *Fugu* (Fr) and zebrafish (Dr) are represented. Amino acids identical in all sequences are shaded *black*, those different in one species are *dark gray*, and those different in two species are *light gray*.

Figure 2.3.1. See previous page for legend.

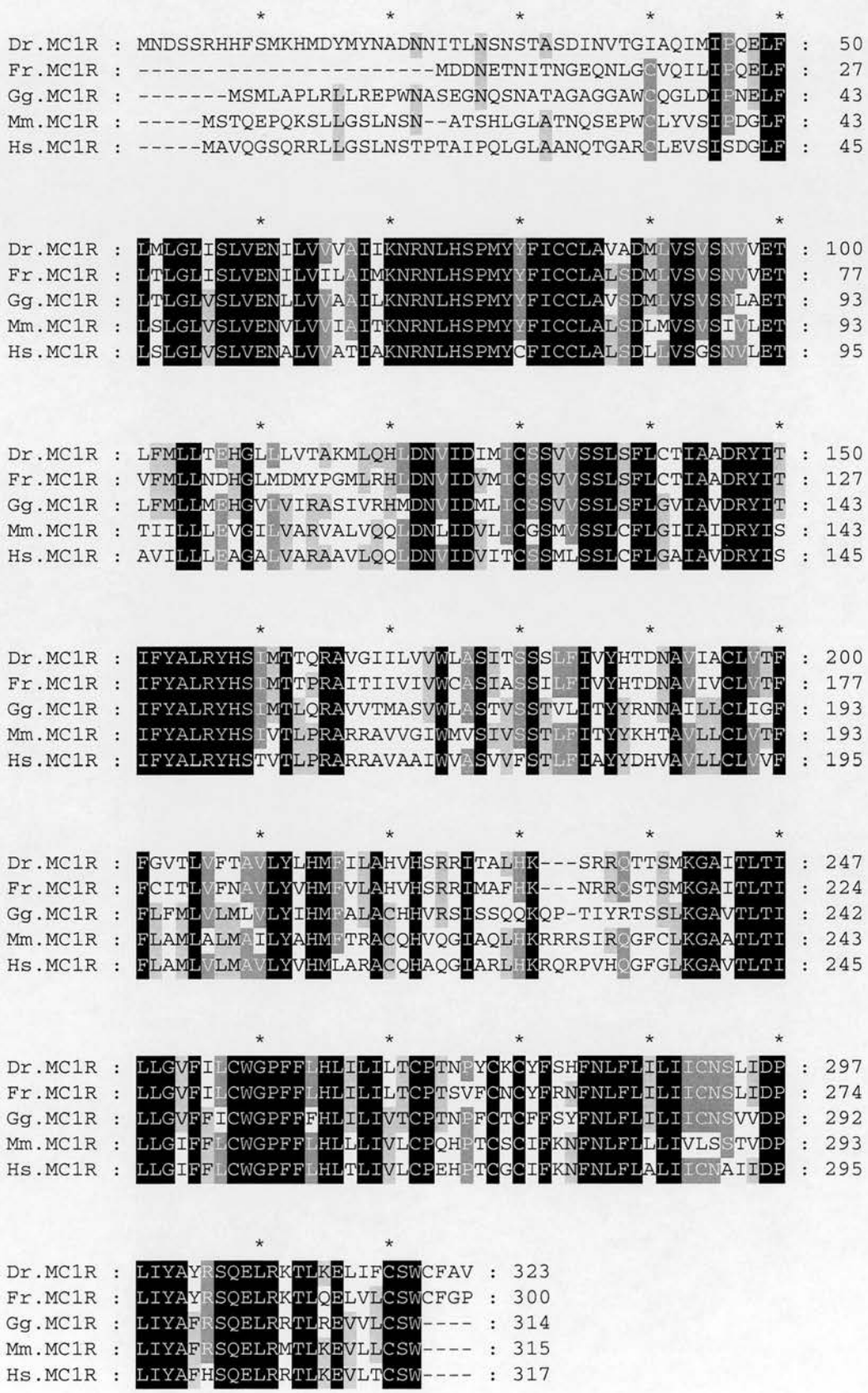

The region containing these important residues is not well conserved in fish. It is three amino acids shorter than the mammalian receptor, and although K226 and K238 flanking the domain are conserved in the fish MC1R, the intervening amino acids are quite different. The sequence is, however, very basic in charge, similar to the region in humans (and the poorly conserved mouse region). It will be informative to determine whether specific amino acid residues are required for coupling, or whether it is the basic nature that is important.

Another difference between the fish and most other MC1R proteins is at the C-terminus. Most GPCRs have a cysteine residue in the intracellular, C-terminal tail. This has been shown to be modified by palmitoylation, and to be essential for function in some receptors (Morello and Bouvier, 1996). Previously described MC1R proteins contain the C-terminal tripeptide motif CSW, and truncation of the C-terminal 13 amino acids of MC1R in dog appears to cause loss of receptor function (Newton *et al.*, 2000). Although both zebrafish and *Fugu* MC1R proteins have the CSW motif, it is not directly at the end of the protein. Both have an additional four residues, including another cysteine residue, which may be an alternative target for palmitoylation

Despite strong phylogenetic evidence that the fish sequence termed MC1R really is an orthologue of its mammalian counterpart, a stronger case could be made if a syntenic relationship could be established. Therefore the location of zebrafish *mc1r* was determined by analysis of radiation hybrids (Hukriede *et al.*, 1999). The gene was successfully mapped to linkage group (LG) 18, 318cR (LOD = 22.2). This places the gene very close to zebrafish cytochrome oxidase subunit 4 (*cox4*) and distal of tyrosine aminotransferase (*tat*). Analysis of human and mouse genome assemblies, revealed orthologous genes are found in the same order within a 20Mb region on human chromosome 16 and mouse chromosome 8 (Fig. 2.3.1). This hints at physical linkage between these genes in an ancestor of zebrafish and mammals and thus provides strong evidence for orthology.

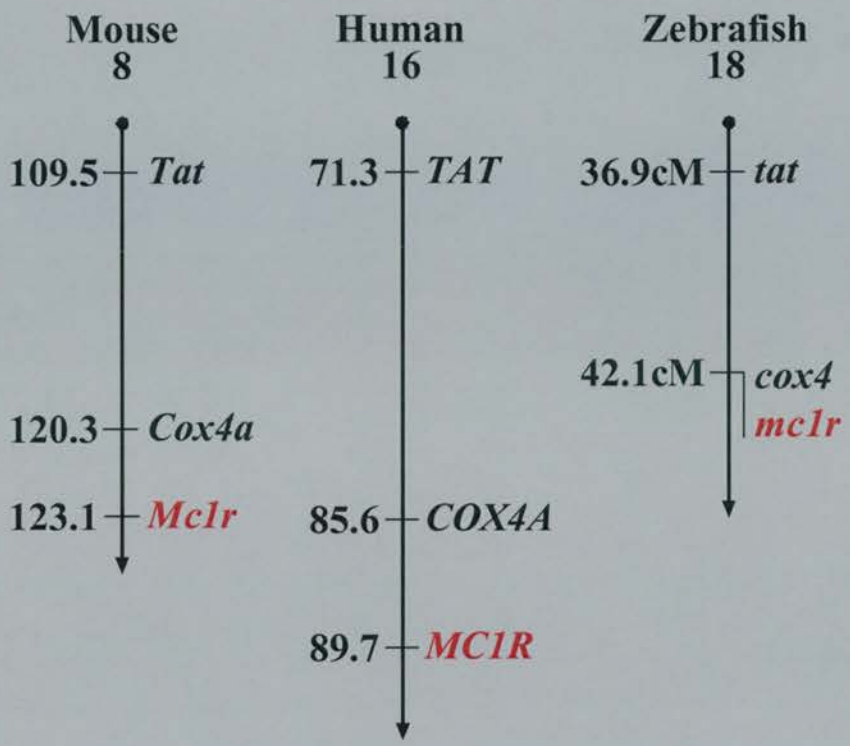

Figure 2.3.2. Conserved synteny around MC1R. Chromosome numbers from human and mouse are indicated (from Ensembl Human v15.33.1 and Mouse v15.30.1) with the relative position of each gene marked in megabases. The zebrafish linkage group is noted, with gene positions estimated from centiRay distance by radiation hybrid mapping.

In order to assess whether the zebrafish *mc1r* gene is transcribed, reverse-transcription-PCR was performed on mRNA from different stages of zebrafish development and from adults. Figure 2.3.3 shows that *mc1r* is expressed throughout larval development. It is during this period that fish melanophores differentiate and develop. In adult fish this gene has a lower apparent signal from head RNA than body. This observation is consistent with the smaller number of melanophores found in the head, although quantitative RT-PCR would be required to confirm this difference. Therefore, not only does fish MC1R have a strong phylogenetic and syntenic link to mammalian MC1R, but it has an expression pattern consistent with a role in melanophore function.

In an attempt to further detail the temporal and spatial expression pattern of zebrafish *mc1r*, a labelled RNA probe covering the first 800bp of the gene was generated for whole mount *in situ* hybridisation histochemical studies. Previous attempts at studying mouse melanocortin receptor expression by *in situ* hybridisation histochemistry have failed (Jackson, personal communication and data not shown) and no reports of successful whole mount *in situ* hybridisation histochemistry to melanocortin receptor transcripts have been published. Consistent with this, no signal in 48hpf, 72hpf and 96hpf zebrafish embryos in melanophores or elsewhere could be detected (Fig. 2.3.4), despite mRNA being detected from 48hrs by RT-PCR (Fig. 2.3.3).

Figure 2.3.3. RT-PCR assayed expression of melanocortin receptors in zebrafish. The embryo ages, tissue origin and controls (neg. = negative control, DNA = positive control) are indicated at the top of the figure with the genes denoted at either side. Zebrafish *b-actin* was used as a control for RNA quality. Zebrafish *mc2r* amplification shows a second, smaller, PCR fragment in all RNA samples. Sequencing indicates that this is a PCR artefact unrelated to *mc2r* sequence.

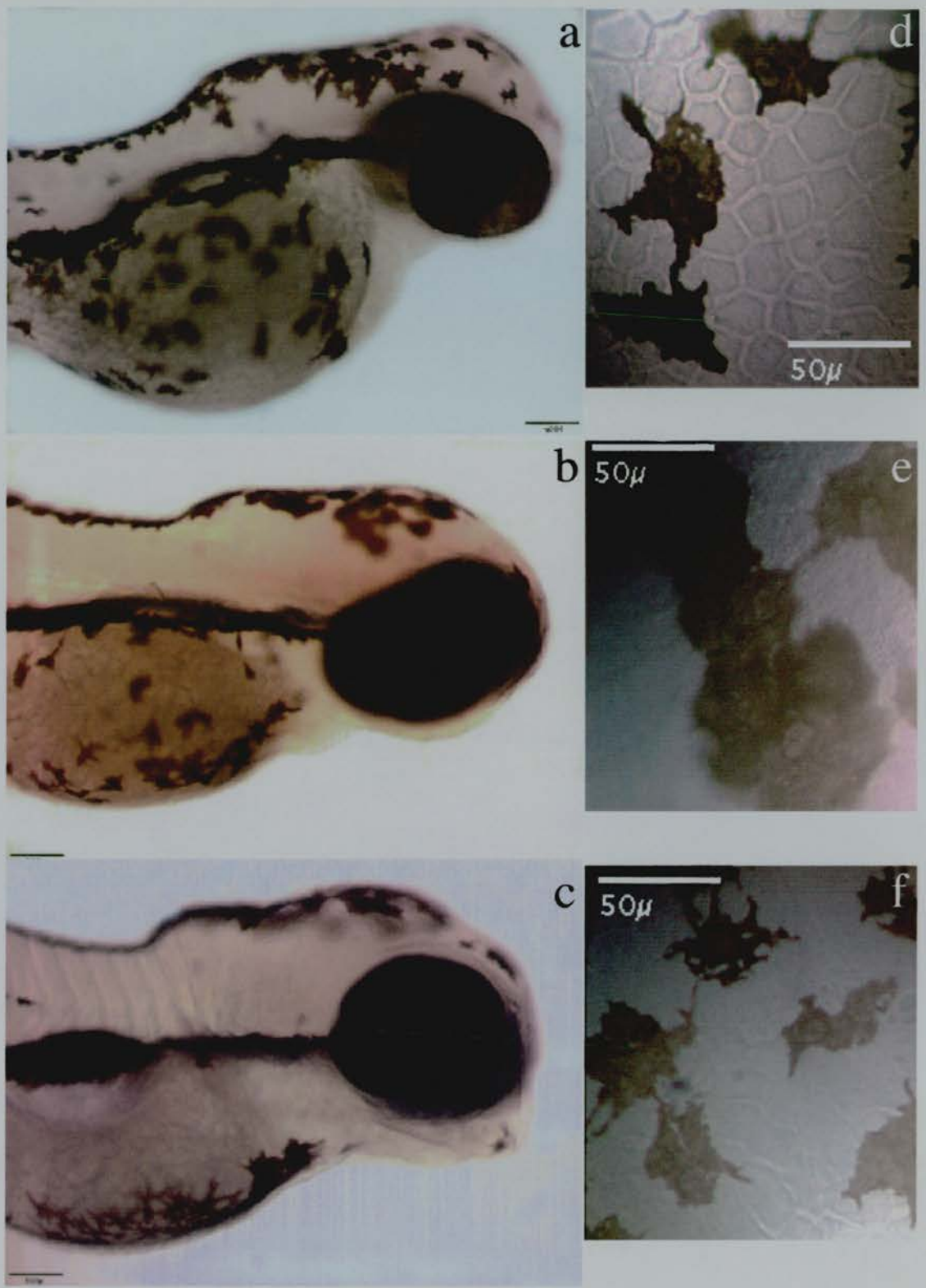

Figure 2.3.4. *mc1r* expression in zebrafish is not detected by *in situ* hybridisation. a-c, lateral view of embryos probed with *mc1r* at 48hpf (**a**), 72hhp (**b**) and 96hpf (**c**). **d-e**, melanophores from the dorsum of a 48hpf (**d**) and 96hpf (**e**) embryo probed with *mc1r* and **f**, a 48hr unprobed embryo. Scale bar: 100μm (**a-c**), 50μm (**d-f**).

2.3.2 The melanocortin 2 receptor and melanocortin 5 receptors.

Figure 2.2.1 and Table 2.2.1 show that MC2R amino acid sequences are the most divergent of all the receptors not only between fish and mammals (<50% identity), but also between *Fugu* and zebrafish (see also Fig. 2.3.10). There is no data available on the impact of specific amino acids on MC2R function in animal models, however mutations associated with human familial glucocorticoid deficiency identify important residues (Penhoat *et al.*, 2002; Fluck *et al.*, 2002). Of the seven mutated amino acids reported, all but one are conserved between fish and humans. The single difference is at human V142 located in the second intracellular loop. A Val to Leu change at that residue renders human MC2R unresponsive to ACTH, yet both fish and chicken have a methionine at that position (Fig. 2.3.5). Although a Met side chain is more similar to Leu than Val in structure and size, functional studies would be needed to assess the implications this has for MC2R signalling in fish.

In contrast to MC2R, both zebrafish mc5r sequences show the highest level of amino acid conservation between fish and mammals receptors (Table 2.2.1, Fig. 2.2.1). This is intriguing in terms of when the zebrafish *mc5r* duplication took place. The phylogenetic relationship of the zebrafish and pufferfish MC5R proteins suggests that the genes duplicated early in ray finned fish evolution, and that one of them (orthologous to zebrafish *mc5ra*) was lost in the pufferfish lineage. This duplication is therefore consistent with a hypothesis of tetraploidization in the teleost lineage (Amores *et al.*, 1998; Taylor *et al.*, 2003). However, it is possible that the duplication happened after the zebrafish/pufferfish lineages separated, and selective constraints on one of the pair may have relaxed, allowing it to rapidly diverge. Figure 2.3.6 shows the difference between zebrafish mc5r amino acid sequences in comparison with those from human, mouse and chicken. The major differences of note include an apparent insertion of an Asp codon at N230 in zebrafish mc5ra and a Cys to Phe substitution at F312 in mc5rb, altering what may be a target for palmitoylation (Qanbar and Bouvier, 2003).

Figure 2.3.5 (overpage). Alignment of MC2R amino acid sequences. Proteins from human (Hs), mouse (Mm), chicken (Gg), *Fugu* (Fr) and zebrafish (Dr) are represented. Amino acids identical in all sequences are shaded *black*, those different in one species are *dark gray*, and those different in two species are *light gray*.

Figure 2.3.5. See previous page for legend.

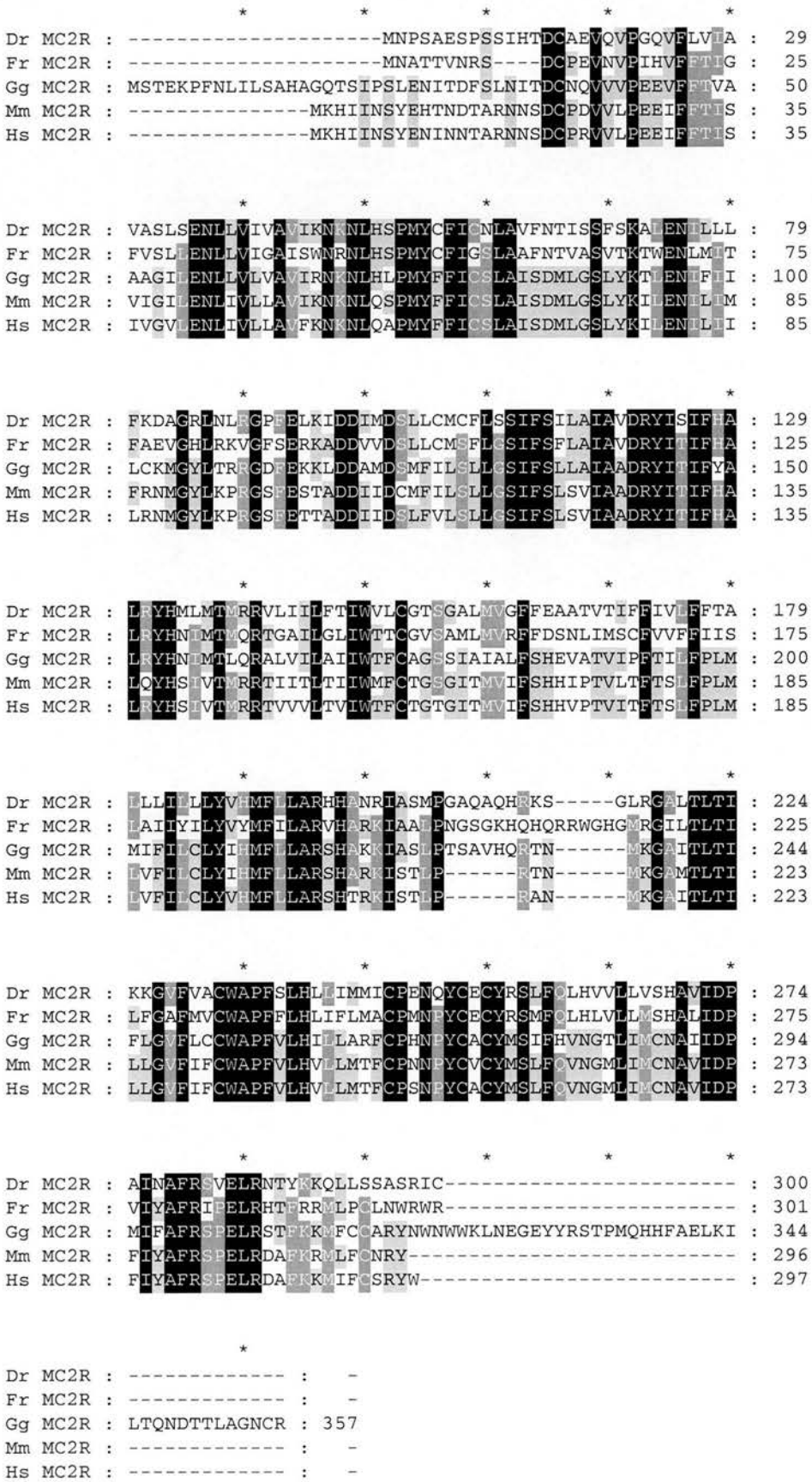

Figure 2.3.6. See following page for legend.

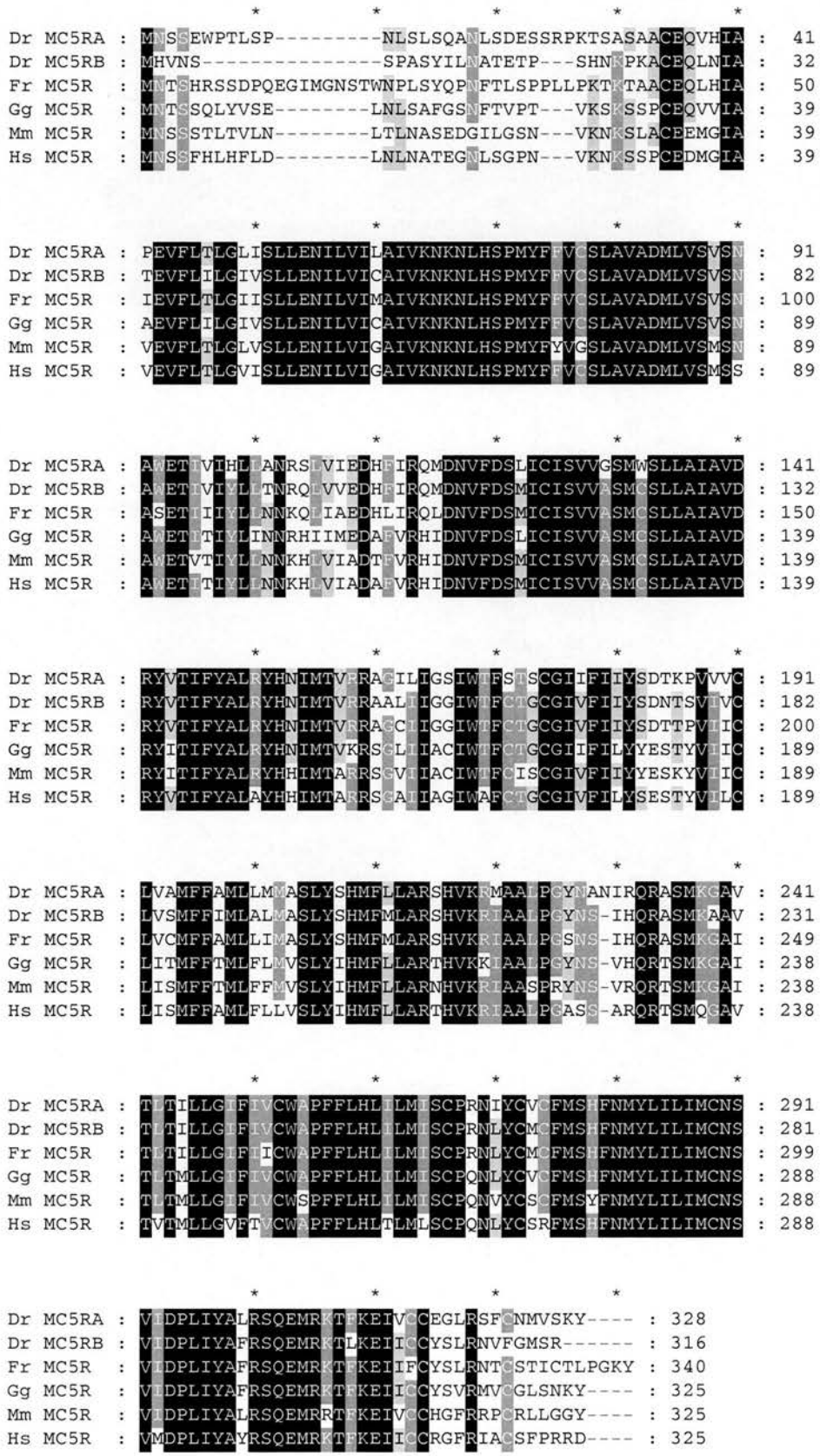

Figure 2.3.6 (previous page). Alignment of MC5R amino acid sequences. Proteins from human (Hs), mouse (Mm), chicken (Gg), *Fugu* (Fr) and zebrafish (Dr) are represented. Amino acids identical in all sequences are shaded *black*, those different in one species are *dark grey*, and those different in two species are *light grey*.

Using radiation hybrids both *mc5r* genes were mapped to zebrafish linkage groups. mc5ra maps to LG 16, 308cR (LOD = 15.7) and mc5rb to LG 19, 174.2cR (LOD = 11.5). The duplicated *mc5r* genes are both linked to genes that are also duplicated in the zebrafish genome, which have themselves a single orthologue in the mouse and in humans (Fig. 2.3.7). However, radiation hybrid mapping of zebrafish *mc2r* places it on LG 16, 313cR (LOD = 16.5), around 5cR from *mc5ra*. This gene pair has also been closely linked by genetic mapping in the mouse to chromosome 18 and by cytogenetic analysis on human chromosomes to 18p11.2 (Magenis *et al.*, 1994; Chowdhary *et al.*, 1995). It therefore appears that the duplicated chromosomal segment that contains the novel zebrafish paralogue (*mc5rb*) has subsequently lost *mc2r*. RT-PCR of mRNA transcripts shows that zebrafish *mc2r* is expressed from the fifth day of development and, like mammals where the gene is expressed in the adrenal cortex (Mountjoy *et al.*, 1992), *mc2r* transcripts are seen only in the torso and not the head of adults (Fig. 2.3.3). Both zebrafish *mc5r* genes are expressed, though in temporally different patterns. It appears that *mc5ra* is largely embryo specific; no transcript can be identified in adult head (though adult body gives a weak signal. By contrast, *mc5rb* has a robust signal in both embryonic and adult mRNA (Fig. 2.3.3).

To further investigate the conserved *MC2R/MC5R* synteny, the genome sequence assemblies for mouse and human (mouse Ensembl release v15.30.1, 6 May 2003, human Ensembl release v15.33.1, 2 July 2003) were examined. It was apparent that both mouse and human *MC2R* and *MC5R* genes are very closely linked, and are convergently transcribed from opposite DNA strands (Fig. 2.3.8). Furthermore, they are separated by a 57.9kb (human) and 67.6kb (mouse) interval that, in both cases, contains no predicted genes.

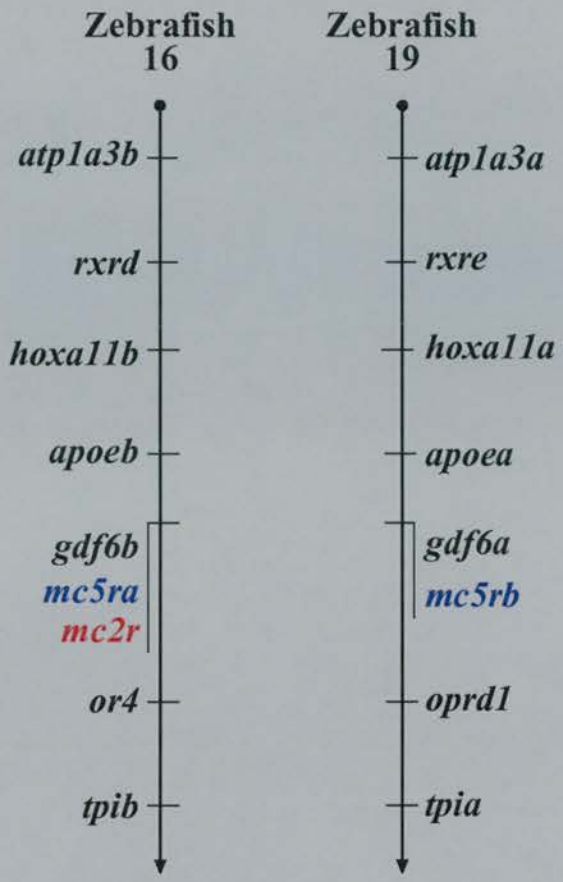

Figure 2.3.7. Paralogous genes on zebrafish LG16 and LG19. Previously reported paralogues are indicated in *black* (Taylor *et al.*, 2003). The *mc5r* duplicates (in *blue*) are found on both linkage groups. In comparison, *mc2r* (in *red*) is found only on LG16. Relative gene position taken from integrated maps at Zfin (www.zfin.org), but intergenic distances are not to scale.

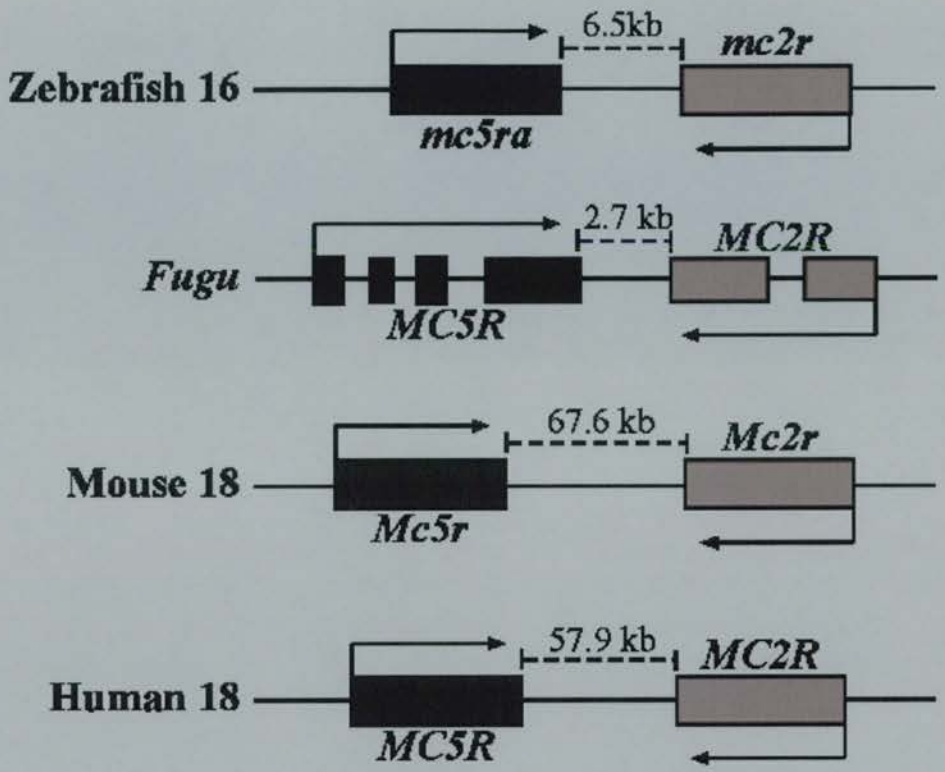

Figure 2.3.8. Linkage between *MC5R* and *MC2R* throughout vertebrate evolution. Species are indicated along with chromosome number where known. The direction of *MC5R* (*black* boxes) and *MC2R* (*grey* boxes) transcription is indicated by arrows. Each box represents a single exon, the lines between boxes of the same color indicate introns. The single intron in *Fugu MC2R* is in an identical position and phase to the third intron in *Fugu MC5R*. Intergenic distances (dashed lines) are calculated from genomic assemblies.

The genomic sequence was obtained downstream of both *Fugu MC5R* and *MC2R* using Zebedee, to find if they could be assembled into a single contiguous sequence. This revealed that in *Fugu* these genes are also convergently transcribed, and that the termination codons of the two coding regions are separated by only a few kilobases. The intergenic distance between this gene pair in *Fugu* has thus been compressed by 20-30 fold relative to mammals. The release of the second *Fugu* genome assembly and zebrafish whole genome shotgun assembly (Ensembl release v14.2.1, 3 April 2003) confirmed the *MC5R* to *MC2R* intergenic distances as 2.7kb and 6.5kb respectively (Fig 2.3.8). A comparison of the *Fugu*, zebrafish, mouse and human intergenic sequences show there are no conserved sequence elements, suggesting a lack of genes in this region (Fig. 2.3.9). The higher levels of sequence conservation between zebrafish and *Fugu* may represent regulatory elements, but there is no strong evidence for a selective pressure to maintain MC5R and MC2R linkage throughout 450 Mya of evolution. Interestingly, the conserved synteny would implicate *Fugu MC5R* as the orthologue of zebrafish *mc5ra* (Fig. 2.3.8). However, phylogentic analysis suggests otherwise (Fig 2.2.1). This can be reconciled in one of two ways. Either the phylogeny is incorrect and *Fugu* has not lost a second *MC5R* gene, or there was a duplication of the genomic segment containing both *MC5R* and *MC2R* in teleosts and one syntenic gene pair was maintained in zebrafish while the other was kept in *Fugu*.

None of the full-length melanocortin receptor genes thus far reported, of which there are over 40, have introns in the coding region (with the possible exception of a spliced variant of human *MC1R* that is of unknown significance (Tan *et al.*, 1999)). However, it is clear that both *Fugu MC2R* and *MC5R*, do contain introns. The *MC5R* gene contains three introns in the coding region: situated after amino acid E52 and interrupting S88 and R151 (Fig. 2.3.6). *Fugu MC2R* contains only one intron, interrupting R118. However, this intron is in an identical position and phase relative to the third *MC5R* intron, as both interrupt the invariant Arg of the DRY motif in phase two (Fig. 2.3.5 and 2.3.6). Analysis of the orthologous *Tetraodon* genes showed an identical gene structure. In all cases each exon/intron boundary is defined by the appropriate consensus sequences and consecutive exons are in phase, suggesting this predicted gene structure is the correct one.

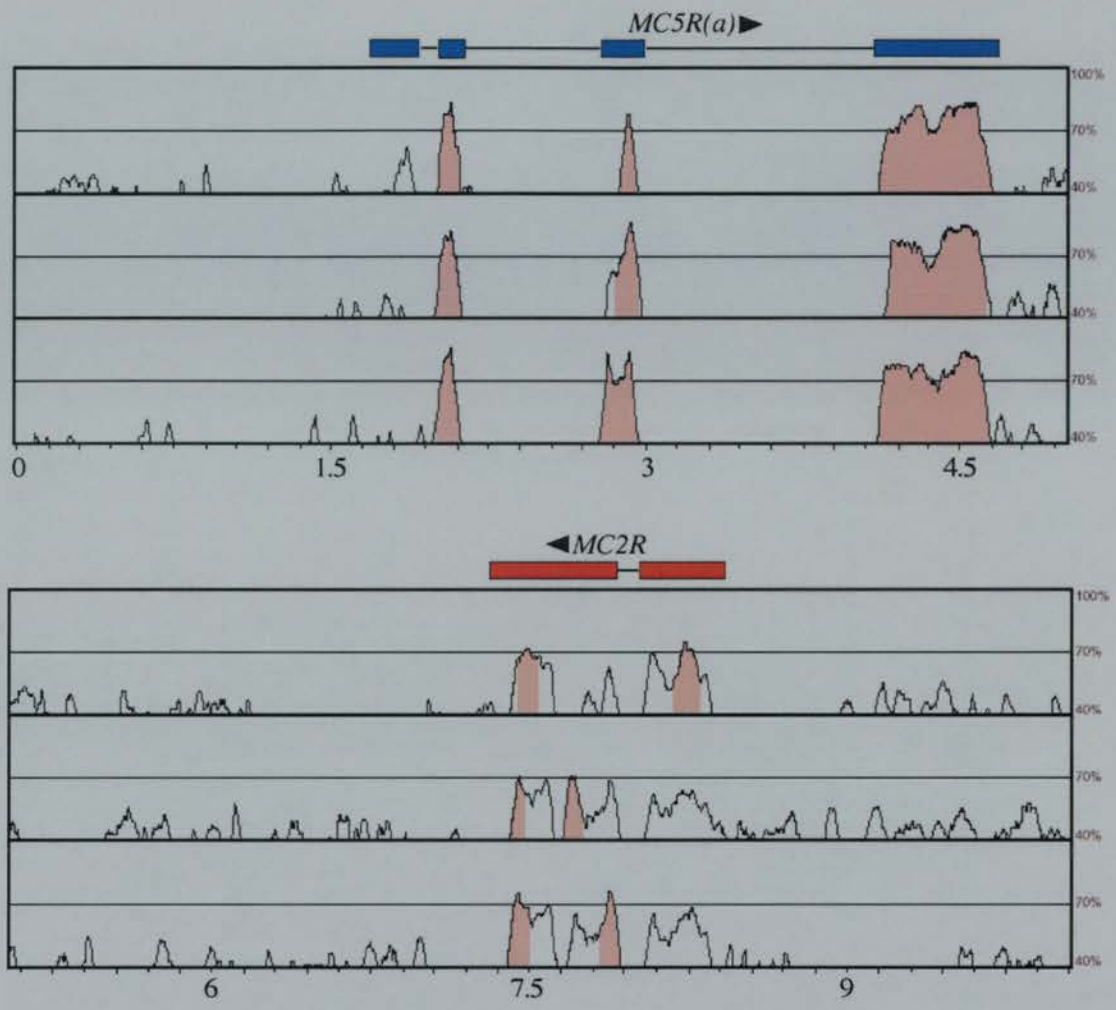

Figure 2.3.9. Comparison of MC2R/MC5R intergenic regions. Zebrafish (top), mouse (middle) and human (bottom) DNA sequences are compared to *Fugu* over rolling 75bp windows. The percentage identity between *Fugu* and each species is plotted, with all significant matches (>70%) occuring between exonic sequences (*pink* fill). The length of DNA from each species consists of the intergenic distance between (and including) MC2R and MC5R (zebrafish *mc5ra*) plus 2kb at either end.The length of the *Fugu* sequence is marked in kbp and the position and orientation of each gene (*black* arrowhead) and each exon (MC5R, *blue*; MC2R, *red*) is indicated. All sequences are from Ensembl alignments and the plot generated by mVISTA (www-gsd.lbl.gov/vista/).

There have been previous reports of intronless genes whose *Fugu* orthologues contain introns, and of additional introns present in *Fugu* (Venkatesh and Brenner, 1997; Aparicio *et al.*, 2002). This example, however, gives a useful insight into the evolution of the melanocortin receptor genes. *MC2R* and *MC5R* are among the most diverged in the gene family (Fig. 2.2.1), and yet share a common intron in *Fugu* and *Tetraodon* that is absent from the other family members in these species and from all family members currently identified in other species. Considering the syntenic relationship of the genes (Fig. 2.3.8), one explanation for this is that the intron is an ancient one that has been lost from virtually all members of the gene family, but has been retained in *MC2R* and *MC5R* in pufferfish. The alternatives are that an intron has inserted into neighbouring genes at an identical position, or that localised gene conversion has taken place between *MC2R* and *MC5R* thereby copying the intron. The implications this intron has for understanding melanocortin receptor gene evolution, and that of other G-protein coupled receptors is discussed further in Chapter 3.

2.3.3 The melanocortin 3 receptor and melanocortin 4 receptors.

Due to their involvement in regulating food intake and energy homeostasis in mice (Huszar *et al.*, 1997; Chen *et al.*, 2000), the phenotype/genotype correlation of MC3R, and particularly MC4R human variants has been subjected to scrutiny (Yeo *et al.*, 1998; Vaisse *et al.*, 2000; Schalin-Jantti *et al.*, 2003). Nine human MC4R variants with missense mutations associated with familial obesity have been functionally tested and shown to display a disrupted cAMP response (Yeo *et al.*, 1998). Of these important amino acids, only two are not conserved in fish (Fig. 2.3.10). Firstly, human MC4R is unable to bind NDP-MSH when I125 is mutated to Lys. In both fish species the equivalent amino acid is Phe. A more interesting difference is at human MC4R residue175. If this amino acid is changed from Ala to Thr, then there is a restricted cAMP response despite apparently normal NDP-MSH binding.

Figure 2.3.10 (following page). Alignment of MC4R amino acid sequences. Proteins from human (Hs), mouse (Mm), chicken (Gg), *Fugu* (Fr) and zebrafish (Dr) are represented. Amino acids identical in all sequences are shaded *black*, those different in one species are *dark grey*, and those different in two species are *light grey*

Figure 2.3.10. See previous page for legend.

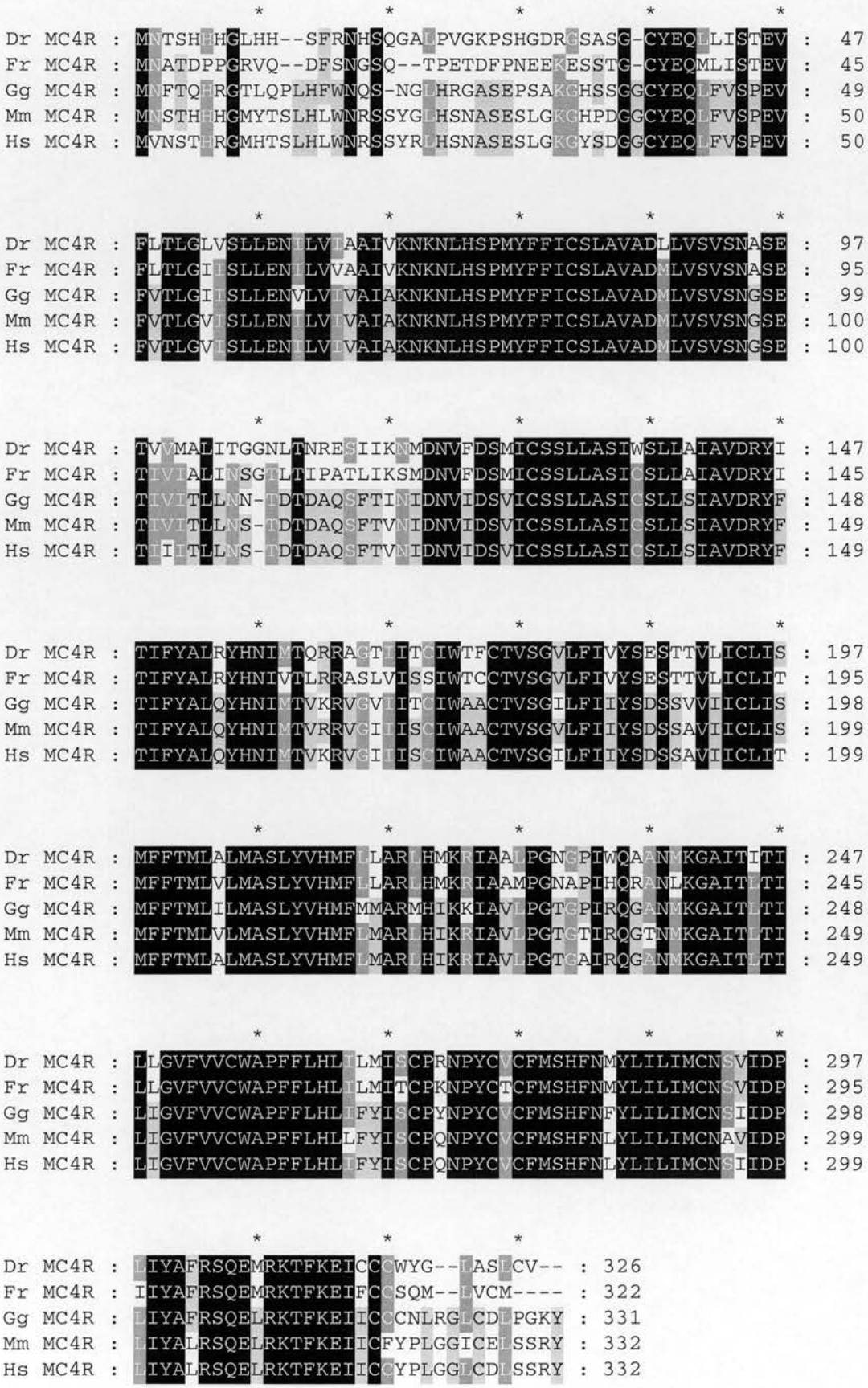

Figure 2.3.11. See following page for legend.

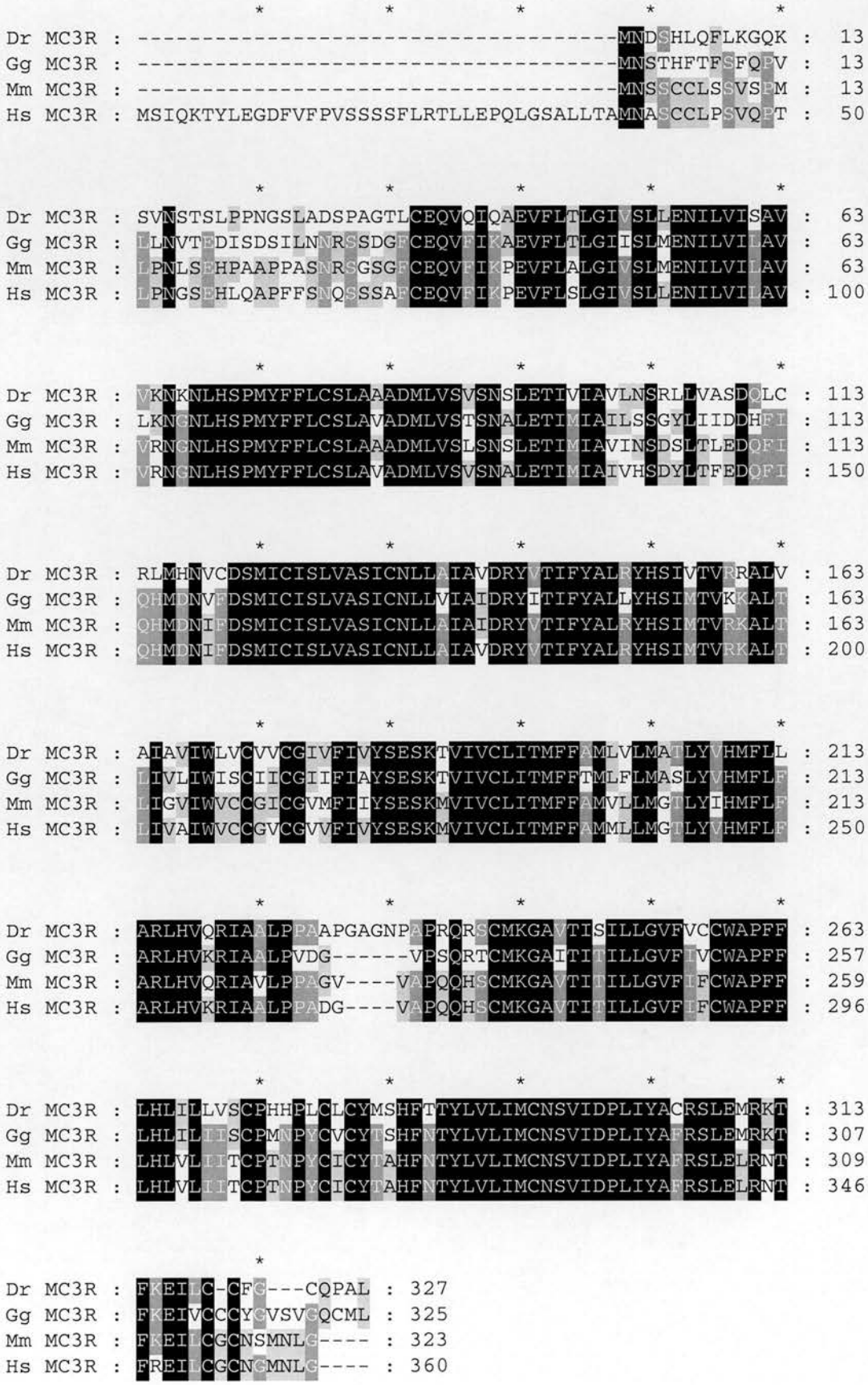

Figure 2.3.11 (previous page). Alignment of MC3R amino acid sequences. Proteins from human (Hs), mouse (Mm), chicken (Gg), *Fugu* (Fr) and zebrafish (Dr) are represented. Amino acids identical in all sequences are shaded *black*, those different in one species are *dark grey*, and those different in two species are *light grey*

Interestingly, both fish have Thr at the equivalent position. This might suggest that fish MC4R is less sensitive to αMSH than its mammalian counterpart, although other sequence differences between fish and mammals may compensate. Figure 2.3.11 shows an alignment of human MC3R proteins. There is less data available on the functional effect of MC3R variants, What is known from domain swapping experiments, is that the third extracellular loop is responsible for the ~30 fold difference in γMSH binding affinity between MC3R and MC4R (Oosterom *et al.*, 1999). Mutation of individual amino acids shows that residue Y268 of MC4R is particularly important, as it is thought to impair binding of γMSH in MC4R. At the equivalent positions, human MC3R has the much less bulky Leu-Ile. Zebrafish mc3r has Leu-Leu (Fig. 2.3.11) and mc4r has Leu-Met (Fig. 2.3.10), both of which are most similar to human MC3R. However, as γMSH is missing in teleost fish (see Chapter 2.5), it is probable that any pressure to distinguish between these residues has been lost.

Analysis of radiation hybrids revealed zebrafish *mc3r* maps to LG8, 320cR (LOD = 16.4) and *mc4r* maps to LG2, 365cR (LOD = 14.2). Despite the statistical probability that MC3R is missing in the pufferfish lineage, the second Ensembl *Fugu* assembly was searched for orthologues of genes closely linked to *MC3R* in mouse, humans and zebrafish. The two nearest genes downstream of mammalian *MC3R* (*STK6* and *TFAP2C*) are found on different *Fugu* scaffolds and the nearest upstream gene (*CBLNL1)* appears not to have a *Fugu* orthologue at all. In comparison, the neighbouring gene to zebrafish *mc3r* (*slc13a3*) is also found in the conserved syntenic region in mammals. These data are consistent with the disruption of synteny in pufferfish and the subsequent or concomitant loss of *MC3R*.

MC3R and MC4R in mammals have exclusively postnatal functions. However, the level of transcription of their orthologues in zebrafish appears in both larval RNA and in adults (Fig. 2.3.3). Furthermore, transcription of both genes in adult fish appears to be higher in the head than the body tissues, consistent with these receptors having a role similar to their mammalian function.

2.4 Teleost melanin-concentrating hormone receptor genes

2.4.1 The teleost melanin-concentrating receptor gene repertoire

The pigmentary function of αMSH in teleost fish, presumably mediated by one of the melanocortin receptors described here, is functionally antagonised by the action of MCH (Baker, 1993). It is also possible, by analogy with the mammalian energy homeostasis pathways, that the function of MC3R and MC4R may be balanced by action of MCH in the central nervous system. Therefore, having characterised teleost melanocortin receptors, the same method was used to identify melanin-concentrating hormone receptors. At the time of analysis, only human MCHR2 and human and mouse MCHR1 were publicly available. Therefore the human receptor sequences were used as a template for a Zebedee search of zebrafish and *Fugu* whole genome shotgun databases. Two *Fugu* and three zebrafish *MCHR* genes were identified. These were then cloned and sequenced by Miss Kayleene Pagan, a summer student in the lab.

A neighbour-joining tree showing the relationship between the fish sequences and representative mammalian MCHR protein sequences is in Figure 2.4.1. Subsequent to the identification of these genes in fish, a report noting the existence of one MCHR gene in rodents and lagomorphs, but two in primate, ferret and dog was published (Tan *et al.*, 2002). The authors speculate that *MCHR1* and *MCHR2* may have diverged from an ancestral gene early in mammalian evolution. However, this analysis shows that, like melanocortin receptors, an initial duplication of the *MCHR* gene took place before the divergence of the vertebrate lineage as both zebrafish and *Fugu* have clear *MCHR1* and *MCHR2* orthologues. As *MCHR2* is present in fish, the loss reported by Tan *et al* must have occurred after the separation of the super-order Glires from other mammals. The third MCH receptor gene in zebrafish is a late duplication in fish evolution. Unlike the duplicated *mc5r*, it appears from the phylogeny that a duplication of *mchr1* has taken place after the divergence of pufferfish from the zebrafish lineage (Fig. 2.4.1), although loss from the former lineage is possible. A search of *Ciona savignyi*, *Drosophila melanogastor* and *Caenorhabditis elegans* genomes elicited no further *MCHR* genes, suggesting the melanin-concentrating hormone system is vertebrate specific.

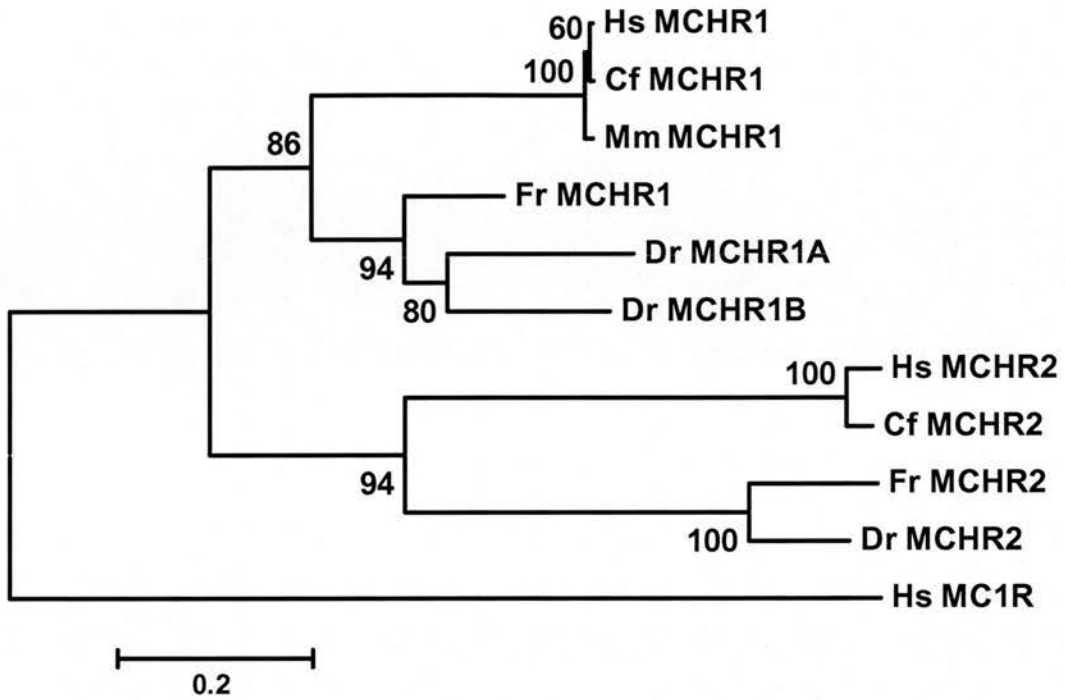

Figure 2.4.1. Phylogeny of melanin-concentrating hormone receptor protein sequences. Proteins from human (Hs), mouse (Mm), dog (Cf), zebrafish (Dr) and *Fugu* (Fr) are included. The tree uses a Poisson correction distance between the two sequences where the proportion of amino acid sites at which the two differ is corrected for multiple substitutions at the same site. Thus, the distance is equal to –ln(1-p), where p is the proportion of sites that differ. The number at each branch is the percentage of bootstrap replicates of the node from 1000 repetitions. The phylogeny is based on a 446aa alignment with gapped sites removed. The tree is rooted against human melanocortin 1 receptor (Hs MC1R).

To investigate the nature of the teleost duplication, the location of the zebrafish *mchr1* genes was determined by analysis of a radiation hybrid panel. Zebrafish *mchr1b* maps to LG3, 184cR (LOD = 18.9), near to the zebrafish orthologues of human ribosomal protein L3 (*RPL3*), mini-chromosome maintenance deficient 5 (*MCM5)* and eukaryotic translation initiation factor 3 subunit 7 (*EIF3S7*). These genes, and human *MCHR1*, are all located within a 10Mb region of human chromosome 22. No synteny was identified between human *MCHR* and zebrafish *mchr1a*, which maps to LG6, 291cR (LOD = 15.9). However, other similarly duplicated genes were found: *mchr1a* maps slightly distal of netrin 1a (*ntn1a*) on LG6, while *mchr1b* maps slightly distal of netrin 1 (*ntn1*) (Fig. 2.4.2). It appears that the gene content around *mchr1b* on LG3 and *mchr1a* on LG6 is syntenic with regions of human chromosomes 17 and 22 as orthologues of genes on those human chromosomes are found on one or both of the zebrafish linkage groups. This is consistent with the duplication of a chromosomal segment in the zebrafish lineage with the subsequent loss of some duplicated genes from one segment or the other. Other genes, like the ancestral *ntn1* or *mchr1*, were maintained in the genome as duplicates. Having established the shared linkage between *ntn1* and *mchr1* paralogues in zebrafish, The *Fugu* genome assembly was searched for *ntn1* orthologues and only one could be identified, providing further evidence that this particular genomic segment may have duplicated after *Fugu*/zebrafish divergence.

Figure 2.4.3 shows the expression of the zebrafish *mchr* genes, assayed by RT-PCR of mRNA transcripts. It appears that *mchr1a* is larvae specific as no transcripts are detected in adult tissues, and progressively weaker signals were found in larvae younger than 5 days. Expression of *mchr1b* appears more widespread than *mchr1a*. It can be detected in adults and young embryos with the signal strongest between days 4 and 7 of development. The expression of *mchr2* seems to parallel that of *mc1r* (Fig. 2.4.3); it can be detected from the earliest time point, throughout the period of larval melanophore function and appears to be expressed at higher levels in adult body compared to head. Again, quantitative assays would be required to confirm this. However, based on RT-PCR determined expression patterns, it seems probable that either mchr1b or mchr2 is likely to be the receptor that acts to regulate pigmentation in zebrafish.

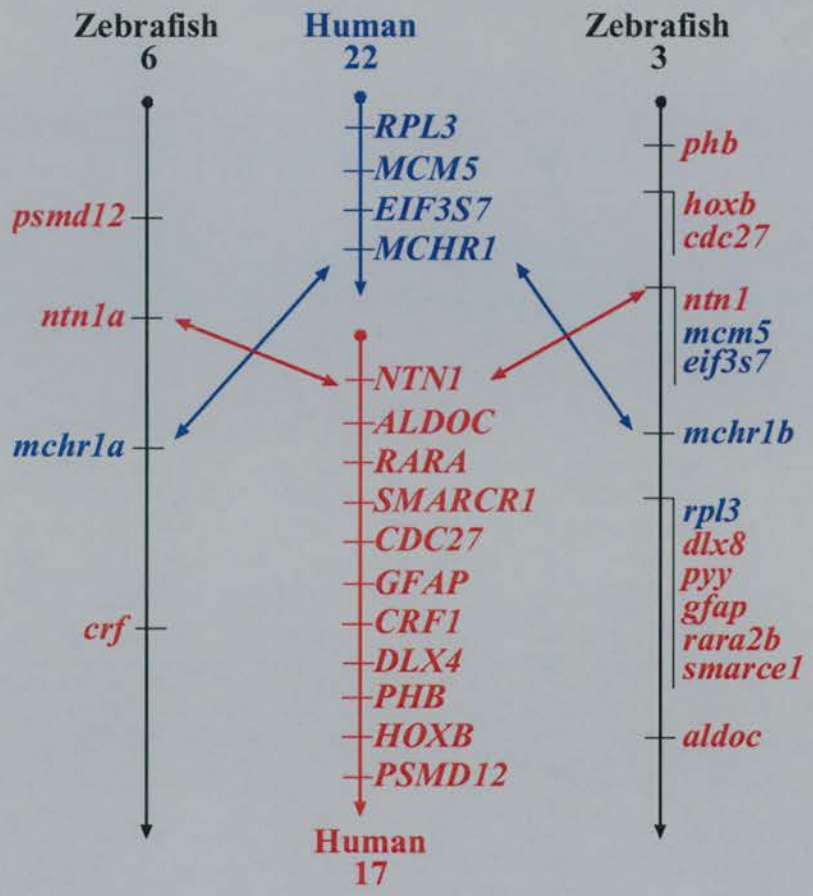

Figure 2.4.2. Conserved linkage between *mchr1* paralogues in zebrafish and synteny with human chromosomes. Species are indicated along with chromosome number or linkage group. Genes on human chromosome 17 and their zebrafish orthologues are *red*. Genes on human chromosome 22 and their zebrafish orthogues are *blue*. Arrows link the genes duplicated in zebrafish with their human orthologues. Gene positions are from a genetic zebrafish map (www.zfin.org) or the Ensembl human genome assembly (v15.33.1), but are not to scale.

Figure 2.4.3. RT-PCR assayed expression of MCH receptors in zebrafish. The embryo ages, tissue origin and controls (neg. = negative control, DNA = positive control) are indicated at the top of the figure with the genes denoted at either side. Zebrafish *b-actin* was used as a control for RNA quality.

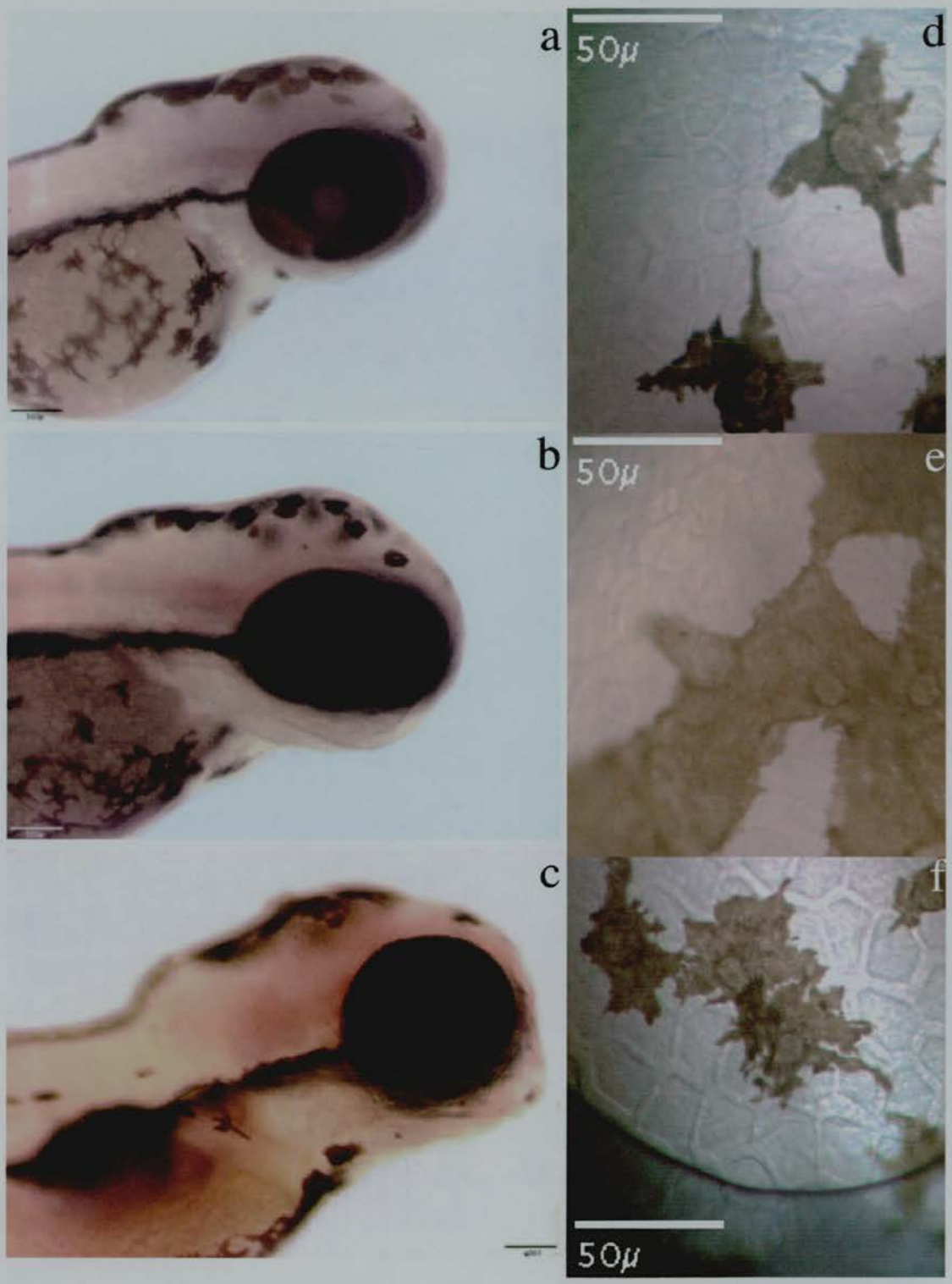

Figure 2.4.4. *mchr1a* expression in zebrafish is not detected by *in situ* hybridisation. a-c, lateral view of embryos probed with *mchr1a* at 48hr (**a**), 72hr (**b**) and 96hr (**c**). **d-e**, melanophores from the dorsum of a 48hr (**d**) and 96hr (**e**) embryo probed with *mchr1a*. **f**, melanophores from the dorsum of a 48hr unprobed embryo. Scale bar: 100μm (**a-c**), 50μm (**d-f**).

To further investigate the temporal and spatial expression of each of the melanin-concentrating hormone receptors in zebrafish, anti-sense riboprobes were generated and *in situ* hybridization histochemistry was carried out. However, as was the case with *mc1r*, specific expression could not be seen with any melanin-concentrating hormone receptor probe in melanophores or elsewhere between 18 and 96hrs. This despite RT-PCR analysis confirming the presence of transcripts. Figure 2.4.4 shows a representative sample of embryos probed with an antisense *mchr1a* probe.

2.5 Pro-opiomelanocortins in teleost fish

2.5.1 Gene identification and characterisation

Pro-opiomelanocortin (POMC) is a pre-pro-hormone that is cleaved by pro-hormone convertases into small peptide hormones (Eipper and Mains, 1980). These peptides have been identified in primitive vertebrate species, mainly by chromatographic separation and protein sequencing (Takahashi *et al.*, 1995a; Takahashi *et al.*, 2003). Subsequently, the pro-opiomelanocortin gene (*POMC*) has been characterised in these species (Takahashi *et al.*, 1995b; Amemiya *et al.*, 1999a; Amemiya *et al.*, 2000). All known POMC gene sequences were conceptually translated and added to the known protein sequences to create a Hidden Markov Model (HMM) using HMMER (Eddy, 1998). This model was used to search the *Fugu*, *Tetraodon* and zebrafish Project-BLAST databases, translated in all frames. In all three species, two distinct trace sequences were identified that showed high identity with the HMM. However these high identity hits were to different, non-overlapping regions of the HMM, suggesting that two exons from a single *POMC* gene had been found. Further analysis of the gene sequences identified splice consensus sites in the correct phase for these potential exons to be spliced together.

Using iterative BLAST, an intervening intron was identified in *Fugu* and *Tetraodon* sequences, confirming the *POMC* gene contained at least two exons. A pairwise comparison of the *POMC* coding sequences of the puffer fish suggests the presence of a second, short intron in these fish. The *Tetraodon* ORF is identical to that found in *Fugu*, so again, for the sake of clarity, only *Fugu* and zebrafish will be discussed further.

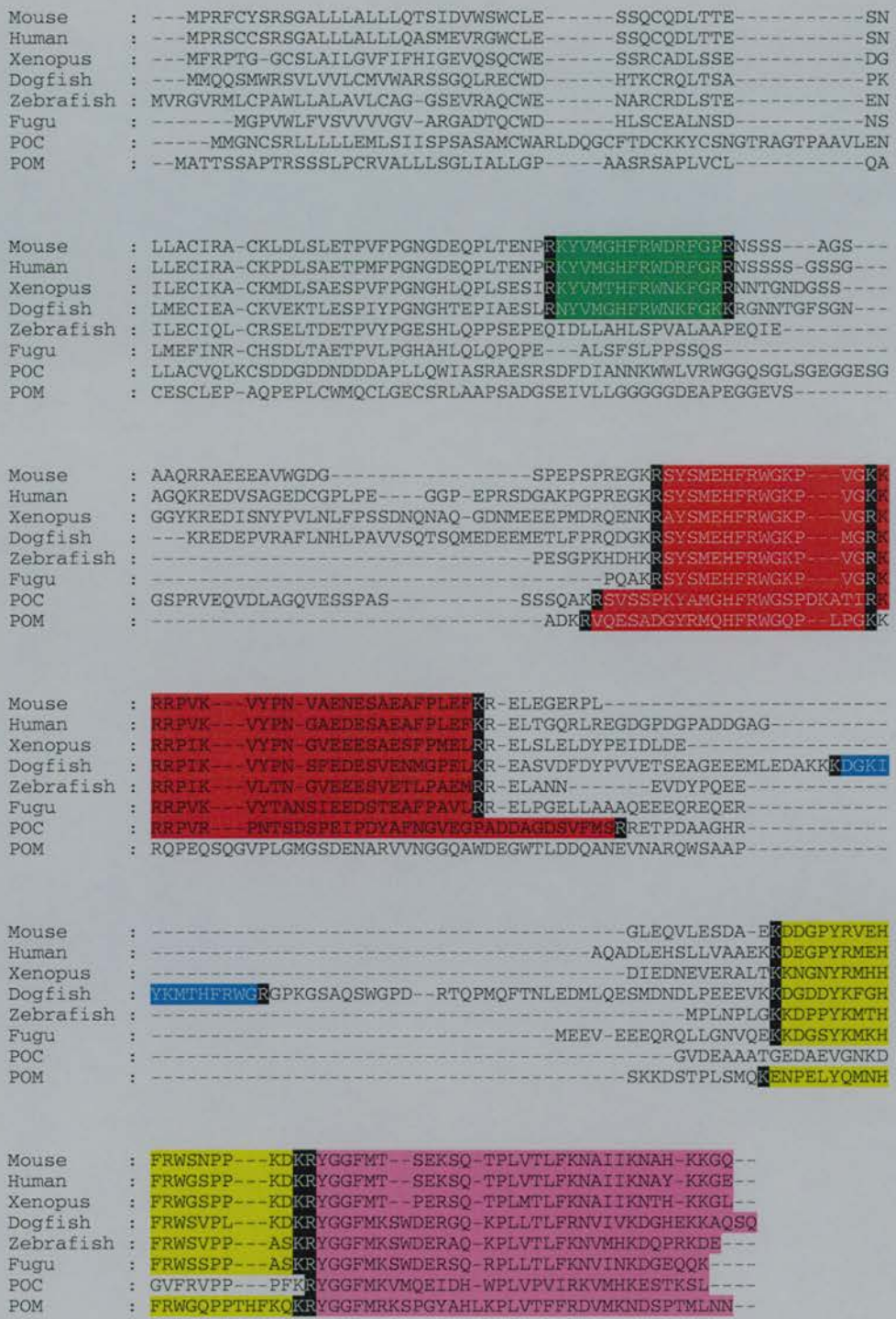
Mouse : ---MPRFCYSRSGALLLALLLQTSIDVWSWCLE------SSQCQDLTTE----------SN
Human : ---MPRSCCSRSGALLLALLLQASMEVRGWCLE------SSQCQDLTTE----------SN
Xenopus : ---MFRPTG-GCSLAILGVFIFHIGEVQSQCWE------SSRCADLSSE----------DG
Dogfish : ---MMQQSMWRSVLVVLCMVWARSSGQLRECWD------HTKCRQLTSA----------PK
Zebrafish : MVRGVRMLCPAWLLALAVLCAG-GSEVRAQCWE------NARCRDLSTE----------EN
Fugu : -------MGPVWLFVSVVVVGV-ARGADTQCWD------HLSCEALNSD----------NS
POC : -----MMGNCSRLLLLLEMLSIISPSASAMCWARLDQGCFTDCKKYCSNGTRAGTPAAVLEN
POM : --MATTSSAPTRSSSLPCRVALLLSGLIALLGP-----AASRSAPLVCL----------QA
Mouse : LLACIRA-CKLDLSLETPVFPGNGDEQPLTENPRKYVMGHFRWDRFGPRNSSS---AGS---
Human : LLECIRA-CKPDLSAETPMFPGNGDEQPLTENPRKYVMGHFRWDRFGRRNSSSS-GSSG---
Xenopus : ILECIKA-CKMDLSAESPVFPGNGHLQPLSESIRKYVMTHFRWNKFGRRNNTGNDGSS----
Dogfish : LMECIEA-CKVEKTLESPIYPGNGHTEPIAESLRNYVMGHFRWNKFGKKRGNNTGFSGN---
Zebrafish : ILECIQL-CRSELTDETPVYPGESHLQPPSEPEQIDLLAHLSPVALAAPEQIE---------
Fugu : LMEFINR-CHSDLTAETPVLPGHAHLQLQPQPE---ALSFSLPPSSQS----------
POC : LLACVQLKCSDDGDDNDDDAPLLQWIASRAESRSDFDIANNKWWLVRWGGQSGLSGEGGESG
POM : CESCLEP-AQPEPLCWMQCLGECSRLAAPSADGSEIVLLGGGGGDEAPEGGEVS--------
Mouse : AAQRRAEEEAVWGDG----------SPEPSPREGKRSYSMEHFRWGKP---VGKK
Human : AGQKREDVSAGEDCGPLPE----GGP-EPRSDGAKPGPREGKRSYSMEHFRWGKP---VGKK
Xenopus : GGYKREDISNYPVLNLFPSSDNQNAQ-GDNMEEEPMDRQENKRAYSMEHFRWGKP---VGRK
Dogfish : ---KREDEPVRAFLNHLPAVVSQTSQMEDEEMETLFPRQDGKRSYSMEHFRWGKP---MGRK
Zebrafish : ----------PESGPKHDHKRSYSMEHFRWGKP---VGRK
Fugu : ----------PQAKRSYSMEHFRWGKP---VGRK
POC : GSPRVEQVDLAGQVESSPAS----------SSSQAKRSVSSPKYAMGHFRWGSPDKATIRK
POM : ----------ADKRVQESADGYRMQHFRWGQP--LPGKK
Mouse : RRPVK---VYPN-VAENESAEAFPLEFKR-ELEGERPL----------
Human : RRPVK---VYPN-GAEDESAEAFPLEFKR-ELTGQRLREGDGPDGPADDGAG----------
Xenopus : RRPIK---VYPN-GVEEESAESFPMELRR-ELSLELDYPEIDLDE----------
Dogfish : RRPIK---VYPN-SFEDESVENMGPELKR-EASVDFDYPVVETSEAGEEEMLEDAKKKDGKI
Zebrafish : RRPIK---VLTN-GVEEESVETLPAEMRR-ELANN-------EVDYPQEE----------
Fugu : RRPVK---VYTANSIEEDSTEAFPAVLRR-ELPGELLAAAQEEEQREQER----------
POC : RRPVR---PNTSDSPEIPDYAFNGVEGPADDAGDSVFMSRRETPDAAGHR----------
POM : RQPEQSQGVPLGMGSDENARVVNGGQAWDEGWTLDDQANEVNARQWSAAP----------
Mouse : ----------GLEQVLESDA-EKDDGPYRVEH
Human : ----------AQADLEHSLLVAAEKKDEGPYRMEH
Xenopus : ----------DIEDNEVERALTKKNGNYRMHH
Dogfish : YKMTHFRWGRGPKGSAQSWGPD--RTQPMQFTNLEDMLQESMDNDLPEEEVKKDGDDYKFGH
Zebrafish : ----------MPLNPLGKKDPPYKMTH
Fugu : ----------MEEV-EEEQRQLLGNVQEKKDGSYKMKH
POC : ----------GVDEAAATGEDAEVGNKD
POM : ----------SKKDSTPLSMQKENPELYQMNH
Mouse : FRWSNPP---KDKRYGGFMT--SEKSQ-TPLVTLFKNAIIKNAH-KKGQ--
Human : FRWGSPP---KDKRYGGFMT--SEKSQ-TPLVTLFKNAIIKNAY-KKGE--
Xenopus : FRWGSPP---KDKRYGGFMT--PERSQ-TPLMTLFKNAIIKNTH-KKGL--
Dogfish : FRWSVPL---KDKRYGGFMKSWDERGQ-KPLLTLFRNVIVKDGHEKKAQSQ
Zebrafish : FRWSVPP---ASKRYGGFMKSWDERAQ-KPLVTLFKNVMHKDQPRKDE---
Fugu : FRWSSPP---ASKRYGGFMKSWDERSQ-RPLLTLFKNVINKDGEQQK----
POC : GVFRVPP---PFKRYGGFMKVMQEIDH-WPLVPVIRKVMHKESTKSL----
POM : FRWGQPPTHFKQKRYGGFMRKSPGYAHLKPLVTFFRDVMKNDSPTMLNN--

Figure 2.5.1. (Previous page). Alignment of POMC amino acid sequences. *Fugu* and zebrafish sequences are aligned with representative proteins from a range of vertebrate classes, including mammals (human and mouse), amphibians (*Xenopus laevis*), chondrichthyes (spiny dogfish) and agnathans (sea lamprey). Lamprey has two POMC-like proteins, termed pro-opiocortin (POC) and pro-opiomelanotropin (POM). Hormone sequences are indicated by coloured shading: γMSH (*green*), ACTH (*red*), δMSH (*blue*), βMSH (*yellow*) and β-endorphin (*pink*). αMSH is a subsequence of ACTH and is indicated by *red* shading and *white* text. All hormones are bordered by dibasic pro-hormone convertase cleavage sites (*black* shading).

At the time of analysis, the zebrafish sequence coverage in Project-BLAST was not comprehensive enough to obtain a single contig across the entire gene. However sequencing of the reverse transcribed mRNA confirmed two exons of a single *pomc* gene had been identified. The first intron position in *Fugu* and in zebrafish, is found at a position equivalent to the single coding intron in mouse and human *POMC*. This is strong evidence that these teleost genes are orthologues of mammalian *POMC*. The subsequent genome alignments made available on Ensembl confirmed the genomic structure predictions described above. However, similar *in silico* analysis of *Drosophila*, *Anopheles* and *C. elegans* genome assemblies, plus the *Ciona savignyi* Project-BLAST database failed to identify a recognisable POMC like sequence.

When the conceptual translation of zebrafish and *Fugu POMC* are compared with other POMC sequences, the constitutive peptide hormones can be identified (Fig. 2.5.1). The N-terminal peptide sequences tend to be quite diverse, as do the connecting sequences between each hormone, but β-endorphin and the melanocortins themselves are highly conserved. The *Fugu* and zebrafish αMSH sequences are completely identical to the characterised peptide in mouse and human and ACTH, βMSH, β-endorphin are very similar. In each melanocortin, the active pharmacore (HFRW) is invariant and can be clearly identified, as can the bordering dibasic pro-hormone convertase cleavage sites. The exception to this is in γMSH, which is clearly absent in both *Fugu* and zebrafish. This is not unexpected, as previous reports have found γMSH lacking in the teleost lineage (Kitahara *et al.*, 1988; Lee *et al.*, 1999), but present in chondrichthyans (Takahashi *et al.*, 1999). Another difference between bony and cartilaginous fish POMC is the absence of δMSH from both teleosts. This particular melanocortin is also missing

in other cloned teleost POMC genes and has currently only been found in two elasmobranch species (Amemiya *et al.*, 1999b; Amemiya *et al.*, 2000)

Figure 2.5.2 illustrates the phylogeny of the entire POMC protein sequences from a diverse range of species. It shows that zebrafish and *Fugu* POMC sequences are grouped in two separate teleost clades. Zebrafish groups with the American eel (*Anguilla rostrata*) and the common carp (*Cyprinus carpio*), while the *Fugu* POMC sequence is more similar to tilapia (*Oreochromis mossambicus*), big-eye tuna (*Thunnus obesus*) and Japanese flounder (*Paralichthys olivaceus*). Perhaps unsurprisingly, the lobe-finned African lungfish (*Protopterus annectens*) is more similar to tetrapod POMCs than ray finned fish, while elasmobranchs are more distant.

To investigate a potential syntenic relationship between teleost and mammalian POMC genes, the zebrafish gene was mapped to LG17, 275cR (LOD = 12.6) by radiation hybrid mapping and its neighbouring genes were identified. Figure 2.5.3a illustrates the conserved synteny between zebrafish and mammalian *POMC*. Both SRY-related HMG-box 11 (*SOX11*) and inhibitor of DNA-binding 2 (*ID2*) map near *POMC* in mouse, human and zebrafish. In addition, a human orthologue of *Drosophila orthodenticle* (*OTX1*) maps distal of human *POMC* while zebrafish *otx1* maps proximal of *pomc*. Mouse *Otx1* is found on chromosome 11, probably as a result of a lineage specific translocation. Taken together, these results suggest the teleost sequences identified here are orthologous to mammalian *POMC*. To begin to understand the functional role of teleost *pomc* the zebrafish gene was cloned and expression analysis carried out by a rotation student in the lab, Miss Sally Burn. These data indicate that *pomc* is expressed throughout larval development (Figure 2.5.3b) and in adult brain (not shown).

2.5.2 The spatial and temporal expression of zebrafish pomc.

To further characterise the expression of *pomc* in the brain, and to investigate when this is first initiated, sense and anti-sense riboprobe were generated for an *in situ* hybridization analysis of whole embryos and larvae. The probes spanned the 528bp second coding exon of zebrafish *pomc* and were labelled with DIG.

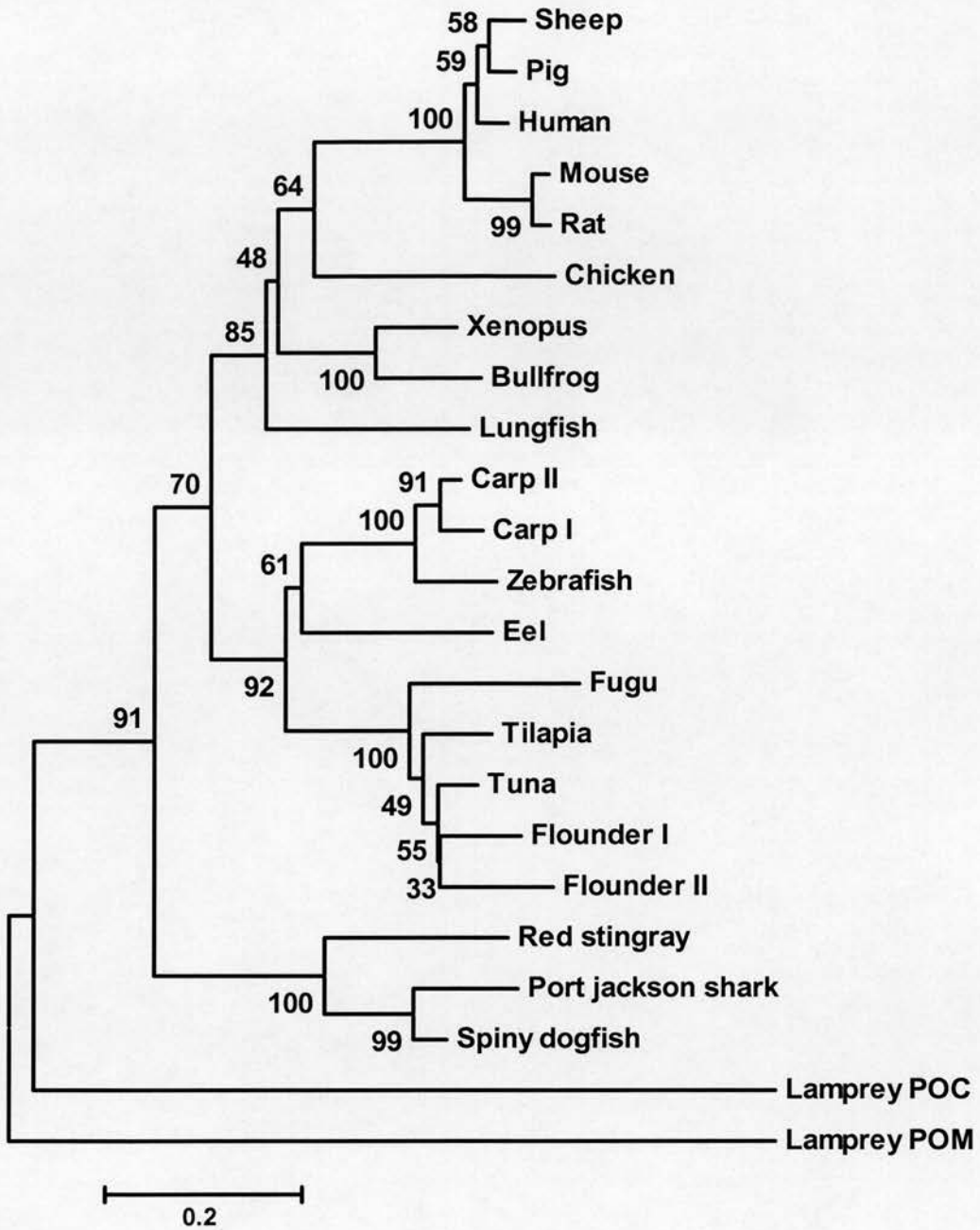

Figure 2.5.2. Phylogeny of POMC protein sequences. Proteins from a selection of vertebrate species are included. The tree uses a Poisson correction distance between the two sequences where the proportion of amino acid sites at which the two differ is corrected for multiple substitutions at the same site. Thus, the distance is equal to –ln(1-p), where p is the proportion of sites that differ. The number at each branch is the percentage of bootstrap replicates of the node from 1000 repetitions. The phylogeny is calcuated from the full-length protein alignment (Fig. 2.5.1) with gapped sites removed. The tree is rooted against two lamprey POMC-like proteins, pro-opiocortin (POC) and pro-opiomelanotropin (POM).

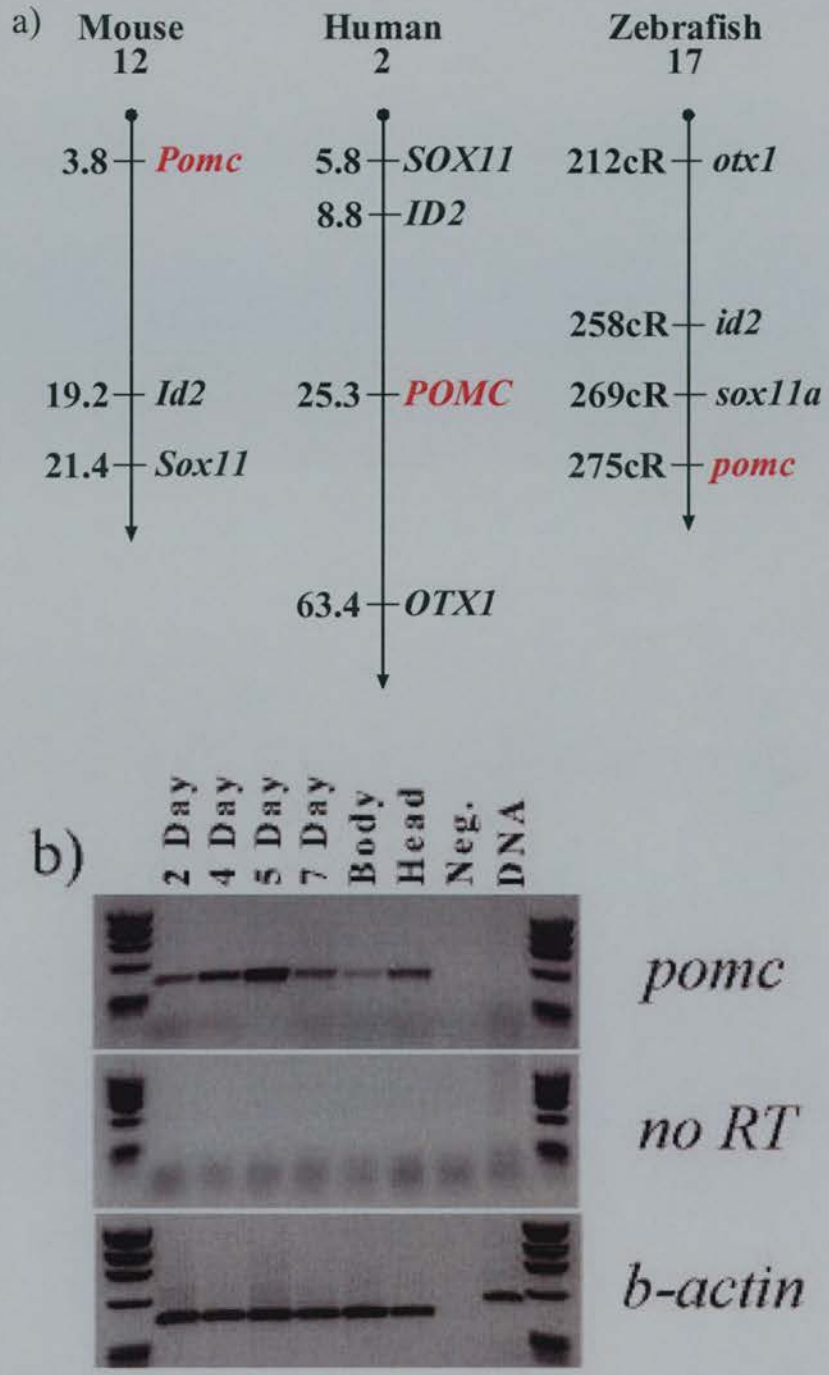

Figure 2.5.3. Zebrafish *pomc* is expressed and displays conserved synteny with mammals. a, Conserved synteny around *POMC*. Chromosome numbers from human and mouse are indicated (from Ensembl Human v15.33.1 and Mouse v15.30.1) with the relative position of each gene marked in megabases. The zebrafish linkage group is noted, with gene positions estimated from centiRay distance by radiation hybrid mapping. **b,** RT-PCR expression analysis. The embryo ages, tissue origin and controls (neg. = negative control, DNA = positive control) are indicated at the top of the figure. Zebrafish *b-actin* was used as a control for RNA quality. Expression data reproduced with permission of Miss Sally Burn.

Figure 2.5.4 shows the *pomc* expression pattern in the developing zebrafish head. At the 21-somite stage (20 hpf) no *pomc* expression could be detected (Fig. 2.5.4a), however by 24 hpf two very strong domains of bilateral expression could be seen at the anterior neural ridge (Fig.2.5.4b). By 28 hpf these domains have fused, forming a single expression domain lateral to the anterior midline (Fig. 2.5.4c). The *pomc* expressing cells continue to proliferate and, by 32 hpf, the expression domain has begun to condense around the midline (Fig.2.5.4d). Then, over the next 16 hours, the cells become arranged in a highly organised pattern, forming one distinct bilateral domain and two medial domains by 48hpf (Fig.2.5.4e, g). This pattern then consolidates by 72hpf (Fig.2.5.4h, i) and remains static until at least 120 hpf (not shown). The most anterior expression domain is shaped like a bilateral arc along the anterior/posterior (AP) axis and is found slightly lateral of the midline (Fig. 2.5.4g, i, *red* arrowheads). The other two domains appear to be roughly circular in shape and are found at the midline (Fig.2.5.4g, i, *black* arrowheads). When compared with the expression pattern of mouse *Pomc* (Japon *et al.*, 1994), zebrafish *lim3*, a marker of early pituitary development (Glasgow *et al.*, 1997), and the distribution of cell types in the adult teleost pituitary (Norris, 1997), it is evident that these domains are separate *pomc* expressing cell populations. The longitudinal arcs mark β-endorphin producing neurons in the hypothalamic stalk while the duel circular domains probably correspond to ACTH producing corticotropes (anterior domain) and MSH producing melanotropes (posterior domain) in the anterior pituitary.

In mammals the neurohypophysis (posterior pituitary) derives from the hypothalamic infundibulum while the adenohypophysis (anterior pituitary) develops from Rathke's pouch, a dorsal invagination of the oral ectoderm at the anterior neural ridge (Treier and Rosenfeld, 1996). However, the organogenesis of the lower vertebrate pituitary is not well understood. Therefore the zebrafish anterior pituitary cells, marked by *pomc* from a very early stage, were analysed for evidence of a similar morphogenetic mechanism.

Figure 2.5.4. (overpage) Zebrafish *pomc* is expressed in the developing adenohypophysis. a, There is no staining detected at 20 hpf. **b-d**, at 24 (**b**), 28 (**c**) and 32 hpf (**d**) *pomc* expression is seen. **e-g, i**, At 48 hpf (**e, g**) and 72 hpf (**f, i**) distinct expression domains are seen. **h**, No expression is seen in a 48 hpf larve probed with a sense control. **a-c,** anterior views; **d-h**, ventral views. **g, i**, 2x magnification of **e** and **f**. All scale bars are 100μm.

Figure 2.5.4. (Previous page)

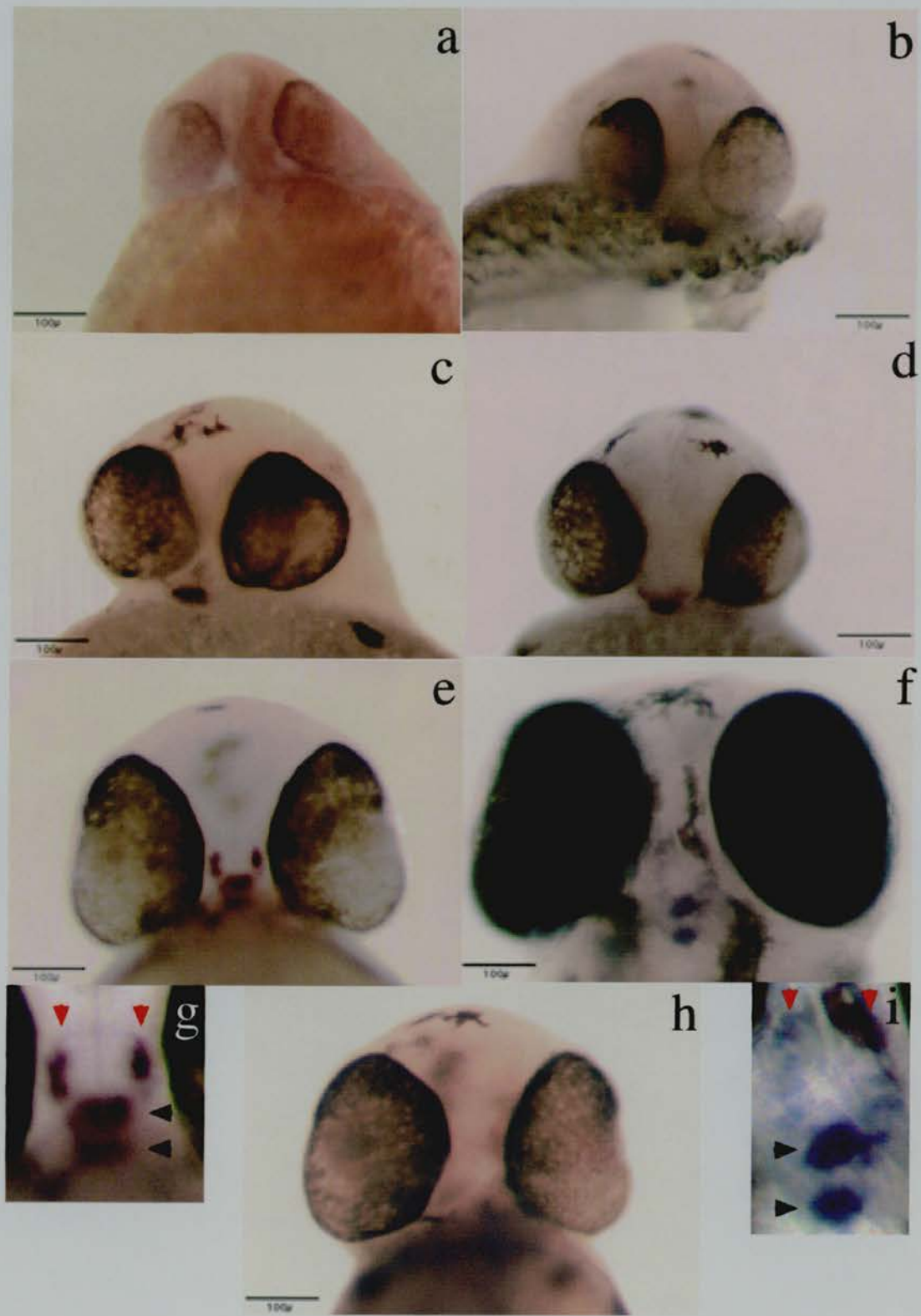

As previously mentioned, the first appearance of *pomc* expressing cells is around 24 hpf at the anterior ridge (Fig. 2.5.4b, 2.5.5a). This is different in mouse, where *Pomc* expression is only detected after the separation of Rathke's pouch from the oral ectoderm, as the pituitary anlage migrates towards the diencephalon. The zebrafish melanotropes and conticotropes migrate towards the midline and appear to proliferate as they begin to migrate towards the posterior (Fig. 2.5.5b,c,d). This movement begins soon after 24 hpf and coincides with oral cavity formation, an invagination of the stomodeal ectoderm that will eventually fuse with the foregut to form a continuous tube.

Is it the case that the posterior movement of the zebrafish pituitary primordium is driven by oral cavity formation rather than by a pituitary specific morphogenic mechanism as is seen in the mouse? There are several lines of evidence that support this. Firstly, after the zebrafish cells organise into separate *pomc* expressing domains cells they continue moving towards the posterior (Fig. 2.5.5e) until they are positioned on the midline just posterior of the optic cups, where they remain (Fig. 2.5.5f). This position on the AP axis coincides with where the invagination of the stomodeal ectoderm terminates, as it fuses with the foregut. Secondly, the relative dorsoventral (DV) position of the migrating primordium differs in mouse and zebrafish. While the pituitary specific morphogenesis in the mouse, forming Rathke's pouch, is essentially a dorsal invagination, there is no primordial internalisation in the zebrafish. Throughout the posterior movement, the *pomc* expressing cells remain in a ventral position (best seen in Fig 2.5.5b), dorsal only to the roof of the oral cavity. Finally, the patterning of the mature pituitary appears to be different in zebrafish and mouse. The mouse adenophyopthysis is patterned along the (DV) axis, presumably due to the cellular distribution resulting from the dorsal invagination of Rathke's pouch (Treier and Rosenfeld, 1996). However, it appears that the zebrafish anterior pituitary may be patterned along the AV axis, with bands of *pomc* expressing cells separated by other pituitary cell types (Fig. 2.5.4i). The different patterns are probably a result of the contrasting morphogenetic mechanisms occurring in zebrafish and mammals. This is discussed further in Chapter 2.6.6.

There is another separate domain of *pomc* expression seen in developing zebrafish larvae. From 72 hpf there is strong bilateral *pomc* expression in a subset of cells in the otic vesicle (Fig. 2.5.6b, e). This is not seen in otic vesicles from 48 hpf (Fig. 2.5.6a, d) or 24 hpf (not shown) larvae, but is maintained through to 96 hpf at least (Fig. 2.5.6c, f).

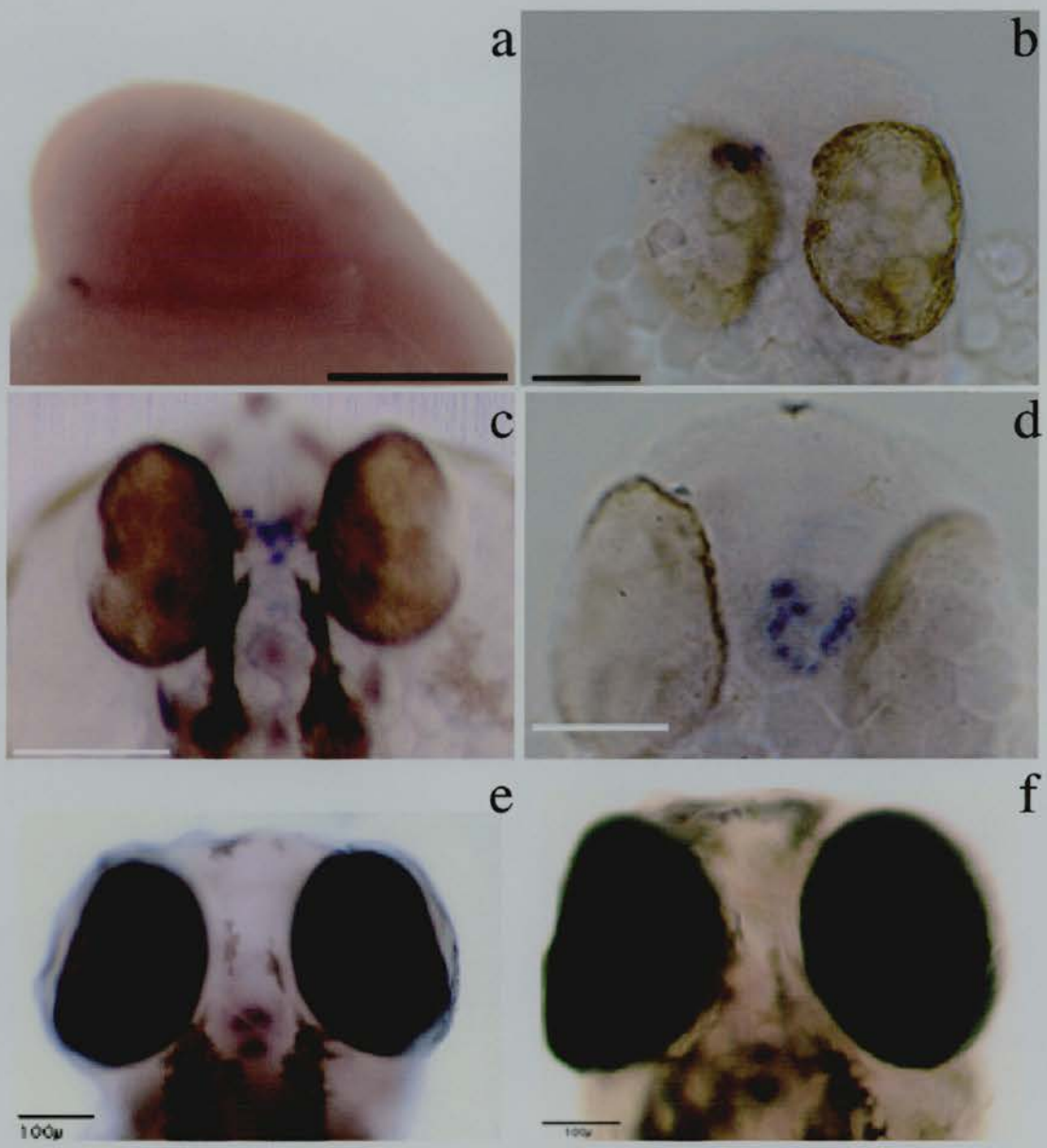

Figure 2.5.5 Morphogenesis of the zebrafish adenohypophysis. a, The pituitary primordium expresses *pomc* bilaterally at the anterior neural ridge around 24 hpf. **b**, These cells proliferate and have moved towards the midline by 28 hpf, but remain in a ventral position.**c-d**, By 32 hpf, the ventrally located pomc expressing cells are moving towards the posterior posterior in an apparantly disorganised manner. **e**, By 72 hpf the cells are more posterior still, but have organised into three expressing domains. **f**, by 96 hpf the adenohypophysis is at the ventral midline posterior to the eyes. **a,** lateral view; **b**, ventrolateral view; **c**, dorsal view; **d-f**, ventral views. Scale bar: 100µm (**a,c,e-f**). Scale bar: 50µm (**b,d**).

Figure 2.5.6. (legend overpage).

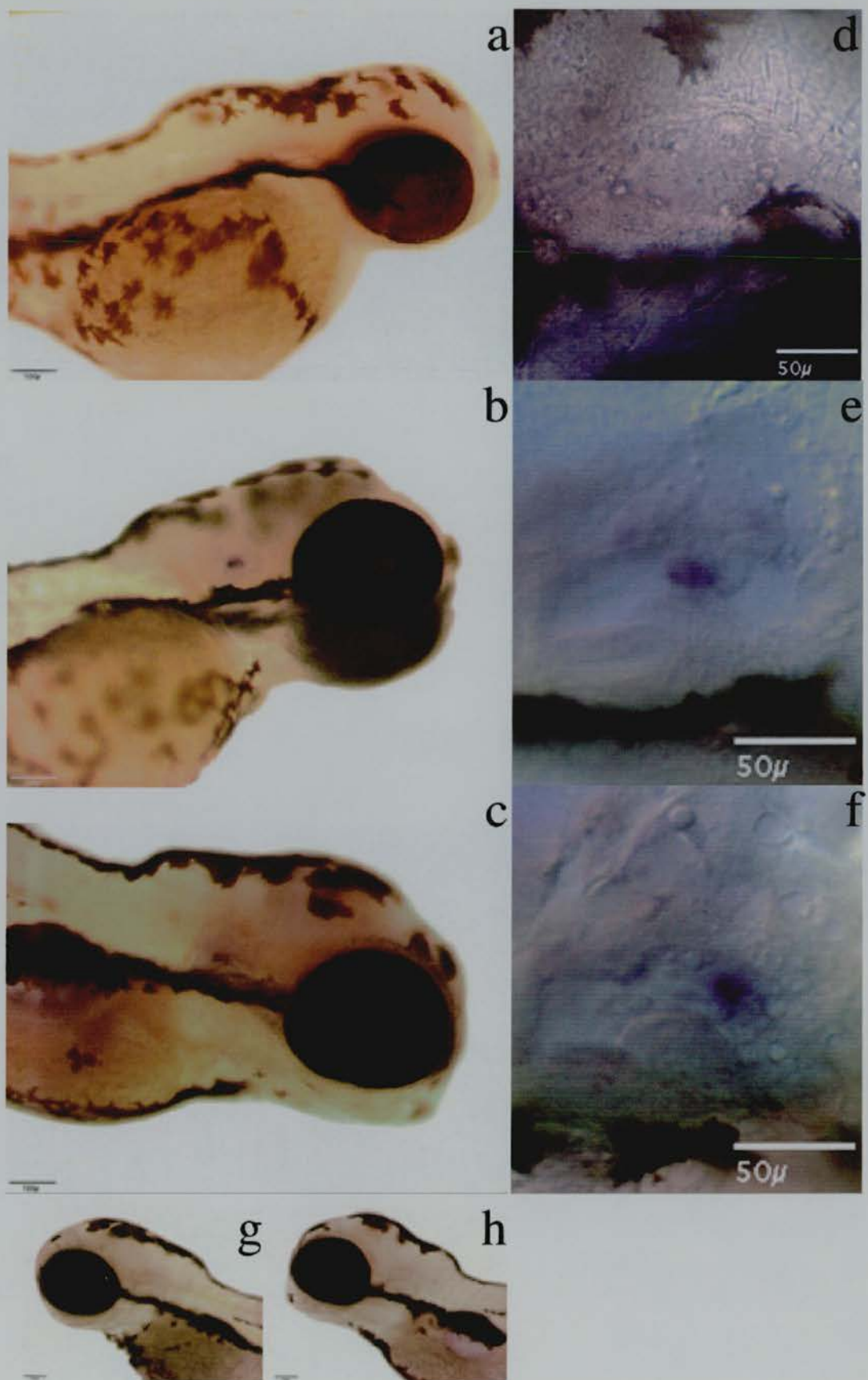

Figure 2.5.6. Zebrafish pomc is expressed in the developing otic vesicle. a, d, No *pomc* expression is seen in 48 hpf larva. **b-c**, **e-f**, A discrete population of cells do express the gene at 72 hpf (**b,e**) and 96 hpf (**c, f**). **g-h**, Larvae probed with a sense control show not otic vesicle staining at 72 hpf (**g**) or 96 hfp (**h**). **a-c**, lateral view with anterior to the right; **d-h**, lateral view, anterior to the left. Scale bar: 100μm (**a-c, g-h**). Scale bar: 50μm (**d-f**).

There have been no previous reports of *pomc* expression detected in mammalian ears despite the presence of pigmented melanocytes in the organ (Steel and Barkway, 1989) and it is not known if there are melanophores in the teleost ear, although no pigmented cells can be seen. However, the very specific and repeatable staining suggests a discrete number of cells are expressing *pomc* in the developing zebrafish ear. Furthermore, fish hybridised with a sense control probe show no staining in the otic vesicle at 72 or 96 hpf fish (Fig 2.5.6g, h), suggesting it is not due to artefactual trapping in the chambers of the ear.

2.6 Discussion

2.6.1. Prospects for identifying orthologous genes in silico

The identification of specific genes in any particular species is greatly aided by knowing the genomic sequence of the orthologous gene in a closely related species. Numerous genes first identified in mouse were then used to identify their human equivalent. In fact, some of the mammalian melanocortin receptor genes themselves were identified in this manner. Traditionally, PCR with degenerate primers targeted at a conserved motif may be used to identify a fragment of the gene. This fragment can then be used to find the entire length of the gene, either by rapid amplification of cDNA ends (RACE) or by screening a cDNA library. While this is often successful when searching for genes between closely related species, it can be problematic when searching for orthologous genes between species that diverged hundreds of millions of years previously. Not only will more distant species show greater variation in sequence at the DNA level, but it may become more difficult to predict where the gene might be expressed from one species to another.

The fruitless attempt to identify zebrafish *mc1r* using these techniques probably failed for a number of reasons. An alignment of full-length zebrafish and chicken MC1R cDNA sequence shows that there is only ~45% conservation at the DNA level. Even between the highly conserved transmembrane domains, conservation is only in the range of 50%. Using a fragment of chicken MC1R to probe a gridded cDNA library was similarly unsuccessful. A search of human cDNA libraries shows *MC1R* is represented at a very low level. Out of 23478 transcripts in a human melanocyte library (Soares melanocyte 2NbHM), none coded for MC1R (Hillier *et al.*, 1996) and when five melanotic melanoma libraries containing over 100,000 transcripts are considered, MC1R only accounts for 0.016%. It is perhaps not surprising therefore, that fish *mc1r* was not identified by *ex situ* hybridisation with a DNA probe derived from such a distant orthologue.

The success of whole genome sequencing is illustrated by the availability of *Drosophila melanogastor*, *Caenorhabditis elegans,* human and mouse genome assemblies prior to the analysis discussed in this chapter. The release of the first draught sequence assemblies, coupled with the appropriate bioinformatic tools, greatly improved orthologous gene identification between distant species. Software such as BLAST2 (Altschul *et al.*, 1997), that can virtually translate sequences at high speed and identify similar sequences using a heuristic algorithm, permits one to probe entire genomes for orthologues that show low identity at the DNA level, but show some similarity at the protein level. Even more sophisticated software, such as HMMER, allows one to combine the information from multiple orthologues into a single model with which to search (Eddy, 1998). However, to use this software the genome data must be accessible and those generating the sequence data will often only release draught assemblies in such a format. Therefore in the years it takes to generate sufficient genome coverage to create an assembly, the sequence data may not be accessible to translated searches. The creation of project-BLAST by Dr Martin Taylor, using hardware available at the HGMP, allows immediate access to sequence traces as and when they are released. Using these databases, it was possible to identify and characterise melanocortin receptor genes and MCH receptor genes from three fish species before the release of a genomic assembly. The success of this strategy, in terms of speed and cost, makes it attractive to apply to other gene families and species, however this depends on the large-scale genome sequencing efforts of others.

The African clawed frog, *Xenopus laevis*, is an excellent model organism for studying embryonic development and cell biology. Pigment dispersal and aggregation in *X. laevis* melanophores has also been studied (Abe *et al.*, 1969a; Abe *et al.*, 1969b; Daniolos *et al.*, 1990; Potenza and Lerner, 1992). However, *X. laevis'* usefulness as a genetic model is limited by a long generation time and its allotetraploid genome (Bisbee *et al.*, 1977). A frog better suited to genetic approaches is *Xenopus tropicalis*, close relative of *X. laevis* (de Sa and Hillis, 1990). *X. tropicalis* shares virtually all of *X. laevis*' advantages as an experimental system. In addition, it features a much shorter generation time, and a smaller diploid genome (Tymowska and Fischberg, 1973). These features inspired a joint initiative to sequence the *X, tropicalis* genome. There is currently over 5Gb of genome sequence publicly available, with 6-8X coverage predicted by 2006 (www.xenbase.org). During this time, a Zebedee mediated search for melanocortin and MCH receptors in *X. tropicalis* would be highly informative. Not only does amphibia occupy a key phylogenetic position between mammals and fish, but the identification of these receptor genes would complement the work already done in *X. laevis* melanophore signalling. The advantage of a genetically characterised melanophore assay system is further discussed in Chapter 4.

The prospects of using *in silico* methods to identify melanocortin or MCH receptors in yet more distant vertebrates seem slim. The smallest cartilaginous fish genome is around 8 times larger than the compact *Fugu* genome (Gregory, 2001) making it an unlikely candidate for genome sequencing. Subsequent to the work described here, a single melanocortin receptor gene (probably *MC4R*) was cloned from the spiny dogfish, *Squalus acanthias* (Ringholm *et al.*, 2003). Therefore at least one melanocortin receptor is present in cartilaginous fish. A more promising candidate may be the lamprey. Lampreys are of the class agnatha that diverged from the jawed gnathostome lineage around 560Mya, making them among the most primitive extant vertebrates. Furthermore, lamprey genomes are more akin to the zebrafish in size and they have been used as a model of vertebrate development and endocrinology (Sower and Kawauchi, 2001; Kuratani *et al.*, 2002). It is probable that at least some melanocortin and MCH receptors are present in lamprey, as both hormones have been identified (Baker, 1993; Takahashi *et al.*, 1995a; Takahashi *et al.*, 1995b). Lampreys have also been shown to have neural crest derived melanophores that can undergo melatonin induced colour

change (Joss, 1973; McCauley and Bronner-Fraser, 2003). However, until a decision is made on when (or indeed if) a primitive vertebrate genome is to be sequenced, any attempts to identify melanocortin or MCH receptor genes will have to utilise more traditional methods.

Having established that the urochordate *Ciona savignyi* is lacking genes encoding melanocortin or MCH receptors and that primitive vertebrates probably possessed them, investigation of an organism that diverged from the vertebrate lineage after urochordates would be informative. The cephalochordate amphioxus (*Branchiostoma*) is the closest living invertebrate relative of vertebrates, and an established model for studying body plan evolution (Garcia-Fernandez and Holland, 1994). Furthermore, it has been reported that amphioxus does have a primordial neural crest but, unlike vertebrate neural crest derivatives, its cells do not differentiate and migrate into melanophores (Shimeld and Holland, 2000; Holland and Holland, 2001). Although brief analysis of a recently published catalogue of almost 10,000 amphioxus ESTs failed to reveal any melanocortin or MCH receptor sequences (Panopoulou *et al.*, 2003), the lack of available genome sequence traces means the presence of these genes cannot be ruled out. However, because of its position near the root of the vertebrate tree, it is likely that the amphioxus genome will be sequenced in the near future.

2.6.2. The evolution of melanocortin and MCH receptors

The data presented in this chapter proves that the entire MC and MCH receptor families were present before the divergence of the ray-finned fish from the tetrapod lineage around 450 million years ago. The same search methods failed to find melanocortin or MCH receptors in the genomes of the invertebrates *Anopheles gambiae, Drosophila melanogaster*, *Caenorhabditis elegans* and *Ciona intestinalis*, suggesting this sub-family of 7 transmembrane GPCRs may be vertebrate specific. However, there are differences between the teleost and mammalian gene repertoires: zebrafish has duplicate *mc5r* and *mchr1* genes while *Fugu* is lacking *MC3R*. How and when duplications and losses may have occurred will now be discussed.

Independent of the efforts to identify zebrafish melanocortin receptor genes described here, Ringholm and colleagues characterised zebrafish *mc4r*, *mc5ra* and *mc5ra*, using a

genomic library to aid identification (Ringholm *et al.*, 2002). As well as confirming the sequences for each of the genes, their mapping data concurs with the results described here. They find no conserved synteny between mammalian and zebrafish *MC5R*, largely because they have not mapped the closely linked zebrafish *mc2r* gene. They do, however, agree that the paralogous *mc5r* genes are probably a result of a duplicated chromosome. This is consistent with a hypothesis of tetraploidization in the teleost lineage (Amores *et al.*, 1998; Taylor *et al.*, 2003). Although it is possible that multiple gene duplications could have could have occurred independently, if this were the case then one would not expect to find multigene blocks of parology. Fourteen such paralogous genome regions have now been reported in zebrafish (Gates *et al.*, 1999; Postlethwait *et al.*, 2000; Barbazuk *et al.*, 2000; Taylor *et al.*, 2003) including LG 16 and LG 19, on which seven other paralogous pairs colocalise with *mc5ra* and *mc5rb*. However, consistent with single *MC5R* and *MCHR1* orthologues in pufferfish, analysis of the *Fugu* genome fails to find similar numbers of duplicated genes (Elgar *et al.*, 1999; Aparicio *et al.*, 2002). Therefore to explain the existence of duplicate genes in zebrafish but not in *Fugu*, one must either accept that large-scale gene loss in pufferfish occurred after a teleosts became tetraploid (Taylor *et al.*, 2003), or believe zebrafish underwent tetraploidization after divergence from pufferfish (Robinson-Rechavi *et al.*, 2001a). Although it is clear lineage specific genome duplications have occurred in some teleost fish (Uyeno and Smith, 1972; Ferris and Whitt, 1977; Ludwig *et al.*, 2001), the compactness of the *Fugu* genome stands testament to its genomic plasticity since divergence from zebrafish, suggesting large-scale gene loss is not impossible. Indeed, the absence of *MC3R* in pufferfish is the first definitive example of melanocortin receptor loss in any species. While proponents of each theory continue debate the matter (Taylor *et al.*, 2001; Robinson-Rechavi *et al.*, 2001b), it appears that, irrespective of when teleost tetraploidization occurred, some zebrafish duplicate genes were maintained (*mc5r* and *mchr1*) while others were first duplicated then lost (e.g. *mc2r*). The potential functional consequences of this are further discussed in Chapter 2.5.3.

It is clear that teleost melanocortin and MCH receptors are informative examples of zebrafish specific gene duplications, but does their identification shed light on the evolution of each gene family? It has been argued that evolution of vertebrate genomes involved multiple large-scale gene duplications (Ohno, 1970). Proponents of this so called "2R hypothesis" suggest that two separate rounds of large-scale duplication took

place in the vertebrate lineage, resulting in as many as four copies of a vertebrate gene from each pre-vertebrate ancestor (Ohno, 1970; Holland *et al.*, 1994; Panopoulou *et al.*, 2003). Although there is extensive debate over the scale and time of the proposed duplications (Friedman and Hughes, 2001; Hughes *et al.*, 2001; Pennisi, 2001; Larhammar *et al.*, 2002) paralogous chromosomal regions within, and synteny between vertebrate genomes are consistent with the hypothesis (Lundin, 1993; Burt *et al.*, 1999; Postlethwait *et al.*, 2000; Popovici *et al.*, 2001). So is there evidence that the evolution of melanocortin and MCH receptor gene could have been shaped by 2R?

With only two members to compare in the vertebrate lineage, one can only speculate about the genome changes that generated the MCH receptor family, but the five melanocortin receptor genes do show a phylogeny consistent with both large and small scale duplications. Figure 2.6.1a is a simplified tree representing the melanocortin receptor gene phylogeny with high bootstrap support. It is clear that *MC2R* and *MC5R* are evolutionarily distant, yet they in close physical proximity in human, mouse, *Fugu* and zebrafish. These genes could have resulted from a local gene duplication of the ancestral melanocortin receptor, prior to any hypothetical tetraploidization event. Subsequent large-scale duplications could then have generated *MC3R*, *MC4R* and *MC5R* from one of those duplicates and *MC2R* and *MC1R* from the other (Fig. 2.6.1b). If there are functional pressures maintaining the *MC2R/MC5R* synteny, this would be relaxed in the duplicates allowing their dispersal through the genome. If there were two rounds of tetraploidization, then three duplicates must have been subsequently lost (Fig 2.6.1b). However, it is equally possible that duplications were large-scale, involving multiple chromosomes, but not whole genomes. Although the origin of melanocortin receptors will probably remain in the realm of supposition unless a primitive vertebrate with a subset of genes is discovered, evidence is mounting for this hypothesis. Schioth *et al* recently reported the mapping of melanocortin receptor genes in chicken, illustrating conserved synteny between mammalian and avian genes including the *MC5R/MC2R* linkage (Schioth *et al.*, 2003). They also propose the receptors evolved through a combination of small-scale duplications and tetraploidization events, citing paralogon analysis as evidence. They show that all the human melanocortin receptors are found on the 8q/16q/18/20q paralogon (Popovici *et al.*, 2001)

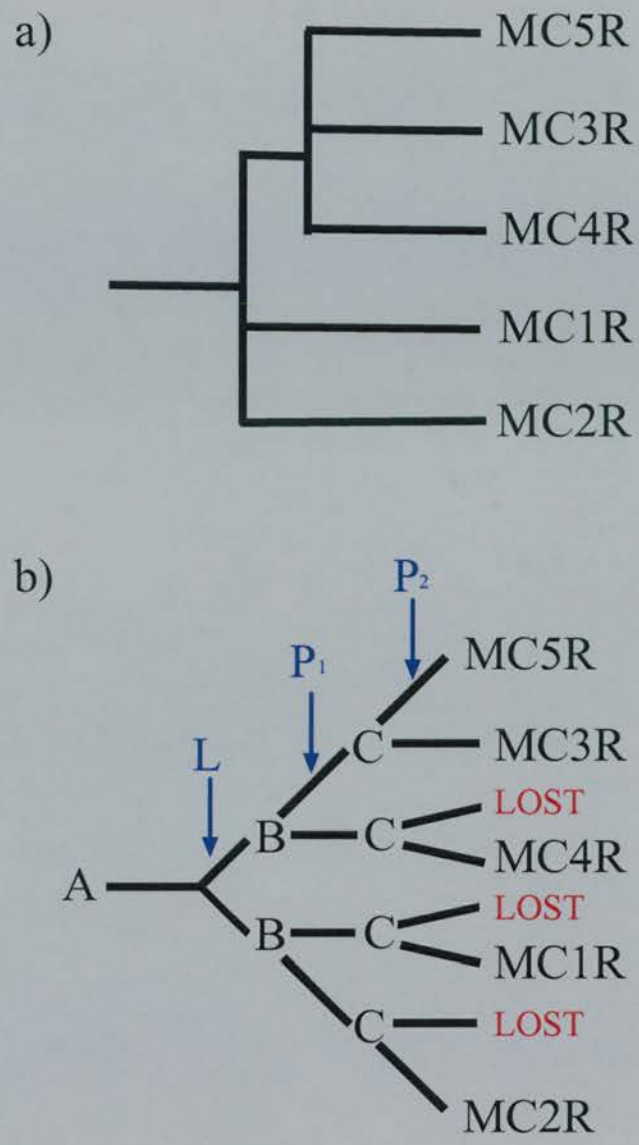

Figure 2.6.1. Large and small scale gene duplications shaped the melanocortin receptor gene family. **a,** a simplified representation of melanocortin receptor protein sequence phylogeny, based on Figure 2.2.1. **b,** A hypothetical scheme for vertebrate melanocortin receptor evolution where the ancestral receptor (A) underwent one local duplication (L) and two tetraploidization events (P). Note that the positions of MC3R, MC4R and MC5R are interchangable.

suggesting large-scale duplication must have taken place. This, of course, is analogous to the more recent melanocortin receptor gene duplication in zebrafish described here. Schioth *et al* concludes that the evolutionary origin of melanocortin receptors is reflected, to some extent, by their function. They suggest that *MC3R*, *MC4R* and, more speculatively, *MC5R* have all been implicated in CNS function and are expressed in the brain, while in comparison *MC1R* and *MC2R* have distinct roles in the periphery (Schioth *et al.*, 2003). Although it is tempting to invoke similar functional characteristics as an indicator evolutionary origin, this particular association is somewhat compromised by mammalian *MC5R* being widely expressed in peripheral tissues and having a defined role in exocrine function (Labbe *et al.*, 1994; Chen *et al.*, 1997). However, understanding what function melanocortin and MCH receptors may have in zebrafish provide clues to their origin.

2.6.3. Implications for melanocortin and MCH receptor function

The remarkable conservation of amino acid sequence and synteny between fish and mammalian melanocortin and MCH receptors suggests that, after the family appeared, at least some of receptors have maintained an evolutionarily conserved role in normal vertebrate physiology. But prior to this study, with the exception of the documented effect of melanocortins and MCH on melanophores, evidence of melanocortin or MCH receptor function in teleosts was scarce. However, there does appear to be scope for teleost conservation of other mammalian systems involving melanocortins and MCH. For example, it has been reported that both melanocortins and MCH are expressed in teleost brain nuclei (Bird *et al.*, 1989) and it is becoming clear that some of the systems regulating mammalian food intake are present in fish (Lin *et al.*, 2000; Narnaware and Peter, 2001). Therefore it is very possible that there are melanocortin and MCH receptors involved in teleost energy homeostasis. Furthermore, teleost fish have a functional equivalent of the mammalian adrenal cortex, the interrenal gland, where melanocortin receptor mediated regulation of steroidogenesis could take place (Grassi *et al.*, 1997). To begin to address the question of function, an attempt was made to identify the spatial and temporal expression pattern of each gene. To do this, RT-PCR of mRNA transcripts was

carried out throughout zebrafish larval development and followed with limited *in situ* hybridisation histochemistry.

Based upon the results of melanin translocation experiments (see Chapter 4), one can conclude that there is probably at least one melanocortin receptor and one MCH receptor expressed in zebrafish melanophores. Based solely on phylogeny, zebrafish *mc1r* is the obvious candidate melanocortin receptor and its expression, monitored from 2dpf onwards, is consistent with the development of pigmented melanophores. As there is little evidence of a role for MCH in mammalian pigmentation, choosing a MCH receptor candidate proved more difficult. Like *mc1r*, zebrafish *mchr1b* and *mchr2* are expressed continuously from the earliest time point tested, but *mchr1a* only seems to be expressed in larvae from 4dpf and not in adults. So, DIG labelled *in situ* hybridisation histochemistry (ISHH) analysis was carried out with all four genes in whole embryos at 1-4dpf, but consistently failed to pick up any expression whatsoever. This lack of signal with melanocortin or MCH receptor gene probes is puzzling. Despite being cloned over 10 years ago, there have been no publications describing melanocortin receptor gene expression by ISHH in mammalian or avian embryos. The only ISHH reported using melanocortin receptor genes is on sectioned adult brains using radio-labelled probes (Gantz *et al.*, 1993; Mountjoy *et al.*, 1994; Cerda-Reverter *et al.*, 2003a). Similarly, MCH receptor gene expression has also been monitored in sectioned adult tissue, but not in whole embryos (Tan *et al.*, 2002). Of course, one could argue that these receptors are not expressed in mammalian embryos, but a search of expressed Unigene clusters indicates that *MCHR2* is expressed in fetal brain. Instead, it is likely that whole embryo ISHH with DIG labelled probes is simply not sensitive enough to detect melanocortin and MCH receptor transcripts. A reason for this is not obvious, but it could be because they are expressed at relatively low levels. As is the case with MC1R, other melanocortin and MCH receptor transcripts are very poorly represented in the Unigene dataset (http://www.ncbi.nlm.nih.gov/). Whatever the reason ISHH was unable to indicate which receptors are involved in melanophore function, therefore other techniques were implemented (see Chapter 4).

The zebrafish *mc2r* orthologue is only expressed in adult body tissues, which is consistent with interrenal gland expression. Recent studies have shown the developing zebrafish interrenal primordium first appears at 20-22hpf and begins to produce steroids

two hours later (Hsu *et al.*, 2003). Although *mc2r* expression is not seen until 4 days later it remains possible that it has a similar function in fish as it does in mammals.

Zebrafish *mc3r* and *mc4r* are expressed from 2dpf onwards, making it difficult to predict their function. It is unlikely that these receptors have an exclusive role in food regulation, as zebrafish larvae do not feed until ~5dpf. In addition to cloning and mapping zebrafish *mc4r, mc5ra* and *mc5rb* Ringholm *et al* undertook expression and functional analysis of the receptors. They report that *mc4r* is expressed in zebrafish brain, eye, GI tract and ovaries and that the receptor shares an almost identical pharmacological profile to human MC4R (Ringholm *et al.*, 2002). It therefore appears as if mc4r has a more diverse functional role in fish compared to mammals, where expression is confined to the CNS. Whether this is also true for mc3r is unknown. The similarity in pharmacological profile between human and zebrafish MC4R is remarkable, both showing the highest affinity for βMSH and low affinity for γMSH (Schioth *et al.*, 1996; Ringholm *et al.*, 2002). Since the completion of the work in this chapter, MC4R has been characterised in both goldfish and spiny dogfish MC4R (Ringholm *et al.*, 2003; Cerda-Reverter *et al.*, 2003a). These authors report similar MC4R affinity profiles for melanocortins is these species. Furthermore, Cerda-Reverter *et al* shows that goldfish *MC4R* is expressed in the food-intake control regions of the adult brain and that melanocortin receptor agonists and antagonists influence feeding in a similar manner to mammals. The same authors recently reported the identification of a gene encoding goldfish agouti related protein (*AGRP*) Like mammalian *AGRP*, the teleost gene is expressed in hypothalamic neurons and is upregulated in response to fasting (Cerda-Reverter and Peter, 2003). Together, these data strongly suggest that the role MC4R plays in energy homeostasis is conserved in teleost fish (Cerda-Reverter *et al.*, 2003b). It is possible, however, that teleost MC4R has other roles outside the CNS that are not seen in mammals. Particularly interesting is that there appears to be opposing dorso-ventral gradients of *MC4R* and *AGRP* expression in goldfish skin (Cerda-Reverter and Peter, 2003; Cerda-Reverter *et al.*, 2003a). A potential role for zebrafish mc4r in pigmentation is discussed in Chapter 4.

Predicting a function for fish MC3R is complicated by the absence of the gene in *Fugu*. It is interesting to note that mammalian MC3R is the only receptor that shows high affinity for all melanocortins, including γMSH (Roselli-Rehfuss *et al.*, 1993). In

comparison, the other mammalian receptors have much lower γMSH affinity. As there is no functional γMSH peptide in *Fugu* or zebrafish, or any other teleost (Takahashi *et al.*, 2001), the pressure to maintain a high affinity γMSH receptor would be relaxed. This could explain the absence of MC3R in pufferfish, with another receptor perhaps compensating for its response to the other melanocortins. It would be informative to investigate the tissue expression of *mc3r*, especially in comparison to *mc4r* expression in the brain, to evaluate the importance of this receptor in zebrafish.

The classical model of evolution suggests that, on the rare occasion a paralogous gene survives after a duplication event, one of the genes must have acquired a new beneficial function (Ohno, 1970). Examples of this include the evolution of antifreeze proteins in fish and colour vision in new-world monkeys (Cheng and Chen, 1999; Dulai *et al.*, 1999). However, more recently the duplication-degeneration-complementation (DDC) model has been proposed to explain why more duplicate genes survive than might be expected (Force *et al.*, 1999). Under the DDC model, there is a partitioning of the ancestral gene function between daughter paralogues, often in the context of temporal and/or spatial expression. There is now a growing body of evidence suggesting the DDC model can explain the excess of duplicate genes observed in zebrafish (Pfeffer *et al.*, 1998; Force *et al.*, 1999; Lister *et al.*, 2001). It is therefore possible that both zebrafish *mc5r* and *mchr1* paralogues have undergone DCC and have near identical functions but are expressed in different places or at different times. The evidence available appears consistent with this. *mc5ra* is largely larvae specific while its paralogue is expressed strongly in both larvae and adults. Furthermore, the mc5r paralogues show very similar melanocortin affinity profiles (Ringholm *et al.*, 2002), suggesting there is little functional difference between the two. The mchr1 paralogues show an even more striking difference in temporal expression pattern, though there is no data available on their ligand binding affinities.

2.6.4 The evolution of POMC

The data presented in this chapter demonstrate that both zebrafish and *Fugu* have a single *POMC* gene that codes for teleost equivalents of all the mammalian melanocortin hormones, with the exception of γMSH. Unlike their receptors, melanocortins have been

previously identified in numerous non-mammalian vertebrate species, including ray-finned fish (Kitahara *et al.*, 1988), lobe-finned fish (Amemiya *et al.*, 1999a), cartilaginous fish (Amemiya *et al.*, 2000) and an agnathan (Takahashi *et al.*, 1995b). This is because the hormones can be extracted from pituitaries with relative ease and protein sequencing allows characterisation of the peptides. More recently, the genomic organisation of the melanocortins within the *POMC* locus has been reported for several species, providing insights into the molecular evolution of the gene (Fig. 2.6.2) (Takahashi *et al.*, 2001).

It appears that early vertebrates probably had one or two *POMC* genes each containing γ, α, βMSH and β-endorphin, duplication occurring just before or after the divergence of agnathans from gnathostomes. In lamprey, the two *POMC* orthologues (*POC* and *POM*) underwent internal deletion or degeneration, losing γ and βMSH and γMSH respectively (Fig. 2.6.2). In the sarcopterygian lineage the POMC gene maintained its melanocortin repertoire, as observed in mammals today. In the actinopterygian lineage γMSH has been lost, as demonstrated in zebrafish and *Fugu POMC* (Fig. 2.5.1).

Interestingly, some actinopterygians (including advanced teleosts such as carp and salmonids) have duplicate POMC genes (Okuta *et al.*, 1996; Arends *et al.*, 1998). However, these genes are always sequentially similar and have the same melanocortin content. Phylogenetic analysis (Fig. 2.5.2) suggests that they are probably the result of species-specific tetraploidizations that have been previously documented (Uyeno and Smith, 1972; Ferris and Whitt, 1977; Ludwig *et al.*, 2001); there does not appear to be a *POMC* duplicate in *Fugu* or zebrafish. A novel melanocortin hormone, δMSH, is found in chondrichthyans (McLean and Lowry, 1981; Amemiya *et al.*, 1999b). Sequence analysis suggests this is due to an internal duplication of the 3' end of the gene after which the duplicate βMSH sequence was selected for and evolved into δMSH and the duplicate β-endorphin degenerated (Amemiya *et al.*, 1999b; Amemiya *et al.*, 2000).

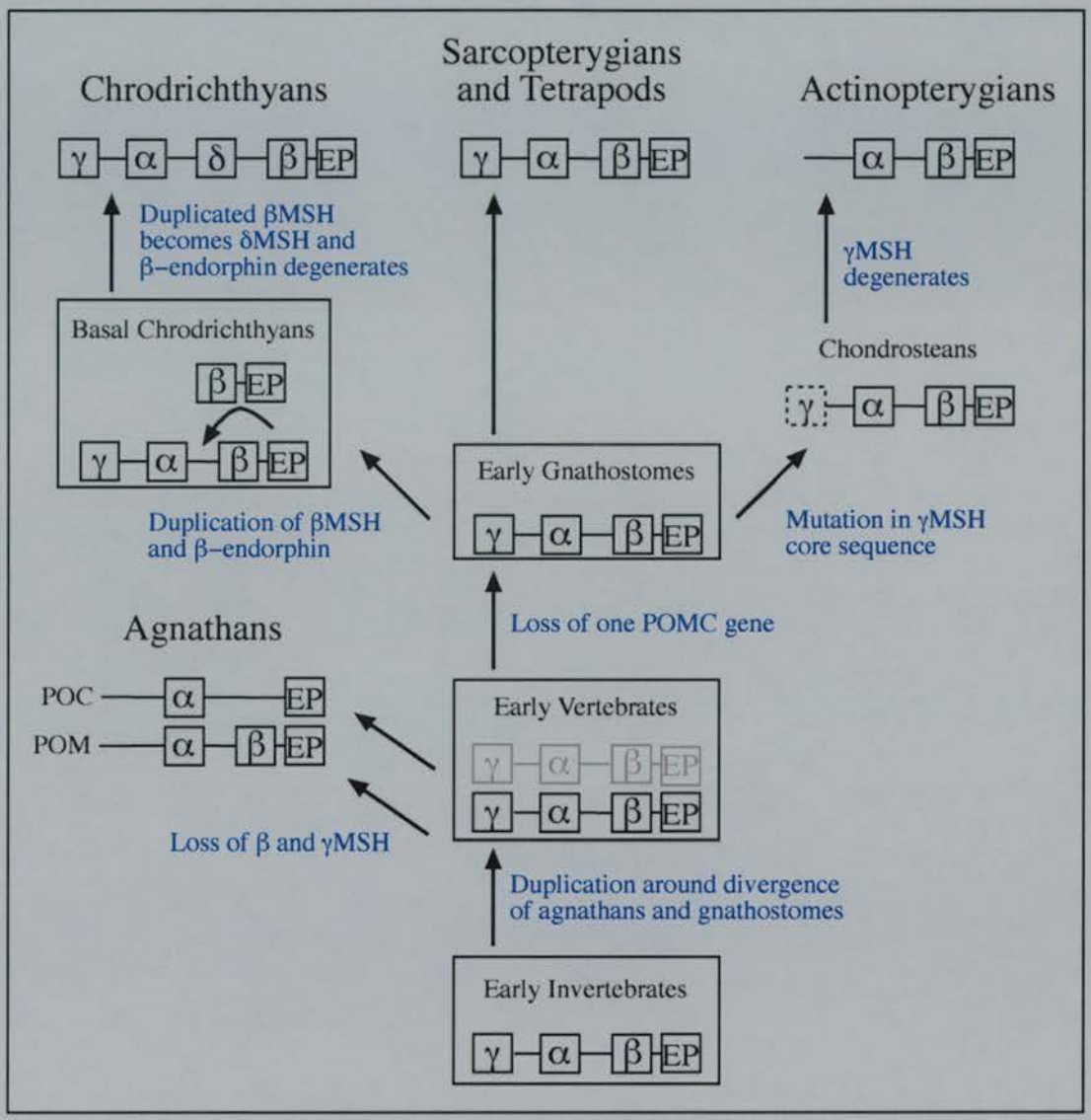

Figure 2.6.2. Evolution of the vertebrate POMC gene. A model for melanocortin (α, β, γ, and δMSH) and β-endorphin peptide (EP) evolution within the POMC pro-hormone. Boxes surround the POMC structure of hypothetical species and unboxed gene structures are based upon extant species. *Blue* text describes the proposed change in gene content. Figure modified from one previously published (Takahashi *et al.*, 2001)

2.6.5 Co-evolution of melanocortins and their receptors?

It appears that the mammalian *POMC* gene content is probably similar to that found in very early vertebrates. This may suggest that the melanocortin receptor repertoire has remained relatively stable throughout this time too. As most of the mammalian melanocortin receptors can bind multiple melanocortin hormones (albeit with different activation profiles), there is unlikely to be a simple co-evolutionary relationship between receptors and *POMC* content. Nevertheless, it is intriguing that *MC3R* is currently the only example of melanocortin receptor loss and it occurred in a teleost, where its most potent ligand (γMSH) is also missing. Considering the differences observed in lamprey and elasmobranch melanocortin content, it would be very interesting to characterise the melanocortin receptor family in these species to see whether there is an associated change in receptor number.

It is likely that the ancestral *POMC* gene arose through internal duplications, with a single melanocortin pharmacore giving rise to α, β and γMSH in a similar manner to how δMSH arose later. One might propose that this diversification of melanocortins coincided with the expansion of the melanocortin receptor family in an early vertebrate, since examples of receptor genes could not be found in invertebrates (see Chapter 2.6.2). It is therefore surprising that a *POMC* gene has been identified in three invertebrate species, a leech (*Theromyzon tessulatum*), a flatworm (*Schistosoma mansoni*) and the blue mussel, *Mytilus edulis* (Duvaux-Miret *et al.*, 1990; Salzet *et al.*, 1997; Stefano *et al.*, 1999). Moreover, the three ancient melanocortins peptides (α, β, and γMSH) are encoded in these genes in the same sequential order as in vertebrates (Fig 2.6.2), suggesting the invertebrate and vertebrate *POMC* genes have the same origin. As both *T. tessulatum* and *S. mansoni* are vertebrate parasites, it was proposed that *POMC* appeared in these species by horizontal transfer from a vertebrate host, possibly through a viral mechanism (Duvaux-Miret *et al.*, 1990; Salzet *et al.*, 1997). However, *M. edulis* is a free-living bivalve mollusc, making it less likely that its *POMC* gene is of vertebrate origin. The functional role of melanocortins in invertebrates is not yet clear, but they appear to be expressed in haemocytes, and are therefore thought to have a role in immune regulation (Stefano *et al.*, 1999). G-protein coupled receptors are notoriously

promiscuous in their ligand binding (Pierce *et al.*, 2002). Thus it may be that invertebrate melanocortins do not have exclusive receptors and the melanocortin receptor family appeared subsequent to the origin of the vertebrate pituitary, when melancortins evolved into endocrine signalling molecules. However, until the mechanism of invertebrate melanocortin function is elucidated, it remains possible that the melanocortin receptor family predates the divergence of vertebrates from invertebrates, as it appears POMC does. The fact that neither POMC nor melanocortin receptors are found in *Drosophila*, *Anopheles*, *C.elegans* or *Ciona savignyi* may simply imply that the melanocortin system has been lost some invertebrate lineages.

2.6.6. pomc expression in the developing zebrafish

Zebrafish *pomc* expression proved to be an excellent tool for studying the morphogenesis of the teleost adenohypophysis. The gene is first expressed in cells in the pituitary anlage at the anterior neural ridge in 24 hpf larvae. These cells first moved medially, then to the posterior, becoming organised and patterning the mature pituitary along the AV axis (see Fig. 2.5.4 and 2.5.5). Independent of the analysis reported in this chapter, two studies characterising zebrafish *pomc* were published (Herzog *et al.*, 2003; Hansen *et al.*, 2003). Hansen and coworkers identified the gene using similar *in silico* methods. They went on to map the gene, characterise its melanocortin content and carry out phylogenetic analysis, in each case arriving at the same conclusions as described here. Hertzog *et al.* cloned zebrafish *pomc* from RNA, along with genes encoding other pituitary hormones including prolactin (*prl*), thyroid stimulating hormone (*tsh*) and growth hormone (*gh*). They then carried out a very elegant study of pituitary development using the hormones as ISHH markers for each of the adenohypophyseal cell types. Their findings are in agreement with data discussed in Chapter 2.5.2, except they do not report any otic vesicle expression. They do confirm, however, that the zebrafish anterior pituitary is patterned along the AP axis by showing the zone between the two *pomc* expressing domains contain *gh* expressing somatotropes and *tsh* producing thyrotropes (Herzog *et al.*, 2003).

A further report by the same researchers describes the characterisation of transgenic zebrafish expressing green fluorescent protein (GFP) from the *pomc* promotor (Liu *et al.*, 2003). The GFP expression pattern is almost identical to that observed by ISHH, but

there are some differences. They suggest that bilateral GFP expression is observed at the anterior neural ridge by 20 hpf, slightly earlier that is seen by ISHH. This discordance may simply be due to the relative insensitivity of ISHH to low-level gene expression however. Interestingly, Lui *et al* demonstrates the presence of GFP in the otic vesicle of a 20 hpf embryo, but claims this expression later disappears. This is in contrast to ISHH staining pattern, where *pomc* expression is only seen from 72 hpf onwards (Fig 2.5.6). While insensitivity may explain why early otic vesicle expression is not detected by ISHH, it is unlikely that GFP expression would be overlooked in older larvae. How, therefore, can this discordance be explained? One explanation would be that the later otic vesicle *pomc* expression is driven by a regulatory element missing from the GFP transgene. This is entirely possible, as an immunohistochemical analysis using antibodies against rabbit melanocortins, showed GFP colocalises with ACTH expression but not αMSH expression in the adenohypophysis of 13 day-old transgenic fish (Liu *et al.*, 2003). This is perhaps unexpected, as the corresponding *Pomc* promotor region in mouse drives reporter gene expression in both cell lineages (Liu *et al.*, 1992) and there is a well-defined mechanism for control of melanocortin peptide production by regulation of prohormone convertases (Marcinkiewicz *et al.*, 1993). Nevertheless, this data suggests there are probably different regulatory elements driving *pomc* expression in zebrafish corticotrophs and melanotrophs. Liu and colleagues' analysis also sheds light on the relative position of different *pomc* expressing cell types in the pituitary. It appears that, as previously suggested, the anterior *pomc* expression domain consists entirely of ACTH expressing cells (corticotrophs). However, the posterior domain appears to be sub-patterned again along the AP axis, with melanotrophs towards the anterior and corticotrophs at the posterior (Liu *et al.*, 2003). The mechanism through which this cellular pattern emerges from the disorganised cell mass seen before 48 hpf (Fig. 2.5.5c, d) is not clear, but time-lapse experiments using the *pomc*-GFP transgenic fish, may resolve the matter.

It is tempting to propose that because neither the otic vesicle expression nor the melanotroph expression appears to be driven off the promotor driving GFP in corticotropes, both domains are primarily producing αMSH. That, however, is not necessarily the case because GFP is not expressed in arcuate nucleus either, where β-endorphin is the primary product. Nevertheless, based on data from experiments in mammals, one might argue that a melanocortin is the most likely product of *pomc*

expression in the ear. Treatment with melanocortins have been shown to protect against cisplatin induced ototoxicity in guinea pigs (Heijmen *et al.*, 1999). However it is not known whether there is endogenous melanocortin expression in the mammalian ear, nor is the mechanism though which this protection occurs known (Smoorenburg *et al.*, 1999). The melanocytes of the stria vascularis are essential for normal ear function (Steel and Barkway, 1989) where they are thought to maintain a potassium gradient in the endolymph (Di Palma *et al.*, 2002), but there is debate over whether the melanin content of strial melanocytes effects their otoprotective function. Some reports suggest eumelanin protects against noise induced trauma, but phaeomelanin does not (Barrenas and Holgers, 2000) while others suggest difference in melanin content does not explain variable otoprotective qualities (Bartels *et al.*, 2001). Thus it currently unresolved as to whether melanocortin induced melanogeneis has functional role in strial melanocytes, but could there be a similar system in the zebrafish ear? It seems unlikely, as there are no visible pigmented melanophores present in wild-type fish and zebrafish does not have strictly defined stria vascularis. However there is preliminary evidence of some neural crest derived cells present in the zebrafish otic vesicle that, under certain conditions, can be driven down a pigmented melanocyte lineage (Kelsh, R; personal communication). Therefore there may be unpigmented melanoblast present in the otic vesicle on which melanocortins could act. Work is underway to identify the nature of these cells.

2.7 Conclusions and future directions

This chapter describes the identification, mapping and expression of the full complement of melanocortin and MCH receptors in three species of teleost fish. These were the most primitive species in which the receptors have been identified until recently, when a single receptor gene was cloned from spiny dogfish (Ringholm *et al.*, 2003). RT-PCR analysis shows all the genes are expressed in larval zebrafish, though *in situ* hybridisation histochemistry analysis failed to detect spatial expression patterns. The receptor gene families show evidence of having been shaped by both small and large-scale gene duplications, both in early vertebrates and in the teleost fish lineage. These genome changes probably resulted in the expansion of the melanocortin receptor repertoire from a single ancestral gene in a primitive vertebrate, or even invertebrate species, to a complete five-member family before the divergence of ray-finned fish from

tetrapods. Then, in the teleost lineage, further large-scale duplications took place, probably in form of a tetraploidization event. This resulted in an expanded repertoire of both melanocortin and MCH receptors in zebrafish, with the duplicated genes probably having complementary functions. Also reported is the first example of a species with less than five melanocortin receptors, the pufferfish *Fugu rubripes* and *Tetraodon nigroviridis* are both lacking a *MC3R* gene.

This chapter also describes the identification and expression analysis of zebrafish *pomc*, the melanocortin hormone precursor gene. Consistent with other actinopterygian *POMC* genes, both zebrafish and *Fugu* lack γMSH, but they do encode α and βMSH as well as β-endorphin. Expression analysis of zebrafish *pomc* reveals it to be a robust marker for anterior pituitary development. By following the migration of pomc expressing cells in larvae, it is clear that the morphogenesis of zebrafish pituitary occurs in a different manner to that seen in mammals. In addition, this chapter reports the first example of a discrete set of *pomc* expressing cells in the developing vertebrate ear.

It is clear that melanocortins, their receptors and MCH receptors are good candidates for involvement in a range of processes in fish, including background adaptation and feeding regulation, and that their identification in zebrafish provides an excellent system in which to further investigate their function. Radioligand binding assays and transfection into mammalian cells will reveal the functional characteristics of each receptor (Ringholm *et al.*, 2002) and morpholino knockdown of zebrafish *pomc* may provide clues to the range of processes mediated by melanocortin receptors during development in the fish (Nasevicius and Ekker, 2000). By matching the phenocopy of individual melanocortin receptor morphants with that observed in *pomc* morphants, a functional role for each receptor could be identified.

The discovery that zebrafish *pomc* is strongly expressed in cells in the earliest stages of the pituitary primordium makes it an excellent marker for studying developmental processes (Herzog *et al.*, 2003). It could be used, in conjunction with other pituitary markers, to study mutant zebrafish strains with defects in oral cavity formation, brain development or with midline deformations. Furthermore, finding *pomc* expressing cells in the otic vesicle could develop into a potentially interesting line of work. While the

nature of these cells is currently unknown, a thorough histological examination should define their position and perhaps their function.

The melanin-concentrating hormone signalling system is much less well understood than the melanocortin system. Preliminary studies suggest there may be duplicate *MCH* genes in zebrafish and *Fugu* (data not shown). A more thorough analysis of these genes, followed by ISHH may illustrate the role of MCH in teleost fish and indicate whether it is important in processes other than regulating pigmentation. In addition, the discovery of a recently duplicated *mchr1* gene provides the opportunity to investigate potential sub-functionalisation. Thus the influence of *mchr1a* and *mchr1b* on different tissues or at different stages of development may be researched independently in zebrafish, something that would prove more complex in mammalian models.

In conclusion, the identification of the teleost genes described in this chapter not only provides an insight into the evolution of their mammalian orthologues mammals, but provides a whole new model in which to investigate their function. With respect to melanogenic research, it is now possible to revisit the pioneering work in the field, the study of pigment translocation in lower vertebrates, using a system that is genetically amenable. Chapter 4 discusses the further development of such an experimental system.

Chapter 3

The Evolution of Rhodopsin-like G-Protein Coupled Receptor Genes

That great tragedy of Science –
the slaying of a beautiful hypothesis by an ugly fact.

T. H. Huxley
Collected Essays, Biogenesis and Abiogenesis

3.1 Preface

The G-protein coupled receptors (GPCRs) are a large super-family of membrane spanning proteins that transduce extra-cellular signals by the activation of GDP-GTP exchange on heterotrimeric G-proteins. These can then activate or inhibit a number of effectors including adenylyl cyclases, ion channel and phospholipases (Pierce *et al.*, 2002). GPCRs are activated by a diverse range of ligands and have evolved to regulate many cellular functions. Their dysfunction results in various pathologies, and they are the targets of over half of the therapeutics currently used (Pierce *et al.*, 2002; George *et al.*, 2002). As they are found in most eukaryotic species (including diploblasts, yeasts, plants, invertebrates and vertebrates) and are widely thought to be the largest single family of proteins (Baldwin, 1994; Strader *et al.*, 1994), GPCRs provide an opportunity to study the evolution of gene structure within a single super-family. Interestingly, the repertoire of genes encoding GPCRs in both mouse and humans are reported to have an unusual feature. It appears that large numbers of GPCR encoding genes in these species contain no introns, in contrast to the GPCR encoding genes in *Drosophila* and *C. elegans*, neither of which have been reported as being enriched in intronless genes (Gentles and Karlin, 1999; Brody and Cravchik, 2000). However, these observations have not been qualified by a genome wide analysis of GPCR gene structure in any species other than *Saccharomyces cerevisiae*, which has only two (intronless) genes (Goffeau *et al.*, 1996).

In Chapter 2, two unusual pufferfish GPCR-encoding genes are discussed. *Fugu MC2R* and *MC5R* have introns identical in position and phase, but their mammalian and zebrafish orthologues are intronless. The other two members of this family in *Fugu*, and all members in all other species examined thus far lack introns in the coding region. As the divergence of *MC5R* and *MC2R* probably preceded that of other family members, it seems likely that this intron was present in an ancestral melanocortin receptor gene but was subsequently lost by most of the derived family members (Chapter 2.3.2). While this particular example provides evidence for GPCR intron loss during vertebrate evolution it, like other studies of specific intron loss or gain, covers only a small group of closely related paralogues in a few species (Perler *et al.*, 1980; Kersanach *et al.*, 1994; Logsdon, Jr. *et al.*, 1995; Venkatesh and Brenner, 1997; Frugoli *et al.*, 1998; Venkatesh *et al.*,

1999). For an intron to be accurately mapped, the coding sequence it interrupts must be conserved at the protein level. While this is often the case in orthologous genes that show high amino-acid identity throughout, it is uncommon for large gene families to have a recognisable, conserved domain that is interrupted by an intron. Although the Fugu MC5R and MC2R proteins are only about 40% identical, it was possible to conclude that their genes contained an intron with a common origin. This is because in both genes the intron is found between the second and third bases of the codon for a conserved Arg, located within a conserved sequence motif (the E/DRY cage). This motif is conserved in the majority of rhodopsin-like GPCRs (Dohlman *et al.*, 1991; Baldwin *et al.*, 1997) where it has been shown to be important for receptor activation (Ballesteros *et al.*, 1998 ; Oliveira *et al.*, 1994; Scheer *et al.*, 1997; Scheer *et al.*, 2000).

With the provision of extensive genome sequence from *Drosophila*, *C. elegans*, human and mouse (C.elegans Sequencing Consortium, 1998; Adams *et al.*, 2000; International Human Genome Sequencing Consortium, 2001; Venter *et al.*, 2001; Mouse Genome Sequencing Consortium, 2002), it is now possible to undertake a genome wide analysis of GPCRs and compare their intron contents. This chapter compares the intron content from the largest subfamily of GPCRs (Family A, subsequently referred to as GPCR-A) in two vertebrate and two invertebrate species. As the conserved intron seen in *Fugu MC5R* and *MC2R* can be mapped in GPCR-A genes, it is possible to determine whether this intron is found throughout the gene family or if it is restricted to *Fugu* melanocortin receptors. Therefore this chapter details an investigation of introns disrupting the E/DRY cage in six diverse species, and discusses its implications for understanding GPCR intron evolution.

3.2 Creating GPCR-A gene datasets

The work described in this chapter was completed in collaboration with Dr. Robert Bryson-Richardson, who wrote all the UNIX batch scripts. These scripts automated the protein to genome alignment, genome retrieval and intron identification process in the Swiss-Prot/TrEMBL dataset.

3.2.1 GPCR-As from SwissProt and TrEMBL

To generate a dataset of GPCR-A proteins, the Swiss-Prot (v41) and TrEMBL (v24) protein databases were used (Boeckmann *et al.*, 2003). Swiss-Prot is a curated protein sequence database that provides a high level of annotation and a minimal level of redundancy. TrEMBL is a computer-annotated supplement that contains all the translations of EMBL nucleotide sequence entries not yet integrated in Swiss-Prot. To retrieve appropriate sequences from these databases SRS was used to select for certain criteria (Etzold *et al.*, 1996). Firstly, proteins annotated with the rhodopsin-like GPCR super-family InterPro domain, IPR000276 were selected (Apweiler *et al.*, 2000; Mulder *et al.*, 2003). InterPro is a database of protein families, motifs and functional sites in which identifiable features found in known proteins are grouped into domains. IPR000276 defines Family-A GPCRs by signatures and patterns common to all proteins in the family, including the conserved sequence encompassing the E/DRY cage (Attwood and Findlay, 1993; Attwood and Findlay, 1994). There are 7540 proteins annotated with IPR000276 in Swiss-Prot and TrEMBL. These were immediately parsed by annotation. Only proteins annotated as being from human, mouse, *Drosophila melanogaster* and *Caenorhabditis elegans* were required and any sequences described as "partial", "incomplete" or containing a gene "fragment" were disregarded. This left a dataset of 3091 proteins (1512 mouse, 977 human, 175 *Drosophila* and 427 *C. elegans*).

Olfactory receptors account for around 80% of mouse and 50% of human expressed GPCR-As (Glusman *et al.*, 2001; Zhang and Firestein, 2002; Fredriksson *et al.*, 2003). These proteins are largely intronless and are found in clusters, due to an expansion within the vertebrate lineage through duplication and recombination (Ben Arie *et al.*, 1994; Issel-Tarver and Rine, 1997; Glusman *et al.*, 2001; Zhang and Firestein, 2002). As this sub-family expansion is vertebrate specific, and because it has occurred rapidly and through a defined mechanism, the olfactory receptors were removed from the dataset and considered separately in the following experiments. For each of the remaining protein sequences in this dataset, the corresponding genomic sequence was identified using TBLASTN against the whole genome alignment for each organism. Proteins for which there was not a genomic match showing >95% identity over the entire sequence were discounted. Only one protein match was selected from each locus. This purged the dataset of splice forms of the same gene (in these cases the longest isoform was selected)

and also removed duplicate entries. The remaining genomic sequences were then extracted from the genome data using the coordinates of the TBLASTN alignment, together with 5kb flanking sequence. This resulted in a final Swiss-Prot and TrEMBL (SPTr) dataset of 246 human, 232 mouse, 71 *Drosophila*, and 318 *C. elegans* proteins with their corresponding genomic sequence.

3.2.2 GPCR-As from Ensembl

The recent publication of the whole genome sequence of the pufferfish, *Tetraodon rubripes* and the mosquito *Anopheles gambiae* provided a further resource to investigate GPCRs. However, there is a dearth of protein sequences from these species deposited in Swiss-Prot and TrEMBL as only 38 *Fugu* and 3 *Anopheles* sequences that matched the requirements could be identified. Therefore Ensembl predicted protein sequences annotated as containing Interpro domain IPR000276 were used. These were taken from genome assembly releases: *Fugu* v16.2.1 and *Anopheles* v16.2.1 and proteins that were not complete over the length of the 7-TM domain disregarded. Of those annotated as such, 95 *Anopheles* and 347 *Fugu* protein sequences were confirmed as genuine rhodopsin-like GPCRs by alignment with the full-length Pfam model for IPR000276 (Bateman *et al.*, 2002).

Ensembl protein predictions are translations of cDNA transcripts. Therefore, by aligning each transcript with its genomic locus, it was possible to analyse the sequence containing the E/DRY motif for the presence, or absence, of introns. As this Ensembl method of dataset selection differed in some respects from the SPTr dataset, it seemed prudent to compare the two methods. Therefore, a similar selection process was carried on Ensembl *Drosophila* asembly v10.3.1 and *C. elegans* assembly v13.98.1. The *Drosophila* Ensembl dataset contained 99 GPCR-A proteins: a difference of 28 between the two selection procedures. The *C. elegans* Ensembl dataset contained 406 GPCR-A proteins, a difference of 88 (22%). Therefore it is clear that, while the SPTr dataset may contain a representative example of GPCRs, perhaps between 70-80%, it is not exhaustive. However, as the Ensembl dataset has some genes identified by gene prediction algorithms, it remains possible that it overestimates the GPCR repertoire.

3.3. The intron content of the GPCR-A family

3.3.1 Quantitative analysis of intron content

In order to investigate the hypothesis that there has been extensive intron loss throughout evolution of the GPCR family, the total number of introns in the coding sequence of each full-length gene in human, mouse, *Drosophila* and *C. elegans* was determined. Figure 3.3.1a shows that, as previously suggested, the majority of mammalian rhodopsin-like GPCRs are indeed intronless. Over 55% of both mouse and human GPCR-A encoding genes in the dataset have no introns. There is then a progressive decrease in the proportion of genes as the number of introns increases: for example 18% of mouse genes have one intron, 9% have two, 5% have three and so forth. This is in contrast to the intron content of *Drosophila* and *C. elegans* GPCR-A genes in the dataset. Both invertebrates species show no enrichment of single exon genes, in our dataset *Drosophila* have 7% and *C. elegans* have no intronless GPCR genes. The mean and median GPCR-A intron frequency was then compared to the average frequency of introns reported for each species (Deutsch and Long, 1999) (Fig. 3.3.1b). Far from having a lack of introns, we found that both *Drosophila* and *C. elegans* GPCR-A genes have a significant increase in mean intron number compared to that observed in the rest of the genome (χ^2 test, $P<0.001$). In both cases the genome average is closer to the median value for GPCR-A genes. In contrast, the mouse and human GPCR-A genes in the dataset have a large and significant reduction in mean intron frequency, to ~35% and ~25% of the genome mean respectively (χ^2 test, $P<0.001$). Furthermore, as over half of both human and mouse GPCR-A genes in the dataset are intronless, the median intron content is zero in both species. It is important to note that these quantifications do not include the mammalian olfactory receptors. If these were included, around 90% of mouse and 75% of human GPCR-A genes in the dataset would be intronless.

Although the relative difference in intron content between mammals and invertebrates is both consistent and striking, there could be factors that introduce bias. Intron content measured on a per gene basis does not account for length of the gene. Therefore genes that have shorter coding sequences may be less likely to have introns than those with longer sequences.

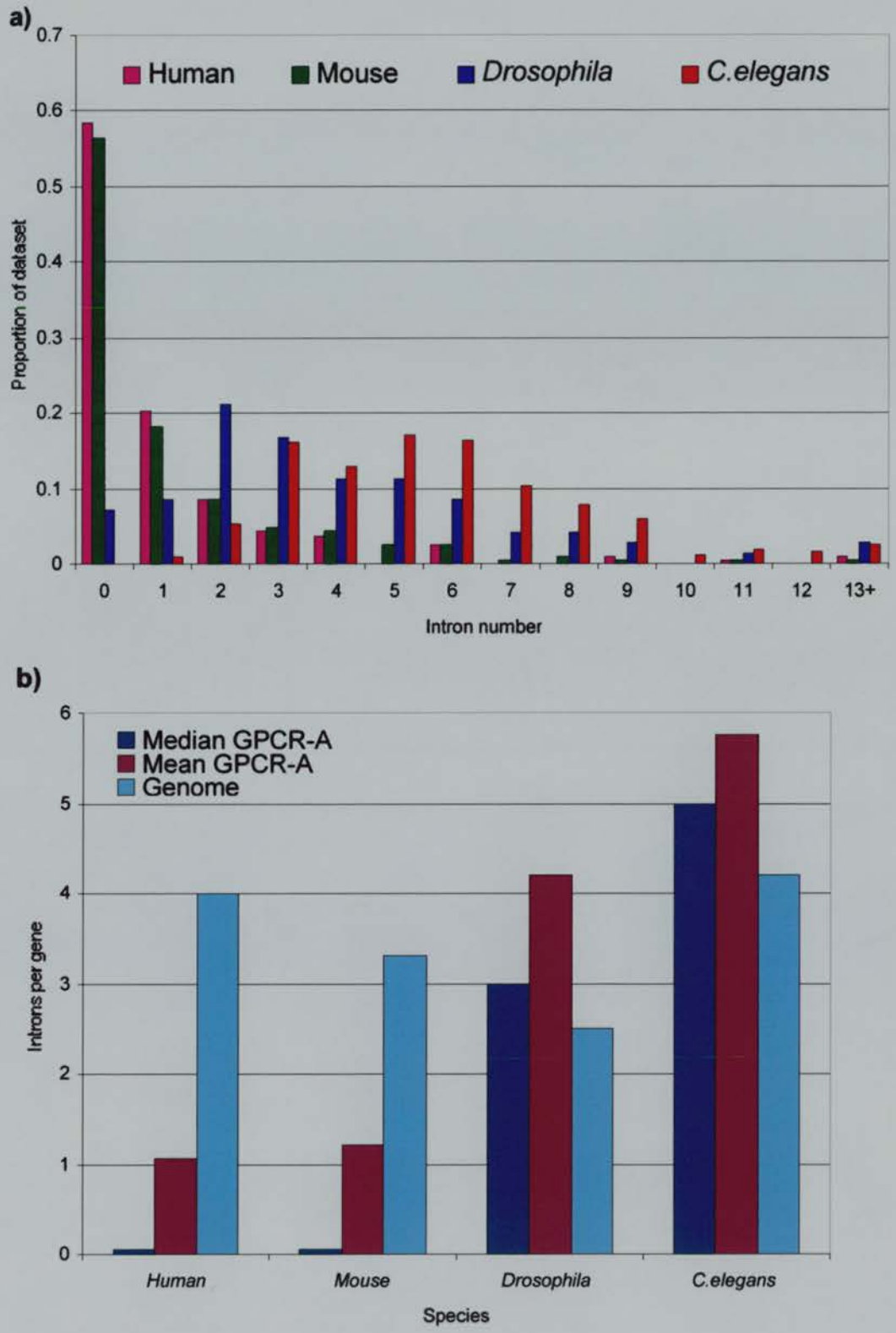

Figure 3.3.1. Intron content of GPCR-As, measured per gene. Only introns interrupting the coding sequence of genes are included. **a**, the distribution of intron number in GPCR-As from four species. **b**, the mean and median values for intron numbers represented in Fig.3.3.1a. The values for whole genomes are published (Deutsch and Long, 1999).

As invertebrate GPCR-As tend to be larger (mean = 442aa) than mammalian proteins (mean = 386aa), gene content measured per Kb of coding sequences would be less biased. Furthermore, it remained possible that the variation observed in intron frequency between species was due to variation in the N-terminal (extracellular) and C-terminal (intracellular) regions. The theory of exon shuffling predicts introns are more likely to be found between units or modules of protein function than within such units (Gilbert, 1987; Gilbert *et al.*, 1997). As the core 7-transmembrane (7-TM) sequence is the most highly conserved region in GPCR proteins, it could be considered a functional protein unit and therefore less likely to contain introns than either terminus. The GPCR termini can be highly variable in sequence and length, not only between divergent proteins, but also between orthologous proteins in different species. If the difference in protein size between vertebrates and invertebrates is due to variable terminal length, then this too may explain the striking difference in intron content.

To address these points, intron quantification was repeated using only the 7-TM regions and the content was calculated per Kb of sequence. Figure 3.3.2a shows that, when the 7-TM regions of proteins in the SPTr dataset are considered alone, there is a similar pattern of intron content as found when using the entire proteins. The increased number of introns seen in invertebrate species, compared to mammals, is therefore not due to introns in terminal regions alone. Figure 3.3.2b illustrates the mean intron content, measured per Kb of coding sequence, of whole GPCR-A genes, the 7-TM regions of those genes and of the genome average. The human and mouse GPCR-As both have around 1 intron per Kb compared to the genome mean of around 5.3 (Deutsch and Long, 1999), representing a highly significant decrease (χ^2 test, $P<0.001$). In contrast, *Drosophila* GPCR-As have an almost identical intron content to the rest of the genome (2.3 introns per Kb compared to 2.2, χ^2 test, $P=0.59$) while *C. elegans* GPCR-A genes have more introns than average (4.7 introns per Kb compared to 3.6, χ^2 test, $P<0.001$). These data show that the relative difference between mammals and invertebrate GPCR-A intron content is not due to gene length. In addition, when the content of the 7-TM regions are represented in a similar format, it is clear that the intron content is the same as the entire gene (χ^2 test, all data $P>0.05$). This quantification suggests that, as previously proposed (Gentles and Karlin, 1999), GPCR encoding genes are bereft of introns in mammals even when the olfactory receptors are discounted.

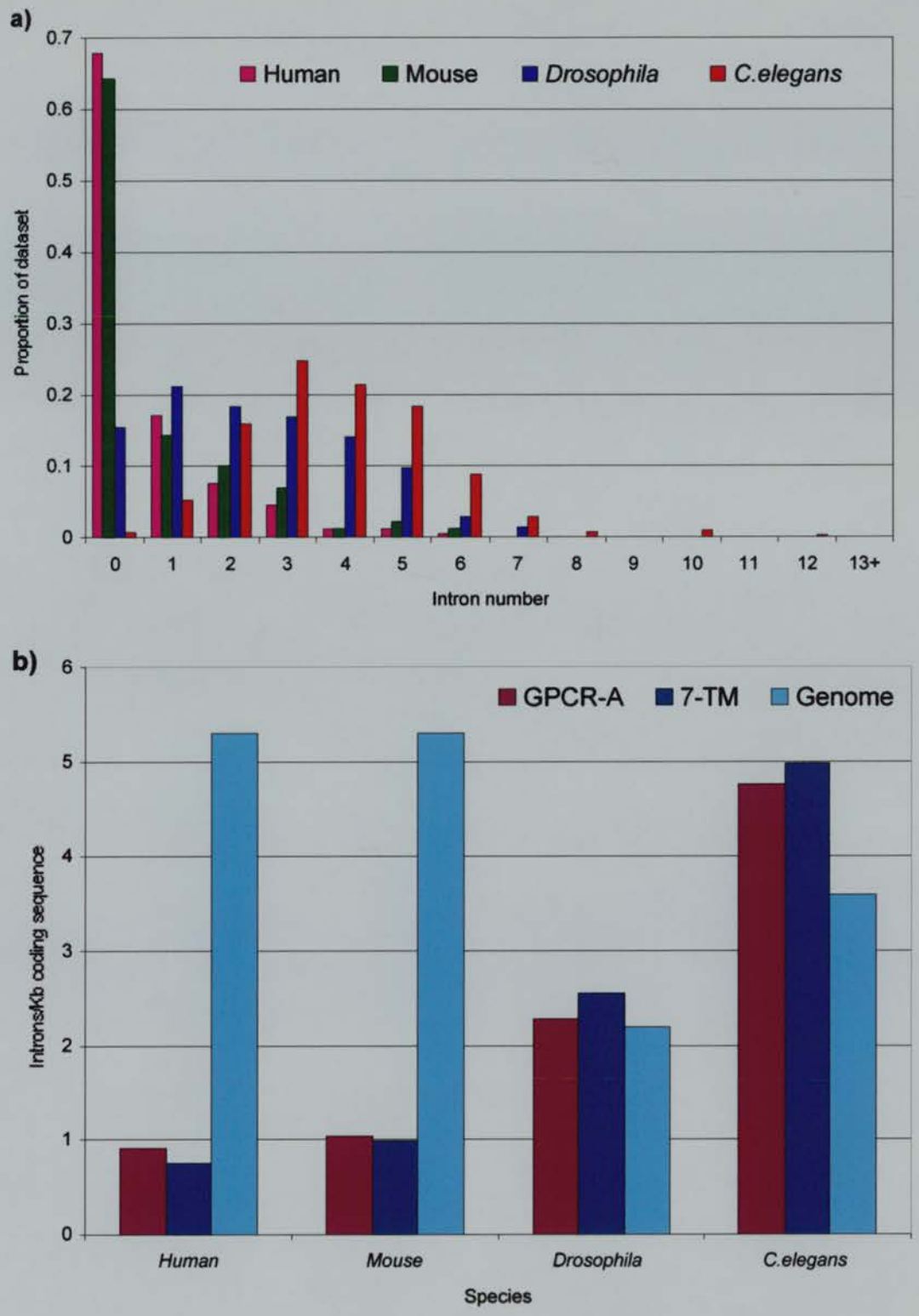

Figure 3.3.2. The intron content of whole GPCR-As and 7-TM regions. Only introns in the coding regions of genes are included. **a,** the distribution of intron number in SPTr GPCR-A 7-TM regions from four species. **b,** the mean value for intron number per kb of whole GPCR-As, 7-TM regions and whole genomes. The values for whole genomes are as published (Deutsch and Long, 1999).

The same is not true for *Drosophila* or *C. elegans*, both of which have GPCR-A intron contents similar to, or greater than, the rest of the genome.

3.3.2 Identification of an intron conserved in GPCR-A genes

The paucity of introns in mammalian GPCR-A genes suggests that introns have been lost in the mammalian GPCR lineage. However it is also possible to argue that the observed differences are due to intron insertion in the *Drosophila* and *C. elegans* lineages. To distinguish between loss or gain of any particular intron, its position must be identifiable. The conserved intron in *Fugu MC5R* and *MC2R* (described in Chapter 2.3.2) is ideal for this purpose. Not only is it found in a conserved functional motif, the E/DRY cage, but it interrupts the Arg codon, which is the only invariant residue in the motif. Therefore, the dataset was analysed for the presence or absence of the conserved intron interrupting the E/DRY cage.

The proteins from each species were aligned and the position of the E/DRY motif within the alignment was identified using Genewise (Birney and Durbin, 2000). All of the genes that contain a phase-2 intron interrupting the conserved Arg (a "DRY-intron") were identified. This comprised 58 genes in the SPTr dataset, some of which were in invertebrates (Tables 3.3.1 and 3.3.2). Of the 318 *C.elegans* SPTr GPCR-As, 13 (4%) have a DRY-intron. To ascertain completeness if the SPTr dataset, it was compared the *C. elegans* Ensembl. In the 406 GPCRA genes in *C. elegans* Ensembl, 19-DRY introns were identified (4.7%), including all the genes in the SPTr dataset (Table 3.3.2). Given the reduction in intron frequency in human and mouse GPCR-As, orthologues of genes containing the DRY-intron were examined in these species to determine whether intron loss had occurred in these lineages. In the SPTr dataset, 17 human and 18 mouse DRY-introns were identified (Table 3.3.1, *black* text). Of these genes containing this intron, 13 orthologous pairs were identified. Where a corresponding orthologue was not present in the SPTr dataset, reciprocal BLAST was used against whole genome assemblies to identify it. This analysis identified 7 further DRY-intron containing genes in mouse and human (Table 3.3.1, *blue* text). These are clearly orthologous genes with conserved genomic structure and sequence, but have incomplete or absent SPTr submissions and were therefore not present in the SPTr dataset.

Table 3.3.1. Vertebrate genes with DRY-introns. Boxed genes indicates orthology and genes in *blue* text were not in the SPTr dataset. Genes that are missing in a lineage are marked (N/A) and orthologues not yet identified are indicated (*). Mammalian genes are named with the SPTr or Ensembl ID included (brackets). Only the five *Fugu* genes with unique DRY-introns are named, otherwise Ensembl IDs are used.

Human	*Mouse*	*Fugu*
HTR4 (ENSG00000164270)	Htr4 (5H4_MOUSE)	SINFRUG00000154525 SINFRUG00000130788
HTR7 (P34969)	Htr7 (5H7_MOUSE)	SINFRUG00000136751 SINFRUG00000132197
BRS3 (P32247)	Brs3 (BRS3_MOUSE)	*
DRD2 (Q9NZR3)	Drd2 (D2DR_MOUSE)	SINFRUG00000122766 SINFRUG00000144962
DRD3 (ENSG00000151577)	Drd3 (D3DR_MOUSE)	SINFRUG00000149153
DRD4 (P21917)	Drd4 (D4DR_MOUSE)	SINFRUG00000141159 SINFRUG00000134728
EDNRA (P25101)	Ednra (ET1R_MOUSE)	SINFRUG00000126554 SINFRUG00000148271
EDNRB (ENSG00000136160)	Ednrb (ETBR_MOUSE)	SINFRUP00000163212 SINFRUG00000133129 SINFRUG00000142012
GALR2 (O43603)	Galr2 (GALS_MOUSE)	SINFRUG00000149324
GALR3 (O60755)	Galr3 (GALT_MOUSE)	*
GRPR (P30550)	Grpr (GRPR_MOUSE)	SINFRUG00000147286 SINFRUG00000152285
NFFR1 (Q9GZQ6)	Nffr1 (Q8BKR6)	SINFRUG00000148491 SINFRUG00000146151
GPR74 (Q9Y5X5)	Gpr74 (ENSMUSG00000035528)	SINFRUG00000146487
TACR1 (P25103)	Tacr1 (NK1R_MOUSE)	SINFRUG00000151158 SINFRUG00000130917
TACR2 (P21452)	Tacr2 (NK2R_MOUSE)	SINFRUG00000139853 SINFRUG00000125465
TACR3 (P29371)	Tacr3 (NK3R_MOUSE)	SINFRUG00000127798
NMBR (P28336)	Nmbr (NMBR_MOUSE)	SINFRUG00000141437
Putative GPCR (O75963)	Putative GPCR ENSMUSG00000040836	SINFRUG00000130429
Putative GPCR (Q14439)	Putative GPCR (ENSMUSG00000040133)	SINFRUG00000124059
GPR73 (ENSG00000169618)	Gpr73 (Q9JKL1)	SINFRUG00000131784
GPR73L1 (ENSG00000101292)	Gpr73l1 (ENSMUSG00000050558)	SINFRUG00000139426 SINFRUG00000145142
MCHR2 (Q969V1)	N/A	SINFRUG00000136750
N/A	Trhr2 (Q9ERT2)	?
		MC2R SINFRUG00000127905
		MC5R SINFRUG00000127904
		ACM3 SINFRUG00000150991
		P2YR SINFRUG00000133368
		GPR10 SINFRUG00000155598

Genome searches for paralogues of those genes already identified revealed only two more DRY-introns, in mouse and human prokineticin receptor 2. When these 9 further genes are taken into account, all but one of 22 DRY-introns identified in mouse are also present in human. The exception is in mouse thyrotropin hormone receptor 2 (*Trhr2*) gene. Although present in the rat and mouse lineage, this gene appears to be absent from the human genome (Itadani *et al.*, 1998; Cao *et al.*, 1998). Additionally, the human melanin-concentrating hormone receptor 2 (*MCHR2*) gene, which does not have an orthologue in the mouse (Tan *et al.*, 2002), also contains a DRY-intron. This analysis failed to find any instances of DRY-intron loss or gain in human and mouse since the divergence of the two species. However it did show that the DRY-intron is not unique to *Fugu* melanocortin receptor genesas the intron is present in about 7% of mammalian non-olfactory GPCR-A genes in the SPTr dataset.

Table 3.3.2. Invertebrate genes with DRY-introns. Boxed genes indicates orthology, shaded genes in *blue* text were not in the SPTr dataset. Genes are labelled with species-specific names or ID numbers. Where different, the SPTr or Ensembl IDs are included in brackets.

Drosophila	*Anopholes*	*C.elegans*
CG6515	GPRTAK1 (ENSANGG00000013698)	Y23H5B.4 (Q9N476)
CG7887	GPRTAK2 (ENSANGG00000015654)	Y69A2AR.15 (Q95XI5)
CG15113 (Q9V8Q3)	GPR5HT1B ENSANGG00000003778	Y49C4A.5 (Q965U4)
CG16720	GPR5HT1A ENSANGG00000016350	C02H7.2 (Q17594)
CG11325	GPRGNR1 ENSANGG00000016873	C24A8.1 (P91096)
CG3171 (Q9NDM2)	GPRMTN ENSANGG00000009167	K09G1.4 (P90927)
CG9569 (Q8IS45)	GPRDOP3 ENSANGG00000003066	F59D12.1 (O17899)
CG31351 (Q8INI7)	GPRNNA3 ENSANGG00000016173	T14E8.3 (Q22490)
CG16752 (Q8SWR3)	GPRNNA16 ENSANGG00000006708	Y37E11AL.1 (Q9N441)
CG7431 (Q9VEG1) CG16766 (Q9VEG2)	GPRNNA4A ENSANGG00000003214	ZK1307.7 (Q09650) C56G3.1 (Q8MQ94)
CG31350 (Q9VG57) CG6989 (Q9VG54) CG6919 (Q9VCZ3)	GPRNNA2 ENSANGG00000016315	F42D1.3 (Q93704) K02F2.6 (O44986) C02D4.2
	GPROP7 (ENSANGG00000015219)	C25G6.5
		F47D12.1
		C52B11.3
		R13H7.2
		T27D1.3

Mouse and man diverged approximately 100 Mya, providing only a relatively short time for evolution of genomic structure to occur. To study DRY-intron gain or loss over a longer evolutionary period, a comparison of orthologous genes in the Diptera *Drosophila melanogaster* and *Anopheles gambiae* was undertaken (Table 3.3.2). Each of the 10 *Drosophila* genes identified in the SPTr dataset has an *Anopheles* orthologue that also contains a DRY-intron. This only amounted to 7 *Anopheles* genes, as there appears to be duplicate orthologues in *Drosophila*. However, a further 5 DRY-intron containing *Anopheles* genes were found in the Ensembl dataset. Of these, 4 have DRY-intron containing *Drosophila* orthologues that were not in our SPTr dataset, the fifth is an *Anopheles* opsin gene (GPROP7) orthologous to *Drosophila Rh3* or *Rh4*, neither of which contain the DRY-intron (Carulli *et al.*, 1994). To investigate possible examples of *Drosophila* genes with a DRY-intron that are not in the SPTr dataset, but have an *Anopheles* orthologue without the intron, the Ensembl *Drosophila* dataset was searched. This dataset contained all 10 DRY-intron containing genes in the SPTr dataset, plus the four orthologues of *Anopheles* DRY-intron containing genes described above. No other DRY-introns were identified. This suggests the entire repertoire of DRY-intron containing genes has been identified in *Drosophila* and there is a single, confirmed example of DRY-intron change since the divergence of *Drosophila* and *Anopheles* approximately 250 Mya.

In order to investigate the loss or gain of DRY-introns between vertebrates more distant than human from mouse, a similar search for DRY-introns in GPCR-A genes in *Fugu* Ensembl was undertaken. Of the 347 genes in the dataset, 37 DRY-intron containing genes were identified (Table 3.3.1). Reciprocal BLAST searches suggest 32 of these have clear mammalian orthologues that also contain a DRY-intron. However, as well as the *MC5R* and *MC2R* genes, three further examples of DRY-intron loss/gain were uncovered. These are in a *Fugu* P2 purinoceptor gene (SINFRUG00000133368), a M3 muscarinic acetylcholine receptor gene (SINFRUG00000150991) and an orthologue of the mammalian *GPR10* gene (SINFRUG00000155598).

3.3.3 Phylogenetic analysis of DRY-intron distribution

Having established that conserved DRY-introns are present in GPCR-A genes from a range of species, it is also clear that either gain or loss of the intron has occurred between

some orthologous genes. To further explore the evolution of the DRY-intron in this gene family, a phylogenetic analysis using the SPTr protein dataset was undertaken. Figure 3.3.3 is a p-distance tree showing the relationship between all family members. It clearly shows that the DRY intron is present in distantly related members of the family. There are two possible explanations for the presence of an identical genomic structure at the E/DRY cage such a diverse range of genes. It could be that the intron was present in the common ancestor of these genes and has been lost in the other members of the family. The alternative would be the independent origin, on multiple occasions, of an intron in the same position and phase throughout the GPCR-A family.

Closer inspection reveals that, in some cases, genes that encode smaller subfamilies of receptors do share the common intron (Fig. 3.3.4). For example, analysis of the mammalian neurokinin receptor subfamily demonstrates that all three human receptor genes have the DRY-intron, as does their murine orthologues. The most closely related protein to this subfamily is encoded by the *Drosophila* CG7887 gene which also contains the DRY-intron (Fig. 3.3.4a). An associated clade contains genes without the DRY-intron, including human and mouse GPR10. It is interesting to note that the *Fugu* GPR10 orthologue does contain a DRY-intron (Table 3.3.1), suggesting the other genes is this clade may have lost it. A similar observation can be made in the endothelin/bombesin receptor sub-family (Fig. 3.3.4b). The three human bombesin receptors that each contain the DRY-intron group together, with their murine orthologues, into a single clade. A related clade contains the human and mouse endothelin receptors. However within each of these clades there are other sequences that do not contain DRY-introns. A further associated clade contains the *Drosophila* CG6515 protein (with DRY-intron). Discounting multiple, independent intron insertion events, this would suggest that an ancient ancestor of neurokinin and endothelin/bombesin subfamilies had a DRY-intron that has been subsequently lost in some descendants (the endothelin-like receptors for example) but maintained in others.

A proposed model of intron insertion holds that there are "proto-splice" sequences that are preferred sites of insertion (Dibb and Newman, 1989). It could be argued that the DNA sequence encoding the E/DRY motif contains a robust proto-splice site for transposable elements.

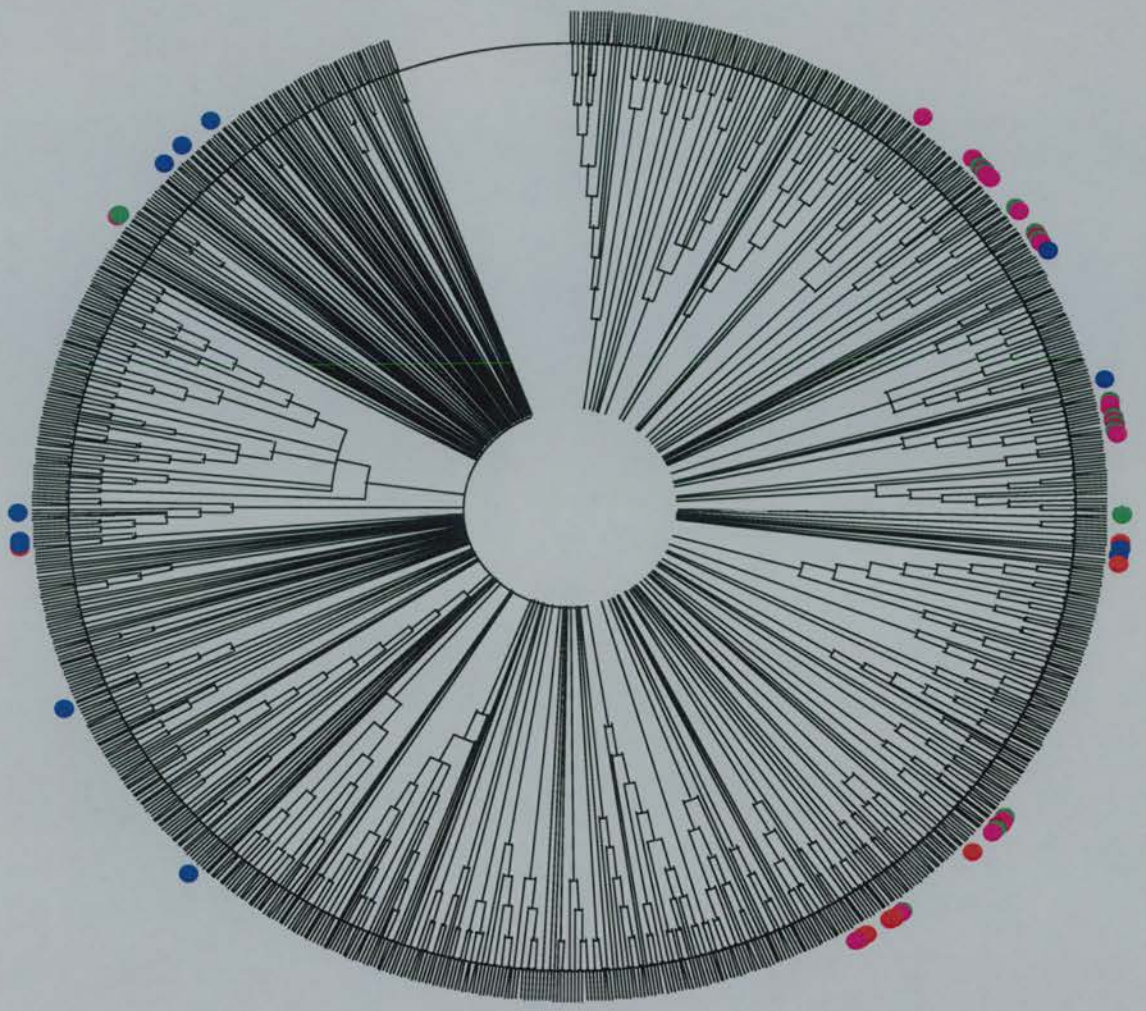

Figure 3.3.3. The phylogeny of GPCR-A proteins. Coloured circles represent proteins that have DRY-introns in their genes (human proteins: *pink*, mouse: *green*, *Drosophila*: *red* and *C. elegans*: *blue*). The tree is calculated using a p-distance method, a bootstrap consensus is shown: all nodes represented have >50% bootstrap confidence from 1000 replicates with a random seed.

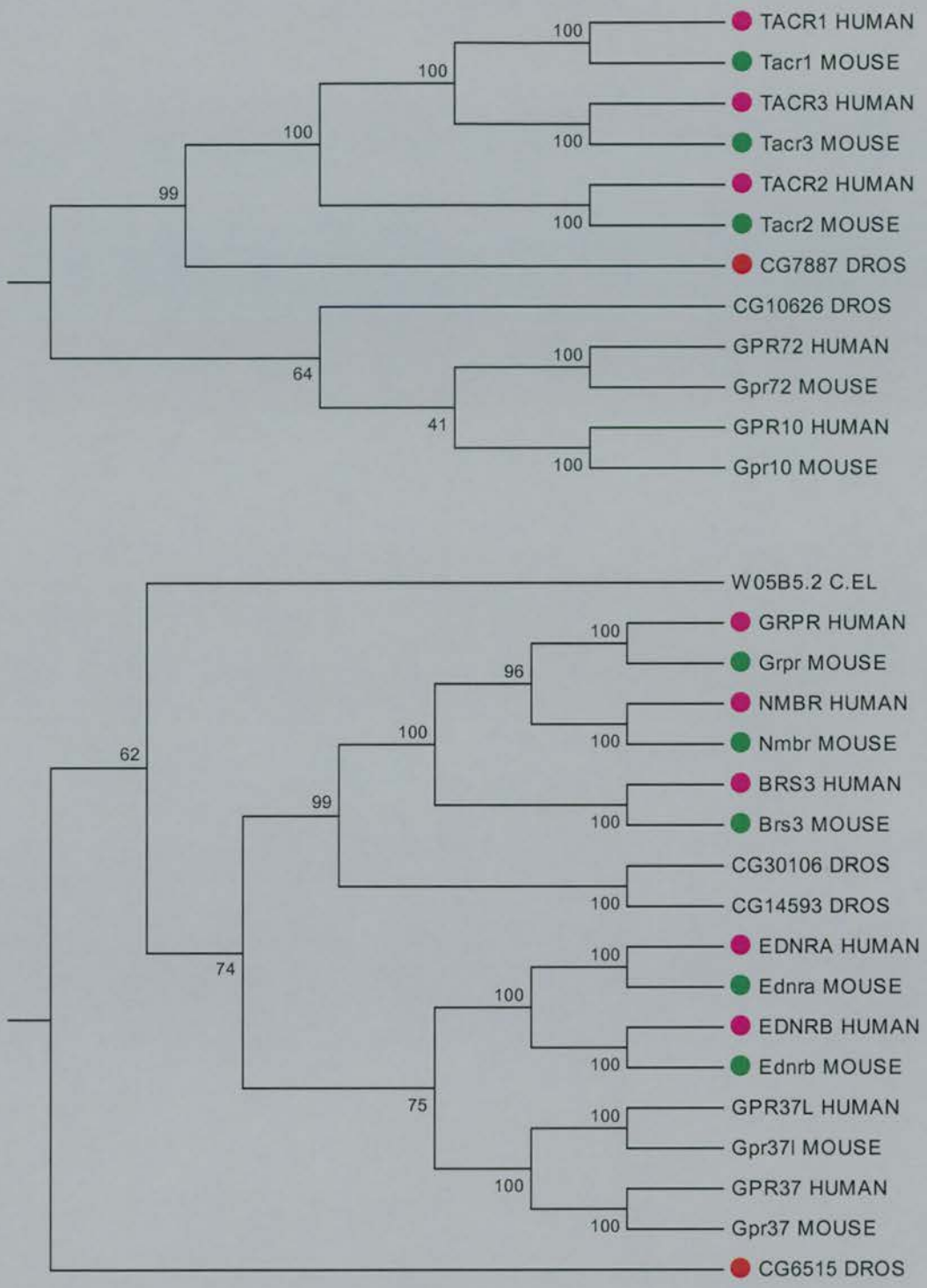

Figure 3.3.4. Enlarged view of clades from the GPCR-A phylogeny. Each clade is enlarged from Fig. 3.3.3. All nodes are shown beside associated bootstrap values from 1000 replicates with a random seed. Protein names are indicated with species of origin. Coloured circles represent proteins that have DRY-introns in their genes (human proteins: *pink*, mouse: *green*, *Drosophila*: *red*). **a,** a clade containing the mammalian nuerokinin receptors. **b,** a clade containing the mammalian endothelin, endothelin-like and bombesin receptor families.

The functional importance of the motif would conserve the proto-splice site thereby increasing the chance of multiple intron insertions in the same position and phase. This could explain how DRY-introns have inserted multiple times in different lineages. To determine whether there is evidence of a proto-spice site at E/DRY motifs that have introns compared to those that are intron free, a Logo analysis (Schneider and Stephens, 1990) of the exonic sequences immediately neighbouring E/DRY motifs was undertaken (Fig. 3.3.5). Unfortunately, the results proved inconclusive. As expected from codons for the E/DRY cage, the nucleotides at positions 1 and 2 of each codon are highly conserved in genes with and without an intron.

However, at the third nucleotide of each codon, DRY-intron containing genes show less variation. Most strikingly, genes that contain a DRY-intron almost all have the dinucleotide AG preceding the intron, whilst those without have a relatively even split between CG and AG at the equivalent position (Fig. 3.3.5). It could be argued that AG is part of a proto-splice site that has been a preferred target for insertion of the DRY-intron. However, intron-splicing machinery appears to have a preference for AG immediately preceding an intron (Mount, 1982; Zhang, 1998). Therefore, if a DRY-intron is present in a gene, there may be selection to maintain this sequence for efficient splicing to occur. If there is no DRY-intron then the only pressure on this sequence is to code for an Arg residue. As Arg codons can begin either with AG or CG dinucleotides, in the absence of an intron an even split between these might be expected.

3.4 Discussion

3.4.1 How complete are the datasets?

In 1999, Gentles and Karlin studied the intron content of 136 vertebrate and 60 *C. elegans* GPCR encoding genes from Genbank (Gentles and Karlin, 1999). Now a more extensive dataset is available due to the publication of the draft genomes of multiple model species. In addition, the characterisation of a functional motif in the largest subfamily of GPCRs means that all members of that family can be mined from the genome assemblies. This should provide a complete dataset from each species with a sequenced genome to compare and contrast.

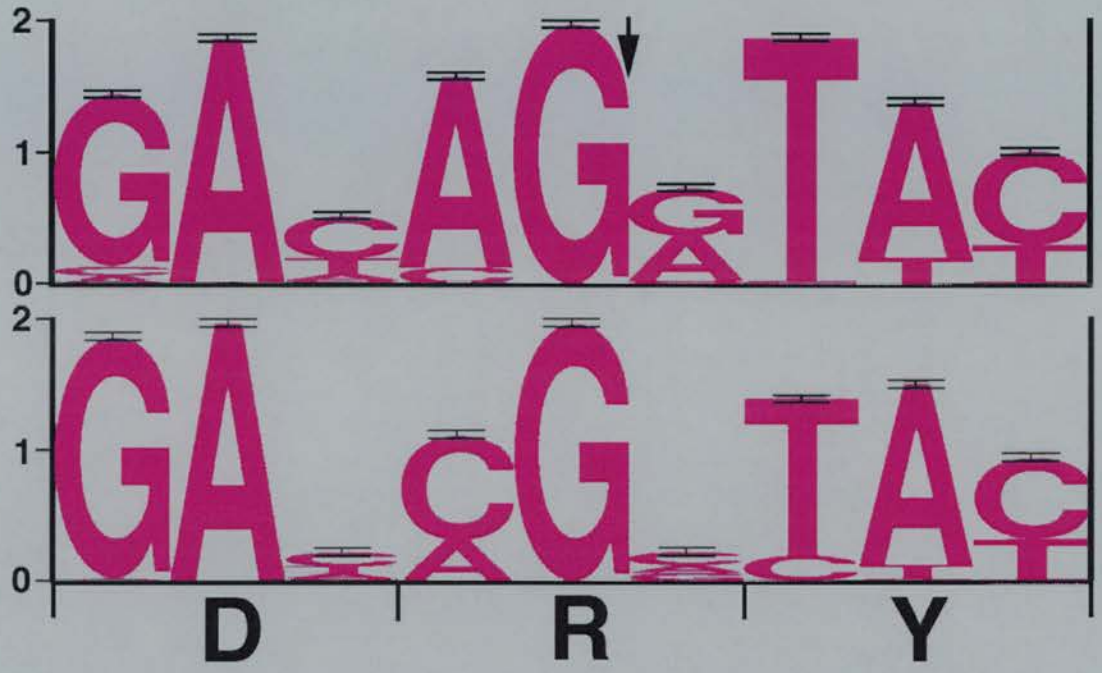

Figure 3.3.5. Analysis of E/DRY codons in genes with and without DRY-introns. The top sequence is a representation of 77 E/DRY codons with the DRY-intron from mouse, human, *Drosophila* and *C. elegans*. The bottom sequence is of the 71 most closely related genes without DRY-introns (according to phylogeny) from the same species. Each logo displays the frequencies of bases at each position as the relative heights of letters. The degree of sequence conservation is shown by the total height of a stack of letters measured in "informative bits", with a maximum of 2 bits possible at each position. The arrow indicates the position of the DRY-intron in the top logo. The amino acid coded by each codon is indicated in *black*. Logos were generated using Weblogo, using previously published formulae (Schneider and Stephens, 1990).

While the genome assemblies available at Ensembl provide a valuable resource for gene mining, there are problems when using then for intron quantification. Many genes are predicted by exon recognition software and are associated with poor quality transcript or protein evidence. In these cases the predicted gene structure may be inaccurate. Other annotated genes are missing the 5' or 3' (and occasionally both) ends of the coding sequence, making it impossible to measure accurate intron content. Furthermore, the low level of annotation makes it very difficult to parse the full length, validated genes from the incomplete ones. For these reasons, the Swiss-Prot/TrEMBL databases were chosen to select GPCR-As for intron quantification. Not only is Swiss-Prot highly annotated, it is also manually curated and replete in proteins from human, mouse, *C. elegans* and *Drosophila*. Although TrEMBL contains entries annotated by computer, these are based on manually curated nucleotide sequences.

Comparison with other studies of GPCR subfamilies in individual species suggests that, in general, the SPTr dataset has high GPCR-A coverage. A phylogenetic analysis of human proteins published subsequent to this analysis identified 241 non-olfactory Family-A receptors from a total non-olfactory GPCR repertoire of 342 (Fredriksson *et al.*, 2003). After the removal of olfactory receptors, the human SPTr dataset contained 246 sequences. Although there is no data available on the precise number of non-olfactory mouse GPCR-As, there is probably a similar number to that seen in human. This is consistent with the 232 receptors selected from Swiss-Prot and TrEMBL.

The *Drosophila* GPCR-A content has been estimated at 68 by manual curation of predicted gene structures (Brody and Cravchik, 2000; Adams *et al.*, 2000). The SPTr dataset of 71 agrees with this figure very closely. Compared with *Drosphila*, both *C. elegans* datasets have a much larger GPCR-A repertoire (SPTr,318 and Ensembl,406). However, based on analysis of the first genome assembly, a review of genes potentially involved in *C. elegans* neurobiology identified only 148 GPCR-As and around 900 chemo-receptors (Bargmann, 1998). Since these chemo-receptors have been sub-classified and examined more thoroughly, it has become clear that 900 is an over estimation (Sonnhammer and Durbin, 1997; Robertson, 1998) and an examination of Swiss-Prot/TrEMBL reveals only 644 proteins that match IPR000168 (the nematode 7-TM chemo-receptor signature). As some chemo-receptor protein families share sequence

similarities with the GPCR-A family (including a E/DRY like motif), it is difficult to classify these genes based solely on motif recognition. Furthermore, as many as 200 chemo-receptor like proteins may not even be expressed in chemosensory neurons (Troemel *et al.*, 1995; Bargmann, 1998) suggesting a classification system based on sequence similarity may be misrepresentative too. It is therefore probable that 300-400 is a more accurate estimation of *C. elegans* GPCR-A content. A retrospective analysis of the SPTr dataset reveals that 9 proteins are annotated as matching both IPR000168 and IPR000276. While chemo-receptors are generally replete with introns (Robertson, 1998; Robertson, 2000), and the 9 potential chemo-receptors in the SPTr dataset contain from 3 to 11 introns, any future study should parse out dually annotated proteins to prevent non GPCR-A bias.

3.4.2 The intron content of GPCR-A genes vary with species

The suggestion that mammals are enriched in intronless GPCR encoding genes (Gentles and Karlin, 1999) appears to be true. Even after discounting the mouse and human olfactory receptor subgroup (which are entirely intronless), a majority of GPCR-A genes lack introns in the coding region. If olfactory receptors are left in the dataset the proportion of intronless genes is even more striking, so why has this particular group of receptors been removed? Olfactory receptors appear to have undergone a large expansion, around the time amphibians diverged from the mammalian lineage over 400 Mya (Glusman *et al.*, 2001). Then, while the repertoire was maintained in some lineages, in microsmatic species a subsequent pseudogenization occurred (Rouquier *et al.*, 1998; Sharon *et al.*, 1999). This is apparent when olfactory receptor gene and pseudogene content is compared between human (a microsmatic species) and mouse (a macrosmatic species) (Zhang and Firestein, 2002). Moreover, the phylogenetic relationships between genes (and pseudogenes) within and between clusters suggest the family expanded from a single, small gene cluster in an ancient tetrapod (Glusman *et al.*, 2001). While both *Drosophila* and *C. elegans* have expanded chemo-receptor families (see Chapter 3.4.1), neither are included in the GPCR-A subfamily classification. Therefore to include olfactory receptors in a comparative study of vertebrate and invertebrate GPCRs would introduce a bias and serve no purpose in examining intron evolution.

In contrast to mammals, *C. elegans* and *Drosophila* GPCR-A genes have a much higher intron number (Fig. 3.3.1 and 3.3.2). The difference in GPCR-A intron content between the vertebrate species and invertebrate species is intriguing, and poses an interesting question: what was the intron content of the last common ancestor? One might propose that ancestral GPCR-A genes had a "high" GPCR-A gene intron content, and the introns have been lost in the mammalian lineage. Although examples of extensive intron loss are not without precedent (Fink, 1987), it is equally possible that ancestral GPCR-A genes were intron deficient and that *C. elegans* and *Drosophila* have gained introns. After comparison with the genome mean for each species, the data seems to favour the former hypothesis. Not only is the mammalian GPCR-A intron content low compared to invertebrates, but also low when compared to the mean intron content of their genome (Figure 3.3.2b). *C. elegans* and *Drosophila*, in contrast, shown no reduction of GPCR-A introns compared the rest of their genome (Deutsch and Long, 1999). In fact, in the case of *C.elegans*, the GPCR-A genes have slightly more introns. It therefore seems likely that GPCR-A genes in the invertebrate lineage have undergone intron gain and loss at a similar rate as the rest of the genome and in *C. elegans* the balance may have tipped towards intron gain. In the mammalian lineage, the observed data is best explained by preferential loss of GPCR-A gene introns.

In all species examined, rhodopsin-like GPCRs are by far the largest GPCR sub-family, when olfactory receptors are removed. Some reports estimate they account for 70% of all human non-olfactory GPCRs (Fredriksson *et al.*, 2003) and 68% of all non-olfactory *Drosophila* GPCRs (Brody and Cravchik, 2000). Although this data concurs with previous estimates of intron content that encompassed other GPCR families (Gentles and Karlin, 1999; Brody and Cravchik, 2000), it remains true that the conclusions drawn from this study can only be attributed to Family-A receptors. Only a repeat of the extensive analysis described in this chapter on the other sub-families would confirm whether the Family-A dataset is an accurate indicator of GPCR intron content. There is also a danger of using data from two closely related species, such as human and mouse, to suggest an outcome is typical of vertebrates. While one could argue that human and mouse may be evolutionarily distant enough to be representative of mammals, there may be large differences in genome structure in other vertebrate lineages. Despite the eightfold genome size difference between *Fugu* and human, their intron content is roughly similar, however there are 317 examples of intronless human genes that have a

Fugu orthologue that contains at least one intron (Aparicio *et al.*, 2002). Unfortunately, the number of GPCR genes in this number was not investigated, but it remains possible that *Fugu* GPCRs have a higher intron content than mammals.

Although *C. elegans* and *Drosophila* are highly divergent, large differences in genome structure are likely to be found throughout invertebrate species. A comparison of the *Anopheles* genome with that of *Drosophila* shows a remarkable difference in genome structure despite these species being only 250 Mya distant. An examination of orthologous genes suggests that, on average, each gene differs in intron content by two. In addition, the mean *Anopheles* gene content is a quarter smaller than that of *Drosophila* (Zdobnov *et al.*, 2002). It is clear therefore, that large-scale analysis of GPCR gene intron content from more species will be required to prove that there is a consistent difference seen between vertebrates and invertebrates. As the *Fugu* and *Anopheles* genome assemblies undergo better annotation and more transcripts become validated, it will become easier to generate a quantifiable GPCR-A dataset. If, after intron quantification in these species, a consistent difference between vertebrates and invertebrate remains, the GPCR intron content of the urochordate sea-squirt, *Ciona* would be an obvious choice to examine next.

3.4.3 The DRY-intron is a feature of GPCR-As in all species studied

It is often difficult to identify introns as being shared by descent in large protein families, due to variation in the coding sequence and relative position within the gene sequence. However the comparison of intron positions in closely related genes form that basis of innumerable studies of molecular evolution. For many the antiquity of so-called common introns (when an intron is found in the same phase and at an identical position relative to a conserved sequence in multiple genes) is a paradigm for establishing orthology (Marchionni and Gilbert, 1986; Kersanach *et al.*, 1994; Robertson, 1998; Venkatesh *et al.*, 1999; Robertson, 2000). Thus to show that the DRY-intron was common to a number of diverse species is strong evidence that it was present before the species diverged.

Tables 3.3.1 and 3.3.2 show that not only do all six species tested have DRY-introns, but that in the majority of cases the intron is found in orthologous genes in closley related

species. While this provides irrefutable evidence that the DRY-intron is over 450 Mya (when teleosts and tetrapods diverged), it strongly suggests the intron predates the divergence of vertebrates from invertebrates over 1000 Mya. However, the true diversity of the DRY-intron could only be determined by a phylogenetic analysis of the entire family from all species. Firstly this identified orthologous genes between diverse species. If two DRY-intron containing genes are orthologous between vertebrate and invertebrate species, the most parsimonious explanation would be that the intron was present in the last common ancestor. Secondly, a phylogenetic tree shows the distribution of the DRY-intron containing genes, providing information on when the intron appeared during the evolution of the family.

3.4.4 The DRY-intron is ancient and has been lost in the vast majority of GPCR-As

A phylogenetic tree of all 867 proteins in the SPTr dataset reveals clades containing related DRY-intron containing genes from species as diverse as *Drosophila* and human, suggesting that the intron pre-dates the divergence of *Drosophila* and *C. elegans* from vertebrates (~1000 Mya). An illustrated example of this is the *Drosophila* CG7887 protein in Fig. 3.3.4a, which is an invertebrate orthologue of the mammalian neurokinin receptor family. There are other examples of DRY-introns in very distant orthologues in the phylogeney: the SPTr *Drosophila* protein Q8IS45 (CG9569) is an orthologue of mammalian Dopamine receptor-2 (DRD2) and the *C. elegans* orphan receptor proteins Q93704 (F42D1.3) and Q95XI5 (Y69A2AR.15) are most similar to *Drosophila* Q8SWR3 (CG16752). Therefore based on the sequence alignment of a very large dataset, the evidence that this intron was common to some ancestral GPCR-As is very strong; but not all the DRY-intron containing genes group together. In fact, the DRY-introns are found in a diverse range of GPCR-As, distributed throughout the bootstrapped phylogeny. For example, the neurokinin receptor clade (Fig. 3.3.4a) is phylogenetically distant from the endothelin/bombesin receptor clade (Fig. 3.3.4b).

Figure 3.4.1 shows the phylogenetic distribution of clades that have more than two pairs of DRY-intron containing orthologues. While not every gene in these clades has a DRY-intron, the distribution of those that do suggest the gene at the root of each clade must have had one.

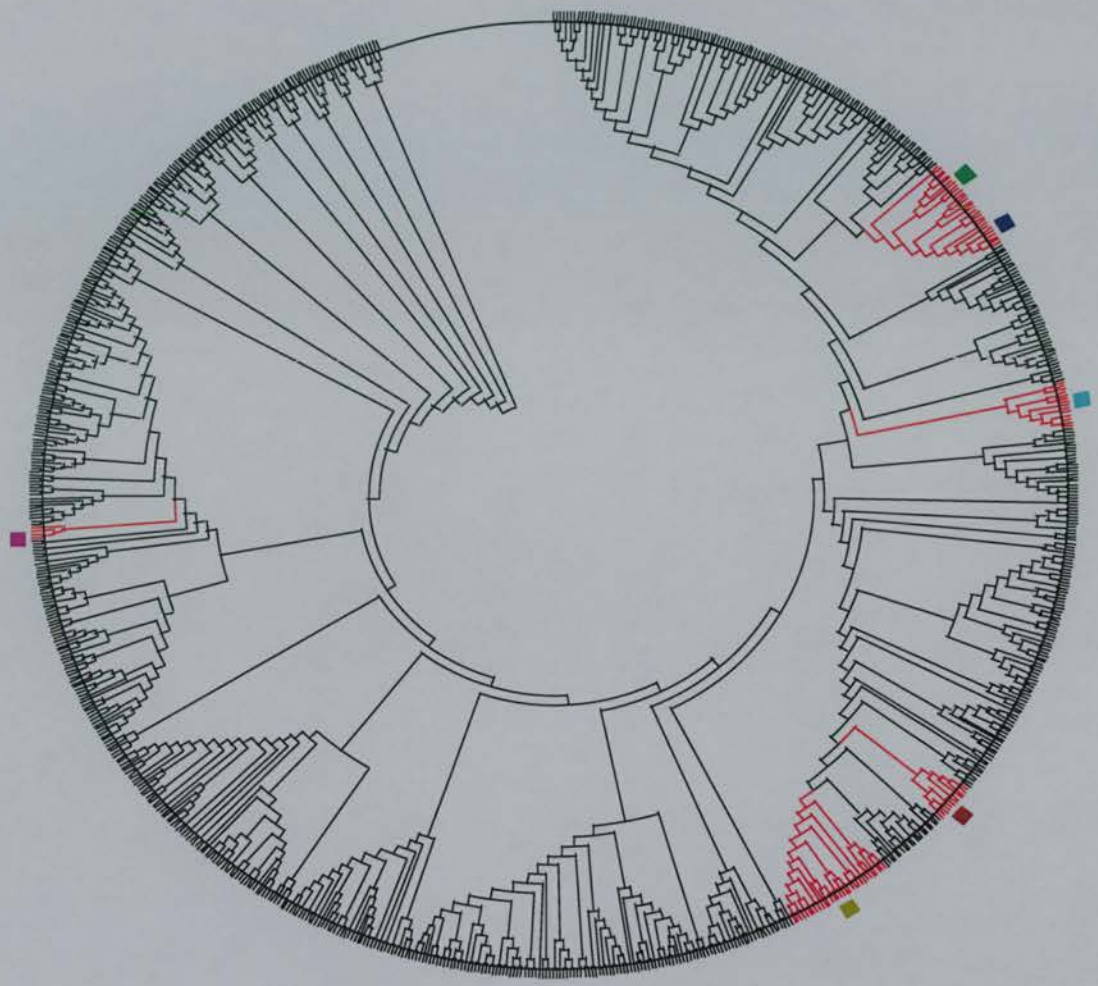

Figure 3.4.1. GPCR-A topology showing clades with multiples examples of DRY-introns. Topology of all nodes are shown. Clades in *red* represent families with more than two examples of genes with DRY-introns from different species. The DRY-introns in each of the clades indicated are highly likely to originate from a single ancestor, positioned at the root. Coloured boxes represent the positions of particular gene familes. Clockwise, from top: neurokinin receptors, *green*; galanin receptors, *dark blue*; endothelin/bombesin receptors, *light blue*; dopamine receptors, *red*; amine receptors, *yellow* and an orphan invertebrate receptor family, *purple*.

For example, if the gene at the root of the neurokinin receptor clade had a DRY-intron, a single intron deletion event could explain the intron content in Figure 3.3.4a. Similarly, 3 independent intron loss events could explain the intron pattern in Figure 3.3.4b, if the gene at the root of the clade had a DRY-intron. Thus, if one assumes that a DRY-intron inserted only once, then not only must the last common neurokinin receptor gene have contained the intron, but also the last common ancestor of endothelin/bombesin receptors, the amine receptors and the invertebrate orphan receptors and so forth. It follows that the DRY-intron probably appeared during the expansion of the GPCR-A family from a single receptor over 1000 Mya.

Although the distribution of the DRY-intron is extensive the actual number of genes containing it is small (6.7% of all sequences in the tree). This means that a large number of genes, probably hundreds, must have undergone loss of the DRY-intron. While this initially might seem improbable, it is perhaps more likely than the alternative: multiple examples of independent DRY-intron insertion. Despite the recent publication of a study showing the conservation of intron positions between plants, animals and fungi strongly supports the antiquity of common introns (Fedorov *et al.*, 2002), there is a model that may justify multiple examples of common intron insertion. The hypothesis holds that there are consensus sequences that are preferred sites for insertion of transposable elements (Dibb and Newman, 1989). If there is such a site conserved within the E/DRY motif, then it may explain how an intron could insert multiple times at the same position in different genes. It is, unfortunately, difficult to prove that common introns are not gained by multiple proto-splice site insertion. There clearly are conserved sequences surrounding most introns (Mount, 1982; Zhang, 1998; Long and Deutsch, 1999), including DRY-introns (Fig. 3.3.5), that are not a result of coding constraint (Fichant, 1992). However Newman and Norman have shown that, in yeasts, exonic nucleotides interact with a splice-factor to enhance splicing (Newman and Norman, 1992). Therefore, while it remains possible that conserved exonic sequences are remnants of proto-splice sites, they are more likely to be a consequence of selection for spliceosomal function.

Long and colleagues have subjected proto-splice site model to two sets of statistical analyses, both times rejecting the null hypothesis (Long *et al.*, 1998; Long and Rosenberg, 2000). Furthermore, a recent comparison of human/mouse/rat orthologous

pairs showed 6 instances of definitive loss in over 11,000 intron positions, but not one instance of gain suggesting, in mammals at least, that intron loss is more common than intron gain (Roy *et al.*, 2003). When compared with analysis of intron structure in other GPCR subfamilies, multiple examples of intron insertion appear even less likely. From phylogenetic analyses of 544 *C. elegans* chemo-receptor genes and pseudogenes, at least 235 independent instances of intron loss were mapped compared to only eight examples of intron gain (Robertson, 1998; Robertson, 2000). Furthermore, each intron insertion event occurred at a different site. This seems to reject the suggestion that, under the proto-splice site model, introns are targeted to identical positions in different members of a gene family (Dibb and Newman, 1989). It is also pertinent to note that *C.elegans* chemoreceptors have an E/DRY-like domain, except in this family the consensus is normally YRY. As the Arg residue is invariable and it is found in a similar position after the third transmembrane domain, it probably has a similar functional role (Parrish *et al.*, 2002). If a proto-splice site was coded by the E/DRY motif, one might expect the chemo-receptor YRY motif to be a target for intron insertion too. However, Robertson failed to find a single example of such an intron in over 500 YRY motifs, while this study identified 58 introns in 867 E/DRY motifs (Robertson, 1998; Robertson, 2000). These data are consistent with the analysis of the GPCR-A family described here, demonstrating that DRY-introns are very likely to be of a single, ancient origin and have subsequently undergone extensive loss throughout evolution.

A time scale for DRY-intron loss can be estimated from orthologue analysis between related species, such as human and mouse. However, this data demonstrated that there has been no DRY-intron loss since the divergence of these species over 90 Mya. To study the loss of DRY-introns over a longer evolutionary period, the GPCR-A family in *Fugu* was compared to human and mouse. 37 DRY-intron containing *Fugu* GPCR-As were identified, of which 32 are orthologous to human or mouse intron containing genes (Table 3.3.1). The increased number of *Fugu* genes is not unexpected, as it is consistent with the genome duplications that have occurred in the teleost lineage (Amores *et al.*, 1998; Aparicio *et al.*, 2002; Taylor *et al.*, 2003). The five cases of DRY-intron discordance between *Fugu* and human/mouse genes, since their divergence over 450 Mya, account for 20% of all DRY-intron containing orthologous sets in these species. A similar comparison of *Drosophila* and *Anopheles* GPCR-A genes reveals one orthologous pair that differs at the DRY-intron. This single example of discordant DRY-

intron loss since *Anopheles* diverged from *Drosophila* accounts for 8.3% of orthologous DRY-intron containing gene sets in these insects. As *Drosophila* and *Anopheles* diverged around 250 Mya, it appears that the more divergent the species compared, the greater the disparity in DRY-introns (Fig. 3.4.2). Interestingly, the rate of DRY-intron change is linear with respect to time. One might expect species with short generation times to show a greater disparity in DRY-intron content (Zdobnov *et al.*, 2002). Because for any change in genomic structure to be transmitted it must occur in the germ line, and the more generations there are per million years, the more likely a change is to be propagated. This however, does not appear to be the case (albeit based on data from only three comparisons). Instead, the rate of DRY-intron change appears to be relatively constant in all five species. While this data is entirely consistent with DRY-introns being ancient and undergoing extensive loss in the GPCR-A family, it is important to note it does not necessarily favour this model *per se*. It is also consistent with a proto-splice site insertion model where DRY-introns have been gained at a constant rate over time. Nevertheless, if DRY-introns have been lost at a similar rate in all species, it has implications for understanding the mechanism of reduced intron content in mammalian GPCR-As.

3.4.5. Selection for net intron loss in the mammalian lineage

While the disputed proto-splice site model is cited to explain targeted intron insertion, there is now a general acceptance that novel introns are generated through transposon insertion (Gilbert *et al.*, 1997). But through what mechanism may GPCR-A intron losses have occurred? There are suggestions that introns could have been lost in some genomes due to a hyperactive reverse transcriptase and a consequent bombardment of the genome with cDNA copies of spliced transcripts (Fink, 1987). Other have shown selection against a large genome size may promote deletion of unneeded DNA, possibly resulting in intron loss (Petrov *et al.*, 1996), although one might expect this to result in introns of shorter length, rather than the accurate removal of introns. A more mechanistically plausible suggestion is that intron losses occur by in-frame deletion through gene conversion (Derr and Strathern, 1993; Robertson, 1998; Roy *et al.*, 2003).

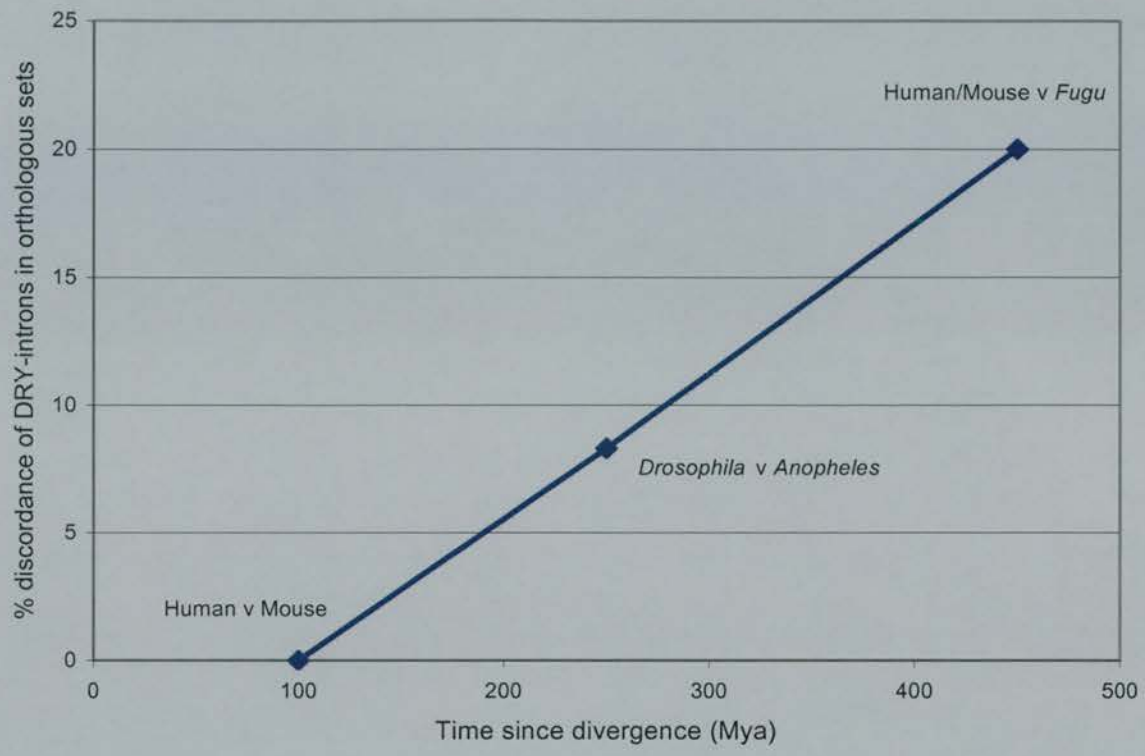

Figure 3.4.2. DRY-intron discordance increases over evolutionary distance. The divergence time is estimated using previously published molecular clock calculations (Blair and Kumar, 2003). Intron loss is calculated from the number of orthologous gene sets in the combined Ensembl and SPTr datasets that show discordance for DRY-introns. The species from which the ortholgous sets are compared are indicated at each time point.

If non-homologous recombination occurred between exon sequences neighbouring an intron and identical sequences in a reverse transcribed mRNA copy of the gene, then single introns could be removed without disturbing the open reading frame. DRY-introns, which have neighbouring exon sequences highly conserved in the entire family, could even have even been removed by gene conversion between a gene with the intron and a paralogue without it.

It is interesting to note, however, in contrast to the situation with total intron number, DRY-introns are not under-represented in the mammalian SPTr dataset when compared to invertebrates. DRY-intron containing genes account for 7-8% of the human and mouse SPTr dataset, 14% in *Drosophila*, but only 4% in *C.elegans* (although lineage differences in GPCR-A gene expansion would influence this data). The rate of DRY-intron change is also consistent with a model where there is no enrichment for DRY-loss in the vertebrate lineage (Fig. 3.4.2). Is it therefore possible that all four genomes have undergone similar levels of GPCR-A intron loss, but that mammals are deficient for the compensatory intron gain seen in invertebrates? Further evidence supporting this includes high rates of intron turnover (loss and gain) reported in at least one *C.elegans* gene family (Gotoh, 1998), while, in the last 100 million years, it appears mammalian genomes have undergone a higher rate of intron loss than gain (Roy *et al.*, 2003).

Debating whether the reduction in intron number in the mammalian GPCR-As is a result of selection for extensive loss or lack of compensatory gain in somewhat extraneous. As with all evolution, intron gains and losses occur without forethought; so it is likely that the same mechanisms that shaped the intron repertoire of the entire genome, shaped the mammalian GPCR-A intron content. The observed net loss is therefore probably due to a selection on both mechanisms: selection for introns that were lost and selection against introns that were gained, although what functional advantage that might result from this not understood. One might predict that unspliced genes are expressed more efficiently, but transgenic experiments suggests introns actually increase the levels of protein produced from a gene through a number of mechanisms (Brinster *et al.*, 1988; Le Hir *et al.*, 2003). One possible explanation for selection against introns could be a requirement for rapid transcription of GPCR-As. While intron splicing can increase the total number of transcripts, the presence of introns may increase the transcriptional delay. This is supported by the observation that the majority of mammalian GPCR-As are expressed in

the central nervous system, where rapid changes in gene expression may be an advantage (Gentles and Karlin, 1999). Such theories are currently the realm of speculation, but investigation of the dynamics of GPCR-A regulation and the study of other intron poor gene families (such the histone encoding genes) may begin to further our understanding of intron selection.

3.5 Conclusions and Future Directions

The discovery of an intron disrupting an invariant codon in such a large gene family provides a unique opportunity to study intron evolution. It is unlikely that many other introns could be mapped in such a manner, therefore the application of the protocols described here to other large protein families appears slim. There is scope to further understand the evolution of introns in GPCRs however. A quantification of intron content in other GPCR families would reveal whether mammalian intron deficiency is unique to the GPCR-A subfamily. As more genomes are sequenced and more proteomes are annotated, the GPCR intron content of more species can be elucidated. This would shed light on the intron evolution in more animal lineages and provide more species with which to carry out analysis of orthologues.

The SPTr dataset could also be used to further investigate properties of GPCR-A introns. For example, quantification of total intron phase or correlation could be carried out, as ancient and inserted intron models predict statistical differences in these values (Long *et al.*, 1995; Gilbert *et al.*, 1997). A particularly interesting analysis would involve determining whether GPCR-A introns correlate with protein structure. While it is clear that introns are distributed equally between the 7-TM domain and both termini (Figure 3.3.2b), there are suggestions that within the 7-TM domain, introns are enriched in the loops between each transmembrane pass (Gentles and Karlin, 1999). If this is the case, it would provide evidence that these introns are ancient and define the boundaries of protein modules (Gilbert and Glynias, 1993; de Souza *et al.*, 1997). The question could be resolved by dissecting each aligned SPTr protein into short sequences representing transmembrane or loop regions, then the corresponding DNA sequences could be studied and intron content quantified. Another application for the SPTr dataset could be the further investigation of the proto-splice site hypothesis (Dibb and Newman, 1989). If

DRY-introns have inserted multiple times at a defined exonic sequence, then an analysis how many such sequences exist and what proportion are interrupted with introns would be informative.

This chapter describes the first quantitative analysis of intron content in GPCR-As: the largest subfamily of G-protein coupled receptors and among the largest gene families represented in sequenced animal genomes. As previously suggested (Gentles and Karlin, 1999), there is a large and significant reduction in intron number in the mammalian lineage, while invertebrate species show no reduction. Additionally, it explains how a conserved intron is present in diverse members of the family across several species, strongly suggesting widespread loss of a specific intron in the evolution of the family. On comparison of intron content in different lineages, there is evidence for the loss of this intron in recent evolutionary history, as well examples of ancient intron loss. Taken together, these data demonstrate that the low intron frequency in mammalian GPCR-As is probably due to intron loss, and that ancient G-protein coupled receptor genes had introns. The alternative scenario, that a parallel intron has been gained at identical positions numerous times in multiple species throughout evolution is both phylogenetically, and statistically unlikely (Long *et al.*, 1998; Long and Rosenberg, 2000). However, if parallel insertions have occurred, then the codons for the E/DRY motif must be considered an extremely attractive target for transposon insertion and therefore a robust proto-splice site (Dibb and Newman, 1989).

Chapter 4

Control of Colour Change in the Zebrafish

I know the human being and fish can coexist peacefully.

George W. Bush

In an election address in Saginaw, Michigan, 29 September 2000

4.1 Preface

The physiological colour change observed in lower vertebrates, defined as rapid changes in colour caused by intercellular movement of pigment (Parker, 1948), has intrigued scientists for over 80 years. This pigment translocation can have wide ranging visual effects, from the dramatic social colour changes in chameleons, to the more subtle background adaptation observed in most fish and amphibians.

Since the discovery that the frog pituitary contains a factor that acts on pigment cells (Allen, 1916; Smith, 1916), it has become clear that colour change is largely under hormonal control. However, almost 50 years passed before it was first demonstrated that melanocyte-stimulating hormone (MSH) dispersed melanosomes in amphibians (Bagnara, 1964; Goldman and Hadley, 1969). Originally championed by Hogben in the 1930s (Hogben and Slome, 1931; Waring, 1963), the bihumoral theory of colour control was leant credence by the extraction of melanin-concentrating hormone (MCH) from the catfish (Enami, 1955). However, it was not until much later that the melanosome aggregating activity of MCH was fully characterised (Kawauchi *et al.*, 1983). It has now been established that in many teleost fish species background adaptation is regulated in a bihumoral manner and that the principle mediators of this are MCH and MSH (Fujii, 2000).

Since its emergence as an important model organism, and with its genome currently being sequenced, the zebrafish makes an excellent species in which to study the genetics of physiological colour change. In Chapter 2, a number of genes potentially involved in zebrafish background adaptation are discussed. This chapter introduces background adaptation in the zebrafish and describes the development of a melanophore assay that can be used to study the bihumoral control of colour change. It also discusses the results of some preliminary experiments that investigate the intercellular processes involved in colour change, which illustrate potential future applications for this assay.

4.2 Zebrafish physiological colour change

Background adaptation is the process of changing colour to blend with the hue of the local environment. Although the colour change can occur over periods of seconds to months, in lower vertebrates the term is generally used to describe a rapid and reversible, physiological adaptation. The rate of vertebrate physiological colour change is highly variable and depends on the regulating mechanism, although very little is known about the process in zebrafish. Therefore, background adaptation was studied in both adult and larval zebrafish, and the role of some potential melanogenic regulating genes was investigated.

4.2.1 Background adaptation in adult fish

To investigate the process in adult zebrafish, a number of fish were exposed to either white or black backgrounds for 24 hours, while ambient lighting was maintained. Figure 4.2.1 shows the effect of background colour on zebrafish pigmentation. It is apparent that, from a dorsal perspective, white adapted (WA) fish appear much lighter in colour compared to black adapted (BA) fish (Fig. 4.2.1a,d). As well as an overall lighter hue, the WA fish display a golden stripe along the dorsal midline (Fig. 4.2.1a,b). In BA fish this stripe is replaced by a melanic stripe (Fig.4.2.1d,e). An enlarged view of the dorsal chromatophores from each fish, reveal the mechanism behind the colour change. The melanin in WA melanophores appears to be aggregated, forming punctate spots that cover a small surface area (Fig. 4.2.1c, arrowhead). In comparison, the BA fish melanophores have dispersed melanin covering a larger area of the fish with dark pigment (Fig. 4.2.1f, arrowhead). The melanophores appear to overlay the reflective iridophores, thus in WA fish the iridophores can be seen (Fig.4.2.1c) but in BA fish they are obscured (Fig. 4.2.1f), explaining the absence of the golden stripe.

When white and black adapted fish are viewed from a lateral perspective, the differences in adapted pigmentation are even more evident. The blue/black lateral stripes are highly defined in BA fish (Fig.4.2.1i), but after white adaptation they are less obvious against the largely golden tone (Fig. 4.2.1g).

Figure 4.2.1.Adult zebrafish adapt to the background (legend overpage).

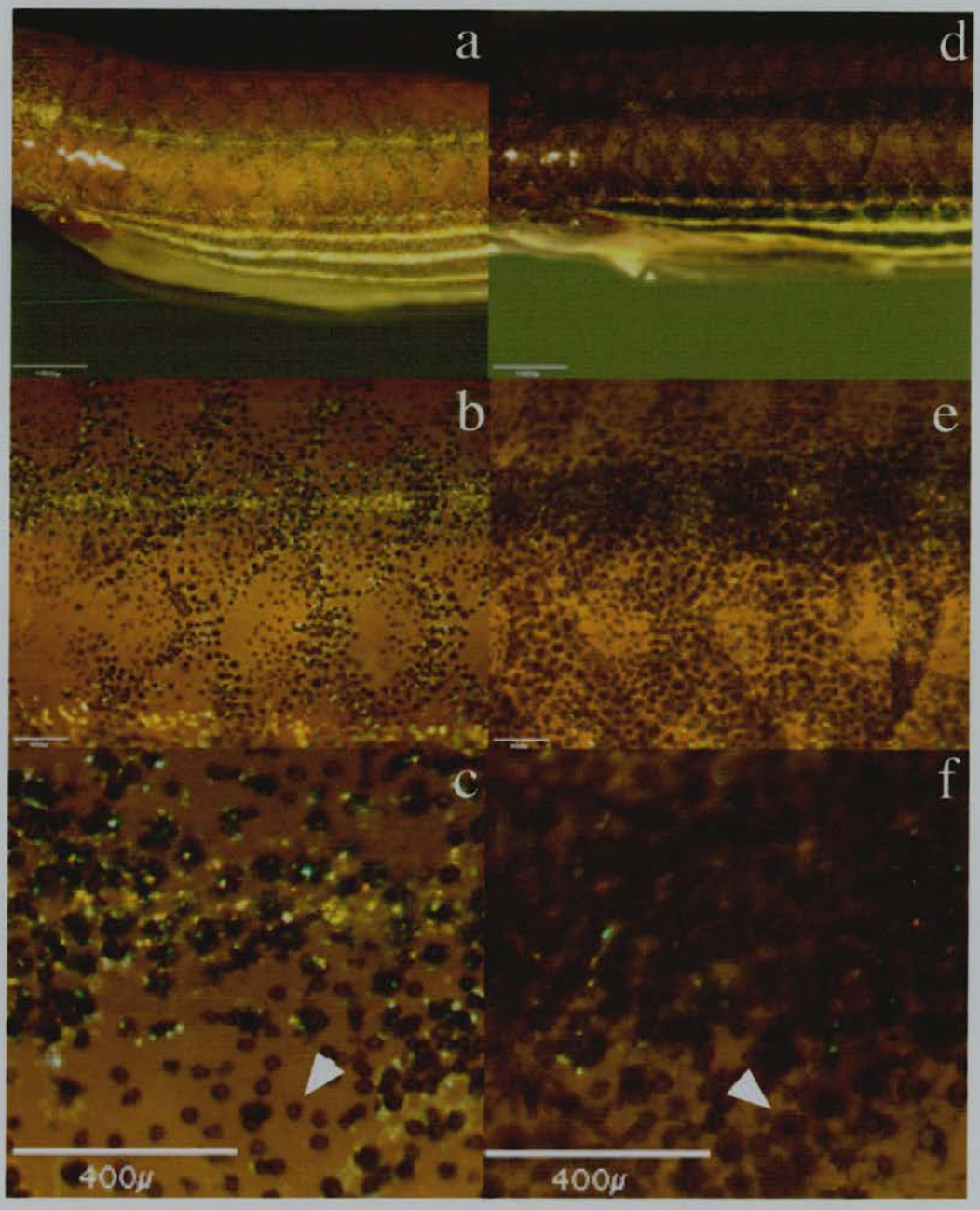

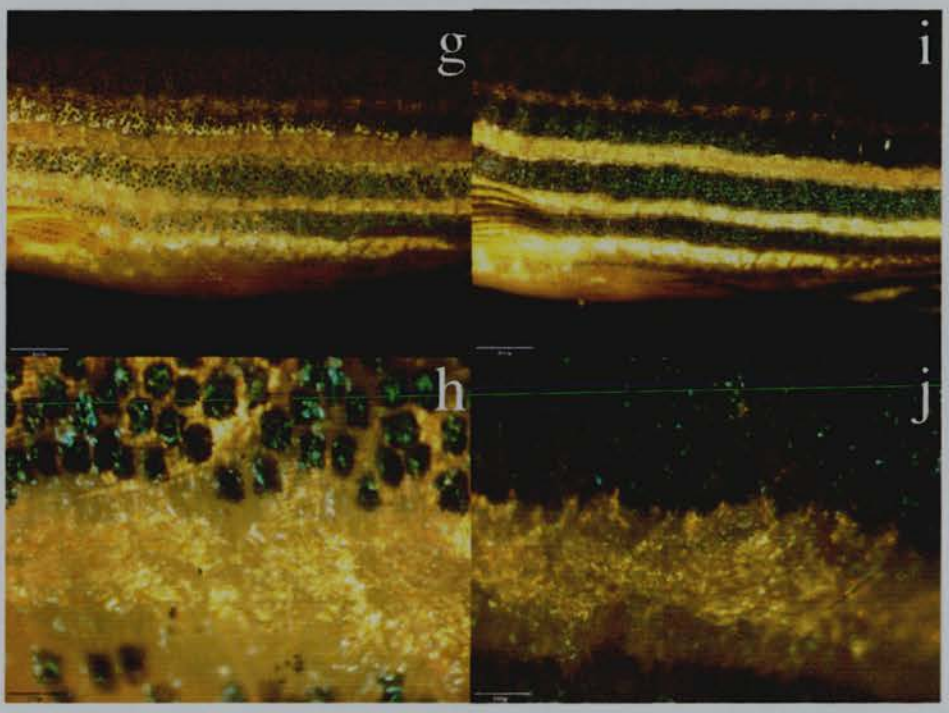

Figure 4.2.1. Adult zebrafish adapt to the background. White adapted fish (**a-c**, **g-h**) appear much lighter in colour compared to black adapted fish (**d-f**, **i-j**). The lighter colour change is due to melanophore aggregation (**c**, arrowhead) and the darker hue is caused by dispersed melanophores (**f**, arrowhead). **a-f**, dorsal view, anterior to left. **g-j**, lateral view, anterior to left. Scale bars: 1600μm (**a,d,g,i**); 800μm (**b,e,h,j**); 400μm (**c,f**).

Furthermore, a magnified view of a stripe reveals there is a overlay of melanophores on iridophores (Fig.4.2.1h,j) similar to those as observed on the dorsum, and that the melanin is dispersed and aggregated in the same manner. There are differences between lateral and dorsal pigmentation. Iridophores cover almost the entire lateral surface making the fish appear iridescent, while on the dorsum the iridophores are concentrated along the midline. In addition, while the dorsal cells are black in hue the lateral melanophores appear blue. This phenomenon, known as Tyndall scattering, is an optical effect produced by a light-absorbing layer (melanophores) overlying a light-reflecting layer (iridophores). Finally, there is a difference in melanophore size (compare Fig. 4.2.1c,f with h,j). Dorsal melanophores appear smaller than the melanophores that form the lateral stripes.

4.2.2 Background adaptation in developing fish

It is clear that adult zebrafish undergo physiological colour change in response to their background, but do larvae respond in the same manner? To investigate this, zebrafish embryos were raised in black or white painted dishes under ambient light conditions. On both backgrounds zebrafish larval melanophores appeared to be fully dispersed from when they first became pigmented (~24 hpf) until 96 hpf (data not shown). However, between 4 and 5 dpf, WA larvae reacted to their tone of the background by aggregating their melanophores (Fig.4.2.2c) while BA larval melanophores remained dispersed (Fig.4.2.2a). The same response was noted in larvae up to 10 dpf and the process is fully reversible: when moved onto different background colours, within a day larvae with dispersed melanophores became aggregated and vice versa.

To better define morphology of adapted melanophores, larval skin was observed using a high-powered light microscope. Figure 4.2.2b shows a melanophore from a 5 dpf BA larva with fully dispersed melanophores. The entire cell can be viewed in a single focal plane with some small areas where there is no melanin (Fig.4.2.2b, arrow). Moreover, an organelle can be distinguished in the same plane (Fig. 4.2.2b, arrowhead). In addition, the boundary of the melanic area is well defined consistent with the edge of the cell itself. This appears to concur with observations of sub-cellular structure in dispersed melanophores. Dr. David Bassett kindly generated transmission electron micrographs of dermal melanophores in 14 dpf zebrafish skin.

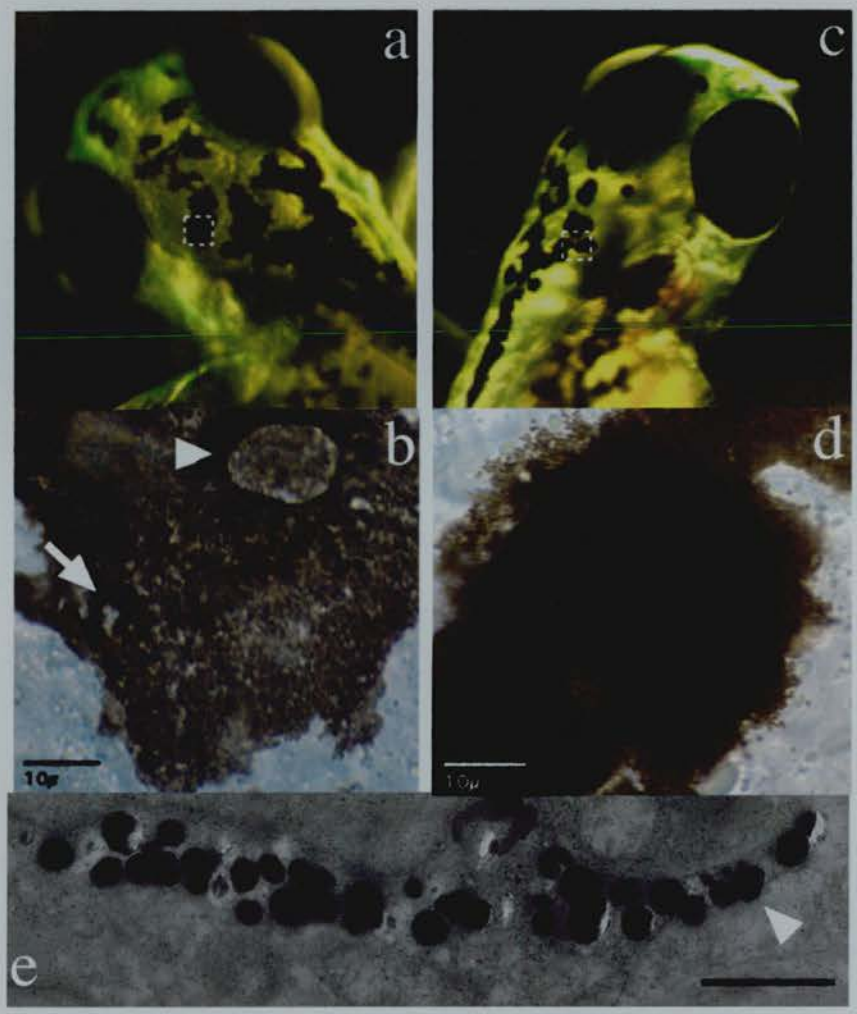

Figure. 4.2.2. Larval melanophores aggregate and disperse melanosomes. a, on a dark background 5 dpf larval melanosomes are dispersed along the flat surface plane of dorsal melanophores. **b**, a detailed view of **a**, *white* box. An organelle (arrowhead) and melanin free holes (arrow) can been seen. **c**, on a light background 5 dpf larval melanosomes are aggregated within the dorsal melanophore. **d**, ,a detailed view of **c**, *white* box. No organelles or holes are visible. **e**, transmission electron micrograph of a sagittal section through the dermis of a 14 dpf zebrafish, showing part of a dispersed melanophore. The melanosomes (arrowhead) are arranged along a plane parallel to the dorsal surface. Kindly reproduced with permission from Dr. David Basset. Scale bars: 10μm (**b,d**); 2μm (**e**).

In these, the pigment containing melanosomes can clearly be observed throughout the cell, largely dispersed along a single, lateral plane (Fig. 4.2.2e, arrowhead). The melanosomes appear to be spherical in form and ~0.5μm in diameter, similar to those reported in other piscine species (Turner *et al.*, 1975). This is in stark contrast to the morphology of a 5 dpf WA larva melanophores with aggregated melanosomes (Fig.4.2.2d). The interior of this cell is raised from the plane of the skin surface. The cell appears darker, suggesting a more dense collection of melanosomes in this area, and there are no melanin deficient spots where the underlying dermis can be seen. No organelles can be visualised (presumably they are obscured by overlying melanosomes), and the boundary of the melanin is irregular and layered with individual melanosomes visible. Taken together, these data suggest that dispersed melanosomes are distributed to the edge of melanophores, along a thin layer parallel to the surface of the skin. On aggregation, the melanosomes are drawn towards the centre of the cell, bunching together in a dense, raised cluster.

4.2.3 Zebrafish deficient in background adaptation

There is a group of zebrafish mutant strains that are deficient in the larval background adaptation process, showing dispersed melanosomes even after 6 dpf on a white background (Kelsh *et al.*, 1996). These were among 894 mutants identified from an ethylnitrosourea (ENU) mutagenesis screen for recessive phenotypes (Haffter *et al.*, 1996). Seven loci have been defined as background adaptation deficient (Table 4.2.1), any of which could be a candidate for a gene involved in melanocortin or MCH signalling. However, a recent screen of mutants for visual defects revealed three background adaptation mutants to be blind (*dropje*, *lakritz* and *noir*) (Neuhauss *et al.*, 1999). As a direct projection from the retina to the hypothalamus provides a sensory input to stimulate the background adaptation response, fish that cannot visually discern changes in background tone generally have dispersed melanophores. Therefore the genetic lesions in these fish are unlikely to be in genes involved in melanogentic regulation. Of the remaining mutant lines, both *melancholic* and *zwart* were not available to study, so only *fata morgana* (*fam*^{te267}) and *submarine* (*sum*^{tr6}) were obtained. All exons from *mc1r*, *mchr1a*, *mchr1b*, *mchr2* and *pomc* were amplified from heterozygous mutant fish (*fam*^{te267}*/AB** and *sum*^{tr6}*/AB**) and wild-type strain (*AB** and *wik*) DNA and sequenced. No strain differences were observed in any of the genes.

Table 4.2.1. Mutant zebrafish strains, deficient in background adaptation. All mutants were identified from an ENU mutagenesis screen (Haffter *et al.*, 1996). The primary phenotypes (Kelsh *et al.*, 1996) and visual defects (Neuhauss *et al.*, 1999) have been previously described.

Gene name	Alleles	Phenotype	Vision
dropje	tr256	DM	Signal transmission defects
fata morgana	te267	DM, later recovers	Normal
lakritz	th241	DM	No retinal ganglion cells
melancholic	tj19e	DM	Not tested
noir	tc22,tp89	DM, motility defects	Signal transmission defects
submarine	tr6	DM, motility defects	Normal
zwart	tj213, tp93a	DM, motility defects	Not tested

The map positions of the *mc1r* gene and the three melanin-concentrating hormone receptor genes were then compared to the linkage groups positions of mapped pigment mutants. Three mutant alleles with pigment phenotypes (*milky*, *pewter* and *tj266c*) were mapped close to *mc1r* in collaboration with Dr. Robert Geisler (Table 4.2.2). As well as a melanophore phenotype, both *milky* and *tj266c* have defects in non pigmentary processes, including cranial development (Heisenberg *et al.*, 1996) and are therefore not obvious candidates for *mc1r* mutations. In contrast, *pewter* has a melanophore specific phenotype, showing an apparent reduction in melanin (Kelsh *et al.*, 1996). Genomic DNA was extracted from each homozygous mutant fish and the *mc1r* gene sequenced. Again, no sequences differences were apparent between the ORF of *mc1r* in mutant and wild-type strains of fish. There are currently no mapped mutants with pigment phenotypes that co-localise with zebrafish *mchr1a*, *mchr1b* or *mchr2* (Geisler, R; personal communication).

Two other pigment mutants were available that could be considered potential candidates for melanocortin or melanin-concentrating hormone receptor defects. The classical melanin deficient strain, *golden*, is located on LG18, but the gene sequence in homozygous mutant fish is identical to that found in wild-type strains. The final mutant strain sequenced was *union jack*. It has dispersed melanophores with a clear, melanin-

free perinuclear spot in each cell (Kelsh *et al.*, 1996). The mutant locus has not been mapped in this strain, so all exons of *pomc*, *mc1r*, *mchr1a*, *mchr1b* and *mchr2* were sequenced. Exon 2 of *pomc* had a single base difference in uni^{tn16} DNA when compared with *AB** and *wik* strains, this however, is a synonomous change and therefore probably polymorphic variation.

Table 4.2.2. Mutant zebrafish strains with pigmentary phenotypes on LG18. All mutants were identified from an ENU mutagenesis screen (Haffter *et al.*, 1996), with the exception of *golden*, which is a spontaneous mutant. The primary phenotypes have been previously described (Streisinger *et al.*, 1986; Kelsh *et al.*, 1996).

Gene name	Alleles	Phenotype	Map position
golden	B1	Melanin pale/absent	2.3cM
milky	tv10	Large melanophores and small eyes	58.4cM
pewter	tm079b	Melanin pale/absent	47.2cM
not named	tj266c	Large melanophores and small eyes	47.2cM
union jack	tn16	Melanophores with clear peri-nuclear spot	Not mapped

4.2.4 The developmental function of mc1r

To further investigate what role mc1r plays in the developing zebrafish, a gene knockdown approach was employed using a morpholino antisense oligo. Morpholinos function by specifically binding to sense mRNA and reducing translation by steric blocking, preventing the assembly of a functional ribosome complex (Nasevicius and Ekker, 2000)(Fig. 4.2.3a).

Figure 4.2.3 (over page). Morpholino knockdown of zebrafish mc1r. a, the morpholino oligo (*pink* bar) is complimentary to the *mc1r* mRNA sequence (*red* line) across the AUG initiator. This inhibits the formation of a ribosome complex (*shaded* circle) resulting in a knockdown of protein production (*green* line). **b-d**, zebrafish larvae injected with 1mM mc1r-MO and imaged on a dark background, after 24 hpf (**b**), 48 hpf (**c**) and 120 hpf (**d**). **e**, a zebrafish larva injected with 1mM mc1r-MO and imaged on a light background, after 120 hpf. **f-h**, un-injected zebrafish larvae imaged on a dark background, after 24 hpf (**f**), 48 hpf (**g**) and 120 hpf (**h**). **i**, an un-injected zebrafish larva imaged on a light background, after 120 hpf. **j**, a plot showing the proportion of injected and un-injected larvae surviving at subsequent days after injection. Error bars: +1 SD. Significance between un-injected and injected fish: Student's t-Test, $P<0.05$ (*), $P<0.01$(**).

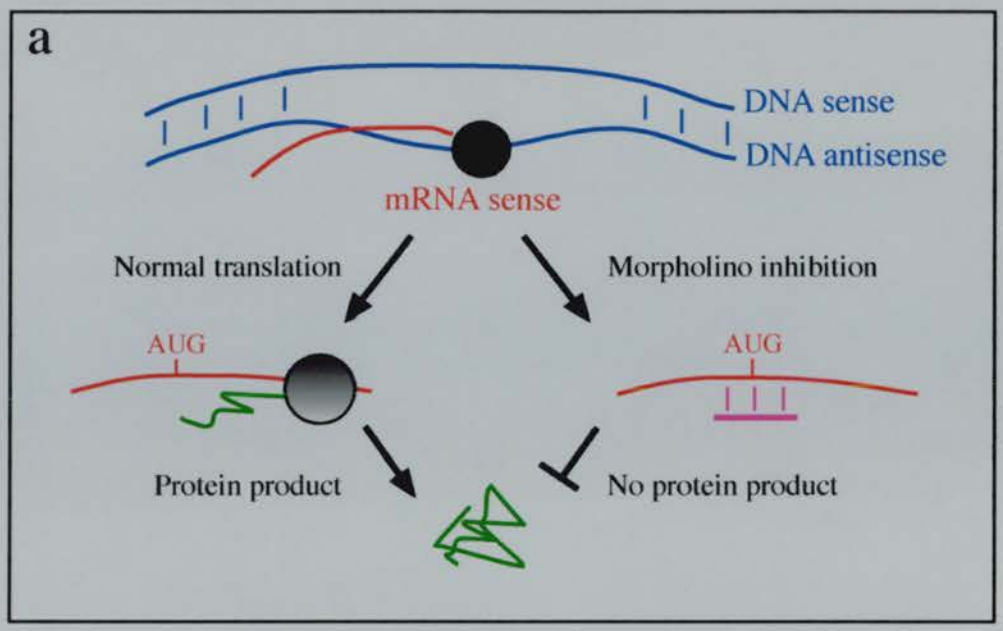
a
DNA sense
DNA antisense
mRNA sense
Normal translation
Morpholino inhibition
AUG
AUG
Protein product
No protein product

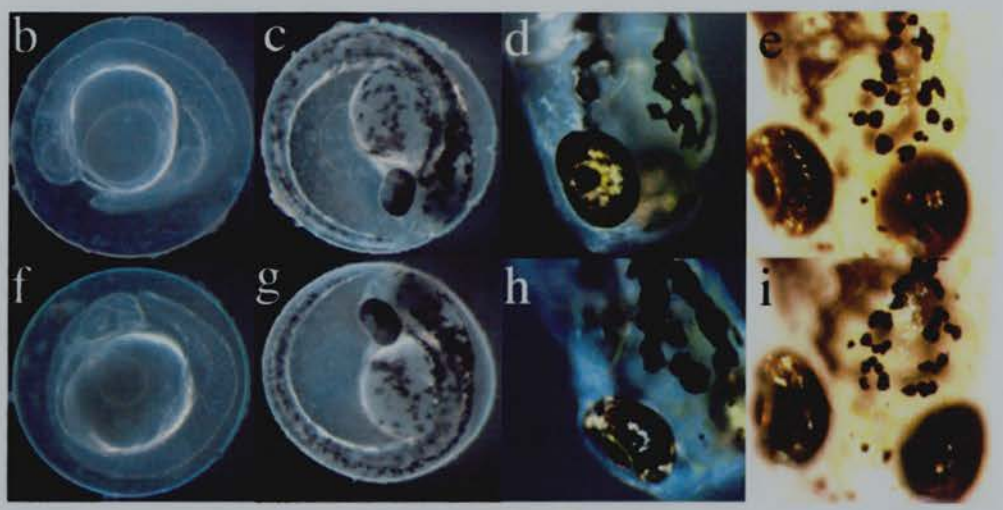
b
c
d
e
f
g
h
i

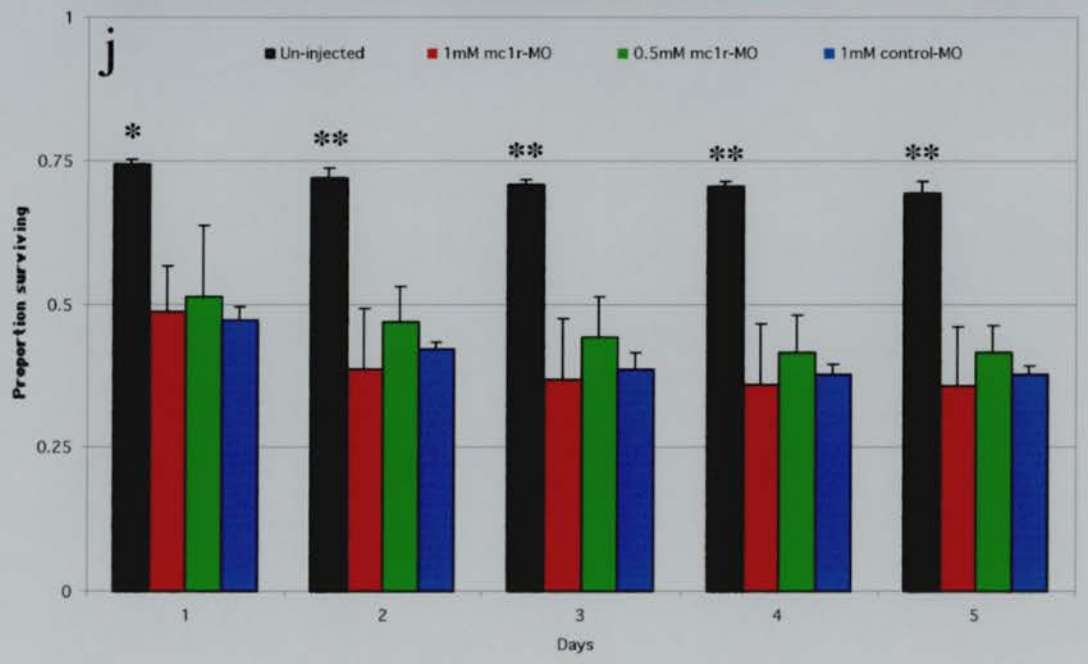
j
Un-injected
1mM mc1r-MO
0.5mM mc1r-MO
1mM control-MO
Proportion surviving
1
0.75
0.5
0.25
0
*
**
**
**
**
1
2
3
4
5
Days

The morpholino designed to inhibit *mc1r* translation (mc1r-MO) was designed to bind across the AUG initiator codon, from position –8 to +16. This sequence is specific for *mc1r* when compared with the zebrafish genome sequence currently available.

In three different experiments, at total of 396 1-2 cell zebrafish embryos were injected with 1mM mc1r-MO, 404 with 0.5mM mc1r-MO, 507 with 1mM of a control morpholino and 297 fish were not injected. These fish were observed on black and white backgrounds until 5 dpf, at which point they were euthanised. Figure 4.2.3b-i illustrates a representative example of 1mM mc1r-MO injected fish compared with un-injected controls. There is no apparent phenotypic difference between the fish at each time point. Both injected and un-injected fish are largely unpigmented at 24 hpf (Fig. 2.4.3b, f), when melanin has just begun to be synthesised. By 48 hpf, however, both have a similar number of typically shaped and pigmented melanophores (Fig. 2.4.3c, g) and these develop normally until 5 dpf (data not shown). On the fifth day both injected and un-injected larvae have aggregated melanophores on a white background (Fig. 2.4.3e, i) and dispersed melanophores on a black background (Fig. 2.4.3d, h). Control injected embryos and 0.5mM mc1r-MO injected embryos have the same phenotype.

To assess whether mc1r knockdown has a lethal or semi-lethal effect, the proportion of embryos surviving each day subsequent to injection was calculated. Figure 2.4.3j shows that, from 1 dpf, there is a significant decrease in fish surviving after injection, compared with un-injected fish (Student's t-Test, all values $P<0.05$). There is, however, no difference between control injected fish and mc1r-MO injected fish, or between difference concentrations of injected morpholino (Student's t-Test, all values $P>0.3$). Thus the increased number of dead fish probably result from the injection itself and is not related to mc1r knockdown.

4.3 An assay for physiological colour change in the zebrafish

Having established that zebrafish respond to the general tone of the background by redistributing the pigment in melanophores, a rapid, *ex vivo* assay was developed to investigate melanosome translocation in cell specific manner. To begin with, a source of melanophores was required that were accessible, easy to immobilise, numerous and have the ability to translocate melanin. Preliminary experiments using dorsal melanophores

from larvae, melanophores from the lateral dermis of adult fish and adult fin melanophores provided unsatisfactory results, mainly due to immobilisation problems and reflected light from associated iridophores (data not shown). However, experiments using the dorsal melanophores of adult fish proved much more successful. These cells are numerous, show melanosome aggregation and dispersion (Fig 4.2.1c,f) and have fewer underlying iridophores (compare reflective cells in Figure 4.2.1a-f with g-j). Moreover, the melanophores are associated with the dermal layer attached to the underside of the dorsal scales, providing a strong surface to support the cells on removal and immobilisation. Therefore an assay system was developed utilising dorsal scale melanophores of adult fish. As licensing restrictions precluded the removal of scales from living fish, dorsal skin tissues were cultured to minimise the number of fish euthanised for these experiments.

4.3.1 Colour change assayed in a single melanophore.

Single scales were removed from skin cultures, inverted, immobilised on agarose and visualised on a Leica stereo microscope. After addition of the compound of interest, individual melanophores were imaged by time-lapse digital photography over a 15 min period. These images were then combined to generate a movie. Figure 4.3.1 shows frame sequences from movies after addition of 1nM αMSH to an aggregated melanophore and of 1nM MCH and a saline solution to dispersed melanophores. It is obvious that αMSH causes the melanin to disperse (Fig. 4.3.1a), that αMCH promotes aggregation (Fig. 4.3.1b) while the control saline solution has no effect (Fig. 4.3.1c). Saline or αMCH added to fully aggregated melanophores also has no effect, nor does MSH addition to fully dispersed melanophores (not shown). Although the gross qualitative effect each compound has can be clearly seen, a quantification protocol was devised for accurate comparison of data across different experiments (see Chapter 5.6).

Figure 4.3.1d shows a merged image of the first and final frame from the movie of αMSH dispersion (Fig. 4.3.1a). Different colour channels are used to illustrate the pigmented area in the first frame and the pigmented area in the final frame. Figure 4.3.1e is a similarly merged image, illustrating the first and final frames from the movie of MCH aggregation (Fig. 4.3.1b). After pseudo-colouring the pigment in each frame, the total number of pseudo-coloured pixels was measured.

Figure 4.3.1. Legend overpage.

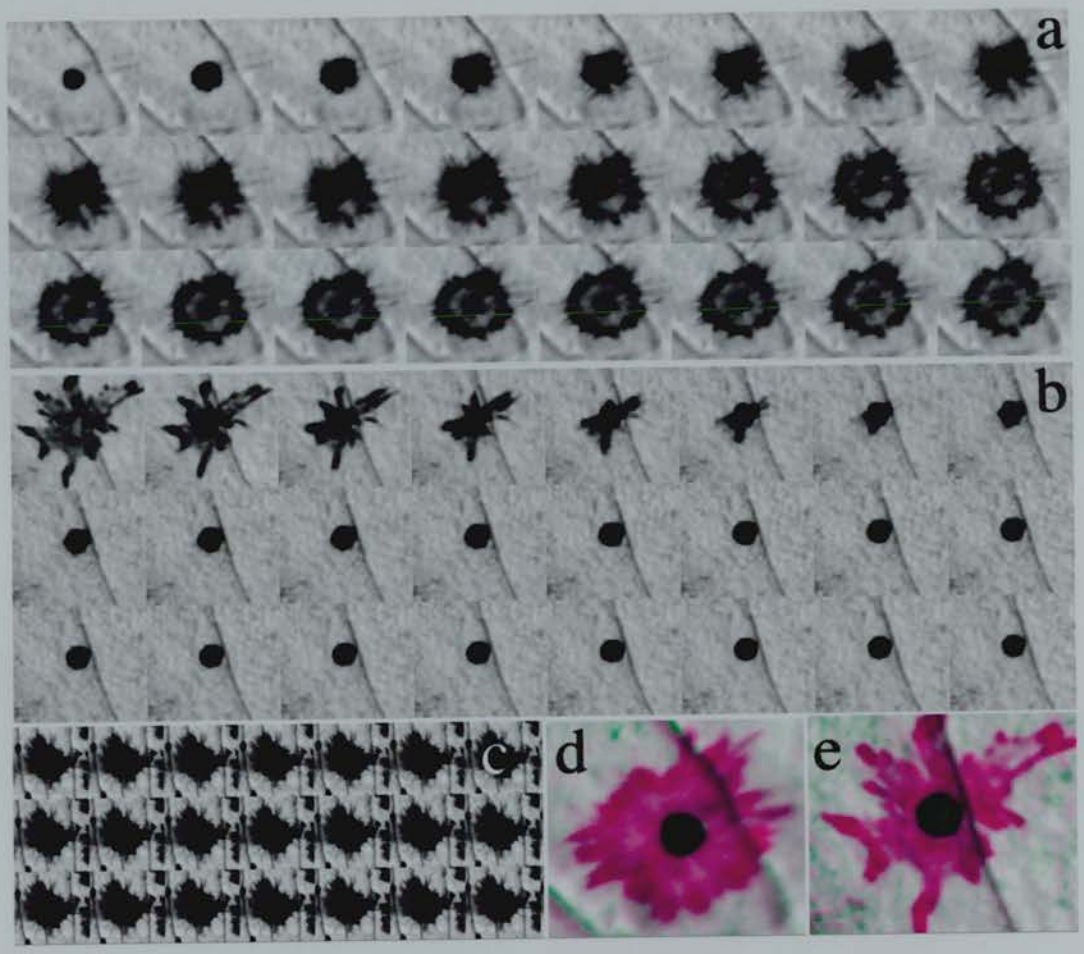

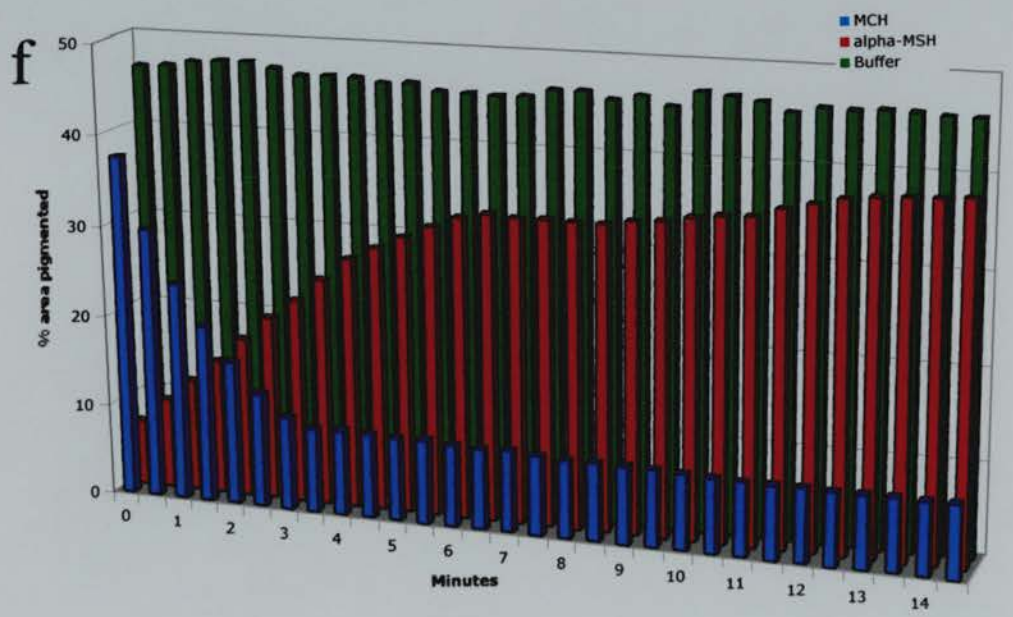

Figure 4.3.1 (previous page) Imaging single melanophores undergoing pigment translocation. a-c, frames from time-lapse movies are represented in three rows from left to right. For illustrative purposes, frames are shown over 36 second intervals beginning immediately after the addition of a compound: 1μM αMSH to a pre-aggregated melanophore (**a**), 1μM MCH (**b**) and PSS (**c**) to dispersed melanophores. **d-e**, merged images of the first and last frame from the movies illustrated in **a** and **b** respectively. Alternative colour channels are used to show the pigmented area when the cells are fully aggregated (*green*) and dispersed (*pink*). **f**, a quantitative analysis of the pigmented area in each frame from the movies represented in **a** (*red*), **b** (*blue*) and **c** (*green*). Frames are taken at 30 sec intervals.

Figure 4.3.1f is a plot of the percentage of pigmented (psuedo-coloured) pixels in each frame of a movie after treatment with αMSH (*red* bars), MCH (*blue* bars) and saline buffer (*green* bars). As melanin appears to be dispersed laterally, across the plane of the scale and because each frame is taken at 30 sec intervals, this assay represents a direct measurement of melanin translocation over time. Quantification shows that in the movies after treatment with αMSH (Fig. 4.3.1a) and MCH (Fig.4.3.1b), the range of melanin translocation is very similar: from ~38% of total frame area when fully dispersed to ~8% when fully aggregated. Furthermore, both aggregation and dispersion occurs rapidly, within 7 min and 4 min respectively. The pseudo-coloured pixel quantification of the movie after saline treatment (Fig. 4.3.1c) shows virtually no change over the 15 min period, remaining around 46% of the total fame area and fluctuating less than 2%. These data illustrate how the effect of hormones on single zebrafish melanophores can be visualised, then precisely and directly measured in a quantitative manner. To generate an accurate and statistically significant account of these effects, however, the data from experiments on numerous melanophores needed to be collected. Therefore this protocol was applied to whole dorsal scales.

4.3.2 Colour change assayed in a dorsal scales.

Adult zebrafish dorsal scales typically have between 20 and 50 melanophores associated with their underlying dermis. As an entire scale must be immobilised to image just a single cell, a quantification of pigment translocation in all the melanophores on the scale would provide a more accurate representation of physiological colour change. Thus the process described in the previous section was applied to entire scales (Fig 4.3.2). Immobilised scales with aggregated melanophores were treated with αMSH and scales with dispersed melanophores treated with MCH or saline buffer, followed by time-lapse

imaging. As demonstrated previously in single cells, it is clear MCH promotes melanin aggregation (Fig. 4.3.2a), that αMSH causes dispersion (Fig. 4.3.2b) and that control saline solution has no effect on melanin translocation (Fig. 4.3.2c). Colouring the translocated pigment by merging first and final frames in different colour channels shows the extent of MCH induced aggregation (Fig. 4.3.2d) and αMSH induced dispersion (Fig. 4.3.2e) on an entire scale. It is interesting to note, however, that even after MCH treatment some melanophores appear to remain dispersed (Fig. 4.3.2a and d, non pseudo-coloured cells). High-powered microscopy reveals that cells have lysed, spilling their contents over the surrounding cells (Fig. 4.3.2f). Such cells never respond to hormone treatment and have probably been damaged during the excision of the scale from the skin of the zebrafish.

As previously described, the total amount of translocated pigment was measured in each scale every 30 sec and represented as a percentage of total area (Fig. 4.3.2g). Although the general trends are similar, there are differences between the data recorded from whole scales to that obtained from single cells (compared Fig. 4.3.2g with Fig. 4.3.1f). Firstly, the measured range of melanin translocation within each frame is much smaller when imaging whole scales; the variance of pseudo coloured pixel area covers ~30% of the frame in single cell imaging but only ~5% of whole scales. Secondly, the measured range of translocation varies greatly between scales. At maximum dispersion, pigment covers 6, 8 and 15% of whole scales in Figure 4.3.2g; the differences due mainly to the variable number of cells found on each scale.

The greater variance observed in whole scale measurements make it difficult to compare data from different experiments, a major drawback for an assay system. However, this was overcome by standardising the quantification of each experiment. Figure 4.3.2h shows the quantification of pigment, in both whole scales and single melanophores, as a percentage of maximum observed pigment area. This representation allows direct comparison of separate experiments across on an identical scale. Moreover, it shows how the data from scales treated with αMSH or MCH, incorporating the translocation profile of tens of melanophores, are comparable to data from a single cell, but reflect a more accurate picture of the dynamic response.

Figure 4.3.2. Legend overpage.

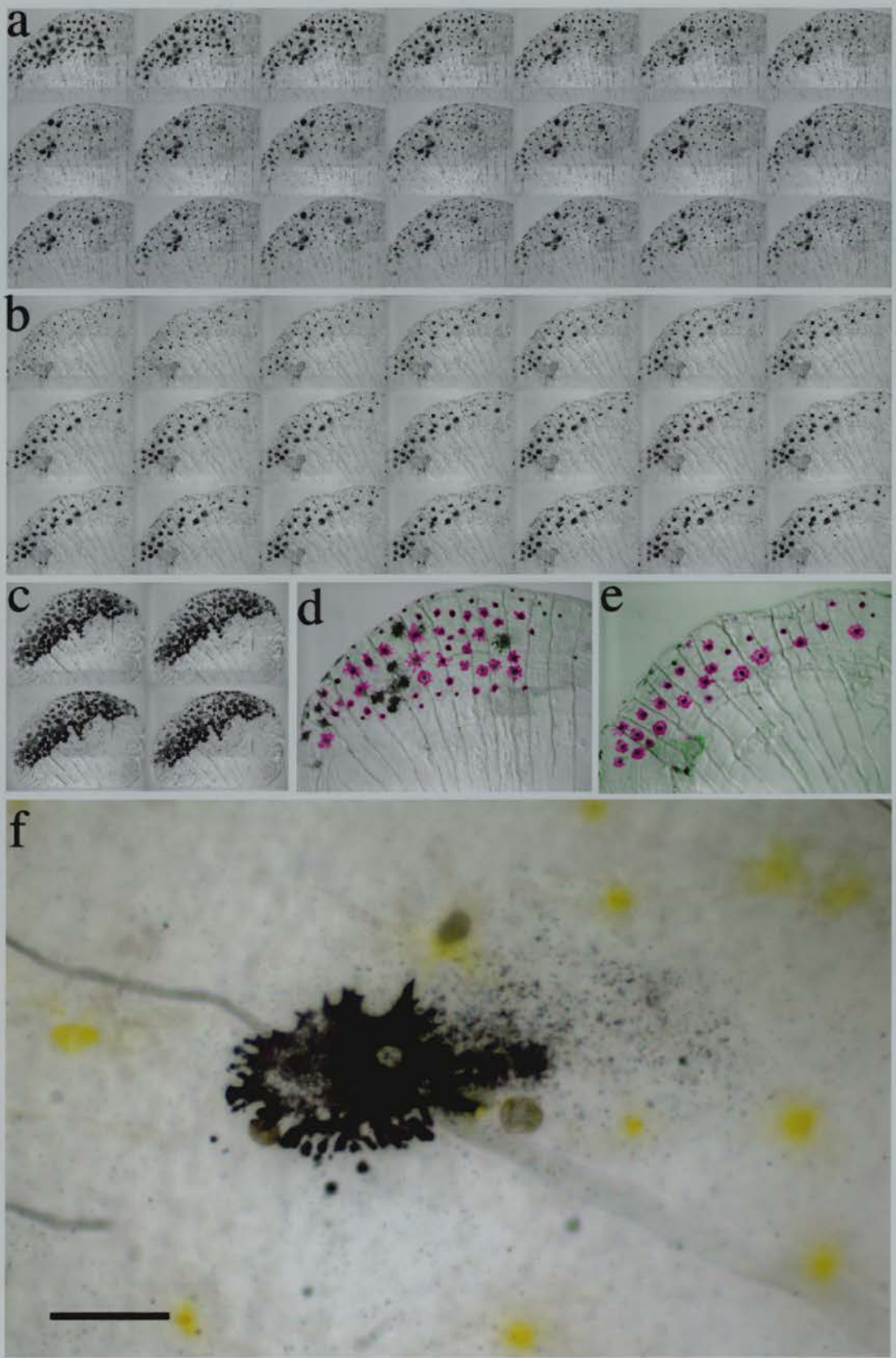

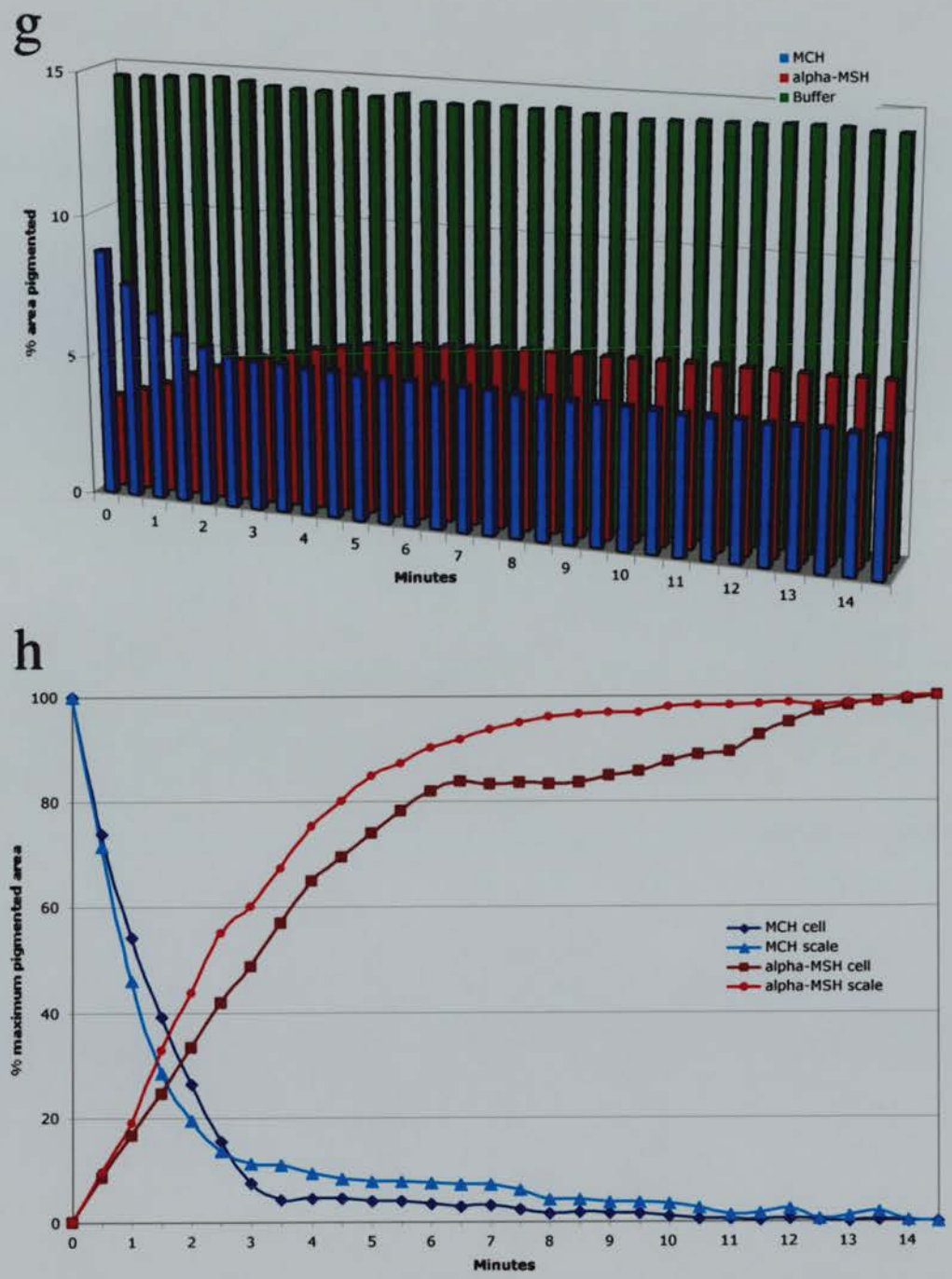

Figure 4.3.2. Imaging scale melanophores undergoing pigment translocation. a-c, frames from time-lapse movies are represented in three rows from left to right. For illustrative purposes, the frames shown are taken over 41 (**a-b**) and 217 (**c**) second intervals, beginning immediately after the addition of a compound: 1μM αMSH to a pre-aggregated melanophore (**a**), 1μM MCH (**b**) and PSS (**c**) to dispersed melanophores. **d-e**, merged images of the first and last frame from the movies illustrated in **a** and **b** respectively. Alternative colour channels are used to show the pigmented area when the cells are fully aggregated (*green*) and dispersed (*pink*). **f**, enlarged view of a non pseudo-coloured cell from **d**. **g**, a quantitative analysis of the pigmented area in all frames from the movies represented in **a** (*red*), **b** (*blue*) and **c** (*green*). **h**, standardised data from **g** and Fig. 4.3.1f, shown as a percentage of the maximum and minimum pigmented areas recorded.

4.4 Hormonal regulation of pigment translocation

It is well established that MCH and MSH are principle regulators of physiological colour change in many teleost fish species (Fujii, 2000). Preliminary experiments using the scale melanophore assay to further characterise the zebrafish response to αMSH and MCH are described in the following section. In each of these experiments, the melanophore translocation profile was recorded from three whole scales, incorporating 60-150 individual cells. The values shown are the mean of the data from these scales.

4.4.1 The effect of MCH on zebrafish melanophores

The activation profile of MCH on zebrafish melanophores was established by measuring the melanin translocation response to sequential dilutions of hormone concentration. Figure. 4.4.1 charts the melanophore aggregation observed over 10 min after treatment with a range of MCH concentrations, although each scale was imaged for 30 min to ensure the full response was recorded. After 10 min of treatment with all concentrations (except $1M^{-10}$), the pigment has aggregated to between 0.5-0.3 of the dispersed area (Fig. 4.4.1a). The response to $1M^{-10}$ MCH was much slower, but by 30 min a similar level of aggregation was observed (0.5 of the dispersed state). The maximum observed aggregation levels are not significantly different between each concentration (Student's t-Test, all values $P>0.3$), with the slight variance reflecting the different number and size of functional melanophores on each scale. Thus is appears that, within this concentration range, MCH has a threshold effect on melanophores: if aggregation does happen, then it occurs to its full capacity.

To investigate whether there is a correlation between MCH concentration and rate of aggregation, the data was standardised and compared (Fig. 4.4.1b). While $1M^{-10}$ MCH treated cells aggregate at the slowest rate, it appears that the higher the MCH concentration used, the faster aggregation occurs. To estimate the dynamics of pigment translocation for comparative purposes, a single value was calculated from the standardised plot: D^{50}. This represents the time (in seconds) at which the pigmented area is midway between the maximum and minimum area recorded for each scale.

Figure. 4.4.1. Legend overpage.

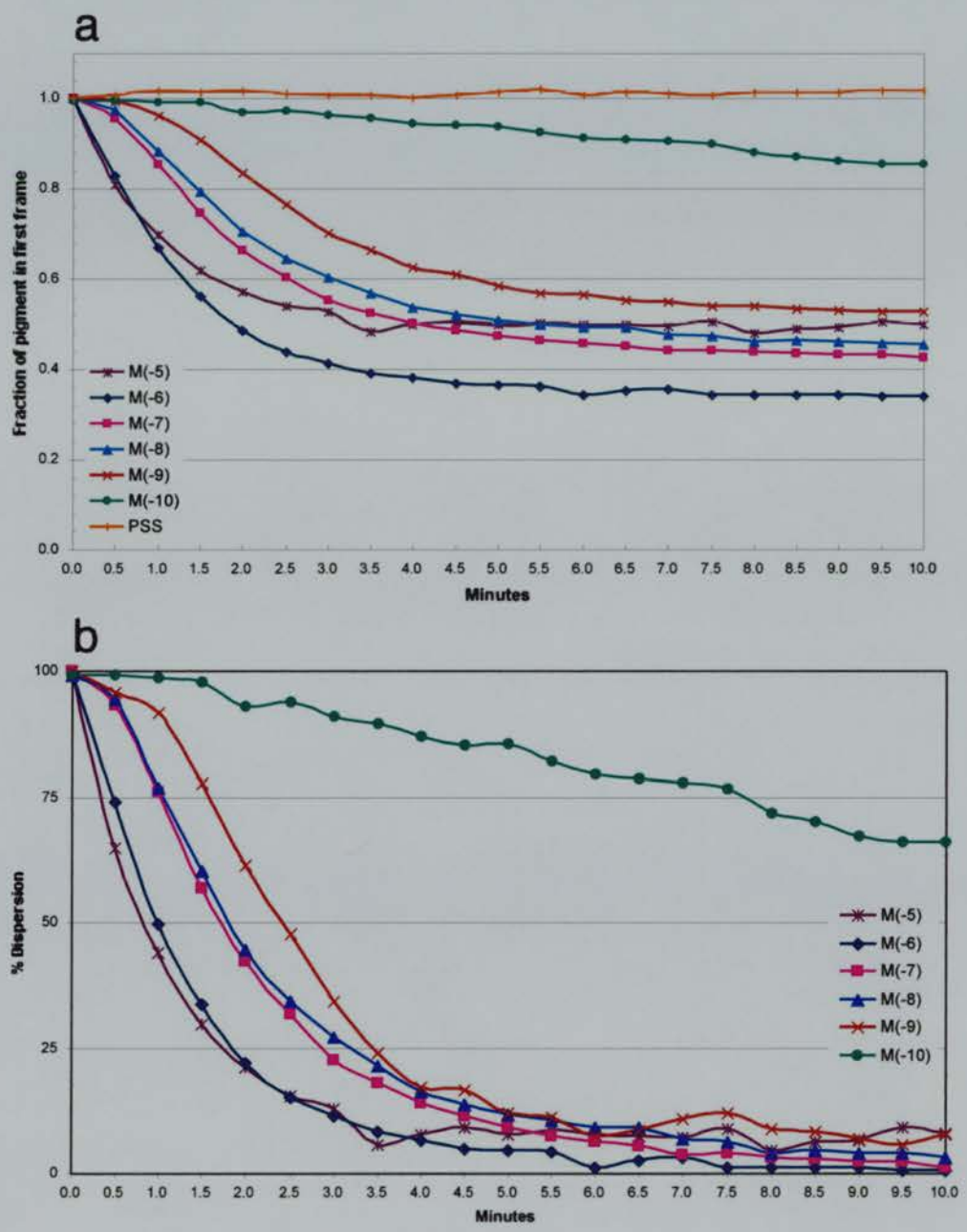

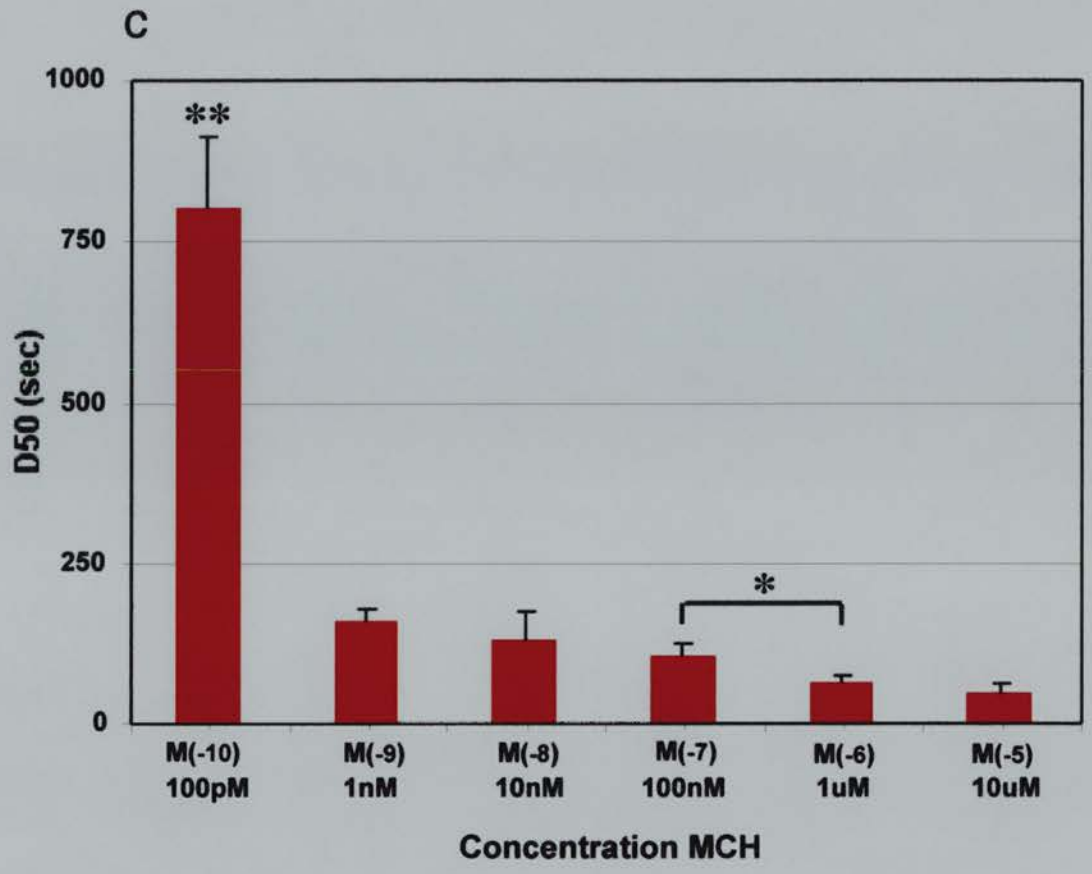

Figure. 4.4.1. Melanophores aggregate in response to MCH. **a**, quantitative analyses of the pigmented area in scales treated with MCH. **b**, standardised data from **a** shown as a percentage of the maximum and minimum pigmented areas recorded over 30 min. **c**, an estimate of translocation rate showing the mean time until 50% of maximum dispersion (D^{50}) for each concentration of MCH. All values are the mean of 3 scales, error bars: +1 SD. Statistical significance: Student's t-Test, $P<0.05$ (*), $P<0.01$(**).

When the D^{50}s of the concentration series are compared the significance of observed differences in aggregation rates can be statistically assessed. Figure 4.4.1c shows the highly significant increase in mean $1M^{-10}$ D^{50} aggregation time when compared with higher concentrations. Although mean D^{50} aggregation time does appear to get shorter with exposure to increasing concentrations of MCH, the subsequent incremental decreases are not statistically significant with the exception of 10^{-7} to 10^{-6}.

4.4.2 The effect of melanocortins on zebrafish melanophores

Having established MCH influences the rate of melanophore aggregation in a dose dependant manner, the effect of αMSH was then investigated. Figure 4.4.2a illustrates the melanin dispersion observed over 15 min after exposure to with a range of αMSH concentrations. Akin to the effect of MCH, the maximal levels of dispersion are variable but uncorrelated with αMSH concentration. However, when compared to MCH aggregation the extent of the response is much smaller (compare Fig. 4.4.1a with Fig. 4.4.2a). This difference is due to the relative position of pigment in melanophores at the beginning of the experiment. If untreated melanophores maintained melanin in an intermediate position, halfway between maximum aggregation and dispersion, then one might expect the MCH and αMSH response to be similar in magnitude. Unfortunately, untreated melanophores are largely dispersed when the fish is euthanised and the skin cultured, so the extent of αMSH-induced dispersion is severely limited.

The reduction in dispersion magnitude has implications for the interpretation of these results. For example, when the data is standardised, artefactual fluctuations caused by minute changes in light intensity during image capture are greatly enhanced. This is apparent when Figure 4.4.1b is compared with Figure 4.4.2b. Furthermore, the dynamics of dispersion may differ between aggregated melanophores and cells that are largely dispersed to begin with. When the mean dispersion times are compared, a decrease in D^{50} dispersion times can be observed with increasing αMSH concentration, but the only incremental difference with statistical significance is between $1M^{-10}$ and $1M^{-9}$ (Fig. 4.4.2c). In an effort to obtain a more accurate representation of melanin dispersion, the range of MSH concentrations was added to fully aggregated melanophores. After removal from the skin culture, but before immobilisation for imaging, scales were incubated in 1nM MCH then washed numerous times with PSS.

Figure. 4.4.2. Legend overpage.

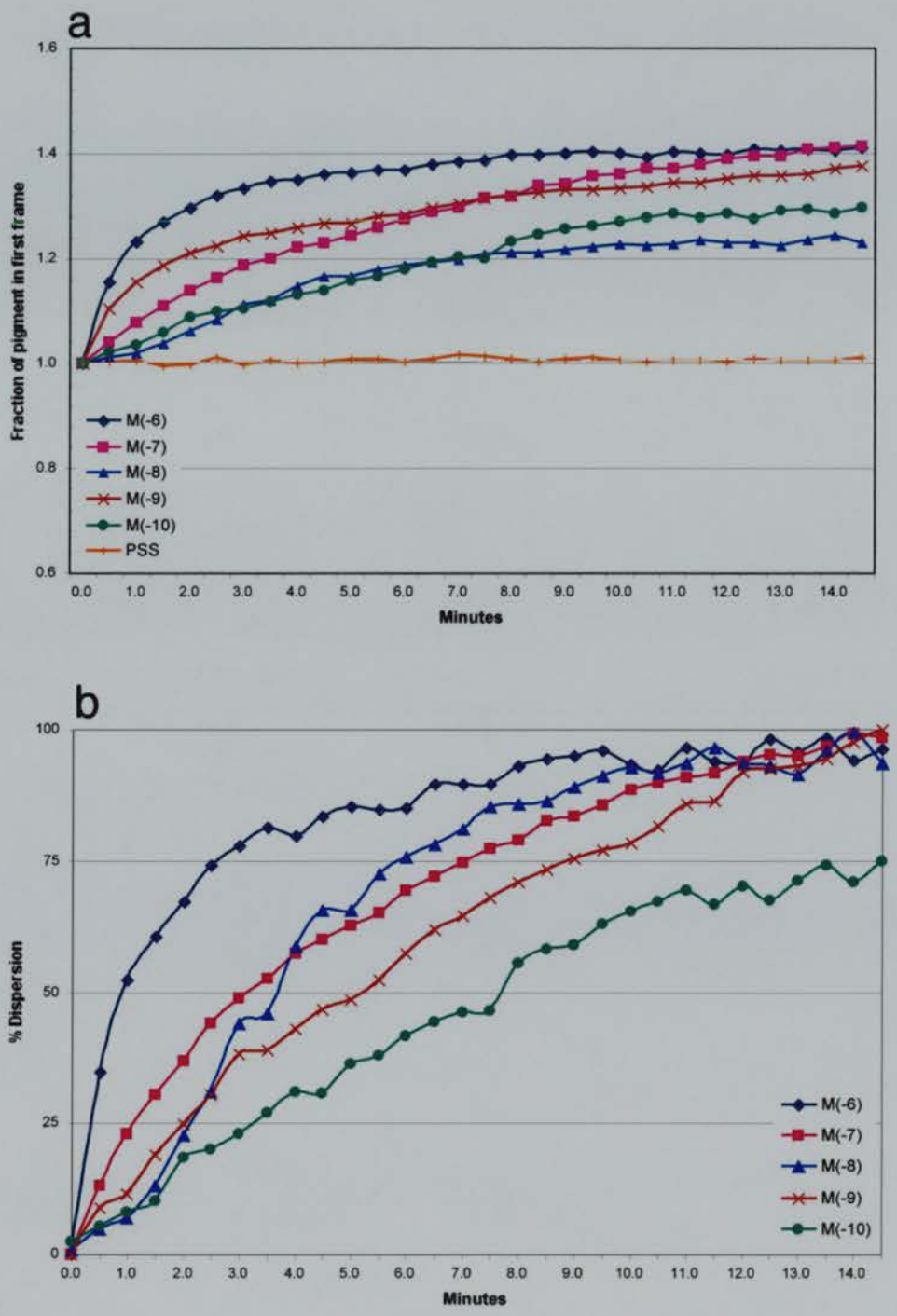

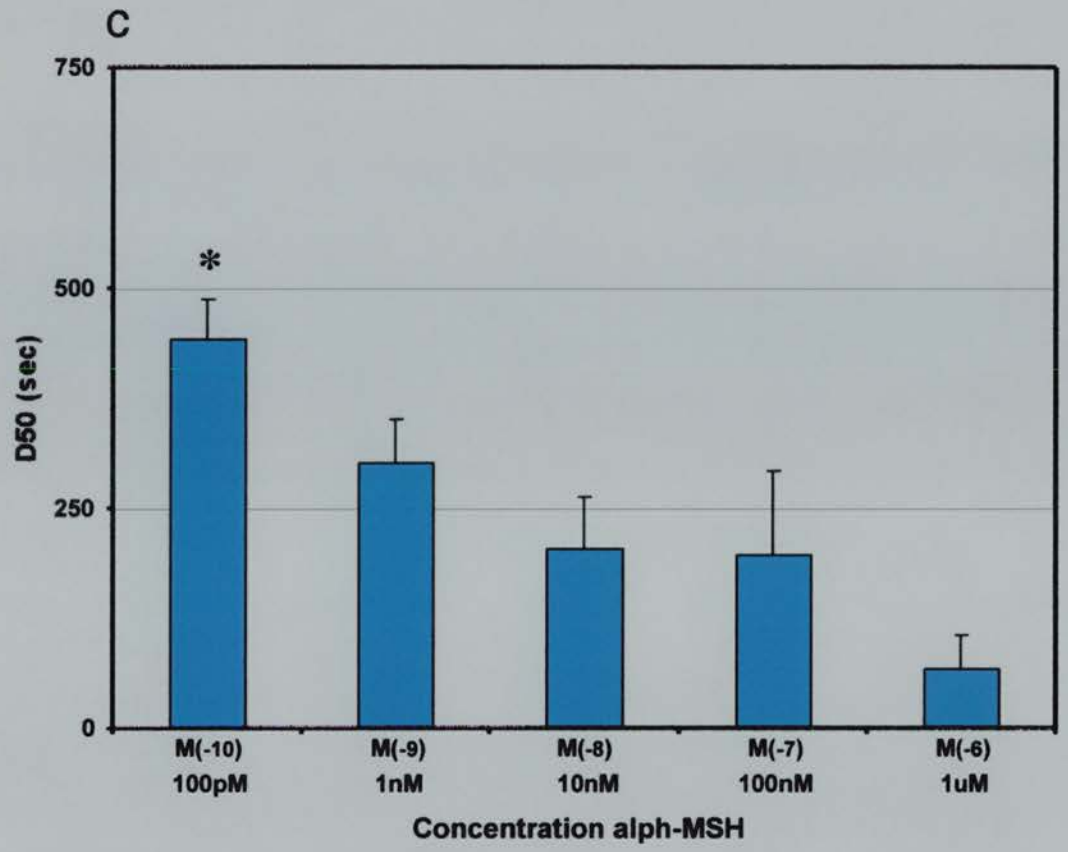

Figure. 4.4.2 Melanophores disperse in response to αMSH. a, quantitative analyses of the pigmented area in scales treated with αMSH. **b**, standardised data from **a** shown as a percentage of the maximum and minimum pigmented areas recorded over 30 min. **c**, an estimate of translocation rate showing the mean time until 50% of maximum dispersion (D^{50}) for each concentration of αMSH. All values are the mean of 3 scales, error bars: +1 SD. Significance: Student's t-Test, $P<0.05$ (*).

As melanin translocation in scale melanophores is a fully reversible process for many hours after excision from the skin (data not shown), pre-aggregation with MCH is unlikely to have any inhibitory effects on subsequent dispersion.

In addition to treatment with MSH, scale melanophores were also treated with sequential dilutions of α, β, γ and [Nle4, D-Phe7]- αMSH (NDP-MSH, a synthetic analogue previously demonstrated to be a very potent activator of mammalian melanocortin receptors) (Haskell-Luevano *et al.*, 1997). For each compound the overall level of pigment was measured to ensure full dispersion was taking place. In all cases the pigment either dispersed to 1.75-2.25 times the aggregated area (full dispersion), or fluctuated within 0.05 of the aggregated state (no dispersion). No intermediate level of dispersion was observed and there was no correlation between extent of dispersion and concentration of melanocortin. Thus, if dispersion did occur, the data was standardised and the time calculated for the melanophores on each scale. Figure 4.4.3 illustrates the mean $1/D^{50}$ time from the melanophores on three scales for each concentration of melanocortin. Within the range tested ($1M^{-10}$ to $1M^{-6}$), a more rapid dispersion is observed with increasing dose of α, β and γMSH. All three naturally produced peptides have rapid dispersing activity at micro-molar concentrations, however γMSH has no effect after dilution to $1M^{-7}$ and βMSH does not disperse at $1M^{-9}$. αMSH continues to disperse melanin at concentrations as low as $1M^{-10}$, but at a slower rate. In comparison, NDP-MSH displays no significant difference in dispersion rate across this range, being the only melanocortin to elicit rapid dispersion at sub-nanomolar concentrations. These data indicate that the melanocortin receptor mediating background adaptation in zebrafish melanophore has an activation profile of NDP-MSH > αMSH > βMSH > γMSH. Furthermore, even with small samples, the melanophore assay system can be used to distinguish between these four hormones at $1M^{-8}$ concentrations.

On binding to mouse Mc1r, the agouti signalling protein (ASP) acts as in inverse agonist to αMSH, promoting a switch from eumelanin to phaeomelanin production (Cone *et al.*, 1996). It is not currently known what role, if any, ASP plays in lower vertebrate pigmentation.

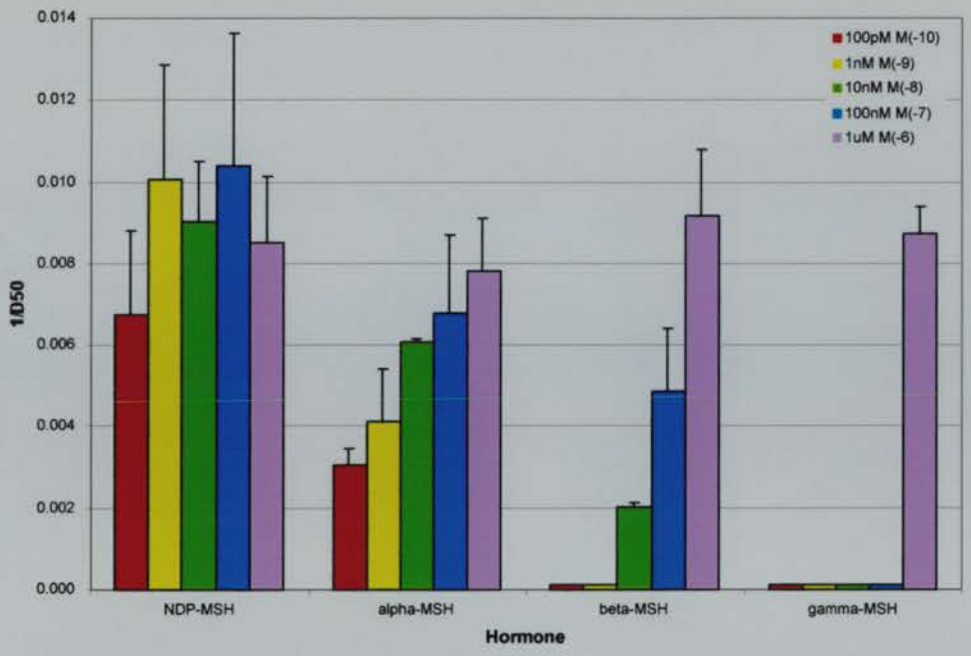

Figure. 4.4.3 The rate of melanophore dispersion in response to melanocortins. An estimate of translocation rate is shown, $1/ D^{50}$, where D^{50} is the time in seconds until 50% of maximum dispersion is reached, for each concentration of melanocortin peptide. Concentrations that failed to induce translocation have $D^{50} = \infty$, thus $1/D^{50} = 0$. All values are the mean translocation from 3 scales measured for 30 minutes. Error bars: + 1 SD.

Therefore a synthetic analogue of mouse ASP was assayed for pigment translocating activity in zebrafish melanophores. AgoutiYY (AYY) is an analogue of the ASP amino acids 90-132, but containing two substitutions (Q115Y and S124Y) that assist synthesis. By itself, concentrations up to $1M^{-7}$ AYY displayed no pigment translocation activity on aggregated or dispersed fish melanophores (Fig. 4.4.4). This suggests that, unlike mammalian MC1R, the melanophore receptor does not undergo "inverse" activation by ASP, but can AYY anatagonise αMSH induced signalling? To test this hypothesis melanophores were co-incubated with $1M^{-7}$ AYY and $1M^{-9}$ αMSH and the dispersion compared with exposure to αMSH alone. Figure 4.4.4 shows there is no significant difference in the rate or extent of $1M^{-9}$ αMSH induced dispersion in the presence or absence of AYY 100 times more concentrated (Student's t-Test, P=0.5). Thus it appears that ASP does not antagonise αMSH at the zebrafish melanophore melanocortin receptor.

4.4.3 Pigment translocation downstream of receptor signalling

Based on data from the zebrafish scale melanophore assay, it is clear that melanocortins and MCHs are initiating an intracellular response resulting in pigment translocation. However, the assay can also be used to investigate the nature of the intracellular signalling cascade and the bio-mechanics of melanosome translocation. The following pilot experiments illustrate the range of processes that can be elucidated using this assay.

After melanocortin activation of MC1R in mammals and amphibians, an increase in intracellular cAMP is observed as a result of adenylyl cylase (AC) activity. In contrast, the MC1R inverse agonist (ASP) decreases cAMP levels, probably by inhibiting AC function (Goldman and Hadley, 1969; Ollmann *et al.*, 1997; Ollmann *et al.*, 1998). To investigate the role of cAMP as an intracellular messenger in zebrafish melanophores forskolin, a specific activator of AC, was used in the melanophore scale assay (Seamon *et al.*, 1981). Figure 4.4.5a shows that after forskolin treatment there is a dispersion of melanosomes comparable to that observed with αMSH exposure (compare with Fig. 4.4.2a).

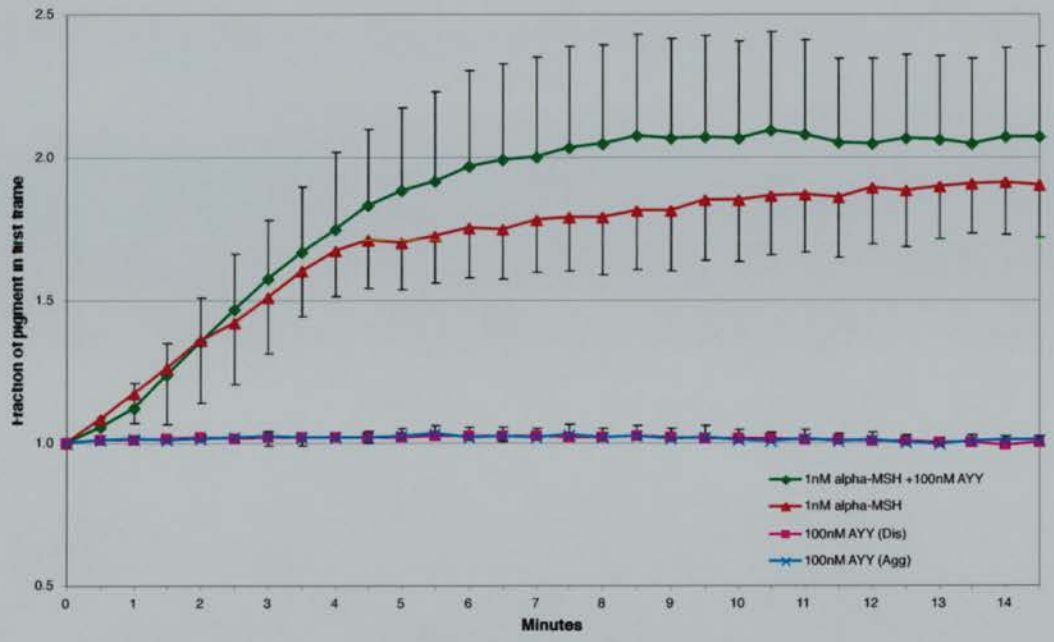

Figure. 4.4.4. AgoutiYY does not antagonise αMSH signalling in fish melanophores. A quantitative analysis of the pigmented area in scales treated with αMSH, AgoutiYY (AYY) or both. AYY was exposed to dispersed cells (Dis, *pink* line) and pre-aggregated cells (Agg, *blue* line). αMSH (*red*) and both proteins (*green*) were exposed to pre-aggregated cells only. All values are the mean of 3 scales, error bars: +1 SD. Further experiments were carried out using lower concentrations of AYY showing similar results.

Figure 4.4.5. Legend overpage.

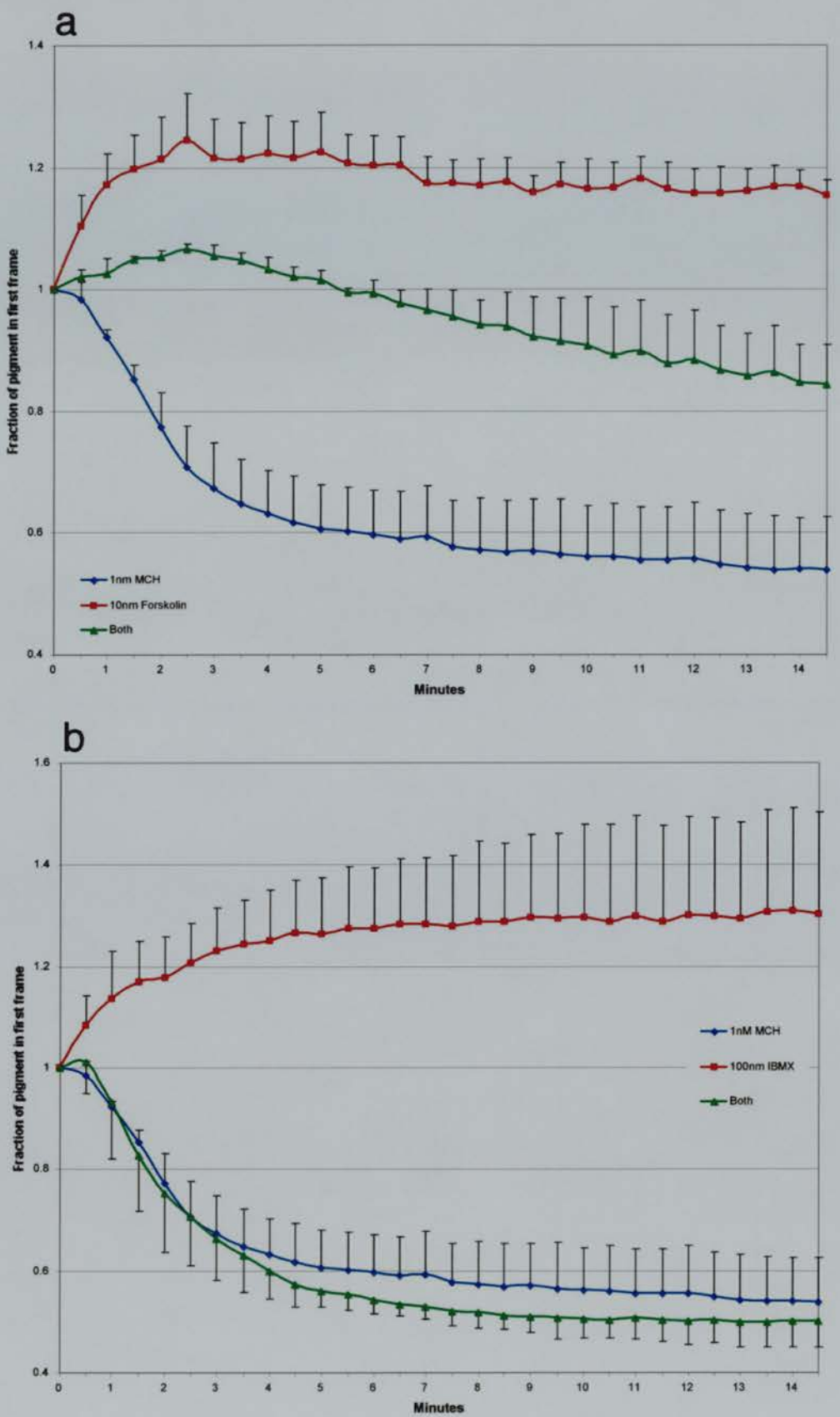

Figure 4.4.5. Intracellular cAMP regulates pigment translocation. a, a quantitative analysis of the pigmented area in scales treated with MCH, forskolin or both. **b**, a quantitative analysis of the pigmented area in scales treated with MCH, IBMX or both. All experiments were carried out in untreated scales, thus melanophores are initially semi-dispersed. All values are the mean of 3 scales, error bars: +/-1 SD.

When forskolin and MCH is added, the response is intermediate to the effect of both compounds alone (Fig. 4.4.5a). This suggests that increased cAMP is a mediator of melanin dispersal in zebrafish melanophores. To further examine the role of cAMP in pigment translocation, this experiment was repeated using 3-isobutyl-l-methylxanthine (IBMX) instead of forskolin. IBMX is a non-specific phosphodiesterase inhibitor that blocks the degredation of cAMP into it AMP, thus potentiating the effect of raised cAMP levels (Fredholm *et al.*, 1976). On exposure to IBMX melanophores undergo dispersion (Fig. 4.4.5b), albeit at a slower rate than when exposed to forskolin (despite being 10 times more concentrated). The effect of IBMX appears to be attenuated by MCH, however, as treatment with both compounds shows aggregation not significantly different than observed after exposure to MCH alone.

The translocation of pigment observed during morphological colour change in mammals involves transport of melanosomes along both microtubules and microfilaments (Jimbow and Sugiyama, 1998). There is some debate about the mechanism of rapid melanosome translocation in lower vertebrates, therefore the scale melanophore assay was used to investigate this in zebrafish. Nocodazole inhibits microtubule formation by binding to tubulin (Head *et al.*, 1985). To examine the effect of nocodazole on zebrafish melanophores, dorsal scales were immobilised then incubated in either nocodazole or physiological saline solution (PSS) for 2 hours, followed by exposure to MCH and αMSH. Figure 4.4.6a shows that pre-incubation in PSS has no adverse effects on the translocation response to αMSH and MCH treatment. In contrast, melanophores preincubated in nocodazole display no aggregation or dispersion after exposure to MCH or αMSH respectively. Even after increasing the concentration of hormones to $1M^{-5}$, no translocation was observed if preincubated in nocodazole (data not shown).

Figure 4.4.6. Legend overpage.

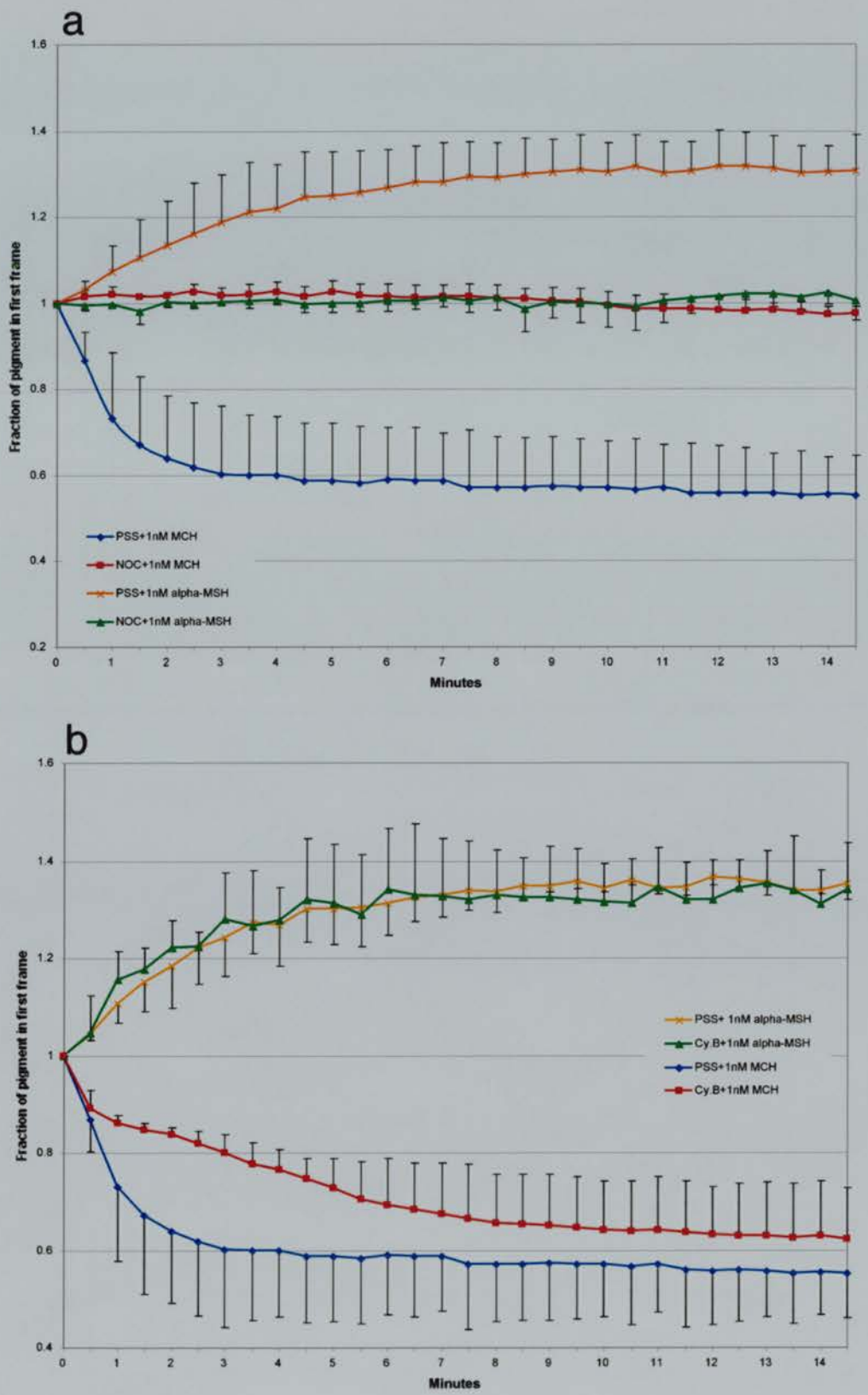

Figure 4.4.6. Microtubules are necessary for pigment translocation. a, a quantitative analysis of the pigmented area in scales preincubated in either nocodazole (NOC) or physiological saline solution (PSS), then treated with αMSH or MCH. **b**, a quantitative analysis of the pigmented area in scales preincubated in either cytochalasin B (Cy.B) or physiological saline solution (PSS), then treated with αMSH or MCH. All values are the mean of 3 scales, error bars: +/-1 SD.

These data indicate that both the anteriograde and retrograde melanosome transport observed in zebrafish physiological colour change is microtubule dependant, but are microfilaments also involved in the process? To resolve this question the above experiment was repeated using cytochalasin B, an inhibitor of actin microfilament formation and interaction (MacLean-Fletcher and Pollard, 1980), in place of nocodazole. Figure 4.4.6b shows that preincubation with cytochalasin B has no effect on the melanosome dispersion, but suggests microfilament disruption may have a subtle effect on melanosome aggregation. The mean D^{50} time for MCH aggregation with and without cytochalasin B preincubation is 175 sec (SD=70) and 63 sec (SD=26) respectively. As the sample sizes being compared in these pilot experiments are very small (n=3), this difference is not quite statistically significant (Student's t-Test, P=0.06), thus further work is required to confirm this difference.

4.5 Discussion

4.5.1 Zebrafish colour change in vivo

Cryptic colouration has not been previously investigated in adult zebrafish, but that it occurs is entirely expected as nearly all lower vertebrates are capable of physiological colour change in response to their surroundings. The form and purpose of background adaptation varies with species and environment. Clearly, an animal matching its colour to the background will render itself less visible to predators or prey. However other poikilotherms use physiological colour change to regulate body temperature or to communicate mood. Chromatophore distribution in the adult zebrafish suggests the background adaptation response provides excellent camouflage from predators. The majority of chromatic cells on the dorsum of the fish are melanophores. Thus when viewed from above the fish appears very dark against a black background (Fig. 4.4.1d).

On a white background the melanophores aggregate and, as there are few iridophores, the underlying flesh gives the dorsum a very pale appearance (Fig. 4.4.1a). The highest density of melanophores is found at the dorsal midline where there are some iridophores, thus on black adaptation the iridescent stripe is completely obscured (Fig 4.4.1b,e). As the ventrum of the fish is largely lacking in melanophores, it is probable that the pigment pattern has evolved to protect the zebrafish from predator attacks from above.

At a higher resolution, it is clear the translocation of melanin is the major factor in the difference in colour observed after 24 hours of adaptation. However it is possible that morphological colour change has been initiated too. Extensive periods of light background adaptation can lead to the degeneration of melanophores (Dickman *et al.*, 1988) while long term dark adaptation appears to produce more melanophores (Fernandez and Bagnara, 1991). Recently, Sugimoto and colleagues compared melanophore density in black and white adapted medaka (*Oryzias latipes*) and found a significant difference within 4 days, due mainly to melanophore apoptosis in light adapted fish (Sugimoto *et al.*, 2000). Whether 24 hour adaptation is sufficient to induce such a morphological response in zebrafish is unclear from these experiments.

Like adult fish, zebrafish larvae also undergo physiological colour change, but not until ~5 dpf. Prior to this time, they have fully dispersed melanophores irrespective of background hue. This is a typical characteristic of lower vertebrate larval development, although the time until adaptation begins varies with species. *Xenopus* has been observed to adapt very early in development while other amphibians, such as *Rana pipiens*, do not adapt for weeks (Bagnara, 1998). It is not yet clear what causes the initiation of background adaptation. Primary phase larval melanophores (non adapting cells) can undergo melatonin-induced aggregation in response to nonretinal light sensing (Binkley *et al.*, 1988), suggesting the intracellular components of the aggregation response are present and functional. A visually evoked startle response is observed in zebrafish at around 3 dpf, suggesting the larvae can distinguish differences in light reflected from the background 1-2 days before adaptation occurs (Easter, Jr. and Nicola, 1996). It therefore seems unlikely the onset of adaptation response is initiated by perception of background, though the development of neural wiring that connects the retina to the hypothalamus could be the instigating factor. It is possible that, in teleosts at least, the induction of the MCH signalling system marks the beginning of the secondary phase of larval

pigmentation. This hypothesis could be tested in the developing zebrafish. Identification and characterisation of the gene(s) encoding MCH would reveal when the hormone is first expressed. However, it may be expression of melanophore specific receptors that allows aggregation to occur, especially as the zebrafish *mchr1a* gene is expressed from 4-5 dpf.

4.5.2 Identifying genes that influence colour change

To investigate a role for mc1r in the primary phase of zebrafish larval pigmentation a morpholino knockdown method was used. This approach was chosen under the hypothesis that a reduction in pigmentation would occur if mc1r induced melanogenesis. Alternatively, if mc1r mediated primary phase dispersion, more aggregated melanosomes would be observed. Unfortunately mc1r morphant larvae exhibited neither of these features, instead showing identical melanophore content and morphology to wild-type and control injected fish (Fig. 4.3.2). These observations can be interpreted in a number of ways. It may be that mc1r signalling does not regulate melanogenesis in developing zebrafish melanophores and that the protein is not required for the initial dispersion of melanosomes. Furthermore, if the morpholino does knockdown mc1r, it would suggest the protein is not essential for early zebrafish development and survival. However, an alternative explanation would be that the morpholino has simply failed to reduce mc1r levels. Without an antibody against the protein product, it is difficult to prove a morpholino is binding to its target sequence and inhibiting protein production. One method would be to use the morpholino to rescue an over-expression phenotype induced by injection of RNA. Alternatively an expression construct could be engineered linking the morpholino target sequence to a reporter gene (such as GFP). If the morpholino can knockdown the reporter gene expression then it must bind to its target effectively.

At 5dpf, when zebrafish larvae enter the secondary phase of pigmentation, the mc1r morphants displayed a normal background adaptation response. This was expected, as by this time the cellular concentration of morpholino will probably have been diluted to below functional levels (Summerton and Weller, 1997; Nasevicius and Ekker, 2000). It is therefore not possible to deduce what role mc1r may have in background adaptation

from morpholino experiments. For this reason the knockdown of mc1r was not pursued further.

Another method used to investigate the transition of zebrafish larvae from primary to secondary phase of pigmentation involved the use of background adaptation mutants. Initially identified by Kelsh *et al*, this class of mutant fails to enter the secondary phase of larval pigmentation at 5 dpf, though whether they are capable of circadian colour change is unknown (Kelsh *et al.*, 1996). For background adaptation, it is implicit that the animal can visually perceive differences in the background. Thus blinded fish cannot undergo this process instead having dispersed cells on all backgrounds (Bagnara, 1998). Analysis by Neuhuass and colleagues indicated that 3 of the 7 mutants in this class were blind, making them unattractive candidates for melanophore specific defects (Neuhauss *et al.*, 1999). However, it appears that the two available non-blind mutants strains that are deficient in background adaptation have normally functioning *mc1r*, *mchr1a*, *mchr1b*, *mchr2* and *pomc* genes. Although changes in regulatory elements that could adjust normal production of these protein cannot be ruled out as the causative factor in these mutants, the majority of ENU induced phenotypes previously characterised are caused by single base pair changes. Single nucleotide substitutions that display a phenotype are almost always found in coding regions of genes or in conserved splice sites, rarely in untranslated regions (Justice, 2000). Nevertheless, a quantitative comparison of specific RNA or protein content in mutant and wildtype fish should reveal any difference in the expression levels of these genes.

If not deficient in melanocortin or MCH signalling, what might be the cause of lack of background adaptation in these mutants? There are many aspects of pigment translocation not yet fully understood that may result in a dispersed phenotype when disturbed. It appears that, in some teleost fish, melanophores are under both hormonal and neuronal control (Green and Baker, 1989). If this is the case in zebrafish, then mutant genes in the neural control pathway may result in a dispersed phenotype.

A review of genes involved in mammalian pigmentation provides further candidates. For instance, the intracellular cascade that signals downstream of hormonal signalling may be disrupted. An example of this is found in McCune-Albright syndrome, a human disorder that results in hyperpigmentation due to an activating mutation in the Gα

subunit associated with MC1R (Kim *et al.*, 1999). Alternatively, the protein complex that tethers melanosomes to the cytoskeleton for retrograde transport could be dysfunctional, leaving the pigmented vesicles in a permanently dispersed state. There are numerous proteins involved in melanosome transport in mammals that result in a pigmentation phenotype when mutated (Westbroek *et al.*, 2003). One of these, myosin Va, has recently been reported to be associated with fish melanosomes, and is probably involved in tethering the vesicles to the peripheral cytoskeleton (Skold *et al.*, 2002b).

There are probably too many genes involved in the translocation process for identification by candidate sequencing to be successful, certainly with unmapped mutations. Therefore, to assist in the future characterisation of background adaptation mutants and to provide an experimental model to examine the contrasting effects of melanocortin and MCH signalling, a zebrafish melanophore assay system was developed.

4.5.3 An experimental system for measuring colour change.

The use of physiological colour change in lower vertebrate melanophores as an assay system is not new. A frog skin bioassay was first used and colour change measured by a reflectometer (Moller and Lerner, 1966). Subsequently, isolated melanophores from many fish species have been used (for examples see (Oshima *et al.*, 1986; Karlsson *et al.*, 1991; Fujii, 2000; Aspengren *et al.*, 2003)) and the response measured using the melanophore index, a visual approximation of aggregation state. The most popular assay system involves measuring the light transmission through a plate of cultured *Xenopus laevis* melanophore cells before and after drug treatment (Potenza and Lerner, 1992). While this assay has proved useful in characterising agonists and antagonists of melanocortin signalling (Ollmann *et al.*, 1998; Tammler *et al.*, 2003), it has some drawbacks for detailed study of the bihumoral control of colour change. Firstly the receptors and downstream mediators of αMSH have yet to be characterised in this species and the tetraploid nature of the *X. laevis* genome will make it difficult to do so at the genetic level. Secondly, frog melanosomes do not aggregate on treatment with MCH (Ide *et al.*, 1985) thus a bihumoral control system is probably not used in lower tetrapods. Finally, this assay measures aggregation and dispersion indirectly, in a

photometric fashion. To accurately investigate the subtleties of melanin translocation, a direct measurement system would be advantageous.

The zebrafish melanophore assay system described in Chapter 4.3 improves on the *X. laevis* in three respects. As described in Chapter 2, the genes involved in zebrafish pigmentation can be easily identified and characterised. Furthermore, as a teleost, the zebrafish melanophore is responsive to both MCH and melanocortins (see Chapter 4.5.3). Most importantly, the availability of advanced digital imaging software allows the direct visualisation and quantification of pigment translocation.

The protocol used in subsequent experiments measured the combined translocation of pigment in tens of melanophores on a single scale over 60x30 sec time points. This was chosen as a compromise between resolution and computing capacity and proved suitable for quantifying gross changes in pigment translocation. It is technically possible to measure the translocation of all the melanophores on each scale concurrently, or to sample the translocation at time points of less than a second, allowing the collection of very accurate and detailed data. Furthermore, Chapter 4.3.1 illustrates the resolution at which translocation in a single melanophore can be imaged. This provides an opportunity to study subtle changes in pigment cell function or morphology. For example, the *union jack* mutant appears to have a pigment free 'hole' in the centre of its dispersed melanophores (Kelsh *et al.*, 1996). This could be monitored through the aggregation response in a single cell. However as there is a large variability in melanophore size and shape, a large number of individual cells would have to be measured to ensure any observed differences are significant. Thus the pigment translocation on entire scales was measured to ascertain the gross changes associated with physiological colour change.

4.5.4 Melanocortins and MCH in colour change

It is clear from scale assay experiments that both MCH and melanocortins stimulate pigment in a dose dependant fashion (Fig. 4.4.1 and Fig. 4.4.3), however the variation appears to be in the rate of translocation, not the extent of the dispersion or aggregation. The minimum dose of MCH to elicit an aggregation response appears to be between concentrations of $1M^{-11}$ and $1M^{-10}$. After 30 min of exposure to $1M^{-11}$ MCH no

aggregation was observed, compared with the D^{50} aggregation time ~800 seconds observed after $1M^{-10}$ MCH treatment. However, an increase in concentration to $1M^{-9}$ MCH resulted in a more rapid aggregation response (D^{50}=156 sec). These values are within the range of doses reported to cause pigment aggregation in *in vitro* assays in other teleost fish species. The marbled swamp eel (*Synbranchus marmoratus*) has been shown to respond to concentrations of MCH as low as $1M^{-12}$ whereas the minimal dose for the convict cichlid (*Archocentrus nigrofasciatus*) is $1M^{-8}$ (Castrucci *et al.*, 1987; Matsunaga *et al.*, 1989). Although the observed range of effective aggregating concentration between species seem large, diffusional barriers within the skin may account for some of the variation. It is also important to note that rat MCH was used in experiments described here while other assays have used salmonid MCH (Baker, 1993), although early experiments on a close relative of zebrafish (*Danio rerio frankei*) reveal similar results to those described here (Hadley *et al.*, 1987).

Is the minimum effective MCH dose observed in this assay likely to be similar to physiological concentrations in zebrafish after light adaptation? Currently the circulating MCH levels have been measured in only one teleost species, the rainbow trout (*Oncorhynchus mykiss*). Kishida and colleagues demonstrated that dark adapted trout have plasma MCH concentrations of ~$1.4M^{-11}$, rising to ~$5M^{-11}$ after white adaptation (Kishida *et al.*, 1988). As well as being within the range of the minimum effective dose in zebrafish, the difference in these concentrations is relatively small. Therefore it might appear that the pigment translocation response in trout melanophores is sensitive to very subtle changes in MCH concentration. In the trout, however, aggregation *in vivo* is unlikely to occur in response to MCH concentration alone, because denervated melanophores do not become fully aggregated on a white background (Baker *et al.*, 1986). Moreover, it has been demonstrated that noradrenaline and MCH act synergistically on trout melanophores *in vitro* (Green and Baker, 1989) thus, in this species, melanosome aggregation is probably under both hormonal and nervous control. In other teleosts, however, MCH appears to be essential and sufficient to elicit full aggregation (Bowley *et al.*, 1983; Baker, 1993). It is not known if neurotransmitters regulate background adaptation in zebrafish melanophores *in vivo*, but preliminary experiments using the melanophore assay suggest noradrenaline is capable of inducing aggregation *in vitro* (data not shown). Further experiments using both MCH and

noradrenaline will reveal whether these are capable of signalling synergistically in the zebrafish.

In comparison to the role of MCH in teleosts, the effect of αMSH on lower vertebrate melanophores is understood. In amphibia there is a simple unihumoral control system regulating background adaptation: increases of circulating αMSH results in melanophore dispersion and decreases result in aggregation (Bagnara, 1998). In teleosts, the reduction of circulating αMSH is not sufficient for melanophore aggregation (Baker, 1993). This is reflected in the relatively dispersed 'resting' state of zebrafish melanophores *in vitro*. In contrast, isolated amphibian melanophores are aggregated in the absence of αMSH. Like MCH, αMSH translocates melanin in zebrafish in a dose dependant fashion with a minimum effective dose between $1M^{-10}$ and $1M^{-11}$. This is within the same concentration range as MCH suggesting that, *in vitro* at least, zebrafish melanophores display a similar sensitivity to each hormone. Not all teleost fish dispay equally sensitivity, however, as trout melanophores respond to MCH over higher concentrations of αMSH (Baker, 1988). The antagonistic actions of αMSH and MCH on zebrafish melanophores could be examined directly by titrating them against one another and measuring the resulting translocation.

Chapter 2 describes the characterisation of zebrafish *pomc*, demonstrating the presence of highly conserved sequences encoding α and βMSH, but lacking a recognisable γMSH peptide. It is not clear how the function of the melanocortin peptides are delineated in lower vertebrates thus, having established the melanosome translocating activity of αMSH in zebrafish, the effect of other melanocortin peptides were measured. Figure 4.4.3 illustrates the dispersing ability of each naturally occuring melanocortin, plus that of a synthetic analogue. It is clear that the most potent of the naturally occurring melanocortins is αMSH. The other naturally occuring melanocortins do have dispersing activities, but only at concentrations that are probably above physiological levels, confirming αMSH as the hormone most likely to be regulating dispersion in zebrafish. What is more interesting, however, is the comparison of the zebrafish melanophore melanocortin receptor activation profile with that of mammalian receptors. Based on the observed melanocortin potency profile (NDP-MSH > αMSH > βMSH > γMSH), and assuming that zebrafish receptors have similar affinities to their mammalian orthologues, it is unlikely that the receptor expressed in melanophores is mc2r or mc3r. Although

mammalian MC4R, MC5R and MC1R have a αβγ melanocortin profile matching that of the melanophore receptor, they differ in affinity for NDP-MSH. This melanocortin is very potent activator of MC1R and MC4R compared with MC5R (Starowicz and Przewlocka, 2003). NDP-MSH appears to be the most potent of all melanocortins tested, thus the melanophore melanocortin receptor shows the best affinity profile match to mammalian MC1R and MC4R.

It has been long assumed that the melanocortin receptor that mediates background adaptation in lower vertebrates is the orthologue of MC1R. Despite lacking genetic evidence showing the *mc1r* gene is responsible for zebrafish pigment dispersion, the melanocortin activating data is consistent with mammalian MC1R-like function. To further assess how similar the zebrafish melanophore receptor is to mammalian MC1R, its response to an alternative agonist was tested.

Through a mechanism not yet fully understood, agouti signalling protein (ASP) functions as an 'inverse' agonist of mouse Mc1r. On binding to the mouse receptor, it not only inhibits the αMSH signal (to produce eumelanin), but also generates an alternative signal (producing phaeomelanin) (Ollmann *et al.*, 1998). Unfortunately ASP is extremely difficult to purify and is therefore not available to use as a reagent. However, a synthetic analogue, AgoutiYY (AYY), has been produced (McNulty, J; unpublished). Tested against the spectrum of mammalian melanocortin receptors, AYY appears indistinguishable from native ASP in antagonising αMSH induced signalling, but it is more stable and easier to synthesise (Millhauser, GL; personal communication). In the scale assay AYY provoked no pigment translocation at concentrations up to 100nM, suggesting it lacks inverse agonising activity in fish. This is consistent with the lack of dispersion by recombinant ASP in the *X. laevis* photometric assay. In amphibia, however, ASP does inhibit αMSH signalling at the melanophore melanocortin receptor. Furthermore, analysis of the binding kinetics suggests ASP both inhibits αMSH binding to the receptor directly and desensitises the receptor to activation (Ollmann *et al.*, 1998). However, at concentrations much higher than required for inhibition in *X. laevis* melanophores, AYY failed to significantly inhibit either the extent or the rate of pigment dispersion in zebrafish.

Although it is possible that higher concentrations of AYY would show inhibiting activity, the limited amount of protein available made it impossible to test. However, as AYY was 500 times more concentrated than required for detection in the *X. laevis* assay, this seems unlikely. It is also possible that zebrafish ASP is structurally different to its mammalian orthologue and its receptor has co-evolved to the extent that AYY cannot bind. This too seems unlikely, because despite detailed genome sequence analysis in three teleost species (see Chapter 2), no ASP encoding gene could be located. However, one exon of a closely related gene encoding agouti related protein (AGRP) was found (data not shown), suggesting if an ASP gene was present it would have been identified by this analysis. Thus the most likely explanation is that teleost fish have lost the ASP encoding gene and the melanophore melanocortin receptor has lost the ability to bind the protein.

This evolutionary scenario is consistent with the requirement for control of pigmentation. As teleosts have evolved a bihumoral control system, it is possible that the need to directly antagonise melanocortin signalling by ASP was superseded by MCH signalling. In comparison, amphibian hormonal control of background adaptation relies on melanocortins alone. In these species maintaining the ability to inhibit αMSH signalling with ASP, and thus change colour, would have an obvious selective advantage. Although ASP is yet to be described in amphibians, there is evidence of a spatially regulated factor produced in the integument, termed melanization-inhibiting factor (MIF), that blocks the melanogenic effect of αMSH on *Xenopus* neural crest cells (Fukuzawa and Ide, 1988; Fukuzawa and Bagnara, 1989). Further work is required to determine whether MIF acts directly on melanocortin receptors and if it is a true orthologue of mammalian ASP.

Subsequent to this analysis, a study describing the cloning of the AGRP gene in goldfish was published (Cerda-Reverter and Peter, 2003). In addition, the authors report a dorsal/ventral gradient of AGRP expression in the goldfish skin and suggest this may regulate the spatial pigment pattern of goldfish, in the same manner as ASP does in mouse (Vrieling *et al.*, 1994). In mammals AGRP cannot bind to MC1R, and therefore the authors propose MC4R (as opposed to MC1R) may be the melanocortin receptor found in teleost pigment cells (Cerda-Reverter and Peter, 2003). Although the data in this chapter does not disprove this hypothesis, neither does it favour it. Mouse Mc4r can

bind both ASP and AGRP *in vitro* and *in vivo* whereas Mc1r can bind only ASP (Cone *et al.*, 1996). Goldfish AGRP shares with mammalian AGRP and ASP all the important structural features required for melanocortin receptor binding. Moreover, as it is expressed in goldfish brain nuclei also expressing MC4R (Cerda-Reverter *et al.*, 2003a), it probably functions by antagonising this receptor (Cerda-Reverter *et al.*, 2003b). Thus, if MC4R is the teleost chromatophore melanocortin receptor, one might expect ASP to antagonise αMSH signalling in melanophores. This is clearly not the case. It is therefore unlikely that MC4R is the receptor expressed in pigment cells, especially considering the shared ontology between zebrafish melanophores and mammalian melanocytes. Nevertheless, it would be informative to investigate the pigment translocating activity of both goldfish and mammalian AGRP in the melanophore scale assay.

4.5.5 Intracellular control of colour change

Intracellular cyclic AMP (cAMP) levels appear to be the major regulator of mammalian melanogenesis, with MC1R producing an increase or decrease after activation by αMSH or ASP respectively (Suzuki *et al.*, 1997; Yang *et al.*, 1997). It has long been observed that cAMP can mimic the effects of αMSH in frog skin *in vitro* (Abe *et al.*, 1969a; Abe *et al.*, 1969b), and that dispersion as a result of direct stimulation of cAMP is insensitive to ASP inhibition (Ollmann *et al.*, 1998). Although a role for MCH in mammalian melanogenesis has been suggested, it has yet to be elucidated (Hoogduijn *et al.*, 2002). However, MCHR1 signalling in the CNS is thought to occur through multiple intracellular pathways. (Hawes *et al.*, 2000). To assess the effect of cAMP in the zebrafish scale assay forskolin, a direct activator of adenylate cyclase (AC), was used. Consistent with the response observed in the *X. laevis* melanophore assay and in other teleosts (Ollmann *et al.*, 1998; Fujii, 2000), forskolin treatment induced dispersion in zebrafish. When co-incubated with MCH an intermediate response was apparent (Fig. 4.4.5). Thus cAMP is an intracellular regulator of background adaptation in zebrafish melanophores. This data is consistent with, but does not prove that, the zebrafish melanophore melanocortin receptor activates AC directly. It is also consistent with teleost MCH signalling resulting in depression of cAMP levels by AC inhibition (Svensson *et al.*, 1991), though it is also possible that MCH activation initiates a parallel signalling cascade that antagonises forskolin function downstream of AC.

To further investigate the interaction between MCH signalling and cAMP, an inhibitor of cAMP breakdown was used in the assay. Exposure to IBMX resulted in melanin dispersion, although at a slower rate that forskolin. This is perhaps not unsurprising however, considering forskolin actively increases cAMP levels whereas IBMX inhibits its turnover. Interestingly, treatment with IBMX and MCH induces an aggregation response not significantly different from the effect of MCH alone (Fig. 4.4.5b), suggesting there is no accumulation of cAMP. For cAMP not to accumulate its formation must be inhibited, suggesting MCH signalling decreases cAMP levels by acting at, or upstream of, AC. This data is in agreement with similar observations in tilapia melanophores, (Fujii, 2000). However, if the teleost melanophore MCH receptor is similar to its mammalian orthologue, the intracellular mechanism of MCH signalling is unlikely to be simple (Hawes *et al.*, 2000). While it is probable that the melanophore MCH receptor can interact with G_i proteins and inhibit AC directly (Saito *et al.*, 1999), there are other second messengers that can influence AC activity. For example, it has been proposed that intracellular Ca^{2+} levels regulate pigment translocation in some teleosts (Martensson and Andersson, 2000) and recently it has become clear that, in Atlantic cod (*Gadus morhua*), reduced Ca^{2+} levels inhibited melantonin and noradrenalin mediated aggregation (Aspengren *et al.*, 2003). In addition, Fujii concluded that IP_3 is another intracellular messenger that regulates the aggregating activity of melanophores (Fujii, 2000). Fortunately, the zebrafish melanophore assay system is ideal for investigating the potential downstream messengers of MCH signalling. For example, pertussis toxin could be used to determine whether MCH induced aggregation is G_i dependant (Hawes *et al.*, 2000) and treatment with a calcium chelator, such as BAPTA, would reveal whether MCH mediated aggregation is Ca^{2+} sensitive (Aspengren *et al.*, 2003).

Perhaps the most fascinating aspect of background adaptation in lower vertebrates is the cytoskeletal arrangement that permits rapid, co-ordinated, bi-directional translocation of melanosomes. A picture has begun to emerge showing tubulin based transport is essential for melanosome translocation in teleosts. It appears dynein moves melanosomes along microtubules during aggregation, while kinesin motors transport melanosome toward the periphery (Rodionov *et al.*, 1991; Rogers *et al.*, 1997; Nilsson and Wallin, 1997; Nilsson *et al.*, 2001). The role of microfilaments in translocation is less well defined. It has been observed that dispersed melanosomes are found in

periphery of melanophores where microtubules are not present (Nilsson *et al.*, 1996) and that melansomes are tethered to actin filaments in these regions (Rodionov *et al.*, 1998). Only recently, however, has myosin Va been identified as a molecular motor associated with actin based transport in teleost fish (Skold *et al.*, 2002b).

To illustrate how zebrafish melanophores can be used to investigate the cytoskeletal framework involved in pigment translocation, agents that disrupt both microfilament and microtubules were assayed. It is clear that microtubules are essential for both aggregation and dispersion of zebrafish melansomes (Fig. 4.4.5a). However, the effect of microfilament disruption is much more subtle. There is no evidence that dispersion is influenced by actin filaments, however there does appear to be a reduced rate of MCH induced aggregation (Fig. 4.4.5b) from a fully dispersed state. If, as recent evidence suggests, teleost melanosomes are transported in a similar manner to mammalian cells (fully dispersed along microtubules then, at the periphery, transferred to microfilaments) the rate of dispersion is unlikely to be influenced by filament disruption (Skold *et al.*, 2002a). If, however, dispersed melanosomes are tethered to microfilaments, then disruption may increase the time it takes to transfer melanosomes to microtubules resulting in a decreased rate of aggregation. Thus these preliminary experiments are consistent with a role for both microtubules and microfilaments in background adaptation.

4.6 Conclusions and Future Directions

This chapter describes the characterisation of the background adaptation response in adult and larval zebrafish. It further reports the development of a rapid bioassay used to directly assess both the extracellular signals and intracellular responses involved in physiological colour change. Many of the results are consistent with data previously generated using a *X. laevis* bioassay (Potenza and Lerner, 1992), although there are some differences. For example, MCH shows weak dispersing activity in frog melanophores, due to the weak affinity between MCH and melanocortin receptors (Ide *et al.*, 1985). In zebrafish, however, MCH has potent aggregating activity in accordance with its role as a regulator of teleost background adaptation (Baker, 1993). In addition, ASP appears not to inhibit αMSH signalling in teleost fish, but it does in frogs (Ollmann *et al.*, 1998).

Thus an assay using teleost melanophores will prove useful in studying the evolution of background adaptation. More important, however, is that zebrafish is the first lower vertebrate model organism that is both experimentally and genomically accessible. Although the full genome sequence is not yet available, Chapter 2 demonstrates how zebrafish orthologues of mammalian genes are readily identified and easily characterised. Moreover, using the techniques and resources described in this thesis, it is now possible to investigate background adaptation at the genetic level.

Currently, only a few cloned zebrafish genes have been proven to play a role in pigmentation (Parichy *et al.*, 1999; Lister *et al.*, 1999; Kelsh *et al.*, 2000; Parichy *et al.*, 2000; Dutton *et al.*, 2001b; Parichy and Turner, 2003) and they were all identified after studying mutant lines (Kelsh *et al.*, 1996). There are at least two, and as many as four, non-blind mutant fish that are deficient in background adaptation. Having established the response of wild-type fish, investigating melanophores from mutant fish in the scale assay should show where the deficiency lies. Then by recombination mapping the mutant locus and studying its position on the forthcoming genome assembly, candidate genes can be selected and sequenced in mutant and wild-type fish. A gene driven approach could also be taken, using morpholino knockdown in larvae or cultured adult melanophores to mimic loss of function mutations or injecting mRNA to produce an over-expression phenotype (Dutton *et al.*, 2001a).

The zebrafish melanophore assay can also be used to investigate other pathways that control physiological colour change. For example, it has been demonstrated that both melatonin and various catecholamines can induce melanosome tranlocation in amphibians (Abe *et al.*, 1969b) and fish (Fujii, 2000), but few of the genes controlling these pathways have been identified (Ebisawa *et al.*, 1994). In addition, a multitude of other hormones or paracrine factors and have been proposed as being potential regulators of fish physiological colour change to a greater or lesser extent. These include prolactin (Kitta *et al.*, 1993), somatolactin (Zhu and Thomas, 1998), met-enkephalin (Satake, 1980), prostaglandins (Abramowitz and Chavin, 1974) and endothelins (Fujii, 2000). Some chromatophores have inherent light sensing capabilities due to the presence of nonvisual opsins (Daniolos *et al.*, 1990). Although the light sensing capacity of zebrafish melanophores has not been studied, a potential candidate gene encoding a non-visual, non-pineal opsin has recently been described (Moutsaki *et al.*, 2003).

The assay system is not limited to studying melanophore background adaptation, but can be used to investigate pigment translocation in other chromotophores, particularly xanthophores. Figure 4.3.1f demonstrates that xanthophores are present on zebrafish dorsal scales. Little is known about the control of pterinosome translocation *in vivo*, mainly due to the difficulty in visualisation, although some have suggested that they have the same hormone regulators as melanophores (Bagnara, 1998; Fujii, 2000). By adjusting the illumination on an immobilized dorsal scale, it is possible to selectively quantify the area covered by pteridine pigment. However the pale colour of xanthophores has an advantage for studying translocation. Recently it has been demonstrated that GFP, which is optically quenched in melanophores, can be visualised in xanthophores (Parichy *et al.*, 2003). Using scales from GFP expressing fish in a time-lapse assay, the movement of specific proteins could be monitored with respect to pigment translocation.

In conclusion, this thesis has demonstrated that both the melanin-concentrating and melanocortin signalling system was present and functionally active when teleost fish diverged from the tetrapod lineage. At the genomic level the mammalian and teleost MCH and melanocortin receptors show many similarities, although differences in genomic structure provide evidence for large-scale loss of ancient introns. However, it is at a functional level that the remarkable conservation of opposing melanocortin and MCH signals in mammals and teleosts becomes apparent. Having developed the zebrafish pigment cell as a model, the evolution of the antagonistic relationship between these hormones can now be fully explored at the genetic level. This will provide valuable insight not only into the evolution pigmentation, but also the regulation of complex feeding behaviour in mammals.

Chapter 5

Materials and Methods

Scientific method has always been, at the very *best*, 20-20 hindsight.
It's good for seeing where you've been.

Robert T. Pirsig
Zen and the Art of Motorcycle Maintenance, Pt. III, Ch. 24.

5.1 Nucleic Acid Manipulation

5.1.1 Solutions

All chemicals were purchased from Sigma and solutions were stored at room temperature unless otherwise stated.

EDTA

EDTA (ethyldiaminetetra-acetic acid di-sodium salt) was dissolved in distilled water. The solution was adjusted to pH 8 by adding NaOH.

Tris.HCl

Tris base (tris[hydroxymethyl]aminomethane) was dissolved in distilled water. HCl was used to adjust the pH to the required value.

TE buffer

10mM Tris.HCl (pH 7.5), 1mM EDTA.

TBE buffer, 20X

Tris base	216g
Boric acid	110g
EDTA	18.6g

Distilled water was added to a final volume of 1 litre. 20X stock was diluted to 1X with distilled water prior to use.

TAE buffer, 50X

Tris base	242g
Glacial acetic acid	57.1ml
EDTA	18.6g

Distilled water was added to a final volume of 1 litre. 50X stock was diluted to 1X with distilled water.

Gel loading buffer, 10X

Reagents were added to distilled water to obtain a final concentration of 100mM EDTA, 20% Ficoll and 1% Orange G.

PCR Primers

Primers were purchased as lyophilised, desalted compounds (MWG Biotech). Stocks were made up to 1mg/ml using TE buffer and stored at 4°C. Working stocks were diluted to 100ng/µl with distilled water and stored at –20°C.

dNTPs

dNTPs were purchased as individual stocks of 100mM (ABgene). Working stocks of 10mM were made by mixing 10µl of each of the dNTPs (dATP, dCTP, dGTP, dTTP) with 60µl distilled water to a final volume of 100µl. Stocks were stored at –20°C.

5.1.2 Gel electrophoresis

Agarose gels were routinely used to determine the presence or size of nucleic acid molecules. The required amount of High pure agarose (BioGene) was dissolved in 1X TBE by heating. Ethidium bromide was then added to a final concentration of 500ng/ml agarose. The molten agarose was poured into sealed plastic trays and allowed to set. DNA size markers were run alongside experimental samples to estimate the size and amount of DNA in the samples. The size markers used were ϕX174 digested with *Hae*III and 100bp DNA Ladder (both Promega). Samples were run in 1X gel loading buffer. When nucleic acid molecules >1kb in size needed to be resolved, NuSieve 3:1 agarose (FMC Bioproducts) was used dissolved in 1X TAE. After electrophoresis, gels were visualised by UV trans-illumination and a photographic record produced.

5.1.3 Determining concentrations of nucleic acids

Nucleic acid concentrations were estimated by agarose gel electrophoresis alongside samples of a known concentration. Accurate measurements of nucleic acid concentration were taken using a GeneQuant spectrophotometer (Amersham) according to the manufacturers instructions.

5.1.4 Digestion by restriction enzymes

Digests were carried out using Roche or New England Biolabs enzymes and buffers. The restriction enzyme was normally added to a final concentration of 10u/μg DNA in 50μl reaction with the appropriate buffer, and incubated in a 37°C waterbath for 2 hours. Any deviation from this protocol was on the recommendation of the manufacturer.

5.1.5 Ligations

All ligations were carried out using the pGEM-T Easy vector system (Promega). An amplified PCR product, purified by a PCR purification kit (Qiagen), was used as an insert. Table 5.1.1 lists the primers used to amplify inserts.

Table 5.1.1. PCR primers used to clone zebrafish genes. The forward primer binds to the antisense strand, the reverse primer to the sense strand. All oligos are represented in a 5' to 3'orientation.

Gene	ID	Forward Primer	ID	Reverse Primer
mc1r	H1801	TCAAAAGGACTGTGGAAGGG	J1386	GGCAACATTAGCAGATTGAACA
mc2r	N1139	CGATCTGCACATTGCAAAATTA	N1144	CCTGGTTCTCATTCAAGCAC
mc3r	H1813	GCTGCAACATCTGACTCTGC	N1137	GCTTGACCTCGGAATGAGAA
mc4r	N1952	GGGATCAATCAGACGATTCAA	N1953	TCCAGTTGCTAAGTGCTGTCA
mc5ra	K1967	TCATCGCCTCTTACCAGACC	K1970	CAGCTGTCGAGTTCCTCC
mc5rb	N1954	ATGCATGTCAACTCCAGTCC	N1955	AAGACGGAGAGTTTTGAAGTGA
mchr1a	M1775	AAATGCCAGGCTAAACAAACA	M1776	AAGACGAAGGGACACAGTGG
mchr1b	M1779	TGGTGTGGATCCTCTCACTG	M1780	CCGGATGGCAACAATAAACT
mchr2	N1721	TTGCAATCGTCCATCCTACA	N1722	CTGGTGGGATGCTGGATACT
Pomc	SBF1	TGCAGGTCTGAACTTACAGAT	SBF2	TGACCAGTGGTTTCTGAGCA

To maximise efficiency, ligation reactions were set up with the following vector: insert molar ratios: 1:3, 1:1 and 3:1. A vector only control and an insert DNA control were also routinely carried out. The following reagents were mixed in a 200µl centrifuge tube to a total reaction volume of 10µl:

pGEM-T Easy vector	(50ng/µl)		1µl
Rapid Ligation Buffer	(2X)		5µl
T4 DNA Ligase	(3 Weiss u/µl)		1µl
Insert DNA		up to	3µl

Ligations were incubated at 4°C overnight.

5.1.6 Polymerase chain reaction (PCR)

PCRs using Ampli*Taq* polymerase, buffer and $MgCl_2$ (Applied Biosystems) were carried out to amplify specific regions of genomic DNA. After defrosting on ice, the following reagents were mixed for a single 25µl reaction in a 200µl centrifuge tube:

Ampli*Taq*	(5u/µl)	0.2µl
Buffer	(10X)	2.5µl
$MgCl_2$	(25mM)	1.5µl
dNTPs	(10mM)	0.5µl
Primer F	(100ng/µl)	0.5µl
Primer R	(100ng/µl)	0.5µl
DNA	(50ng/µl)	1.0µl
dH_2O		18.3µl

To control for contamination, a reaction with water replacing the DNA was always carried out, as was a positive DNA control whenever possible. After mixing and briefly centrifuging, the reactions were placed in a Peltier Thermal Cycler (MJ Research). A standard cycling programme was used: 5 min denaturation at 94°C, then 60s at 94°C, 60s at 60°C and 90s at 72°C for 35 cycles, then a final elongation of 10 min at 72°C. If a

product of greater than 1.5kb was expected, the elongation time was increased 30s for every 0.5kb during the cycle.

5.1.7 Reverse-transcribed polymerase chain reaction (RT-PCR)

Total RNA was reverse-transcribed using First Strand cDNA Synthesis reagents (Roche). After defrosting on ice, the following were mixed for a single 20µl reaction in a 200µl centrifuge tube:

AMV-RT	(25u/µl)	1.0µl
AMV Buffer	(5X)	4.0µl
RNAse Inhibitor	(40u/µl)	0.5µl
dNTPs	(10mM)	2.0µl
Random Hexamers	(100µM)	1.0µl
RNA	(100ng/µl)	2.0µl
dH_2O		9.5µl

After mixing, the reaction was incubated at 42°C for 1hr, then 75°C for 8 min. 2µl of the cDNA product was then used as a template for PCR as described previously. A PCR with non-reverse transcribed total RNA was used as a negative control to detect for DNA contamination. Whenever possible a PCR with a suitable DNA template was used as positive control. Unused cDNA was stored at –20°C.

5.1.8 DNA sequencing

DNA sequencing reactions were performed using the ABI PRISM BigDye Terminator cycle sequencing method (Applied Biosystems). If PCR products were being sequenced, they were first cleaned using a PCR purification kit (Qiagen) and the concentration calculated. If plasmid DNA was being sequenced cleaning was not required. Routinely 200-500ng DNA was used per reaction. The following reagents were mixed in a 200µl centrifuge tube:

DNA in dH_2O	11µl
Big Dye Terminator RR mix	8µl
Primer (3.2µM)	1µl

After briefly centrifuging, the reactions were placed in a Peltier Thermal Cycler (MJ Research). A standard cycling programme was used: 30s at 96°C, 15s at 50°C and 4 min at 60°C for 24 cycles. After cycling, the reaction was transferred to a 1.5ml centrifuge tube, 80µl of 80% isopropanol was added and the solution mixed. Then the reaction was left at room temperature for 20 min then centrifuged at 13,000g for 20 min. The pellet was washed once in 80% isopropanol then allowed to air-dry. The DNA was analysed on an ABI-377 automated sequencer (Applied Biosystems) by a sequencing service operator. The sequence trace files were aligned and compared with database assemblies using Sequencher v.4.0.5 (Gene Codes). Novel finished sequences have been submitted to GenBank. Table 5.1.2 lists the primers used to sequence each gene.

Table 5.1.2. PCR primers used to sequence genes. The forward primer binds to the antisense strand, the reverse primer to the sense strand. All oligos are represented in a 5' to 3' orientation.

Gene	ID	Forward Primer 5' to 3'	ID	Reverse Primer 5' to 3'
mc1r	H1801	TCAAAAGGACTGTGGAAGGG	J1386	GGCAACATTAGCAGATTGAACA
mc2r	N1139	CGATCTGCACATTGCAAAATTA	N1144	CCTGGTTCTCATTCAAGCAC
mc3r	H1813	GCTGCAACATCTGACTCTGC	N1137	GCTTGACCTCGGAATGAGAA
mc4r	N1952	GGGATCAATCAGACGATTCAA	N1953	TCCAGTTGCTAAGTGCTGTCA
mc5ra	K1967	TCATCGCCTCTTACCAGACC	K1970	CAGCTGTCGAGTTCCTCC
mc5rb	N1954	ATGCATGTCAACTCCAGTCC	N1955	AAGACGGAGAGTTTTGAAGTGA
mchr1a	M1212	GCGCTGTGGTCATTAAGTTT	M1215	CAGGGGTACCTCAGGTTGAGT
mchr1b	M1219	TGACTTTGGACCGATACTTGG	M1220	CGTGCTCATTACGGACACAA
mchr2	N1721	TTGCAATCGTCCATCCTACA	N1722	CTGGTGGGATGCTGGATACT
Pomc	SBF1	TGCAGGTCTGAACTTACAGAT	SBF2	TGACCAGTGGTTTCTGAGCA

5.1.9 Radiation hybrid mapping

The mapping of zebrafish genes was performed using the LN54 radiation hybrid panel (Hukriede *et al.*, 1999). The panel contains DNA from 93 radiation hybrids plus three controls in a 96 well format. The DNA from each hybrid was amplified by PCR using

primers specific for the zebrafish gene to be mapped. This reaction was then analysed for the presence or absence of a product by electrophoresis on agarose gels. Each reaction was performed twice and discordance between duplicate assays remained below 5% for the whole panel. Map placement was calculated using an online programme, RHMAPPER (http://mgchd1.nichd.nih.gov:8000/zfrh/beta.cgi). Table 5.1.3 lists the primers used to map each gene.

Table 5.1.3. PCR primers used in radiation hybrid mapping. The forward primer binds to the antisense strand, the reverse primer to the sense strand. All oligos are represented 5' to 3'.

Gene	ID	Forward Primer 5' to 3'	ID	Reverse Primer 5' to 3'
mc1r	H1801	TCAAAAGGACTGTGGAAGGG	H1807	AAAGTCACGAGACAGGCGAT
mc2r	N1139	CGATCTGCACATTGCAAAATTA	H1811	GCCACAATCACCAAGAGGTT
mc3r	H1813	GCTGCAACATCTGACTCTGC	H1815	CAAACGCACAAATTGGTCAC
mc4r	H1817	TCTGCCTCATCAGCATGTTC	H1875	CACCCTAAAACAGCACGTCA
mc5ra	K1967	TCATCGCCTCTTACCAGACC	K1972	CAGGCTGTGTGTCCGAGTAG
mc5rb	H1819	GCTTGTGGTGGAAGACCATT	H1820	GGGACAGGAAATCATGAGGA
mchr1a	M1214	GGTGTGGGCACTCTCTCTTA	M1215	CAGGGGTACCTCAGGTTGAGT
mchr1b	M1219	TGACTTTGGACCGATACTTGG	M1220	CGTGCTCATTACGGACACAA
mchr2	N1721	TTGCAATCGTCCATCCTACA	N1722	CTGGTGGGATGCTGGATACT
Pomc	SBF3	TGTGCAGGATTTTCTTTCCA	SBR2	TGACCAGTGGTTTCTGAGCA

5.2 Microbiology

Aseptic technique was observed for all procedures involving the growth of bacterial cells (setting up cultures, selecting single colonies, and storing bacterial stocks).

5.2.1 Solutions

All chemicals were purchased from Sigma and solutions were stored at 4°C unless otherwise stated. Bacterial growth media stocks were prepared in dated batches then autoclaved by technical staff.

Luria-Bertani Broth

Tryptone	10.0g
Yeast extract	5.0g
NaCl	10.0g
Glucose	1.0g

Distilled water was added to a final volume of 1 litre and the solution was autoclaved.

Luria-Bertani Agar

Tryptone	10.0g
Yeast extract	5.0g
NaCl	10.0g
Agar	15.0g

Distilled water was added to a final volume of 1 litre and the solution autoclaved.

Ampicillin, 1000X

100mg Ampicillin (D-[-]-α-aminobenzylpenicillin sodium salt) was diluted in 2ml ethanol and stored at -20°C.

X-gal, 500X

40mg X-Gal (5-bromo-4-chloro-3-indolyl-β-D-galactoside) was diluted in 2ml N,N,dimethylformamide (DMF) in a polypropylene tube.

5.2.2 Transformations

Heat shock transformations were performed by adding 2µl of the DNA ligation reaction to 50µl of thawed DH5α sub-cloning efficiency *E. coli* (Life Technologies) in a 1.5ml centrifuge tube on ice. The DNA/cell suspension was incubated on ice for 30 min, then immersed in a 42 °C waterbath for 20 sec followed by incubation in ice for a further 2 min. The transformed bacteria were then suspended in 1ml of Luria-Bertani broth and incubated at 37 °C for 1 hour in an orbital shaker. Then, using an inoculation loop, the bacteria were spread on a Luria-Bertani agar plate containing 1X ampicillin (to select for antibiotic resistance) and 1X X-gal (for blue/white insert selection). Normally three plates would be used for each transformation, one spread with 1µl of bacterial

suspension, one with 10µl and one with 100µl. The agar plates were then inverted and incubated at 37°C overnight and then stored at 4°C. A control transformation of the plasmid, pUC19 (Life Technologies) was carried out alongside experimental samples to determine efficiency.

5.2.3 Isolation of plasmid DNA

Plasmid DNA was prepared using a commercially available kit (Qiagen). For the extraction of a small amount of plasmid DNA (minipreps), a single white colony was spotted onto a duplicate plate then used to inoculate 10ml Luria broth containing 1X ampicillin. This culture was left at 37°C overnight in an orbital shaker. The following morning, plasmid DNA was extracted using the kit according to the manufacturer's instructions. The concentration of the isolated DNA was determined either by agarose gel electrophoresis or by spectrophotometry.

5.2.4 Storage of bacterial stocks

Once a plasmid containing the correct insert was identified, the host bacterial colony was lifted off the duplicate plate and used to inoculate 10ml Luria-Bertani broth containing 1X ampicillin. This culture was left at 37°C overnight in an orbital shaker. The bacteria was then harvested by centrifugation and resuspended in 1ml Luria-Bertani broth. 800µl of this suspension was added to 200µl 80% glycerol, and stored in 1.5ml centrifuge tubes at -70°C.

5.3 RNA* in situ *hybridisation histochemistry

5.3.1 Solutions

PBS

NaCl	8g
KCl	0.2g
Na_2PO_4	1.44g
KH_2PO_4	0.24g

800ml of distilled water was added, then the pH adjusted to 7.4 with 1M HCl. More distilled water was added to a final volume of 1L. The solution was sterilized by autoclaving. PBS was prepared in dated batches by technical staff then autoclaved.

DEPC treated water/PBS

500µl DEPC (diethyl pyrocarbonate) was added to 500ml of either liquid and left to stand overnight in a fumehood. The solution was then autoclaved.

PBT

250µl of 20% Tween-20 was added to 50ml DEPC treated PBS. Stored at room temperature.

4% PFA in PBS or PBT

2g of PFA (paraformaldehyde) was added to 50ml DEPC treated PBS or PBT. The suspension was heated to 65°C until the PFA fully dissolved. The solution was used within 48hrs of making.

SSC, 20X

Sodium Citrate	8.82g
NaCl	17.5g

DEPC treated water added to a final volume of 100ml and the pH was adjusted to 7 with 1M HCl. Stored at room temperature.

Hybridisation buffer

De-ionised formamide		25ml
SSC	(20X)	12.5ml
Yeast tRNA	(50mg/ml)	0.5ml
Heparin	(10mg/ml)	0.25ml
Tween-20	(20%)	0.25ml

DEPC treated water added to a final volume of 50ml and the pH was adjusted to 6 with 1M citric acid.

MAB

Maleic acid 5.8g

NaCl 4.38g

DEPC treated water added to a final volume of 500ml and the pH was adjusted to 7.5 with 1M NaOH. Stored at room temperature.

MABT

250µl of 20% Tween-20 was added to 50ml MAB. Stored at room temperature.

MABBP

100mg of blocking powder (Roche) was added to 5ml MAB.

NTMT

NaCl	(5M)	1ml
Tris.HCl, pH 9.5	(1M)	5ml
$MgCl_2$	(1M)	2.5ml
Tween-20	(20%)	0.25ml
DEPC water		41.25ml

This solution was made immediately prior to use from concentrated stocks.

Staining solution

3.4µl of 100mg/ml NBT (nitro blue tetrazolium) (Life Technologies) was added to 1ml NTMT buffer. This solution was mixed before 3.5µl of 50mg/ml BCIP (5-bromo-4-chloro-3-indolyl phosphate) (Life Technologies) was added.

5.3.2 Labelling riboprobes with digoxygenin

Riboprobes were labelled with digoxygenin (DIG) for *in situ* hybridisation histochemistry. The polymerases, DIG labelling mix, and transcription buffer were purchased (Roche). RNA products were kept on ice as much as possible and gloves worn throughout to prevent degredation by RNAses. Electrophoresis equipment was soaked in 0.1% SDS and rinsed in DEPC-treated water to destroy RNAses.

The plasmid (1μg) containing the riboprobe sequence (amplified using primers in Table 5.1.3) was linearised with an appropriate restriction enzyme. The linearised plasmid was precipitated in $1/10^{th}$ volume of 3M sodium acetate and 2 volumes of ethanol. After centrifugation, the supernatant was removed and the pellet resuspended in 5μl distilled water. The choice of restriction enzyme and of RNA polymerase depended on the direction of the DNA cloned into the pGEM-T Easy vector (Table 5.3.1).

Table 5.3.1. Restriction enzymes and RNA polymerases used to generate riboprobes. All were used according to the manufacturer's instructions (New England Biolabs or Roche).

Gene	**Clone**	**Antisense Probe**		**Sense Probe**	
		Polymerase	Enzyme	Polymerase	Enzyme
mc1r	PGMC1	Sp6	*Nco*I	T7	*Spe*I
mc2r	PGMC2	T7	*Sal*I	Sp6	*Nco*I
mc3r	PGMC3	T7	*Spe*I	Sp6	*Sac*II
mc4r	PGMC4	T7	*Spe*I	Sp6	*Sac*II
mc5ra	PGMC5a	T7	*Spe*I	Sp6	*Nco*I
mc5rb	PGMC5b	Sp6	*Nco*I	T7	*Spe*I
mchr1a	PGMCH1a	T7	*Spe*I	Sp6	*Sac*II
mchr1b	PGMCH1b	Sp6	*Sac*II	Sp6	*Spe*I
mchr2	PGMCH2	Sp6	*Sac*II	T7	*Spe*I
pomc	PGPOM	T7	*Spe*I	Sp6	*Sph*I

The labelling reaction was set up in a 200μl centrifuge tube to a total volume of 20μl:

dH_2O		8μl
Transcription buffer	(10X)	2μl
linearised DNA	(200ng/μl)	5μl
dNTP (from DIG RNA labelling kit)	(10X)	2μl
Human placenta RNAse inhibitor	(40u/μl)	1μl
Polymerase (T7 or Sp6)	(20u/μl)	2μl

After mixing, the reaction was incubated at 37°C for 2 hours. Then the template DNA was removed by adding 2µl RNAse-free DNAse1 and incubating at 37°C for a further 15 min. This digestion was stopped by adding 2µl of 0.2M EDTA, pH8.0. The DIG labelled RNA was precipitated by adding 2.5µl of 4M LiCl and 75µl of ethanol then incubating overnight at -20°C. The following day, the RNA was centrifuged for 10 min at maximum speed and the pellet was washed with 50µl ice-cold 70% ethanol. The pellet was resuspended in 110µl DEPC-treated water and 1µl RNAse inhibitor was added. The integrity of the RNA was checked by gel electrophoresis and the probe stored at -20°C until use.

5.3.3 In situ hybridization of riboprobes

In situ probe hybridisations were modified from a protocol previously described (Jowett, 1999). Unless otherwise stated, the washes were carried out at room temperature in RNAse free 1.5ml centrifuge tubes. Typically, 5-25 zebrafish embryos would be used in each hybridisation reaction. The zebrafish embryos were fixed in their chorions with 4% PFA in PBS for 2hrs at room temperature or overnight at 4°C. Then they were washed twice in PBT at 4°C before dechorionation in a glass dish using watchmaker's forceps. The embryos were then dehydrated through a wash series of methanol/PBT (1:3, 1:1 and 3:1 solutions of methanol/PBT) before two final washes with methanol alone. The incubation time in each solution was 10 min. At this stage the embryos could be stored indefinitely at -20°C, though typically they would be left overnight.

The following morning the embryos were re-hydrated through a reverse methanol/PBT series (3:1, 1:1 and 1:3 methanol/PBT) then finished with three washes of PBT. Again, each incubation period was 10 min. If the embryos were older than 24 hours they were treated with proteinase K (10µg/ml in PBT) for 10-20 min. The digestion was stopped by washing the embryos in 4% PFA in PBT for 20 min, followed by two further washes with PBT for 5 min each. Next the embryos were washed in hybridisation buffer for 5 min then they were incubated at 60°C in more hybridisation buffer for a minimum of 2hrs. This was replaced with 200µl of preheated hybridisation buffer containing 1µl of riboprobe in DEPC treated water. The probe was hybridised overnight at 65°C.

The following day, a series of washes were carried out at 65°C for 10 min each. Firstly, three washes with 50% hybridisation buffer, 50% 2X SSC. Then a single wash with 2X SSC, 0.1% Tween-20 and four washes with 0.2X SSC, 0.1% Tween-20. A second series of washes were carried out at room temperature with gentle shaking for 5 min each. One wash of 3:1, 1:1 and 1:3 0.2X SSC:MABT then a single wash in MABT alone. Following a brief wash in MAB, the embryos were pre-blocked with MABBP for at least 1 hour at room temperature with gently shaking. This was replaced with 5000:1 MABBP:anti-DIG F_{ab} antibody fragments conjugated to alkaline phosphatase (Roche). The embryos were incubated overnight at 4°C with gentle shaking.

Unbound antibody fragments were removed by eight 15 min washes in PBT while gently shaking, then three 5 min washes in NTMT buffer were carried out to equilibrate the embryos to pH 9.5. Staining solution was applied to the embryos and left, in the dark, for 0.5-48 hours until staining appeared. If required, the staining reaction was speeded up or slowed down by incubating at 37°C or 4°C respectively. When the appropriate staining had developed, the reaction was stopped by washing with PBT for 5 min, then the stain fixed by incubation in 4% PFA in PBS overnight at 4°C.

5.3.4 Mounting probed embryos for microscopy

NBT/BCIP stained embryos were cleared in a series of 50% ethanol, 100% ethanol and 1:2 benzyl benzoate:benzyl alcohol for at least 5 min at each step. Yolk sacs were removed, if required, when the embryos were in 50% ethanol. A protective well was made on glass slides by stacking two sets of two No.1 cover-slips (Chance Propper) for embryos aged up to 24 hours, three cover-slips thereafter. These stacks run parallel, with a 3mm gap between the nearest edges. The embryos were then mounted in DePeX (Merck) within the protective well and a final coverslip placed on top, bridging the stacks and sealing the embryo in the well.

5.3.5 Imaging probed zebrafish embryos

Unmounted embryos were imaged in their storage buffer or 80% glycerol using a MZFLIII stereo fluorescence microscope (Leica Microsystems) with a fibre optic cold light source and illuminated base for incident/transmission illumination. Image acquisition was with a Photometrics CoolSnap colour CCD camera (Roper Scientific) controlled by scripts written by Dr. Paul Perry for IPLab Spectrum v3.2 (Scanalytics). Mounted images were captured using a Zeiss Axioplan II fluorescence microscope (Carl Zeiss) equipped with colour additive filters (Andover Corp) for sequential colour imaging and a Photometrics CoolSnap HQ monochrome CCD camera (Roper Scientific). Images were captured using scripts written by Dr. Paul Perry for IPLab Spectrum v3.6 (Scanalytics) which controlled camera capture and filter selection via motorised filter wheels (Ludl Electronic Products).

5.4 Computational Methods

Many of the computational methods described here were completed in collaboration with (or with the assistance of) various bioinformaticians at the MRC Human Genetics Unit. The individuals are credited for their work in the description of each method.

5.4.1 Programs and databases

Table 5.4.1. Computer programmes, websites and databases used in analysis.

Programme	Version	Reference
BLAST package	2.1.3	(Altschul *et al.*, 1997)
Clustalw	1.74	(Thompson *et al.*, 1994)
Mega2	2.1	(Kumar *et al.*, 2001)
Phrap	N/a	(Ewing and Green, unpublished)
Phred	0.000925.c	(Ewing and Green, 1998)
RepeatMasker	07/07/2001	(Smit, unpublished)
HMMER	2.2	(Eddy, unpublished)
Zfin	N/a	(Sprague *et al.*, 2001)
Ensembl	N/a	(Clamp *et al.*, 2003)
Project BLAST	11/03/02	(Taylor, unpublished)
Zebedee	N/a	(Semple and Bryson-Richardson, unpublished)
Wise2	2-1-22c	(Birney and Durbin, 2000)
ForCon	1.0	(Raes and Van der Peer, unpublished)
GeneDoc	2.6.002	(Nicholas et al, unpublished)
Vista	N/a	(Mayor *et al.*, 2000)
SRS	7.1.1	(Etzold *et al.*, 1996)
Web Logo	2.2	(Crooks, unpublished)

5.4.2 Genomic sequence assembly

Sequence assemblies for *Anopheles gambiae, Drosophila melanogaster, Caenorhabditis elegans, Caenorhabditis briggsae, Homo sapiens and Mus musculus* were available for analysis at Ensembl (http://www.ensembl.org). However, at the time of analysis there were either no, or very limited, genomic sequence assemblies from *Danio rerio, Fugu*

rubripes, Ciona savignyi and *Tetraodon nigroviridis*. Genes from these species were identified by analysis and assembly of individual sequence traces. An indexed BLAST database was created from the publicly available DNA sequence repositories. A script was written by Dr Martin Taylor (Project-BLAST) to automatically update these databases with the latest sequence trace releases on a daily basis. The indexed database was then searched with a protein sequence using TBLASTN. Once the sequences were retrieved they were assembled using Phred/Phrap. Any contiguously assembled sequences (contigs) were compared to the original query sequence. If they matched to a significant level over their entire length, the contigs were then used to search the databases again by BLAST. This process was repeated over periods of time in order to extend the contigs in length. This method was later accelerated by using an online batch script, Zebedee (http://longrow.hgu.mrc.ac.uk/zebedee), written by Drs Colin Semple and Robert Bryson-Richardson. The program automated the process described above, attempting to extend the contigs on a daily basis. The only difference with Zebedee's analysis was that automated BLAST results were parsed by identity instead of significance to try and improve the identification of homologous sequences. When a complete coding sequence was identified, the sequence was confirmed by PCR or RT-PCR and resequencing. Extensive *Danio rerio* and *Fugu rubripes* genome assemblies were subsequently made available at Ensembl.

5.4.3 Gene predictions

Coding sequences were occasionally spread over multiple exons. In these cases, gene predications were first made using Wise2. If this was unsuccessful, alignments of orthologous amino acid sequences were made using ClustalW. Hidden Markov Models (HMM) were created from ClustalW outputs using HMMbuild, part of the HMMER package. The predicted intron/exon boundaries were then inspected manually and compared to the gene structure of known orthologues. Finally, testing by RT-PCR was carried out whenever possible.

5.4.4 Phylogenetic analysis

Protein sequence alignments were created using ClustalW. The output of the alignment was visualised using GeneDoc, then converted to Mega2 format using ForCon. Mega2

was used to construct and bootstrap the phylogenetic trees. When closely related sequences were aligned, neighbour joining with complete deletion and Poisson correction was used to construct the phylogeny. For alignments of more diverse sequences, such as the GPCR protein family, a pairwise deletion and p-distance model of phylogeny was used. Bootstrapping was carried out with 1000 repetitions and a random seed.

5.4.5 Comparative mapping

Comparative mapping was used to find a positional relationship between fish genes and their mammalian orthologues. Neighbouring genes were identified from the genetic and physical maps at the Zebrafish Information Network (ZFIN), (http://zfin.org/). They were used in a TBLASTX search against the human and mouse whole genome assembly. The best match was then used in a reciprocal TBLASTN search against the zebrafish BLAST database. If this identified the original zebrafish sequence as the best hit, the genes were designated as orthologous. Syntenic relationships were established by cross-referencing neighbouring zebrafish genes with the chromosomal position of their mammalian orthologues.

5.4.6 GPCR protein selection

Protein sequences in Swiss-Prot and TrEMBL containing the Interpro domain for rhodopsin-like G-coupled receptors (IPR0000276) were retrieved using SRS (http://www.ebi.ac.uk). Descriptions of the proteins were retrieved and olfactory receptors and sequences annotated as fragments or partial sequences were removed. This generated a final GPCR dataset (the SPTR dataset) of 246 human proteins, 232 mouse proteins, 71 *Drosophila* proteins and 318 *C. elegans* proteins. A further dataset containing GPCR proteins were obtained by retrieving IPR0000276 annotated peptides translated from Ensembl gene predictions. The predictions were based on the following genome assemblies: *Fugu* v16.2.1, *Anopheles* v16.2.1, *Drosophila* v10.3.1 and *C. elegans* v12.95.1 (all at http://www.ensembl.org). After purging incorrectly annotated or partial sequences this Ensembl dataset contains 347 *Fugu* proteins, 95 *Anopheles* proteins, 406 *C. elegans* proteins and 99 *Drosophila* proteins.

5.4.7 GPCR gene identification

The corresponding genomic sequence for each protein in the SPTR dataset was identified using BLAST. Each protein was compared to the whole genome sequence from its organism of origin. The following genome sequence releases were used: human, NCBI release 30; mouse, Mm_mgsc3; *C. elegans*, assembly release 11/11/02 and *Drosophila*, BDGP release 3. Proteins for which there was not a genomic match at >95% for the entire length were discounted. The genomic sequence was extracted from the genome data using the co-ordinates of the BLAST hits, together with 5kb flanking sequence. A batch script was written by Dr. Robert Bryson-Richardson to automate the above process. The corresponding genomic sequences for proteins in the Ensembl dataset were accessed using Ensembl.

5.4.8 Identification of the genomic structure of GPCR genes

Gene structure in the SPTR dataset was determined by aligning the protein to its corresponding genomic sequence using Genewise. The proteins were then aligned using ClustalW and the conserved seven transmembrane region identified using matches to the Pfam domain (7tm_1). The matching co-ordinates were then used to extract the region for each protein. The genomic structures of the seven transmembrane regions were then determined as above, again using Genewise.

5.4.9 Identification of a DRY intron in GPCR genes

The SPTR dataset proteins were aligned using ClustalW and the E/DRY motif identified. The 50aa sequences flanking either side of the arginine of the motif was then extracted and aligned to its corresponding genomic sequence using Genewise. These alignments were then visually inspected for introns that split the arginine in phase two. The transcripts coding for Ensembl dataset proteins were aligned with the Pfam model for IPR000276 (7tm_1) using BLAST to confirm that they were genuine rhodopsin-like GPCR and to identify the DRY signature. Using Ensembl, the intron/exon boundaries were then identified and their position compared to that of the DRY motif. Finally, when a GPCR with an interrupted DRY motif was identified, orthologous genes in other species and paralogous genes within the species were checked for a similar intron.

5.4.10 Logo analysis

Logos were generated using Web Logo (http://weblogo.berkeley.edu/). Each logo consists of stacks of symbols, one stack for each position in the sequence. The overall height of the stack indicates the sequence conservation at that position, while the height of symbols within the stack indicates the relative frequency of each amino or nucleic acid at that position. The conservation for each base is represented in 'informative bits'(R_s) calculated as follows:

$$R_s(1) = 2 - H(1) - e(n),$$

Where,

$$H(1) = -\sum f_i(1)\log_2 f_i(1).$$

$f_i(1)$ is the frequency of nucleotide i (A, T, G or C) at base 1 and

$$e(n) = 3/(2n \log_e 2)$$

where n is the sample size ($n = 77$, for genes with DRY introns; $n = 71$ for genes without DRY introns). $R_s(1) = 0$ when there is no conservation at base 1, while $R_s(1) = 2$ when there is maximum conservation (i.e. when only one nucleotide is present) (Schneider and Stephens, 1990). The genes with DRY introns were identified from both Ensembl and SPTR datasets. The genes without DRY introns are the most closely related to those with the intron, based on phylogeny. The proportions of genes from different species were maintained in both sets.

5.5 Zebrafish Husbandry

Zebrafish were kept and raised in a custom built aquarium according to the standards described by Westerfield (Westerfield, 2000). Feeding, stock management and system cleaning was performed by Mr. David Keenan and Mr. Ross Anderson.

5.5.1 Solutions

Fish Water

100µl of 1% methylene blue in 1L system water.

Tricaine Solution, 12X

400mg of tricaine powder (ethyl m-aminoboenzoate) was added to 98ml distilled, deionised water and 2ml 1M Tris (pH 9). This was adjusted to pH 7 and stored at -20°C.

5.5.2 Zebrafish Strains

All wildtype DNA and RNA were produced from normally pigmented **AB*, a derived line 70 generations removed from the original *AB* cross. All wildtype fish in melanophore adaptation experiments were **AB*, however due to seasonal mating problems, some fish used for *in situ* hybridisation and morpholino injection were *WIK* or *TU*. There was no evidence of variation in the results of these experiments due to strain differences.

Mutant lines *fata morgana* (*fam*^{te267}) and *submarine* (*sum*^{tr6}) were kind gifts from Dr. Hans Georg Frohnhoefer. These were provided as outcrosses to *Tuebingen long fin* (*TL*) and pair mated to generate homozygotes. The mutant, *union jack* (*uni*^{tn16}), was a kind gift from Dr. Robert Kelsh. This line was maintained in homozygous adults. DNA from mutant lines *milky* (*mlk*^{tv10}), *pewter* (*pew*^{tm79b}) and *tj266c* (*unm*(^{tj266c})) were kind gifts from Dr. Robert Geisler.

5.5.3 Raising zebrafish embryos

Embryos were harvested by overnight marbling of large tanks containing multiple fish, or pair-mating tanks containing just two fish. After washing in fish water and removing unfertilised eggs, the embryos were grown in a petri dish of fish water at 28.5°C. Every day the water was changed and dead embryos and larva removed. From day 4-5 the larvae were fed powdered food then from day 7 they were moved to larger tanks and fed

brine shrimp. As they grew they were moved to progressively larger tanks with deeper water until they were large enough to eat adult food.

5.5.4 Morpholino microinjection

A morpholino antisense oligo was designed by an expert at Genetools based on the predicted coding sequence and 5' UTR of zebrafish *mc1r* (MC1R-MO: 5'-GCGAAGAGTCGTTCATGCTCTTAA-3') (Summerton and Weller, 1997). The lyophilised oligo was dissolved in distilled water to a concentration of 1.2mM and stored at -20°C. For injection, an initial injection mixture was made consisting of 0.5mM morpholino and 1% phenol red in distilled water. This was then adjusted upwards to 1mM. Needles used for injection were 1mm boro-silicate capillaries (1mm outer diameter, 0.78mm inner diameter) (Clark Electromedical Instruments) pulled on a CFP microelectrode puller. A needle was broken near the tip using forceps. 2µl of injection solution was spotted onto a microscope slide and the needle filled using the fill function on a IM 300 micro-injector (Narishige). The tip of the needle was then adjusted using forceps such that it passed easily through the chorion of an embryo. Embryos were injected at the 1-2 cell stage, either directly into a cell or into the yolk sac using a Leica MZFLIII stereo microscope (Leica Microsystems). Contol injections were carried out with distilled water and a standard control morpholino (Std-MO: 5'-CCTCTTACCTCAGTTACAATTTATA-3'). This control oligo has no target and no significant biological activity, except in reticulocytes from thallasemic humans having a splice-generating mutation at position 705 in beta-globin pre-mRNA. Injected embryos were raised as previously described and visualised on a Leica MZFLIII stereo microscope (Leica Microsystems).

5.5.5 Background adaptation

Larvae were tested for adaptation by attaching either white or black card to the bottom of their petri dish and exposing to ambient light. For adaptation of adult fish 2L tanks and 1L tanks were painted by Mr Duncan Fletcher. Light background adapted adult fish were kept in tanks painted matte white to 2.5cm under the surface of the water. Dark background adapted adult fish were placed in tanks painted matte black to 2.5cm under

the surface of the water. Fish were typically adapted to their background for 24 hours before use.

5.5.6 Fish euthanasia

Fish were captured in a suitable net and quickly and gently transferred to a plastic beaker containing tricaine solution diluted to 1X in water and chilled to 4°C. Fish were overdosed with tricaine solution for sufficient time to ensure death. Whenever possible, tricaine overdose was followed by decapitation before disposal of the carcass.

5.5.7 Extraction of DNA from fish tissue

DNA was isolated from zebrafish tissue using the DNeasy system (Qiagen). DNA was typically made from the spawn of a large tank of **AB* fish four days post fertilisation. DNA from *Fugu rubripes* was purchased from the Human Genome Mapping Project Resource Centre. DNA was stored at -20°C until required.

5.5.8 Extraction of RNA from fish tissue

Total RNA was isolated from zebrafish tissue using the RNAgents system (Promega) according to the manufacturers instructions. Head and body RNA was obtained by pooling the heads and bodies of a single male and female fish. Zebrafish embryo RNA was obtained from spawn of at defined days post fertilization. Individual tissues were dissected from a carcass immediately after euthanasia and stored at -70°C. The tissue from multiple fish were pooled and RNA extracted as above. The total RNA samples were RNase-Free DNase treated (Roche) at 37°C for 15 min and purified according to the manufacturer's instructions. All RNA samples were stored at -70°C until required. The quantity of nucleic acid in each sample was measured using a GeneQuant spectrophotometer (Amersham).

5.6 Zebrafish Melanophore Assay

5.6.1 Solutions

Penicillin/Streptomycin (pen-strep) solution, 100U/L

62.6mg of penicillin and 128.7mg streptomycin was added to 1ml distilled water. This was stored at -20°C.

L-15 medium with 1000U/ml pen-strep

500µl of pen-strep solution was added to 49.5ml L-15 medium. The solution was stored at 4°C.

Serum-free Culture Solution, 100X

30mg of L-glutamine, 15mg of ascorbic acid and 238mg of hydroxyethylpiperazine ethanesulphonic acid (HEPES) were added to 1ml of distilled water. This was stored at -20°C.

L-15 serum-free culture medium

500µl of 100X serum-free culture solution, 50µl of pen-strep solution and 50µl 1M $NaHCO_3$ was added to 49.4ml L-15 medium. This was stored at -20°C.

Physiological Saline Solution (PSS)

NaCl	(5M)	5.2ml
KCl	(1M)	0.54ml
D-Glucose	(56mM)	20ml
EDTA	(0.5M)	0.4ml
Tris Buffer	(40mM)	250ml

Distilled water was added to a final volume of 200ml. This solution was autoclaved then stored at 4°C.

Melanin-concentrating Hormone (MCH)

MCH was diluted in PSS to make a 100µM stock solution. This was stored at -20°C. Subsequent dilutions were made in PSS, or PSS/DMSO.

Melanocyte Stimulating Hormones (αMSH, βMSH, γMSH)

Each hormone was diluted in PSS to make a 100μM stock solution. This was stored at -20°C. Subsequent dilutions were made in PSS, or PSS/DMSO.

Forskolin

Forskolin was diluted in dimethyl sulfoxide (DMSO) to make a stock solution of 1mM and stored at -20°C. Subsequent dilutions were made in PSS.

IBMX

IBMX was diluted in dimethyl sulfoxide (DMSO) to make a 1mM stock solution and stored at -20°C. Subsequent dilutions were made in PSS.

Nocodazole

Nocadozole was diluted in dimethyl sulfoxide (DMSO) to make a 1mM stock solution. This was stored at -20°C. Subsequent dilutions were made in PSS.

Cytochalasin B

Cytochalasin B was diluted in dimethyl sulfoxide (DMSO) to make a 1mM stock solution. This was stored at -20°C. Subsequent dilutions were made in PSS.

Agouti YY

0.5pmol Agouti YY was a kind gift of Greg Millhauser and Joe McNulty. It was diluted in PSS to make a 1μM stock solution. This was stored at -20°C. Subsequent dilutions were made in PSS.

5.6.2 Skin culture

The zebrafish skin culture protocol was based upon one previously published (Sugimoto *et al.*, 2000) using Leibovitz serum-free culture medium. Euthanised zebrafish were decapitated, the spine and bones were removed and the dorsal trunk dissected into Leibovitz (L-15) medium. The trunk was twice washed for 10 min with L-15 medium, then once for 5 min with L-15 medium with 1000U/ml penicillin and streptomycin. The

trunk was rinsed in L-15 medium again before being incubated in L-15 serum-free culture medium in a six-well culture plate (Greiner Bio-One). One half of the media was changed every day and each culture was maintained for no more than 3 days.

5.6.3 Time lapse imaging

Dorsal scales were carefully removed from cultured zebrafish trunks using forceps and washed briefly in physiological saline solution (PSS) at 4°C. Molten 0.8% agarose was poured to half fill a single well in a four-well plate (Nunc). As the agarose set, a single dorsal scale was inverted and carefully placed on the surface, so the attached dermal layer containing chromatophores was uppermost. The immobilised scale was then covered by 500µl PSS and kept on ice until assayed. In experiments with nocodazole and cytochalasin B, scales were pre-incubated for 2 hours at 4°C. Otherwise the plate was transferred to a Leica MZFLIII stereo fluorescence microscope (Leica Microsystems) and the PSS replaced by a PSS solution containing an active compound.

The level of melanophore aggregation or dispersion was recorded by time-lapse photography using a Photometrics CoolSnap colour CCD camera (Roper Scientific) and controlled by scripts written for IPLab Spectrum v3.2 (Scanalytics). Briefly, high-resolution digital images were captured at fixed intervals over a defined time period (usually every 30 seconds over 15-30 minutes) and stacked into frames to make a movie. Table 5.6.1 illustrates the IPLab script commands written to automate the capture process.

The movie was converted to greyscale and the background of each frame equalised to compensate for variation in lighting throughout the time lapse. Pigment aggregation or dispersion was then measured by masking the pigment with a false colour. The number of false coloured pixels in each frame was measured and quantified using a second IPLab script (Table 5.6.2). After quantification the numerical values per frame were imported into Excel (Microsoft), standardised then plotted.

Table 5.6.1. Commands for time-lapse image capture. All commands were scripted in IPLab v3.2 with help from Dr. Paul Perry.

IPLab Command	Description
Show Variables	Make variables visible
Select All	Use entire image
Clear	Remove previous values from data stack
Enter Variables	A = exposure time, B = lapse time, C = frame number
New Image	Named "image stack"
Mark	Marks point for loop.
Single Exposure	Using variable A, named "temp"
Transfer Frames	Moves temp to image stack
Dispose Window	Removes temp
Pause	Using variable B
Loop	Go to "Mark", (variable C-1) times
Animate	Show image stack sequentially
End	Save image stack

Table 5.6.2. Commands for pigment quantification. All commands were scripted in IPLab v3.2 with help from Dr. Paul Perry.

IPLab Command	Description
Select Frame	Choose frame, variable = F (of total = T)
Enter Variables	A = minimum pigment intensity, B = maximum intensity
Segmentation	Make a segment between variables A and B
Segment at ROI	Capture segment over selected area
Quantify Segments	Count pixels in captured segment, tabulate
Mark	Marks point for loop.
Enter Variables	F = F+1
Select Frame	Choose variable F
Segmentation	Make a segment between variables A and B
Segment at ROI	Capture segment over selected area
Quantify Segments	Count pixels in captured segment, tabulate
Loop	Go to "Mark", (variable T-1) times
End	Save data table

Chapter 6

References

Fine words!
I wonder where you stole them.

Jonathan Swift

Abdel-Malek, Z, Swope, VB, Suzuki, I, Akcali, C, Harriger, MD *et al.* 1995. Mitogenic and melanogenic stimulation of normal human melanocytes by melanotropic peptides. *Proc. Natl. Acad. Sci. U. S A* **92:** 1789-1793.

Abdel-Malek, ZA, Scott, MC, Furumura, M, Lamoreux, ML, Ollmann, M *et al.* 2001. The melanocortin 1 receptor is the principal mediator of the effects of agouti signaling protein on mammalian melanocytes. *J Cell Sci.* **114:** 1019-1024.

Abe, K, Butcher, RW, Nicholson, WE, Baird, CE, Liddle, RA *et al.* 1969a. Adenosine 3',5'-monophosphate (cyclic AMP) as the mediator of the actions of melanocyte stimulating hormone (MSH) and norepinephrine on the frog skin. *Endocrinology* **84:** 362-368.

Abe, K, Robison, GA, Liddle, GW, Butcher, RW, Nicholson, WE *et al.* 1969b. Role of cyclic AMP in mediating the effects of MSH, norepinephrine, and melatonin on frog skin color. *Endocrinology* **85:** 674-682.

Abramowitz, J and Chavin, W. 1974. In vitro response of goldfish (Carassius auratus L.) dermal melanophores to cyclic 3',5'-nucleotides, nucleoside 5'-phosphates and methylxanthines. *J. Cell Physiol* **84:** 301-309.

Adalsteinsson, S, Bjarnadottir, S, Vage, DI, and Jonmundsson, JV. 1995. Brown coat color in Icelandic cattle produced by the loci Extension and Agouti. *J. Hered.* **86:** 395-398.

Adams, MD, Celniker, SE, Holt, RA, Evans, CA, Gocayne, JD *et al.* 2000. The genome sequence of Drosophila melanogaster. *Science* **287:** 2185-2195.

Akiyama, M, Dale, BA, Sun, TT, and Holbrook, KA. 1995. Characterization of hair follicle bulge in human fetal skin: the human fetal bulge is a pool of undifferentiated keratinocytes. *J. Invest Dermatol.* **105:** 844-850.

Allen, BM. 1916. Extirpation of the hypophysis and thyroid glands of *Rana pipiens*. *Science* **44:** 755-757.

Allolio, B and Reincke, M. 1997. Adrenocorticotropin receptor and adrenal disorders. *Horm. Res* **47:** 273-278.

Altschul, SF, Madden, TL, Schaffer, AA, Zhang, J, Zhang, Z *et al.* 1997. Gapped BLAST and PSI-BLAST: a new generation of protein database search programs. *Nucleic Acids Res.* **25:** 3389-3402.

Amemiya, Y, Takahashi, A, Meguro, H, and Kawauchi, H. 1999a. Molecular cloning of lungfish proopiomelanocortin cDNA. *Gen. Comp Endocrinol.* **115:** 415-421.

Amemiya, Y, Takahashi, A, Suzuki, N, Sasayama, Y, and Kawauchi, H. 1999b. A newly characterized melanotropin in proopiomelanocortin in pituitaries of an elasmobranch, Squalus acanthias. *Gen. Comp Endocrinol.* **114:** 387-395.

Amemiya, Y, Takahashi, A, Suzuki, N, Sasayama, Y, and Kawauchi, H. 2000. Molecular cloning of proopiomelanocortin cDNA from an elasmobranch, the stingray, Dasyatis akajei. *Gen. Comp Endocrinol.* **118:** 105-112.

Amores, A, Force, A, Yan, YL, Joly, L, Amemiya, C *et al.* 1998. Zebrafish hox clusters and vertebrate genome evolution. *Science* **282:** 1711-1714.

An, S, Cutler, G, Zhao, JJ, Huang, SG, Tian, H *et al.* 2001. Identification and characterization of a melanin-concentrating hormone receptor. *Proc. Natl. Acad. Sci. U. S A* **98:** 7576-7581.

Aparicio, S. 2000. Vertebrate evolution: recent perspectives from fish. *Trends Genet.* **16:** 54-56.

Aparicio, S, Chapman, J, Stupka, E, Putnam, N, Chia, JM *et al.* 2002. Whole-genome shotgun assembly and analysis of the genome of Fugu rubripes. *Science* **297:** 1301-1310.

Apweiler, R, Attwood, TK, Bairoch, A, Bateman, A, Birney, E *et al.* 2000. InterPro--an integrated documentation resource for protein families, domains and functional sites. *Bioinformatics.* **16:** 1145-1150.

Arends, RJ, Vermeer, H, Martens, GJ, Leunissen, JA, Wendelaar Bonga, SE *et al.* 1998. Cloning and expression of two proopiomelanocortin mRNAs in the common carp (Cyprinus carpio L.). *Mol. Cell Endocrinol.* **143:** 23-31.

Aspengren, S, Skold, HN, Quiroga, G, Martensson, L, and Wallin, M. 2003. Noradrenaline- and melatonin-mediated regulation of pigment aggregation in fish melanophores. *Pigment Cell Res.* **16:** 59-64.

Attwood, TK and Findlay, JB. 1993. Design of a discriminating fingerprint for G-protein-coupled receptors. *Protein Eng* **6:** 167-176.

Attwood, TK and Findlay, JB. 1994. Fingerprinting G-protein-coupled receptors. *Protein Eng* **7:** 195-203.

Bachner, D, Kreienkamp, H, Weise, C, Buck, F, and Richter, D. 1999. Identification of melanin concentrating hormone (MCH) as the natural ligand for the orphan somatostatin-like receptor 1 (SLC-1). *FEBS Lett.* **457:** 522-524.

Bagnara, JT. 1961. Chromatotropic hormone, pteridines and amphibian pigmentation. *Gen. Comp Endocrinol.* 124-133.

Bagnara, JT. 1964. Stimulation of melanophores and guanophores by MSH peptides. *Gen. Comp Endocrinol.* **4:** 290-294.

Bagnara, JT. 1966. Cytology and cytophysiology of non-melanophore pigment cells. *Int. Rev. Cytol.* **20:** 173-205.

Bagnara, JT. 1998. Comparative Anatomy and Physiology of Pigment Cells in Nonmammalian Tissues *in The Pigmentary System: Its Physiology and Pathophysiology.* Oxford University Press. New York.

Bagnara, JT and Hadley, ME. 1970. Endocrinology of the amphibian pineal. *Am. Zool.* **10:** 201-216.

Bagnara, JT and Hadley, ME. 1973. Chromatophores and Color Change: The Comparative Physiology of Animal Pigmentation. Prentice-Hall. Englewood Cliffs, NJ.

Bagnara, JT, Matsumoto, J, Ferris, W, Frost, SK, Turner, WA, Jr. *et al.* 1979. Common origin of pigment cells. *Science* **203:** 410-415.

Bagnara, JT, Taylor, JD, and Hadley, ME. 1968. The dermal chromatophore unit. *J. Cell Biol.* **38:** 67-79.

Bagnara, JT, Taylor, JD, and Prota, G. 1973. Color changes, unusual melanosomes, and a new pigment from leaf frogs. *Science* **182:** 1034-1035.

Baker, BI. 1988. Relative importance of MCH and MSH in melanophore control. *Prog. Clin. Biol. Res.* **256:** 505-515.

Baker, BI. 1993. The role of melanin-concentrating hormone in color change. *Ann. N. Y. Acad. Sci.* **680:** 279-289.

Baker, BI, Bird, DJ, and Buckingham, JC. 1986. Effects of chronic administration of melanin-concentrating hormone on corticotrophin, melanotrophin, and pigmentation in the trout. *Gen. Comp Endocrinol.* **63:** 62-69.

Baldwin, JM. 1994. Structure and function of receptors coupled to G proteins. *Curr. Opin. Cell Biol* **6:** 180-190.

Baldwin, JM, Schertler, GF, and Unger, VM. 1997. An alpha-carbon template for the transmembrane helices in the rhodopsin family of G-protein-coupled receptors. *J. Mol. Biol* **272:** 144-164.

Ballesteros, J, Kitanovic, S, Guarnieri, F, Davies, P, Fromme, BJ *et al.* 1998. Functional microdomains in G-protein-coupled receptors. The conserved arginine-cage motif in the gonadotropin-releasing hormone receptor. *J Biol. Chem.* **273:**10445-53.

Barbazuk, WB, Korf, I, Kadavi, C, Heyen, J, Tate, S *et al.* 2000. The syntenic relationship of the zebrafish and human genomes. *Genome Res.* **10:** 1351-1358.

Bargmann, CI. 1998. Neurobiology of the Caenorhabditis elegans genome. *Science* **282:** 2028-2033.

Barrenas, ML and Holgers, KM. 2000. Ototoxic interaction between noise and pheomelanin: distortion product otoacoustic emissions after acoustical trauma in chloroquine-treated red, black, and albino guinea pigs. *Audiology* **39:** 238-246.

Barsh, GS. 1996. The genetics of pigmentation: from fancy genes to complex traits. *Trends Genet.* **12:** 299-305.

Bartels, S, Ito, S, Trune, DR, and Nuttall, AL. 2001. Noise-induced hearing loss: the effect of melanin in the stria vascularis. *Hear. Res.* **154:** 116-123.

Bateman, A, Birney, E, Cerruti, L, Durbin, R, Etwiller, L *et al.* 2002. The Pfam protein families database. *Nucleic Acids Res.* **30:** 276-280.

Bateman, N. 1961. Sombre, a viable dominant mutant in the house mouse. *J. Hered.* **52:** 186-189.

Baynash, AG, Hosoda, K, Giaid, A, Richardson, JA, Emoto, N *et al.* 1994. Interaction of endothelin-3 with endothelin-B receptor is essential for development of epidermal melanocytes and enteric neurons. *Cell* **79:** 1277-1285.

Beermann, F, Ruppert, S, Hummler, E, Bosch, FX, Muller, G *et al.* 1990. Rescue of the albino phenotype by introduction of a functional tyrosinase gene into mice. *EMBO J.* **9:** 2819-2826.

Ben Arie, N, Lancet, D, Taylor, C, Khen, M, Walker, N *et al.* 1994. Olfactory receptor gene cluster on human chromosome 17: possible duplication of an ancestral receptor repertoire. *Hum. Mol. Genet* **3:** 229-235.

Bennett, DC and Lamoreux, ML. 2003. The color loci of mice--a genetic century. *Pigment Cell Res.* **16:** 333-344.

Binkley, S, Mosher, K, Rubin, F, and White, B. 1988. Xenopus tadpole melanophores are controlled by dark and light and melatonin without influence of time of day. *J. Pineal Res.* **5:** 87-97.

Bird, DJ, Baker, BI, and Kawauchi, H. 1989. Immunocytochemical demonstration of melanin-concentrating hormone and proopiomelanocortin-like products in the brain of the trout and carp. *Gen. Comp Endocrinol.* **74:** 442-450.

Birney, E and Durbin, R. 2000. Using GeneWise in the Drosophila annotation experiment. *Genome Res.* **10:** 547-548.

Bisbee, CA, Baker, MA, Wilson, AC, Haji-Azimi, I, and Fischberg, M. 1977. Albumin phylogeny for clawed frogs (Xenopus). *Science* **195:** 785-787.

Blair, HS and Kumar, S. 2003. Genomic clocks and evolutionary timescales. *Trends Genet.* **19:** 200-206.

Boeckmann, B, Bairoch, A, Apweiler, R, Blatter, MC, Estreicher, A *et al.* 2003. The SWISS-PROT protein knowledgebase and its supplement TrEMBL in 2003. *Nucleic Acids Res.* **31:** 365-370.

Bolognia, JL and Orlow, SJ. 2003. Melanocyte Biology *in Dermatology*. Elsevier Science. New York.

Borowsky, B, Durkin, MM, Ogozalek, K, Marzabadi, MR, DeLeon, J *et al.* 2002. Antidepressant, anxiolytic and anorectic effects of a melanin-concentrating hormone-1 receptor antagonist. *Nat. Med.* **8:** 825-830.

Borsu, L, Presse, F, and Nahon, JL. 2000. The AROM gene, spliced mRNAs encoding new DNA/RNA-binding proteins are transcribed from the opposite strand of the melanin-concentrating hormone gene in mammals. *J. Biol. Chem.* **275:** 40576-40587.

Boston, BA. 1999. The role of melanocortins in adipocyte function. *Ann. N. Y. Acad. Sci.* **885:** 75-84.

Boston, BA and Cone, RD. 1996. Characterization of melanocortin receptor subtype expression in murine adipose tissues and in the 3T3-L1 cell line. *Endocrinology* **137:** 2043-2050.

Bouchard, B, Fuller, BB, Vijayasaradhi, S, and Houghton, AN. 1989. Induction of pigmentation in mouse fibroblasts by expression of human tyrosinase cDNA. *J. Exp. Med.* **169:** 2029-2042.

Bowley, TJ, Rance, TA, and Baker, BI. 1983. Measurement of immunoreactive alpha-melanocyte-stimulating hormone in the blood of rainbow trout kept under various conditions. *J. Endocrinol.* **97:** 267-275.

Brenner, S, Elgar, G, Sandford, R, Macrae, A, Venkatesh, B *et al.* 1993. Characterization of the pufferfish (Fugu) genome as a compact model vertebrate genome. *Nature* **366:** 265-268.

Brinster, RL, Allen, JM, Behringer, RR, Gelinas, RE, and Palmiter, RD. 1988. Introns increase transcriptional efficiency in transgenic mice. *Proc. Natl. Acad. Sci. U. S. A* **85:** 836-840.

Brody, T and Cravchik, A. 2000. Drosophila melanogaster G protein-coupled receptors. *J. Cell Biol* **150:** F83-F88.

Bultman, SJ, Klebig, ML, Michaud, EJ, Sweet, HO, Davisson, MT *et al.* 1994. Molecular analysis of reverse mutations from nonagouti (a) to black-and- tan (a(t)) and white-bellied agouti (Aw) reveals alternative forms of agouti transcripts. *Genes Dev.* **8:** 481-490.

Bultman, SJ, Michaud, EJ, and Woychik, RP. 1992. Molecular characterization of the mouse agouti locus. *Cell* **71:** 1195-1204.

Bultman, SJ, Russell, LB, Gutierrez-Espeleta, GA, and Woychik, RP. 1991. Molecular characterization of a region of DNA associated with mutations at the agouti locus in the mouse. *Proc. Natl. Acad. Sci. U. S A* **88:** 8062-8066.

Burt, DW, Bruley, C, Dunn, IC, Jones, CT, Ramage, A *et al.* 1999. The dynamics of chromosome evolution in birds and mammals. *Nature* **402:** 411-413.

C.elegans Sequencing Consortium. 1998. Genome sequence of the nematode C. elegans: a platform for investigating biology. *Science* **282:** 2012-2018.

Cao, J, O'Donnell, D, Vu, H, Payza, K, Pou, C *et al.* 1998. Cloning and characterization of a cDNA encoding a novel subtype of rat thyrotropin-releasing hormone receptor. *J. Biol. Chem.* **273:** 32281-32287.

Carulli, JP, Chen, DM, Stark, WS, and Hartl, DL. 1994. Phylogeny and physiology of Drosophila opsins. *J Mol. Evol.* **38:** 250-262.

Castrucci, AM, Hadley, ME, and Hruby, VJ. 1987. A teleost skin bioassay for melanotropic peptides. *Gen. Comp Endocrinol.* **66:** 374-380.

Catania, A, Rajora, N, Capsoni, F, Minonzio, F, Star, RA *et al.* 1996. The neuropeptide alpha-MSH has specific receptors on neutrophils and reduces chemotaxis in vitro. *Peptides* **17:** 675-679.

Cerda-Reverter, JM and Peter, RE. 2003. Endogenous Melanocortin Antagonist in Fish: Structure, Brain Mapping and Regulation by Fasting of the Goldfish Agouti-Related Protein Gene. *Endocrinology* **144:** 4552-61.

Cerda-Reverter, JM, Ringholm, A, Schioth, HB, and Peter, RE. 2003a. Molecular cloning, pharmacological characterization, and brain mapping of the melanocortin 4 receptor in the goldfish: involvement in the control of food intake. *Endocrinology* **144:** 2336-2349.

Cerda-Reverter, JM, Schioth, HB, and Peter, RE. 2003b. The central melanocortin system regulates food intake in goldfish. *Regul. Pept.* **115:** 101-113.

Chambers, J, Ames, RS, Bergsma, D, Muir, A, Fitzgerald, LR *et al.* 1999. Melanin-concentrating hormone is the cognate ligand for the orphan G- protein-coupled receptor SLC-1. *Nature* **400:** 261-265.

Chen, AS, Marsh, DJ, Trumbauer, ME, Frazier, EG, Guan, XM *et al.* 2000. Inactivation of the mouse melanocortin-3 receptor results in increased fat mass and reduced lean body mass. *Nat. Genet.* **26:** 97-102.

Chen, W, Kelly, MA, Opitz-Araya, X, Thomas, RE, Low, MJ *et al.* 1997. Exocrine gland dysfunction in MC5-R-deficient mice: evidence for coordinated regulation of exocrine gland function by melanocortin peptides. *Cell* **91:** 789-798.

Chen, Y, Hu, C, Hsu, CK, Zhang, Q, Bi, C *et al.* 2002. Targeted disruption of the melanin-concentrating hormone receptor-1 results in hyperphagia and resistance to diet-induced obesity. *Endocrinology* **143:** 2469-2477.

Cheng, CH and Chen, L. 1999. Evolution of an antifreeze glycoprotein. *Nature* **401:** 443-444.

Chhajlani, V and Wikberg, JE. 1992. Molecular cloning and expression of the human melanocyte stimulating hormone receptor cDNA. *FEBS Lett.* **309:** 417-420.

Chowdhary, BP, Gustavsson, I, Wikberg, JE, and Chhajlani, V. 1995. Localization of the human melanocortin-5 receptor gene (MC5R) to chromosome band 18p11.2 by fluorescence in situ hybridization. *Cytogenet. Cell Genet.* **68:** 79-81.

Clamp, M, Andrews, D, Barker, D, Bevan, P, Cameron, G *et al.* 2003. Ensembl 2002: accommodating comparative genomics. *Nucleic Acids Res.* **31:** 38-42.

Cohen, J and Szabo, G. 1968. Study of pigment donation in vitro. *Exp. Cell Res.* **50:** 418-434.

Cone, RD, Lu, D, Koppula, S, Vage, DI, Klungland, H *et al.* 1996. The melanocortin receptors: agonists, antagonists, and the hormonal control of pigmentation. *Recent Prog. Horm. Res* **51:** 287-317.

Conklin, BR and Bourne, HR. 1993. Mouse coat colour reconsidered. *Nature* **364:** 110-

Copeland, NG, Gilbert, DJ, Cho, BC, Donovan, PJ, Jenkins, NA *et al.* 1990. Mast cell growth factor maps near the steel locus on mouse chromosome 10 and is deleted in a number of steel alleles. *Cell* **63:** 175-183.

Corbo, JC, Di Gregorio, A, and Levine, M. 2001. The ascidian as a model organism in developmental and evolutionary biology. *Cell* **106:** 535-538.

Crnogorac-Jurcevic, T, Brown, JR, Lehrach, H, and Schalkwyk, LC. 1997. Tetraodon fluviatilis, a new puffer fish model for genome studies. *Genomics* **41:** 177-184.

Daniolos, A, Lerner, AB, and Lerner, MR. 1990. Action of light on frog pigment cells in culture. *Pigment Cell Res.* **3:** 38-43.

de Sa, RO and Hillis, DM. 1990. Phylogenetic relationships of the pipid frogs Xenopus and Silurana: an integration of ribosomal DNA and morphology. *Mol. Biol. Evol.* **7:** 365-376.

de Souza, SJ, Long, M, Schoenbach, L, Roy, SW, and Gilbert, W. 1997. The correlation between introns and the three-dimensional structure of proteins. *Gene* **205:** 141-144.

Derr, LK and Strathern, JN. 1993. A role for reverse transcripts in gene conversion. *Nature* **361:** 170-173.

Deutsch, M and Long, M. 1999. Intron-exon structures of eukaryotic model organisms. *Nucleic Acids Res.* **27:** 3219-3228.

Di Palma, F, Belyantseva, IA, Kim, HJ, Vogt, TF, Kachar, B *et al.* 2002. Mutations in Mcoln3 associated with deafness and pigmentation defects in varitint-waddler (Va) mice. *Proc. Natl. Acad. Sci. U. S. A* **99:** 14994-14999.

Dibb, NJ and Newman, AJ. 1989. Evidence that introns arose at proto-splice sites. *EMBO J.* **8:** 2015-2021.

Dickie, MM. 1969. Mutations at the agouti locus in the mouse. *J. Hered.* **60:** 20-25.

Dickman, MC, Schliwa, M, and Barlow, GW. 1988. Melanophore death and disappearance produces color metamorphosis in the polychromatic Midas cichlid (Cichlasoma citrinellum). *Cell Tissue Res.* **253:** 9-14.

Dohlman, HG, Thorner, J, Caron, MG, and Lefkowitz, RJ. 1991. Model systems for the study of seven-transmembrane-segment receptors. *Annu Rev Biochem.* **60:** 653-688.

Dorr, RT, Lines, R, Levine, N, Brooks, C, Xiang, L *et al.* 1996. Evaluation of melanotan-II, a superpotent cyclic melanotropic peptide in a pilot phase-I clinical study. *Life Sci.* **58:** 1777-1784.

Du, J and Fisher, DE. 2002. Identification of Aim-1 as the underwhite mouse mutant and its transcriptional regulation by MITF. *J. Biol. Chem.* **277:** 402-406.

Dube, D, Lissitzky, JC, Leclerc, R, and Pelletier, G. 1978. Localization of alpha-melanocyte-stimulating hormone in rat brain and pituitary. *Endocrinology* **102:** 1283-1291.

Dubern, B, Clement, K, Pelloux, V, Froguel, P, Girardet, JP *et al.* 2001a. Mutational analysis of melanocortin-4 receptor, agouti-related protein, and alpha-melanocyte-stimulating hormone genes in severely obese children. *J Pediatr.* **139:** 204-209.

Duhl, DM, Stevens, ME, Vrieling, H, Saxon, PJ, Miller, MW *et al.* 1994. Pleiotropic effects of the mouse lethal yellow (Ay) mutation explained by deletion of a maternally expressed gene and the simultaneous production of agouti fusion RNAs. *Development* **120:** 1695-1708.

Dulai, KS, von Dornum, M, Mollon, JD, and Hunt, DM. 1999. The evolution of trichromatic color vision by opsin gene duplication in New World and Old World primates. *Genome Res.* **9:** 629-638.

Dutton, K, Dutton, JR, Pauliny, A, and Kelsh, RN. 2001a. A morpholino phenocopy of the colourless mutant. *Genesis.* **30:** 188-189.

Dutton, KA, Pauliny, A, Lopes, SS, Elworthy, S, Carney, TJ *et al.* 2001b. Zebrafish colourless encodes sox10 and specifies non-ectomesenchymal neural crest fates. *Development* **128:** 4113-4125.

Duvaux-Miret, O, Dissous, C, Gautron, JP, Pattou, E, Kordon, C *et al.* 1990. The helminth Schistosoma mansoni expresses a peptide similar to human beta-endorphin and possesses a proopiomelanocortin-related gene. *New Biol.* **2:** 93-99.

Easter, SS, Jr. and Nicola, GN. 1996. The development of vision in the zebrafish (Danio rerio). *Dev. Biol.* **180:** 646-663.

Ebisawa, T, Karne, S, Lerner, MR, and Reppert, SM. 1994. Expression cloning of a high-affinity melatonin receptor from Xenopus dermal melanophores. *Proc. Natl. Acad. Sci. U. S. A* **91:** 6133-6137.

Eddy, SR. 1998. Profile hidden Markov models. *Bioinformatics.* **14:** 755-763.

Eipper, BA and Mains, RE. 1980. Structure and biosynthesis of pro-adrenocorticotropin /endorphin and related peptides. *Endocr. Rev.* **1:** 1-27.

Eizirik, E, Yuhki, N, Johnson, WE, Menotti-Raymond, M, Hannah, SS *et al.* 2003. Molecular genetics and evolution of melanism in the cat family. *Curr. Biol.* **13:** 448-453.

Elgar, G, Clark, MS, Meek, S, Smith, S, Warner, S *et al.* 1999. Generation and analysis of 25 Mb of genomic DNA from the pufferfish Fugu rubripes by sequence scanning. *Genome Res* **9:** 960-971.

Enami, M. 1955. Melanophore-concentrating hormone (MCH) of possible hypothalamic origin in the catfish *Parasilurus*. *Science* **121:** 36-37.

Epstein, DJ, Vekemans, M, and Gros, P. 1991. Splotch (Sp2H), a mutation affecting development of the mouse neural tube, shows a deletion within the paired homeodomain of Pax-3. *Cell* **67:** 767-774.

Etzold, T, Ulyanov, A, and Argos, P. 1996. SRS: information retrieval system for molecular biology data banks. *Methods Enzymol.* **266:** 114-128.

Ewing, B and Green, P. 1998. Base-calling of automated sequencer traces using phred. II. Error probabilities. *Genome Res* **8:** 186-194.

Farooqi, IS, Yeo, GS, Keogh, JM, Aminian, S, Jebb, SA *et al.* 2000. Dominant and recessive inheritance of morbid obesity associated with melanocortin 4 receptor deficiency. *J Clin. Invest* **106:** 271-279.

Fedorov, A, Merican, AF, and Gilbert, W. 2002. Large-scale comparison of intron positions among animal, plant, and fungal genes. *Proc. Natl. Acad. Sci. U. S. A* **99:** 16128-16133.

Fernandez, PJ and Bagnara, JT. 1991. Effect of background color and low temperature on skin color and circulating alpha-MSH in two species of leopard frog. *Gen. Comp Endocrinol.* **83:** 132-141.

Ferris, SD and Whitt, GS. 1977. Loss of duplicate gene expression after polyploidisation. *Nature* **265:** 258-260.

Fichant, GA. 1992. Constraints acting on the exon positions of the splice site sequences and local amino acid composition of the protein. *Hum. Mol. Genet.* **1:** 259-267.

Fink, GR. 1987. Pseudogenes in yeast? *Cell* **49:** 5-6.

Fitzpatrick, TB, Quevedo, WC, Jr., Levene, AL, McGovern, VJ, Mishima, Y *et al.* 1966. Terminology of vertebrate melanin-containing cells: 1965. *Science* **152:** 88-89.

Fluck, CE, Martens, JW, Conte, FA, and Miller, WL. 2002. Clinical, genetic, and functional characterization of adrenocorticotropin receptor mutations using a novel receptor assay. *J. Clin. Endocrinol. Metab* **87:** 4318-4323.

Fong, TM, Mao, C, MacNeil, T, Kalyani, R, Smith, T *et al.* 1997. ART (protein product of agouti-related transcript) as an antagonist of MC-3 and MC-4 receptors. *Biochem. Biophys. Res. Commun.* **237:** 629-631.

Force, A, Lynch, M, Pickett, FB, Amores, A, Yan, YL *et al.* 1999. Preservation of duplicate genes by complementary, degenerative mutations. *Genetics* **151:** 1531-1545.

Frandberg, PA, Doufexis, M, Kapas, S, and Chhajlani, V. 1998. Amino acid residues in third intracellular loop of melanocortin 1 receptor are involved in G-protein coupling. *Biochem. Mol. Biol. Int.* **46:** 913-922.

Fredriksson, R, Lagerstrom, MC, Lundin, LG, and Schioth, HB. 2003. The G-protein-coupled receptors in the human genome form five main families. Phylogenetic analysis, paralogon groups, and fingerprints. *Mol. Pharmacol.* **63:** 1256-1272.

Friedman, R and Hughes, AL. 2001. Pattern and timing of gene duplication in animal genomes. *Genome Res.* **11:** 1842-1847.

Frugoli, JA, McPeek, MA, Thomas, TL, and McClung, CR. 1998. Intron loss and gain during evolution of the catalase gene family in angiosperms. *Genetics* **149:** 355-365.

Fujii, R. 1993. Cytophysiology of fish chromatophores. *Int. Rev. Cytol.* **143:** 191-255.

Fujii, R. 2000. The regulation of motile activity in fish chromatophores. *Pigment Cell Res* **13:** 300-319.

Fukamachi, S, Shimada, A, Shima, A. 2001. Mutations in the gene encoding B, a novel transporter protein, reduce melanin content in medaka. *Nat. Genet.* **28:** 381-385.

Fukuzawa, T and Bagnara, JT. 1989. Control of melanoblast differentiation in amphibia by alpha-melanocyte stimulating hormone, a serum melanization factor, and a melanization inhibiting factor. *Pigment Cell Res.* **2:** 171-181.

Fukuzawa, T and Ide, H. 1988. A ventrally localized inhibitor of melanization in Xenopus laevis skin. *Dev. Biol.* **129:** 25-36.

Galbraith, DB. 1969. Cell mass, hair type and expression of the agouti gene. *Nature* **222:** 288-290.

Gantz, I, Konda, Y, Tashiro, T, Shimoto, Y, Miwa, H *et al.* 1993a. Molecular cloning of a novel melanocortin receptor. *J Biol. Chem.* **268:** 8246-8250.

Gantz, I, Miwa, H, Konda, Y, Shimoto, Y, Tashiro, T *et al.* 1993b. Molecular cloning, expression, and gene localization of a fourth melanocortin receptor. *J Biol. Chem.* **268:** 15174-15179.

Garcia-Fernandez, J and Holland, PW. 1994. Archetypal organization of the amphioxus Hox gene cluster. *Nature* **370:** 563-566.

Gates, MA, Kim, L, Egan, ES, Cardozo, T, Sirotkin, HI *et al.* 1999. A genetic linkage map for zebrafish: comparative analysis and localization of genes and expressed sequences. *Genome Res.* **9:** 334-347.

Gentles, AJ and Karlin, S. 1999. Why are human G-protein-coupled receptors predominantly intronless? *Trends Genet* **15:** 47-49.

George, SR, O'Dowd, BF, and Lee, SP. 2002. G-protein-coupled receptor oligomerization and its potential for drug discovery. *Nat. Rev Drug Discov.* **1:** 808-820.

Gilbert, W. 1987. The exon theory of genes. *Cold Spring Harb. Symp. Quant. Biol.* **52:** 901-905.

Gilbert, W, de Souza, SJ, and Long, M. 1997. Origin of genes. *Proc. Natl. Acad. Sci. U. S. A* **94:** 7698-7703.

Gilbert, W and Glynias, M. 1993. On the ancient nature of introns. *Gene* **135:** 137-144.

Glasgow, E, Karavanov, AA, and Dawid, IB. 1997. Neuronal and neuroendocrine expression of lim3, a LIM class homeobox gene, is altered in mutant zebrafish with axial signaling defects. *Dev. Biol.* **192:** 405-419.

Glusman, G, Yanai, I, Rubin, I, and Lancet, D. 2001. The complete human olfactory subgenome. *Genome Res.* **11:** 685-702.

Goda, G and Fujii, R. 1995. Blue chromatophores in two species of callionymid fish. *Zoolog. Sci.* **12:** 811-813.

Goffeau, A, Barrell, BG, Bussey, H, Davis, RW, Dujon, B *et al.* 1996. Life with 6000 genes. *Science* **274:** 546, 563-546, 567.

Goldgeier, MH, Klein, LE, Klein-Angerer, S, Moellmann, G, and Nordlund, JJ. 1984. The distribution of melanocytes in the leptomeninges of the human brain. *J. Invest Dermatol.* **82:** 235-238.

Goldman, JM and Hadley, ME. 1969. The beta adrenergic receptor and cyclic 3',5'-adenosine monophosphate: possible roles in the regulation of melanophore responses of the spadefoot toad, Scaphiopus couchi. *Gen. Comp Endocrinol.* **13:** 151-163.

Gotoh, O. 1998. Divergent structures of Caenorhabditis elegans cytochrome P450 genes suggest the frequent loss and gain of introns during the evolution of nematodes. *Mol. Biol. Evol.* **15:** 1447-1459.

Goulding, M, Sterrer, S, Fleming, J, Balling, R, Nadeau, J *et al.* 1993. Analysis of the Pax-3 gene in the mouse mutant splotch. *Genomics* **17:** 355-363.

Grassi, ME, Basari, F, and Chimenti, C. 1997. Adrenocortical and adrenomedullary homologs in eight species of adult and developing teleosts: morphology, histology, and immunohistochemistry. *Gen. Comp Endocrinol.* **108:** 483-496.

Green, JA and Baker, BI. 1989. Melanin concentrating hormone. I. Influence of nerves and hormones on the control of trout melanophores. *Life Sci.* **45:** 1127-1132.

Gregory, TR. 2001. Animal Genome Size Database. http://www.genomesize.com/.

Grunwald, DJ and Eisen, JS. 2002. Headwaters of the zebrafish -- emergence of a new model vertebrate. *Nat. Rev. Genet.* **3:** 717-724.

Hadley, ME and Quevedo, WC, Jr. 1967. The role of epidermal melanocytes in adaptive colour change in amphibians. *Adv. Biol. Skin* **8:** 337-359.

Hadley, ME, Zechel, C, Wilkes, BC, Castrucci, AM, Visconti, MA *et al.* 1987. Differential structural requirements for the MSH and MCH activities of melanin concentrating hormone. *Life Sci.* **40:** 1139-1145.

Haffter, P, Granato, M, Brand, M, Mullins, MC, Hammerschmidt, M *et al.* 1996. The identification of genes with unique and essential functions in the development of the zebrafish, Danio rerio. *Development* **123:** 1-36.

Halaban, R and Lerner, AB. 1977. The dual effect of melanocyte-stimulating hormone (MSH) on the growth of cultured mouse melanoma cells. *Exp. Cell Res.* **108:** 111-117.

Halaban, R and Moellmann, G. 1993. White mutants in mice shedding light on humans. *J. Invest Dermatol.* **100:** 176S-185S.

Hani, EH, Dupont, S, Durand, E, Dina, C, Gallina, S *et al.* 2001. Naturally occurring mutations in the melanocortin receptor 3 gene are not associated with type 2 diabetes mellitus in French Caucasians. *J Clin. Endocrinol. Metab.* **86:** 2895-2898.

Hansen, IA, To, TT, Wortmann, S, Burmester, T, Winkler, C *et al.* 2003. The pro-opiomelanocortin gene of the zebrafish (Danio rerio). *Biochem. Biophys. Res. Commun.* **303:** 1121-1128.

Hara, M, Yaar, M, Byers, HR, Goukassian, D, Fine, RE *et al.* 2000. Kinesin participates in melanosomal movement along melanocyte dendrites. *J. Invest Dermatol.* **114:** 438-443.

Harris, JI and Lerner, AB. 1957. Amino acid sequence of α-melanocyte-stimulating hormone. *Nature* **179:** 1346-1347.

Haskell-Luevano, C, Hendrata, S, North, C, Sawyer, TK, Hadley, ME *et al.* 1997. Discovery of prototype peptidomimetic agonists at the human melanocortin receptors MC1R and MC4R. *J. Med. Chem.* **40:** 2133-2139.

Haskell-Luevano, C, Miwa, H, Dickinson, C, Hruby, VJ, Yamada, T *et al.* 1994. Binding and cAMP studies of melanotropin peptides with the cloned human peripheral melanocortin receptor, hMC1R. *Biochem. Biophys. Res. Commun.* **204:** 1137-1142.

Hatta, N, Dixon, C, Ray, AJ, Phillips, SR, Cunliffe, WJ *et al.* 2001. Expression, candidate gene, and population studies of the melanocortin 5 receptor. *J Invest Dermatol.* **116:** 564-570.

Hauschka, TS, Jacobs, BB, and Holdridge, BA. 1968. Recessive yellow and its interaction with belted in the mouse. *J Hered.* **59:** 339-341.

Hawes, BE, Kil, E, Green, B, O'Neill, K, Fried, S *et al.* 2000. The melanin-concentrating hormone receptor couples to multiple G proteins to activate diverse intracellular signaling pathways. *Endocrinology* **141:** 4524-4532.

Head, J, Lee, LL, Field, DJ, and Lee, JC. 1985. Equilibrium and rapid kinetic studies on nocodazole-tubulin interaction. *J. Biol. Chem.* **260:** 11060-11066.

Healy, E, Flannagan, N, Ray, A, Todd, C, Jackson, IJ *et al.* 2000. Melanocortin-1-receptor gene and sun sensitivity in individuals without red hair. *Lancet* **355:** 1072-1073.

Healy, E, Jordan, SA, Budd, PS, Suffolk, R, Rees, JL *et al.* 2001. Functional variation of MC1R alleles from red-haired individuals. *Hum. Mol. Genet.* **10:** 2397-2402.

Hearing, VJ and Tsukamoto, K. 1991. Enzymatic control of pigmentation in mammals. *FASEB J.* **5:** 2902-2909.

Heijmen, PS, Klis, SF, De Groot, JC, and Smoorenburg, GF. 1999. Cisplatin ototoxicity and the possibly protective effect of alpha-melanocyte stimulating hormone. *Hear. Res.* **128:** 27-39.

Heisenberg, CP, Brand, M, Jiang, YJ, Warga, RM, Beuchle, D *et al.* 1996. Genes involved in forebrain development in the zebrafish, Danio rerio. *Development* **123:** 191-203.

Herzog, W, Zeng, X, Lele, Z, Sonntag, C, Ting, JW *et al.* 2003. Adenohypophysis formation in the zebrafish and its dependence on sonic hedgehog. *Dev. Biol.* **254:** 36-49.

Hill, J, Duckworth, M, Murdock, P, Rennie, G, Sabido-David, C *et al.* 2001. Molecular cloning and functional characterization of MCH2, a novel human MCH receptor. *J. Biol. Chem.* **276:** 20125-20129.

Hillier, LD, Lennon, G, Becker, M, Bonaldo, MF, Chiapelli, B *et al.* 1996. Generation and analysis of 280,000 human expressed sequence tags. *Genome Res.* **6:** 807-828.

Hogben, LT and Slome, D. 1931. The pigmentary effector system. VI. The dual character of endocrine coordination in amphibian colour change. *Proc. R. Soc. Lond. B Biol. Sci.* **109:** 10-53.

Holland, LZ and Holland, ND. 2001. Evolution of neural crest and placodes: amphioxus as a model for the ancestral vertebrate? *J. Anat.* **199:** 85-98.

Holland, PW, Garcia-Fernandez, J, Williams, NA, and Sidow, A. 1994. Gene duplications and the origins of vertebrate development. *Dev. Suppl* 125-133.

Hoogduijn, MJ, Ancans, J, Suzuki, I, Estdale, S, and Thody, AJ. 2002. Melanin-concentrating hormone and its receptor are expressed and functional in human skin. *Biochem. Biophys. Res. Commun.* **296:** 698-701.

Hori, Y, Toda, K, Pathak, MA, Clark, WH, Jr., and Fitzpatrick, TB. 1968. A fine-structure study of the human epidermal melanosome complex and its acid phosphatase activity. *J. Ultrastruct. Res.* **25:** 109-120.

Hosoda, K, Hammer, RE, Richardson, JA, Baynash, AG, Cheung, JC *et al.* 1994. Targeted and natural (piebald-lethal) mutations of endothelin-B receptor gene produce megacolon associated with spotted coat color in mice. *Cell* **79:** 1267-1276.

Hsu, HJ, Lin, G, and Chung, BC. 2003. Parallel early development of zebrafish interrenal glands and pronephros: differential control by wt1 and ff1b. *Development* **130:** 2107-2116.

Huang, E, Nocka, K, Beier, DR, Chu, TY, Buck, J *et al.* 1990. The hematopoietic growth factor KL is encoded by the Sl locus and is the ligand of the c-kit receptor, the gene product of the W locus. *Cell* **63:** 225-233.

Hughes, AL, da Silva, J, and Friedman, R. 2001. Ancient genome duplications did not structure the human Hox-bearing chromosomes. *Genome Res.* **11:** 771-780.

Hukriede, NA, Joly, L, Tsang, M, Miles, J, Tellis, P *et al.* 1999. Radiation hybrid mapping of the zebrafish genome. *Proc. Natl. Acad. Sci. U. S A* **96:** 9745-9750.

Hunt, G, Donatien, PD, Lunec, J, Todd, C, Kyne, S *et al.* 1994a. Cultured human melanocytes respond to MSH peptides and ACTH. *Pigment Cell Res.* **7:** 217-221.

Hunt, G, Kyne, S, Ito, S, Wakamatsu, K, Todd, C *et al.* 1995. Eumelanin and phaeomelanin contents of human epidermis and cultured melanocytes. *Pigment Cell Res.* **8:** 202-208.

Hunt, G, Todd, C, Cresswell, JE, and Thody, AJ. 1994b. Alpha-melanocyte stimulating hormone and its analogue Nle4DPhe7 alpha-MSH affect morphology, tyrosinase activity and melanogenesis in cultured human melanocytes. *J. Cell Sci.* **107 (Pt 1):** 205-211.

Huszar, D, Lynch, CA, Fairchild-Huntress, V, Dunmore, JH, Fang, Q *et al.* 1997. Targeted disruption of the melanocortin-4 receptor results in obesity in mice. *Cell* **88:** 131-141.

Ide, H, Kawazoe, I, and Kawauchi, H. 1985. Fish melanin-concentrating hormone disperses melanin in amphibian melanophores. *Gen. Comp Endocrinol.* **58:** 486-490.

Iga, T. 1983. Electric stimulation experiments on leucophores of a freshwater teleost, Oryzias latipes. *Comp Biochem. Physiol C.* **74:** 103-108.

International Human Genome Sequencing Consortium. 2001. Initial sequencing and analysis of the human genome. *Nature* **409:** 860-921.

Issel-Tarver, L and Rine, J. 1997. The evolution of mammalian olfactory receptor genes. *Genetics* **145:** 185-195.

Itadani, H, Nakamura, T, Itoh, J, Iwaasa, H, Kanatani, A *et al.* 1998. Cloning and characterization of a new subtype of thyrotropin-releasing hormone receptors. *Biochem. Biophys. Res. Commun.* **250:** 68-71.

Ito, S. 2003. The IFPCS presidential lecture: a chemist's view of melanogenesis. *Pigment Cell Res.* **16:** 230-236.

Ito, S and Wakamatsu, K. 2003. Quantitative analysis of eumelanin and pheomelanin in humans, mice, and other animals: a comparative review. *Pigment Cell Res.* **16:** 523-531.

Jackson, IJ. 1991. Mouse coat colour mutations: a molecular genetic resource which spans the centuries. *Bioessays* **13:** 439-446.

Jackson, IJ. 1994. Molecular and developmental genetics of mouse coat color. *Annu. Rev. Genet.* **28:** 189-217.

Jackson, IJ. 1997. Homologous pigmentation mutations in human, mouse and other model organisms. *Hum. Mol. Genet.* **6:** 1613-1624.

Jackson, IJ and Bennett, DC. 1990. Identification of the albino mutation of mouse tyrosinase by analysis of an in vitro revertant. *Proc. Natl. Acad. Sci. U. S. A* **87:** 7010-7014.

Jackson, IJ, Chambers, DM, Tsukamoto, K, Copeland, NG, Gilbert, DJ *et al.* 1992. A second tyrosinase-related protein, TRP-2, maps to and is mutated at the mouse slaty locus. *EMBO J* **11:** 527-535.

Japon, MA, Rubinstein, M, and Low, MJ. 1994. In situ hybridization analysis of anterior pituitary hormone gene expression during fetal mouse development. *J. Histochem. Cytochem.* **42:** 1117-1125.

Jenkins, NA, Copeland, NG, Taylor, BA, and Lee, BK. 1981. Dilute (d) coat colour mutation of DBA/2J mice is associated with the site of integration of an ecotropic MuLV genome. *Nature* **293:** 370-374.

Jimbow, K, Ishida, O, Takahashi, H, and Ito, S. 1984. Hair colour and type of melanogenesis in human hair *in Structure and Function of Melanin*. Fuji-Shoin Company. Sapporo

Jimbow, K, Quevedo, WC, Jr., Fitzpatrick, TB, and Szabo, G. 1976. Some aspects of melanin biology: 1950-1975. *J. Invest Dermatol.* **67:** 72-89.

Jimbow, K and Sugiyama, S. 1998. Melanosomal Translocation and Transfer *in The Pigmentary System: Its Physiology and Pathophysiology*. Oxford University Press. New York.

Johnston, HS, McGadey, J, Payne, AP, Thompson, GG, and Moore, MR. 1987. The Harderian gland, its secretory duct and porphyrin content in the woodmouse (Apodemus sylvaticus). *J. Anat.* **153:** 17-30.

Jordan, SA and Jackson, IJ. 1998. Melanocortin receptors and antagonists regulate pigmentation and body weight. *Bioessays* **20:** 603-606.

Joss, JM. 1973. The pineal complex, melatonin, and color change in the lamprey Lampetra. *Gen. Comp Endocrinol.* **21:** 188-195.

Jowett, T. 1999. Analysis of Protein and Gene Expression *in Methods in Cell Biology: The Zebrafish*. Academic Press. San Diego

Justice, MJ. 2000. Capitalizing on large-scale mouse mutagenesis screens. *Nat. Rev. Genet.* **1:** 109-115.

Karlsson, JO, Andersson, RG, Askelof, P, Elwing, H, Granstrom, M *et al.* 1991. The melanophore aggregating response of isolated fish scales: a very rapid and sensitive diagnosis of whooping cough. *FEMS Microbiol. Lett.* **66:** 169-175.

Katsuki, A, Sumida, Y, Gabazza, EC, Murashima, S, Tanaka, T *et al.* 2001. Plasma levels of agouti-related protein are increased in obese men. *J. Clin. Endocrinol. Metab* **86:** 1921-1924.

Kawauchi, H, Kawazoe, I, Tsubokawa, M, Kishida, M, and Baker, BI. 1983. Characterization of melanin-concentrating hormone in chum salmon pituitaries. *Nature* **305:** 321-323.

Keller, C. 1978. How it Began *in Origins of Inbred Mice*. Academic Press. London.

Kelsh, RN, Brand, M, Jiang, YJ, Heisenberg, CP, Lin, S *et al.* 1996. Zebrafish pigmentation mutations and the processes of neural crest development. *Development* **123:** 369-389.

Kelsh, RN and Raible, DW. 2002. Specification of zebrafish neural crest. *Results Probl. Cell Differ.* **40:** 216-236.

Kelsh, RN, Schmid, B, and Eisen, JS. 2000. Genetic analysis of melanophore development in zebrafish embryos. *Dev. Biol.* **225:** 277-293.

Kersanach, R, Brinkmann, H, Liaud, MF, Zhang, DX, Martin, W *et al.* 1994. Five identical intron positions in ancient duplicated genes of eubacterial origin. *Nature* **367:** 387-389.

Kijas, JM, Wales, R, Tornsten, A, Chardon, P, Moller, M *et al.* 1998. Melanocortin receptor 1 (MC1R) mutations and coat color in pigs. *Genetics* **150:** 1177-1185.

Kim, IS, Kim, ER, Nam, HJ, Chin, MO, Moon, YH *et al.* 1999. Activating mutation of GS alpha in McCune-Albright syndrome causes skin pigmentation by tyrosinase gene activation on affected melanocytes. *Horm. Res.* **52:** 235-240.

King, RA, Summers, CG, Haefemeyer, JW, and LeRoy, BS. 2001. Facts about albinism. www.cbc.umn.edu/iac/facts.htm

Kishida, M, Baker, BI, and Bird, DJ. 1988. Localisation and identification of melanocyte-stimulating hormones in the fish brain. *Gen. Comp Endocrinol.* **71:** 229-242.

Kitahara, N, Nishizawa, T, Iida, K, Okazaki, H, Andoh, T *et al.* 1988. Absence of a gamma-melanocyte-stimulating hormone sequence in proopiomelanocortin mRNA of chum salmon Oncorhynchus keta. *Comp Biochem. Physiol B* **91:** 365-370.

Kitta, K, Makino, M, Oshima, N, and Bern, HA. 1993. Effects of prolactins on the chromatophores of the tilapia, Oreochromis niloticus. *Gen. Comp Endocrinol.* **92:** 355-365.

Klaus, SN and Snell, RS. 1967. The response of mammalian epidermal melanocytes in culture to hormones. *J. Invest Dermatol.* **48:** 352-358.

Klebig, ML, Wilkinson, JE, Geisler, JG, and Woychik, RP. 1995. Ectopic expression of the agouti gene in transgenic mice causes obesity, features of type II diabetes, and yellow fur. *Proc. Natl. Acad. Sci. U. S. A* **92:** 4728-4732.

Klungland, H, Vage, DI, Gomez-Raya, L, Adalsteinsson, S, and Lien, S. 1995. The role of melanocyte-stimulating hormone (MSH) receptor in bovine coat color determination. *Mamm. Genome* **6:** 636-639.

Koegler, FH, Grove, KL, Schiffmacher, A, Smith, MS, and Cameron, JL. 2001. Central melanocortin receptors mediate changes in food intake in the rhesus macaque. *Endocrinology* **142:** 2586-2592.

Konrad, K and Wolff, K. 1973. Hyperpigmentation, melanosome size, and distribution patterns of melanosomes. *Arch. Dermatol.* **107:** 853-860.

Krude, H, Biebermann, H, Luck, W, Horn, R, Brabant, G *et al.* 1998. Severe early-onset obesity, adrenal insufficiency and red hair pigmentation caused by POMC mutations in humans. *Nat. Genet.* **19:** 155-157.

Kumar, S, Tamura, K, Jakobsen, IB, and Nei, M. 2001. MEGA2: molecular evolutionary genetics analysis software. *Bioinformatics.* **17:** 1244-1245.

Kuratani, S, Kuraku, S, and Murakami, Y. 2002. Lamprey as an evo-devo model: lessons from comparative embryology and molecular phylogenetics. *Genesis.* **34:** 175-183.

Kuzumaki, T, Matsuda, A, Wakamatsu, K, Ito, S, and Ishikawa, K. 1993. Eumelanin biosynthesis is regulated by coordinate expression of tyrosinase and tyrosinase-related protein-1 genes. *Exp. Cell Res* **207:** 33-40.

Kwon, BS, Haq, AK, Pomerantz, SH, and Halaban, R. 1987. Isolation and sequence of a cDNA clone for human tyrosinase that maps at the mouse c-albino locus. *Proc. Natl. Acad. Sci. U. S A* **84:** 7473-7477.

Kwon, HY, Bultman, SJ, Loffler, C, Chen, WJ, Furdon, PJ *et al.* 1994. Molecular structure and chromosomal mapping of the human homolog of the agouti gene. *Proc. Natl. Acad. Sci. U. S. A* **91:** 9760-9764.

Labbe, O, Desarnaud, F, Eggerickx, D, Vassart, G, and Parmentier, M. 1994. Molecular cloning of a mouse melanocortin 5 receptor gene widely expressed in peripheral tissues. *Biochemistry* **33:** 4543-4549.

Lamoreux, ML, Zhou, BK, Rosemblat, S, and Orlow, SJ. 1995. The pinkeyed-dilution protein and the eumelanin/pheomelanin switch: in support of a unifying hypothesis. *Pigment Cell Res* **8:** 263-270.

Larhammar, D, Lundin, LG, and Hallbook, F. 2002. The human Hox-bearing chromosome regions did arise by block or chromosome (or even genome) duplications. *Genome Res.* **12:** 1910-1920.

Le Hir, H, Nott, A, and Moore, MJ. 2003. How introns influence and enhance eukaryotic gene expression. *Trends Biochem. Sci.* **28:** 215-220.

Lee, J, Danielson, P, Sollars, C, Alrubaian, J, Balm, P *et al.* 1999. Cloning of a neoteleost (Oreochromis mossambicus) pro-opiomelanocortin (POMC) cDNA reveals a deletion of the gamma-melanotropin region and most of the joining peptide region: implications for POMC processing. *Peptides* **20:** 1391-1399.

Lembo, PM, Grazzini, E, Cao, J, Hubatsch, DA, Pelletier, M *et al.* 1999. The receptor for the orexigenic peptide melanin-concentrating hormone is a G-protein-coupled receptor. *Nat. Cell Biol.* **1:** 267-271.

Lin, X, Volkoff, H, Narnaware, Y, Bernier, NJ, Peyon, P *et al.* 2000. Brain regulation of feeding behavior and food intake in fish. *Comp Biochem. Physiol A Mol. Integr. Physiol* **126:** 415-434.

Lister, JA, Close, J, and Raible, DW. 2001. Duplicate mitf genes in zebrafish: complementary expression and conservation of melanogenic potential. *Dev. Biol.* **237:** 333-344.

Lister, JA, Robertson, CP, Lepage, T, Johnson, SL, and Raible, DW. 1999. nacre encodes a zebrafish microphthalmia-related protein that regulates neural-crest-derived pigment cell fate. *Development* **126:** 3757-3767.

Liu, B, Hammer, GD, Rubinstein, M, Mortrud, M, and Low, MJ. 1992. Identification of DNA elements cooperatively activating proopiomelanocortin gene expression in the pituitary glands of transgenic mice. *Mol. Cell Biol.* **12:** 3978-3990.

Liu, NA, Huang, H, Yang, Z, Herzog, W, Hammerschmidt, M *et al.* 2003. Pituitary corticotroph ontogeny and regulation in transgenic zebrafish. *Mol. Endocrinol.* **17:** 959-966.

Logsdon, JM, Jr., Tyshenko, MG, Dixon, C, Jafari, J, Walker, VK *et al.* 1995. Seven newly discovered intron positions in the triose-phosphate isomerase gene: evidence for the introns-late theory. *Proc. Natl. Acad. Sci. U. S. A* **92:** 8507-8511.

Long, M, de Souza, SJ, Rosenberg, C, and Gilbert, W. 1998. Relationship between "proto-splice sites" and intron phases: evidence from dicodon analysis. *Proc. Natl. Acad. Sci. U. S. A* **95:** 219-223.

Long, M and Deutsch, M. 1999. Association of intron phases with conservation at splice site sequences and evolution of spliceosomal introns. *Mol. Biol. Evol.* **16:** 1528-1534.

Long, M and Rosenberg, C. 2000. Testing the "proto-splice sites" model of intron origin: evidence from analysis of intron phase correlations. *Mol. Biol Evol.* **17:** 1789-1796.

Long, M, Rosenberg, C, and Gilbert, W. 1995. Intron phase correlations and the evolution of the intron/exon structure of genes. *Proc. Natl. Acad. Sci. U. S. A* **92:** 12495-12499.

Lu, D, Willard, D, Patel, IR, Kadwell, S, Overton, L *et al.* 1994. Agouti protein is an antagonist of the melanocyte-stimulating-hormone receptor. *Nature* **371:** 799-802.

Ludwig, A, Belfiore, NM, Pitra, C, Svirsky, V, and Jenneckens, I. 2001a. Genome duplication events and functional reduction of ploidy levels in sturgeon (Acipenser, Huso and Scaphirhynchus). *Genetics* **158:** 1203-1215.

Ludwig, DS, Mountjoy, KG, Tatro, JB, Gillette, JA, Frederich, RC *et al.* 1998. Melanin-concentrating hormone: a functional melanocortin antagonist in the hypothalamus. *Am. J. Physiol* **274:** E627-E633.

Ludwig, DS, Tritos, NA, Mastaitis, JW, Kulkarni, R, Kokkotou, E *et al.* 2001b. Melanin-concentrating hormone overexpression in transgenic mice leads to obesity and insulin resistance. *J. Clin. Invest* **107:** 379-386.

Lundin, LG. 1993. Evolution of the vertebrate genome as reflected in paralogous chromosomal regions in man and the house mouse. *Genomics* **16:** 1-19.

MacLean-Fletcher, S and Pollard, TD. 1980. Mechanism of action of cytochalasin B on actin. *Cell* **20:** 329-341.

Magenis, RE, Smith, L, Nadeau, JH, Johnson, KR, Mountjoy, KG *et al.* 1994. Mapping of the ACTH, MSH, and neural (MC3 and MC4) melanocortin receptors in the mouse and human. *Mamm. Genome* **5:** 503-508.

Marchionni, M and Gilbert, W. 1986. The triosephosphate isomerase gene from maize: introns antedate the plant-animal divergence. *Cell* **46:** 133-141.

Marcinkiewicz, M, Day, R, Seidah, NG, and Chretien, M. 1993. Ontogeny of the prohormone convertases PC1 and PC2 in the mouse hypophysis and their colocalization with corticotropin and alpha-melanotropin. *Proc. Natl. Acad. Sci. U. S. A* **90:** 4922-4926.

Marklund, L, Moller, MJ, Sandberg, K, and Andersson, L. 1996. A missense mutation in the gene for melanocyte-stimulating hormone receptor (MC1R) is associated with the chestnut coat color in horses. *Mamm. Genome* **7:** 895-899.

Marsh, DJ, Weingarth, DT, Novi, DE, Chen, HY, Trumbauer, ME *et al.* 2002. Melanin-concentrating hormone 1 receptor-deficient mice are lean, hyperactive, and hyperphagic and have altered metabolism. *Proc. Natl. Acad. Sci. U. S A* **99:** 3240-3245.

Marshall, WS, Howard, JA, Cozzi, RR, and Lynch, EM. 2002. NaCl and fluid secretion by the intestine of the teleost Fundulus heteroclitus: involvement of CFTR. *J. Exp. Biol.* **205:** 745-758.

Marshall, WS and Singer, TD. 2002. Cystic fibrosis transmembrane conductance regulator in teleost fish. *Biochim. Biophys. Acta* **1566:** 16-27.

Martensson, LG and Andersson, RG. 2000. Is Ca2+ the second messenger in the response to melatonin in cuckoo wrasse melanophores? *Life Sci.* **66:** 1003-1010.

Martin, LW, Catania, A, Hiltz, ME, and Lipton, JM. 1991. Neuropeptide alpha-MSH antagonizes IL-6- and TNF-induced fever. *Peptides* **12:** 297-299.

Matsumoto, J. 1965. Studies on fine structure and cytochemical properties of erythrophores in swordtail, Xiphophorus helleri, with special reference to their pigment granules (Pterinosomes). *J. Cell Biol.* **27:** 493-504.

Matsunaga, TO, Castrucci, AM, Hadley, ME, and Hruby, VJ. 1989. Melanin concentrating hormone (MCH): synthesis and bioactivity studies of MCH fragment analogues. *Peptides* **10:** 349-354.

Mayor, C, Brudno, M, Schwartz, JR, Poliakov, A, Rubin, EM *et al.* 2000. VISTA : visualizing global DNA sequence alignments of arbitrary length. *Bioinformatics.* **16:** 1046-1047.

McCauley, DW and Bronner-Fraser, M. 2003. Neural crest contributions to the lamprey head. *Development* **130:** 2317-2327.

McLean, C and Lowry, PJ. 1981. Natural occurrence but lack of melanotrophic activity of gamma-MSH in fish. *Nature* **290:** 341-343.

Menter, DG, Obika, TT, Tchen, TT, and Taylor, JD. 1979. Leucophores and iridophores of Fundus heteroclitus: biophysical and ultrastructural properties. *J. Morphol.* **160:** 103-120.

Mercer, JA, Seperack, PK, Strobel, MC, Copeland, NG, and Jenkins, NA. 1991. Novel myosin heavy chain encoded by murine dilute coat colour locus. *Nature* **349:** 709-713.

Michaud, EJ, Bultman, SJ, Klebig, ML, van Vugt, MJ, Stubbs, LJ *et al.* 1994. A molecular model for the genetic and phenotypic characteristics of the mouse lethal yellow (Ay) mutation. *Proc. Natl. Acad. Sci. U. S. A* **91:** 2562-2566.

Michaud, EJ, Bultman, SJ, Stubbs, LJ, and Woychik, RP. 1993. The embryonic lethality of homozygous lethal yellow mice (Ay/Ay) is associated with the disruption of a novel RNA-binding protein. *Genes Dev.* **7:** 1203-1213.

Millar, SE, Miller, MW, Stevens, ME, and Barsh, GS. 1995. Expression and transgenic studies of the mouse agouti gene provide insight into the mechanisms by which mammalian coat color patterns are generated. *Development* **121:** 3223-3232.

Miller, MW, Duhl, DM, Vrieling, H, Cordes, SP, Ollmann, MM *et al.* 1993. Cloning of the mouse agouti gene predicts a secreted protein ubiquitously expressed in mice carrying the lethal yellow mutation. *Genes Dev.* **7:** 454-467.

Misuraca, G, Prota, G, Frost, SK, and Bagnara, JT. 1977. Identification of the leaf-frog melanophore pigment, rhodomelanochrome, as pterorhodin. *Comp. Biochem. Physiol. A Physiol.* **57B:** 41-43.

Mogil, JS, Wilson, SG, Chesler, EJ, Rankin, AL, Nemmani, KV *et al.* 2003. The melanocortin-1 receptor gene mediates female-specific mechanisms of analgesia in mice and humans. *Proc. Natl. Acad. Sci. U. S. A* **100:** 4867-4872.

Molinoff, PB, Shadiack, AM, Earle, D, Diamond, LE, and Quon, CY. 2003. PT-141: a melanocortin agonist for the treatment of sexual dysfunction. *Ann. N. Y. Acad. Sci.* **994:** 96-102.

Moller, H and Lerner, AB. 1966. Melanocyte stimulating hormone inhibition by acetylcholine and noradrenaline in the frog skin bioassay. *Acta Endocrinol. (Copenh)* **51:** 149-160.

Morello, JP and Bouvier, M. 1996. Palmitoylation: a post-translational modification that regulates signalling from G-protein coupled receptors. *Biochem. Cell Biol.* **74:** 449-457.

Mori, M, Harada, M, Terao, Y, Sugo, T, Watanabe, T *et al.* 2001. Cloning of a novel G protein-coupled receptor, SLT, a subtype of the melanin-concentrating hormone receptor. *Biochem. Biophys. Res. Commun.* **283:** 1013-1018.

Morrison, RL. 1995. A transmission electron microscopic (TEM) method for determining structural colors reflected by lizard iridophores. *Pigment Cell Res.* **8:** 28-36.

Mount, SM. 1982. A catalogue of splice junction sequences. *Nucleic Acids Res.* **10:** 459-472.

Mountjoy, KG, Mortrud, MT, Low, MJ, Simerly, RB, and Cone, RD. 1994. Localization of the melanocortin-4 receptor (MC4-R) in neuroendocrine and autonomic control circuits in the brain. *Mol. Endocrinol.* **8:** 1298-1308.

Mountjoy, KG, Robbins, LS, Mortrud, MT, and Cone, RD. 1992. The cloning of a family of genes that encode the melanocortin receptors. *Science* **257:** 1248-1251.

Mouse Genome Sequencing Consortium. 2002. Initial sequencing and comparative analysis of the mouse genome. *Nature* **420:** 520-562.

Mulder, NJ, Apweiler, R, Attwood, TK, Bairoch, A, Barrell, D *et al.* 2003. The InterPro Database, 2003 brings increased coverage and new features. *Nucleic Acids Res.* **31:** 315-318.

Nachman, MW, Hoekstra, HE, and D'Agostino, SL. 2003. The genetic basis of adaptive melanism in pocket mice. *Proc. Natl. Acad. Sci. U. S. A* **100:** 5268-5273.

Nahon, JL, Presse, F, Bittencourt, JC, Sawchenko, PE, and Vale, W. 1989. The rat melanin-concentrating hormone messenger ribonucleic acid encodes multiple putative neuropeptides coexpressed in the dorsolateral hypothalamus. *Endocrinology* **125:** 2056-2065.

Narnaware, YK and Peter, RE. 2001. Neuropeptide Y stimulates food consumption through multiple receptors in goldfish. *Physiol Behav.* **74:** 185-190.

Nasevicius, A and Ekker, SC. 2000. Effective targeted gene 'knockdown' in zebrafish. *Nat. Genet.* **26:** 216-220.

Neuhauss, SC, Biehlmaier, O, Seeliger, MW, Das, T, Kohler, K *et al.* 1999. Genetic disorders of vision revealed by a behavioral screen of 400 essential loci in zebrafish. *J. Neurosci.* **19:** 8603-8615.

Newman, AJ and Norman, C. 1992. U5 snRNA interacts with exon sequences at 5' and 3' splice sites. *Cell* **68:** 743-754.

Newton, JM, Wilkie, AL, He, L, Jordan, SA, Metallinos, DL *et al.* 2000. Melanocortin 1 receptor variation in the domestic dog. *Mamm. Genome* **11:** 24-30.

Nielsen, HI. 1978. Ultrastructural changes in the dermal chromatophore unit of Hyla arborea during color change. *Cell Tissue Res.* **194:** 405-418.

Nilsson, H, Rutberg, M, and Wallin, M. 1996. Localization of kinesin and cytoplasmic dynein in cultured melanophores from Atlantic cod, Gadus morhua. *Cell Motil. Cytoskeleton* **33:** 183-196.

Nilsson, H, Steffen, W, and Palazzo, RE. 2001. In vitro reconstitution of fish melanophore pigment aggregation. *Cell Motil. Cytoskeleton* **48:** 1-10.

Nilsson, H and Wallin, M. 1997. Evidence for several roles of dynein in pigment transport in melanophores. *Cell Motil. Cytoskeleton* **38:** 397-409.

Ning, Z, Cox, AJ, and Mullikin, JC. 2001. SSAHA: a fast search method for large DNA databases. *Genome Res.* **11:** 1725-1729.

Nishimura, EK, Jordan, SA, Oshima, H, Yoshida, H, Osawa, M *et al.* 2002. Dominant role of the niche in melanocyte stem-cell fate determination. *Nature* **416:** 854-860.

Nocka, K, Tan, JC, Chiu, E, Chu, TY, Ray, P *et al.* 1990. Molecular bases of dominant negative and loss of function mutations at the murine c-kit/white spotting locus: W37, Wv, W41 and W. *EMBO J.* **9:** 1805-1813.

Norman, RA, Leibel, RL, Chung, WK, Power-Kehoe, L, Chua, SC, Jr. *et al.* 1996. Absence of linkage of obesity and energy metabolism to markers flanking homologues of rodent obesity genes in Pima Indians. *Diabetes* **45:** 1229-1232.

Norris, D. O. 1997. Vertebrate Endocrinology. Adademic Press. San Diego

O'Grady, PM and DeSalle, R. 2000. How the fruit fly changed (some of) its spots. *Curr. Biol.* **10:** R75-R77.

Odenthal, J, Rossnagel, K, Haffter, P, Kelsh, RN, Vogelsang, E *et al.* 1996. Mutations affecting xanthophore pigmentation in the zebrafish, Danio rerio. *Development* **123:** 391-398.

Ohno, S. 1970. Evolution by Gene Duplication. Springer-Verlag. New York.

Okuta, A, Ando, H, Ueda, H, and Urano, A. 1996. Two types of cDNAs encoding proopiomelanocortin of sockeye salmon, Oncorhynchus nerka. *Zoolog. Sci.* **13:** 421-427.

Oliveira, L, Paiva, AC, Sander, C, and Vriend, G. 1994. A common step for signal transduction in G protein-coupled receptors. *Trends Pharmacol. Sci.* **15:** 170-172.

Ollmann, MM, Lamoreux, ML, Wilson, BD, and Barsh, GS. 1998. Interaction of Agouti protein with the melanocortin 1 receptor in vitro and in vivo. *Genes Dev.* **12:** 316-330.

Ollmann, MM, Wilson, BD, Yang, YK, Kerns, JA, Chen, Y *et al.* 1997. Antagonism of central melanocortin receptors in vitro and in vivo by agouti-related protein. *Science* **278:** 135-138.

Oosterom, J, Nijenhuis, WA, Schaaper, WM, Slootstra, J, Meloen, RH *et al.* 1999. Conformation of the core sequence in melanocortin peptides directs selectivity for the melanocortin MC3 and MC4 receptors. *J. Biol. Chem.* **274:** 16853-16860.

Orlow, SJ. 1995. Melanosomes are specialized members of the lysosomal lineage of organelles. *J. Invest Dermatol.* **105:** 3-7.

Oshima, N, Kasukawa, H, Fujii, R, Wilkes, BC, Hruby, VJ *et al.* 1986. Action of melanin-concentrating hormone (MCH) on teleost chromatophores. *Gen. Comp Endocrinol.* **64:** 381-388.

Palazzo, RE, Lynch, TJ, Lo, SJ, Taylor, JD, and Tchen, TT. 1989. Rearrangements of pterinosomes and cytoskeleton accompanying pigment dispersion in goldfish xanthophores. *Cell Motil. Cytoskeleton* **13:** 9-20.

Palmer, JS, Duffy, DL, Box, NF, Aitken, JF, O'Gorman, LE *et al.* 2000. Melanocortin-1 receptor polymorphisms and risk of melanoma: is the association explained solely by pigmentation phenotype? *Am. J Hum. Genet.* **66:** 176-186.

Panopoulou, G, Hennig, S, Groth, D, Krause, A, Poustka, AJ *et al.* 2003. New evidence for genome-wide duplications at the origin of vertebrates using an amphioxus gene set and completed animal genomes. *Genome Res.* **13:** 1056-1066.

Parichy, DM, Mellgren, EM, Rawls, JF, Lopes, SS, Kelsh, RN *et al.* 2000. Mutational analysis of endothelin receptor b1 (rose) during neural crest and pigment pattern development in the zebrafish Danio rerio. *Dev. Biol.* **227:** 294-306.

Parichy, DM, Rawls, JF, Pratt, SJ, Whitfield, TT, and Johnson, SL. 1999. Zebrafish sparse corresponds to an orthologue of c-kit and is required for the morphogenesis of a subpopulation of melanocytes, but is not essential for hematopoiesis or primordial germ cell development. *Development* **126:** 3425-3436.

Parichy, DM and Turner, JM. 2003. Temporal and cellular requirements for Fms signaling during zebrafish adult pigment pattern development. *Development* **130:** 817-833.

Parichy, DM, Turner, JM, and Parker, NB. 2003. Essential role for puma in development of postembryonic neural crest-derived cell lineages in zebrafish. *Dev. Biol.* **256:** 221-241.

Parker, GH. 1948. Animal Colour Changes and Their Neurohumours. Cambridge Univeristy Press. London.

Parrish, W, Eilers, M, Ying, W, and Konopka, JB. 2002. The cytoplasmic end of transmembrane domain 3 regulates the activity of the Saccharomyces cerevisiae G-protein-coupled alpha-factor receptor. *Genetics* **160:** 429-443.

Pastural, E, Barrat, FJ, Dufourcq-Lagelouse, R, Certain, S, Sanal, O *et al.* 1997. Griscelli disease maps to chromosome 15q21 and is associated with mutations in the myosin-Va gene. *Nat. Genet.* **16:** 289-292.

Penhoat, A, Naville, D, El Mourabit, H, Buronfosse, A, Berberoglu, M *et al.* 2002. Functional relationships between three novel homozygous mutations in the ACTH receptor gene and familial glucocorticoid deficiency. *J. Mol. Med.* **80:** 406-411.

Pennisi, E. 2001. Molecular evolution. Genome duplications: the stuff of evolution? *Science* **294:** 2458-2460.

Perler, F, Efstratiadis, A, Lomedico, P, Gilbert, W, Kolodner, R *et al.* 1980. The evolution of genes: the chicken preproinsulin gene. *Cell* **20:** 555-566.

Petrov, DA, Lozovskaya, ER, and Hartl, DL. 1996. High intrinsic rate of DNA loss in Drosophila. *Nature* **384:** 346-349.

Pfeffer, PL, Gerster, T, Lun, K, Brand, M, and Busslinger, M. 1998. Characterization of three novel members of the zebrafish Pax2/5/8 family: dependency of Pax5 and Pax8 expression on the Pax2.1 (noi) function. *Development* **125:** 3063-3074.

Pierce, KL, Premont, RT, and Lefkowitz, RJ. 2002. Seven-transmembrane receptors. *Nat. Rev Mol. Cell Biol* **3:** 639-650.

Pissios, P and Maratos-Flier, E. 2003. Melanin-concentrating hormone: from fish skin to skinny mammals. *Trends Endocrinol. Metab* **14:** 243-248.

Popovici, C, Leveugle, M, Birnbaum, D, and Coulier, F. 2001. Homeobox gene clusters and the human paralogy map. *FEBS Lett.* **491:** 237-242.

Postlethwait, JH, Woods, IG, Ngo-Hazelett, P, Yan, YL, Kelly, PD *et al.* 2000. Zebrafish comparative genomics and the origins of vertebrate chromosomes. *Genome Res* **10:** 1890-1902.

Potenza, MN and Lerner, MR. 1992. A rapid quantitative bioassay for evaluating the effects of ligands upon receptors that modulate cAMP levels in a melanophore cell line. *Pigment Cell Res* **5:** 372-378.

Presse, F, Nahon, JL, Fischer, WH, and Vale, W. 1990. Structure of the human melanin concentrating hormone mRNA. *Mol. Endocrinol.* **4:** 632-637.

Price, JS, Burton, JL, Shuster, S, and Wolff, K. 1976. Control of scrotal colour in the vervet monkey. *J. Med. Primatol.* **5:** 296-304.

Puri, N, Gardner, JM, and Brilliant, MH. 2000. Aberrant pH of melanosomes in pink-eyed dilution (p) mutant melanocytes. *J. Invest Dermatol.* **115:** 607-613.

Qanbar, R and Bouvier, M. 2003. Role of palmitoylation/depalmitoylation reactions in G-protein-coupled receptor function. *Pharmacol. Ther.* **97:** 1-33.

Qu, D, Ludwig, DS, Gammeltoft, S, Piper, M, Pelleymounter, MA *et al.* 1996. A role for melanin-concentrating hormone in the central regulation of feeding behaviour. *Nature* **380:** 243-247.

Quevedo, WC, Jr. 1981. Phaeomelanogenesis in the mouse, a review of its genetics and developmental features *in The Pigment Cell 1981.* University of Tokyo Press. Tokyo.

Quevedo, WC, Jr. and Holstein, TJ. 1992. Molecular genetics and the ontogeny of pigment patterns in mammals. *Pigment Cell Res.* **5:** 328-334.

Quevedo, WC, Jr. and Holstein, TJ. 1998. General Biology of Mammalian Pigmentation *in The Pigmentary System: Its Physiology and Pathophysiology.* Oxford University Press. New York

Quevedo, WC, Jr., Holstein, TJ, and Dyckman, J. 1994. Further observations on the nature of of the premature melanocyte death in the hair follicles of Light-Silver mice. *Pigment Cell Res.* **Supp 3:** 31-31.

Raible, DW and Eisen, JS. 1994. Restriction of neural crest cell fate in the trunk of the embryonic zebrafish. *Development* **120:** 495-503.

Rawls, JF, Mellgren, EM, and Johnson, SL. 2001. How the zebrafish gets its stripes. *Dev. Biol.* **240:** 301-314.

Rees, JL. 2000. The melanocortin 1 receptor (MC1R): more than just red hair. *Pigment Cell Res* **13:** 135-140.

Reith, AD, Rottapel, R, Giddens, E, Brady, C, Forrester, L *et al.* 1990. W mutant mice with mild or severe developmental defects contain distinct point mutations in the kinase domain of the c-kit receptor. *Genes Dev.* **4:** 390-400.

Rieder, S, Taourit, S, Mariat, D, Langlois, B, and Guerin, G. 2001. Mutations in the agouti (ASIP), the extension (MC1R), and the brown (TYRP1) loci and their association to coat color phenotypes in horses (Equus caballus). *Mamm. Genome* **12:** 450-455.

Ringholm, A, Fredriksson, R, Poliakova, N, Yan, YL, Postlethwait, JH *et al.* 2002. One melanocortin 4 and two melanocortin 5 receptors from zebrafish show remarkable conservation in structure and pharmacology. *J Neurochem.* **82:** 6-18.

Ringholm, A, Klovins, J, Fredriksson, R, Poliakova, N, Larson, ET *et al.* 2003. Presence of melanocortin (MC4) receptor in spiny dogfish suggests an ancient vertebrate origin of central melanocortin system. *Eur. J. Biochem.* **270:** 213-221.

Ritland, K, Newton, C, and Marshall, HD. 2001. Inheritance and population structure of the white-phased "Kermode" black bear. *Curr. Biol.* **11:** 1468-1472.

Robbins, LS, Nadeau, JH, Johnson, KR, Kelly, MA, Roselli-Rehfuss, L *et al.* 1993. Pigmentation phenotypes of variant extension locus alleles result from point mutations that alter MSH receptor function. *Cell* **72:** 827-834.

Robertson, HM. 1998. Two large families of chemoreceptor genes in the nematodes Caenorhabditis elegans and Caenorhabditis briggsae reveal extensive gene duplication, diversification, movement, and intron loss. *Genome Res.* **8:** 449-463.

Robertson, HM. 2000. The large srh family of chemoreceptor genes in Caenorhabditis nematodes reveals processes of genome evolution involving large duplications and deletions and intron gains and losses. *Genome Res.* **10:** 192-203.

Robinson-Rechavi, M, Marchand, O, Escriva, H, Bardet, PL, Zelus, D *et al.* 2001a. Euteleost fish genomes are characterized by expansion of gene families. *Genome Res.* **11:** 781-788.

Robinson-Rechavi, M, Marchand, O, Escriva, H, and Laudet, V. 2001b. An ancestral whole-genome duplication may not have been responsible for the abundance of duplicated fish genes. *Curr. Biol.* **11:** R458-R459.

Rodionov, VI, Gyoeva, FK, and Gelfand, VI. 1991. Kinesin is responsible for centrifugal movement of pigment granules in melanophores. *Proc. Natl. Acad. Sci. U. S. A* **88:** 4956-4960.

Rodionov, VI, Hope, AJ, Svitkina, TM, and Borisy, GG. 1998. Functional coordination of microtubule-based and actin-based motility in melanophores. *Curr. Biol.* **8:** 165-168.

Rodriguez, M, Beauverger, P, Naime, I, Rique, H, Ouvry, C *et al.* 2001. Cloning and molecular characterization of the novel human melanin-concentrating hormone receptor MCH2. *Mol. Pharmacol.* **60:** 632-639.

Rogers, SL, Tint, IS, Fanapour, PC, and Gelfand, VI. 1997. Regulated bidirectional motility of melanophore pigment granules along microtubules in vitro. *Proc. Natl. Acad. Sci. U. S. A* **94:** 3720-3725.

Roselli-Rehfuss, L, Mountjoy, KG, Robbins, LS, Mortrud, MT, Low, MJ *et al.* 1993. Identification of a receptor for gamma melanotropin and other proopiomelanocortin peptides in the hypothalamus and limbic system. *Proc. Natl. Acad. Sci. U. S. A* **90:** 8856-8860.

Rosenfeld, RD, Zeni, L, Welcher, AA, Narhi, LO, Hale, C *et al.* 1998. Biochemical, biophysical, and pharmacological characterization of bacterially expressed human agouti-related protein. *Biochemistry* **37:** 16041-16052.

Rossi, M, Choi, SJ, O'Shea, D, Miyoshi, T, Ghatei, MA *et al.* 1997. Melanin-concentrating hormone acutely stimulates feeding, but chronic administration has no effect on body weight. *Endocrinology* **138:** 351-355.

Rouquier, S, Taviaux, S, Trask, BJ, Brand-Arpon, V, van den, EG *et al.* 1998. Distribution of olfactory receptor genes in the human genome. *Nat. Genet.* **18:** 243-250.

Roy, SW, Fedorov, A, and Gilbert, W. 2003. Large-scale comparison of intron positions in mammalian genes shows intron loss but no gain. *Proc. Natl. Acad. Sci. U. S. A* **100:** 7158-7162.

Sailer, AW, Sano, H, Zeng, Z, McDonald, TP, Pan, J *et al.* 2001. Identification and characterization of a second melanin-concentrating hormone receptor, MCH-2R. *Proc. Natl. Acad. Sci. U. S A* **98:** 7564-7569.

Saito, Y, Nothacker, HP, Wang, Z, Lin, SH, Leslie, F *et al.* 1999. Molecular characterization of the melanin-concentrating-hormone receptor. *Nature* **400:** 265-269.

Sakai, C, Ollmann, M, Kobayashi, T, Abdel-Malek, Z, Muller, J *et al.* 1997. Modulation of murine melanocyte function in vitro by agouti signal protein. *EMBO J.* **16:** 3544-3552.

Sakurai, T, Ochiai, H, and Takeuchi, T. 1975. Ultrastructural change of melanosomes associated with agouti pattern formation in mouse hair. *Dev. Biol.* **47:** 466-471.

Salzet, M, Salzet-Raveillon, B, Cocquerelle, C, Verger-Bocquet, M, Pryor, SC *et al.* 1997. Leech immunocytes contain proopiomelanocortin: nitric oxide mediates hemolymph proopiomelanocortin processing. *J. Immunol.* **159:** 5400-5411.

Satake, N. 1980. Effect of methionine-enkephalin on xanthopore aggregation. *Peptides* **1:** 73-75.

Satoh, N and Jeffery, WR. 1995. Chasing tails in ascidians: developmental insights into the origin and evolution of chordates. *Trends Genet.* **11:** 354-359.

Schalin-Jantti, C, Valli-Jaakola, K, Oksanen, L, Martelin, E, Laitinen, K *et al.* 2003. Melanocortin-3-receptor gene variants in morbid obesity. *Int. J. Obes. Relat Metab Disord.* **27:** 70-74.

Schauer, E, Trautinger, F, Kock, A, Schwarz, A, Bhardwaj, R *et al.* 1994. Proopiomelanocortin-derived peptides are synthesized and released by human keratinocytes. *J. Clin. Invest* **93:** 2258-2262.

Scheer, A, Costa, T, Fanelli, F, De Benedetti, PG, Mhaouty-Kodja, S *et al.* 2000. Mutational analysis of the highly conserved arginine within the Glu/Asp- Arg-Tyr motif of the alpha(1b)-adrenergic receptor: effects on receptor isomerization and activation. *Mol. Pharmacol.* **57:** 219-231.

Scheer, A, Fanelli, F, Costa, T, De Benedetti, PG, and Cotecchia, S. 1997. The activation process of the alpha1B-adrenergic receptor: potential role of protonation and hydrophobicity of a highly conserved aspartate. *Proc. Natl. Acad. Sci. U. S. A* **94:** 808-813.

Schioth, HB, Chhajlani, V, Muceniece, R, Klusa, V, and Wikberg, JE. 1996a. Major pharmacological distinction of the ACTH receptor from other melanocortin receptors. *Life Sci.* **59:** 797-801.

Schioth, HB, Muceniece, R, and Wikberg, JE. 1996b. Characterisation of the melanocortin 4 receptor by radioligand binding. *Pharmacol. Toxicol.* **79:** 161-165.

Schioth, HB, Phillips, SR, Rudzish, R, Birch-MacHin, MA, Wikberg, JE *et al.* 1999. Loss of function mutations of the human melanocortin 1 receptor are common and are associated with red hair. *Biochem. Biophys. Res. Commun.* **260:** 488-491.

Schioth, HB, Raudsepp, T, Ringholm, A, Fredriksson, R, Takeuchi, S *et al.* 2003. Remarkable synteny conservation of melanocortin receptors in chicken, human, and other vertebrates. *Genomics* **81:** 504-509.

Schneider, TD and Stephens, RM. 1990. Sequence logos: a new way to display consensus sequences. *Nucleic Acids Res.* **18:** 6097-6100.

Schraermeyer, U and Heimann, K. 1999. Current understanding on the role of retinal pigment epithelium and its pigmentation. *Pigment Cell Res.* **12:** 219-236.

Schwalm, PA, Starrett, PH, and McDiarmid, RW. 1977. Infrared reflectance in leaf-sitting neotropical frogs. *Science* **196:** 1225-1227.

Seamon, KB, Padgett, W, and Daly, JW. 1981. Forskolin: unique diterpene activator of adenylate cyclase in membranes and in intact cells. *Proc. Natl. Acad. Sci. U. S. A* **78:** 3363-3367.

Searle, AG. 1968. An extension series in the mouse. *J. Hered.* **59:** 341-342.

Sebhat, IK, Martin, WJ, Ye, Z, Barakat, K, Mosley, RT *et al.* 2002. Design and pharmacology of N-[(3R)-1,2,3,4-tetrahydroisoquinolinium- 3-ylcarbonyl]-(1R)-1-(4-chlorobenzyl)- 2-[4-cyclohexyl-4-(1H-1,2,4-triazol- 1-ylmethyl)piperidin-1-yl]-2-oxo-ethylamine (1), a potent, selective, melanocortin subtype-4 receptor agonist. *J. Med. Chem.* **45:** 4589-4593.

Sharon, D, Glusman, G, Pilpel, Y, Khen, M, Gruetzner, F *et al.* 1999. Primate evolution of an olfactory receptor cluster: diversification by gene conversion and recent emergence of pseudogenes. *Genomics* **61:** 24-36.

Shibahara, S, Taguchi, H, Muller, RM, Shibata, K, Cohen, T *et al.* 1991. Structural organization of the pigment cell-specific gene located at the brown locus in mouse. Its promoter activity and alternatively spliced transcript. *J Biol. Chem.* **266:** 15895-15901.

Shimada, M, Tritos, NA, Lowell, BB, Flier, JS, and Maratos-Flier, E. 1998. Mice lacking melanin-concentrating hormone are hypophagic and lean. *Nature* **396:** 670-674.

Shimeld, SM and Holland, PW. 2000. Vertebrate innovations. *Proc. Natl. Acad. Sci. U. S. A* **97:** 4449-4452.

Shizume, K, Lerner, AB, and Fitzpatrick, TB. 1954. In vitro bioassay for the melanocyte stimulating hormone. *Endocrinology* **54:** 553-560.

Shutter, JR, Graham, M, Kinsey, AC, Scully, S, Luthy, R *et al.* 1997. Hypothalamic expression of ART, a novel gene related to agouti, is up- regulated in obese and diabetic mutant mice. *Genes Dev.* **11:** 593-602.

Silvers, WK. 1979. The Coat Colors of Mice: A model for mammalian gene action and interaction. Springer-Verlag. New York

Siracusa, LD. 1994. The agouti gene: turned on to yellow [published erratum appears in Trends Genet 1995 Mar;11(3):116]. *Trends Genet.* **10:** 423-428.

Skold, HN, Aspengren, S, and Wallin, M. 2002a. The cytoskeleton in fish melanophore melanosome positioning. *Microsc. Res. Tech.* **58:** 464-469.

Skold, HN, Norstrom, E, and Wallin, M. 2002b. Regulatory control of both microtubule- and actin-dependent fish melanosome movement. *Pigment Cell Res.* **15:** 357-366.

Smith, PE. 1916. Experimental ablation of the hypophysis in the frog embryo. *Science* **44:** 280-282.

Smoorenburg, GF, De Groot, JC, Hamers, FP, and Klis, SF. 1999. Protection and spontaneous recovery from cisplatin-induced hearing loss. *Ann. N. Y. Acad. Sci.* **884:** 192-210.

Sonnhammer, EL and Durbin, R. 1997. Analysis of protein domain families in Caenorhabditis elegans. *Genomics* **46:** 200-216.

Sower, SA and Kawauchi, H. 2001. Update: brain and pituitary hormones of lampreys. *Comp Biochem. Physiol B Biochem. Mol. Biol.* **129:** 291-302.

Sprague, J, Doerry, E, Douglas, S, and Westerfield, M. 2001. The Zebrafish Information Network (ZFIN): a resource for genetic, genomic and developmental research. *Nucleic Acids Res.* **29:** 87-90.

Stahl, FW. 1985. George Streisinger (December 27, 1927-August 11, 1984). *Genetics* **109:** 1-2.

Star, RA, Rajora, N, Huang, J, Stock, RC, Catania, A *et al.* 1995. Evidence of autocrine modulation of macrophage nitric oxide synthase by alpha-melanocyte-stimulating hormone. *Proc. Natl. Acad. Sci. U. S. A* **92:** 8016-8020.

Starowicz, K and Przewlocka, B. 2003. The role of melanocortins and their receptors in inflammatory processes, nerve regeneration and nociception. *Life Sci.* **73:** 823-847.

Steel, KP and Barkway, C. 1989. Another role for melanocytes: their importance for normal stria vascularis development in the mammalian inner ear. *Development* **107:** 453-463.

Stefano, GB, Salzet-Raveillon, B, and Salzet, M. 1999. Mytilus edulis hemolymph contains pro-opiomelanocortin: LPS and morphine stimulate differential processing. *Brain Res. Mol. Brain Res.* **63:** 340-350.

Strader, CD, Fong, TM, Tota, MR, Underwood, D, and Dixon, RA. 1994. Structure and function of G protein-coupled receptors. *Annu Rev Biochem.* **63:** 101-132.

Streisinger, G, Singer, F, Walker, C, Knauber, D, and Dower, N. 1986. Segregation analyses and gene-centromere distances in zebrafish. *Genetics* **112:** 311-319.

Streisinger, G, Walker, C, Dower, N, Knauber, D, and Singer, F. 1981. Production of clones of homozygous diploid zebra fish (Brachydanio rerio). *Nature* **291:** 293-296.

Sturm, RA, Teasdale, RD, and Box, NF. 2001. Human pigmentation genes: identification, structure and consequences of polymorphic variation. *Gene* **277:** 49-62.

Sugimoto, M, Uchida, N, and Hatayama, M. 2000. Apoptosis in skin pigment cells of the medaka, Oryzias latipes (Teleostei), during long-term chromatic adaptation: the role of sympathetic innervation. *Cell Tissue Res.* **301:** 205-216.

Summerton, J and Weller, D. 1997. Morpholino antisense oligomers: design, preparation, and properties. *Antisense Nucleic Acid Drug Dev.* **7:** 187-195.

Suzuki, I, Cone, RD, Im, S, Nordlund, J, and Abdel-Malek, ZA. 1996. Binding of melanotropic hormones to the melanocortin receptor MC1R on human melanocytes stimulates proliferation and melanogenesis. *Endocrinology* **137:** 1627-1633.

Suzuki, I, Tada, A, Ollmann, MM, Barsh, GS, Im, S *et al.* 1997. Agouti signaling protein inhibits melanogenesis and the response of human melanocytes to alpha-melanotropin. *J Invest Dermatol.* **108:** 838-842.

Svensson, SP, Norberg, T, Andersson, RG, Grundstrom, N, and Karlsson, JO. 1991. MCH-induced pigment aggregation in teleost melanophores is associated with a cAMP reduction. *Life Sci.* **48:** 2043-2046.

Sweet, HO, Brilliant, MH, Cook, SA, Johnson, KR, and Davisson, MT. 1998. A new allelic series for the underwhite gene on mouse chromosome 15. *J Hered.* **89:** 546-551.

Szabo, G, Gerald, AB, Pathak, MA, and Fitzpatrick, TB. 1969. Racial differences in the fate of melanosomes in human epidermis. *Nature* **222:** 1081-1082.

Takahashi, A, Amemiya, Y, Nozaki, M, Sower, SA, Joss, J *et al.* 1995a. Isolation and characterization of melanotropins from lamprey pituitary glands. *Int. J. Pept. Protein Res.* **46:** 197-204.

Takahashi, A, Amemiya, Y, Nozaki, M, Sower, SA, and Kawauchi, H. 2001. Evolutionary significance of proopiomelanocortin in agnatha and chondrichthyes. *Comp Biochem. Physiol B Biochem. Mol. Biol.* **129:** 283-289.

Takahashi, A, Amemiya, Y, Sakai, M, Yasuda, A, Suzuki, N *et al.* 1999. Occurrence of four MSHs in dogfish POMC and their immunomodulating effects. *Ann. N. Y. Acad. Sci.* **885:** 459-463.

Takahashi, A, Amemiya, Y, Sarashi, M, Sower, SA, and Kawauchi, H. 1995b. Melanotropin and corticotropin are encoded on two distinct genes in the lamprey, the earliest evolved extant vertebrate. *Biochem. Biophys. Res. Commun.* **213:** 490-498.

Takahashi, A, Yasuda, A, Sullivan, CV, and Kawauchi, H. 2003. Identification of proopiomelanocortin-related peptides in the rostral pars distalis of the pituitary in coelacanth: evolutional implications. *Gen. Comp Endocrinol.* **130:** 340-349.

Takayama, Y, Wada, C, Kawauchi, H, and Ono, M. 1989. Structures of two genes coding for melanin-concentrating hormone of chum salmon. *Gene* **80:** 65-73.

Takeuchi, S, Suzuki, H, Yabuuchi, M, and Takahashi, S. 1996. A possible involvement of melanocortin 1-receptor in regulating feather color pigmentation in the chicken. *Biochim. Biophys. Acta* **1308:** 164-168.

Takeuchi, T, Kobunai, T, and Yamamoto, H. 1989. Genetic control of signal transduction in mouse melanocytes. *J. Invest Dermatol.* **92:** 239S-242S.

Tamate, HB and Takeuchi, T. 1984. Action of the e locus of mice in the response of phaeomelanic hair follicles to alpha-melanocyte-stimulating hormone in vitro. *Science* **224:** 1241-1242.

Tammler, U, Quillan, JM, Lehmann, J, Sadee, W, and Kassack, MU. 2003. Design, synthesis, and biological evaluation of non-peptidic ligands at the Xenopus laevis skin-melanocortin receptor. *Eur. J. Med. Chem.* **38:** 481-493.

Tan, CP, McKee, KK, Weinberg, DH, MacNeil, T, Palyha, OC *et al.* 1999. Molecular analysis of a new splice variant of the human melanocortin-1 receptor. *FEBS Lett.* **451:** 137-141.

Tan, CP, Sano, H, Iwaasa, H, Pan, J, Sailer, AW *et al.* 2002. Melanin-concentrating hormone receptor subtypes 1 and 2: species- specific gene expression. *Genomics* **79:** 785-792.

Taylor, JD. 1969. The effects of intermedin on the ultrastructure of amphibian iridophores. *Gen. Comp Endocrinol.* **12:** 405-416.

Taylor, JD and Bagnara, JT. 1972. Dermal chromatophores. *Am. Zool.* **12:** 43-62.

Taylor, JS, Braasch, I, Frickey, T, Meyer, A, and Van de, PY. 2003. Genome duplication, a trait shared by 22000 species of ray-finned fish. *Genome Res.* **13:** 382-390.

Taylor, JS, Van de, PY, and Meyer, A. 2001. Revisiting recent challenges to the ancient fish-specific genome duplication hypothesis. *Curr. Biol.* **11:** R1005-R1008.

Theron, E, Hawkins, K, Bermingham, E, Ricklefs, RE, and Mundy, NI. 2001. The molecular basis of an avian plumage polymorphism in the wild: a melanocortin-1-receptor point mutation is perfectly associated with the melanic plumage morph of the bananaquit, Coereba flaveola. *Curr. Biol.* **11:** 550-557.

Thiboutot, D, Sivarajah, A, Gilliland, K, Cong, Z, and Clawson, G. 2000. The melanocortin 5 receptor is expressed in human sebaceous glands and rat preputial cells. *J Invest Dermatol.* **115:** 614-619.

Thody, AJ, Ridley, K, Penny, RJ, Chalmers, R, Fisher, C *et al.* 1983. MSH peptides are present in mammalian skin. *Peptides* **4:** 813-816.

Thompson, JD, Higgins, DG, and Gibson, TJ. 1994. CLUSTAL W: improving the sensitivity of progressive multiple sequence alignment through sequence weighting, position-specific gap penalties and weight matrix choice. *Nucleic Acids Res* **22:** 4673-4680.

Thompson, RC and Watson, SJ. 1990. Nucleotide sequence and tissue-specific expression of the rat melanin concentrating hormone gene. *DNA Cell Biol.* **9:** 637-645.

Toda, K, Pathak, MA, Parrish, JA, Fitzpatrick, TB, and Quevedo, WC, Jr. 1972. Alteration of racial differences in melanosome distribution in human epidermis after exposure to ultraviolet light. *Nat. New Biol.* **236:** 143-145.

Toumaniantz, G, Bittencourt, JC, and Nahon, JL. 1996. The rat melanin-concentrating hormone gene encodes an additional putative protein in a different reading frame. *Endocrinology* **137:** 4518-4521.

Treier, M and Rosenfeld, MG. 1996. The hypothalamic-pituitary axis: co-development of two organs. *Curr. Opin. Cell Biol.* **8:** 833-843.

Troemel, ER, Chou, JH, Dwyer, ND, Colbert, HA, and Bargmann, CI. 1995. Divergent seven transmembrane receptors are candidate chemosensory receptors in C. elegans. *Cell* **83:** 207-218.

Tsatmalia, M, Wakamatsu, K, Graham, AJ, and Thody, AJ. 1999. Skin POMC peptides. Their binding affinities and activation of the human MC1 receptor. *Ann. N. Y. Acad. Sci.* **885:** 466-469.

Tsukamoto, K, Jackson, IJ, Urabe, K, Montague, PM, and Hearing, VJ. 1992. A second tyrosinase-related protein, TRP-2, is a melanogenic enzyme termed DOPAchrome tautomerase. *EMBO J.* **11:** 519-526.

Turner, WA, Taylor, JD, and Tchen, TT. 1975. Melanosome formation in the goldfish: the role of multivesicular bodies. *J. Ultrastruct. Res.* **51:** 16-31.

Tymowska, J and Fischberg, M. 1973. Chromosome complements of the genus Xenopus. *Chromosoma* **44:** 335-342.

Uyeno, T and Smith, GR. 1972. Tetraploid origin of the karyotype of catostomid fishes. *Science* **175:** 644-646.

Vage, DI, Klungland, H, Lu, D, and Cone, RD. 1999. Molecular and pharmacological characterization of dominant black coat color in sheep. *Mamm. Genome* **10:** 39-43.

Vage, DI, Lu, D, Klungland, H, Lien, S, Adalsteinsson, S *et al.* 1997. A non-epistatic interaction of agouti and extension in the fox, Vulpes vulpes. *Nat. Genet.* **15:** 311-315.

Vaisse, C, Clement, K, Durand, E, Hercberg, S, Guy-Grand, B *et al.* 2000. Melanocortin-4 receptor mutations are a frequent and heterogeneous cause of morbid obesity. *J Clin. Invest* **106:** 253-262.

Valverde, P, Healy, E, Jackson, I, Rees, JL, and Thody, AJ. 1995. Variants of the melanocyte-stimulating hormone receptor gene are associated with red hair and fair skin in humans. *Nat. Genet.* **11:** 328-330.

Valverde, P, Healy, E, Sikkink, S, Haldane, F, Thody, AJ *et al.* 1996. The Asp84Glu variant of the melanocortin 1 receptor (MC1R) is associated with melanoma. *Hum. Mol. Genet.* **5:** 1663-1666.

Van der Ploeg, LH, Martin, WJ, Howard, AD, Nargund, RP, Austin, CP *et al.* 2002. A role for the melanocortin 4 receptor in sexual function. *Proc. Natl. Acad. Sci. U. S. A* **99:** 11381-11386.

Vaughan, JM, Fischer, WH, Hoeger, C, Rivier, J, and Vale, W. 1989. Characterization of melanin-concentrating hormone from rat hypothalamus. *Endocrinology* **125:** 1660-1665.

Venkatesh, B and Brenner, S. 1997. Genomic structure and sequence of the pufferfish (Fugu rubripes) growth hormone-encoding gene: a comparative analysis of teleost growth hormone genes. *Gene* **187:** 211-215.

Venkatesh, B, Ning, Y, and Brenner, S. 1999. Late changes in spliceosomal introns define clades in vertebrate evolution. *Proc. Natl. Acad. Sci. U. S. A* **96:** 10267-10271.

Venter, JC, Adams, MD, Myers, EW, Li, PW, Mural, RJ *et al.* 2001. The sequence of the human genome. *Science* **291:** 1304-1351.

Verlaet, M, Adamantidis, A, Coumans, B, Chanas, G, Zorzi, W *et al.* 2002. Human immune cells express ppMCH mRNA and functional MCHR1 receptor. *FEBS Lett.* **527:** 205-210.

Vink, T, Hinney, A, van Elburg, AA, van Goozen, SH, Sandkuijl, LA *et al.* 2001. Association between an agouti-related protein gene polymorphism and anorexia nervosa. *Mol. Psychiatry* **6:** 325-328.

von Lehmann, E. 1973. Coat Colour genetics of the tobacco-mouse (*Mus poschiavinus Fatio*). *Mouse News Lett.* **48:** 23-23.

Vrieling, H, Duhl, DM, Millar, SE, Miller, KA, and Barsh, GS. 1994. Differences in dorsal and ventral pigmentation result from regional expression of the mouse agouti gene. *Proc. Natl. Acad. Sci. U. S. A* **91:** 5667-5671.

Wakamatsu, K, Graham, A, Cook, D, and Thody, AJ. 1997. Characterisation of ACTH peptides in human skin and their activation of the melanocortin-1 receptor. *Pigment Cell Res.* **10:** 288-297.

Wang, S, Behan, J, O'Neill, K, Weig, B, Fried, S *et al.* 2001. Identification and pharmacological characterization of a novel human melanin-concentrating hormone receptor, mch-r2. *J. Biol. Chem.* **276:** 34664-34670.

Waring, H. 1963. Colour Change Mechanisms of Cold-Blooded Vertebrates. Academic Press. New York.

Weber, A and Clark, AJ. 1994. Mutations of the ACTH receptor gene are only one cause of familial glucocorticoid deficiency. *Hum. Mol. Genet.* **3:** 585-588.

Westbroek, W, Lambert, J, De Schepper, S, Kleta, R, Van Nieuwpoort, F *et al.* 2003. IL-28 Melanosome transport: an update. *Pigment Cell Res.* **16:** 586-

Westerfield, M. 2000. The Zebrafish Book. A guide for the laboratory use of zebrafish. University of Oregon Press. Eugene

Wilson, BD, Ollmann, MM, Kang, L, Stoffel, M, Bell, GI *et al.* 1995. Structure and function of ASP, the human homolog of the mouse agouti gene. *Hum. Mol. Genet.* **4:** 223-230.

Winder, AJ, Wittbjer, A, Rosengren, E, and Rorsman, H. 1993. Fibroblasts expressing mouse c locus tyrosinase produce an authentic enzyme and synthesize phaeomelanin. *J. Cell Sci.* **104 (Pt 2):** 467-475.

Wittkopp, PJ, Carroll, SB, and Kopp, A. 2003. Evolution in black and white: genetic control of pigment patterns in Drosophila. *Trends Genet.* **19:** 495-504.

Wolff, K and Konrad, K. 1971. Melanin pigmentation: an in vivo model for studies of melanosome kinetics within keratinocytes. *Science* **174:** 1034-1035.

Xia, Y and Wikberg, JE. 1996. Localization of ACTH receptor mRNA by in situ hybridization in mouse adrenal gland. *Cell Tissue Res* **286:** 63-68.

Yamamoto, O and Bhawan, J. 1994. Three modes of melanosome transfers in Caucasian facial skin: hypothesis based on an ultrastructural study. *Pigment Cell Res.* **7:** 158-169.

Yang, YK, Ollmann, MM, Wilson, BD, Dickinson, C, Yamada, T *et al.* 1997. Effects of recombinant agouti-signaling protein on melanocortin action. *Mol. Endocrinol.* **11:** 274-280.

Yeo, GS, Farooqi, IS, Aminian, S, Halsall, DJ, Stanhope, RG *et al.* 1998. A frameshift mutation in MC4R associated with dominantly inherited human obesity. *Nat. Genet.* **20:** 111-112.

Yeo, GS, Lank, EJ, Farooqi, IS, Keogh, J, Challis, BG *et al.* 2003. Mutations in the human melanocortin-4 receptor gene associated with severe familial obesity disrupts receptor function through multiple molecular mechanisms. *Hum. Mol. Genet.* **12:** 561-574.

Yokoyama, T, Silversides, DW, Waymire, KG, Kwon, BS, Takeuchi, T *et al.* 1990. Conserved cysteine to serine mutation in tyrosinase is responsible for the classical albino mutation in laboratory mice. *Nucleic Acids Res.* **18:** 7293-7298.

Zdarsky, E, Favor, J, and Jackson, IJ. 1990. The molecular basis of brown, an old mouse mutation, and of an induced revertant to wild type. *Genetics* **126:** 443-449.

Zdobnov, EM, von Mering, C, Letunic, I, Torrents, D, Suyama, M *et al.* 2002. Comparative genome and proteome analysis of Anopheles gambiae and Drosophila melanogaster. *Science* **298:** 149-159.

Zhang, MQ. 1998. Statistical features of human exons and their flanking regions. *Hum. Mol. Genet.* **7:** 919-932.

Zhang, X and Firestein, S. 2002. The olfactory receptor gene superfamily of the mouse. *Nat. Neurosci.* **5:** 124-133.

Zhou, BK, Kobayashi, T, Donatien, PD, Bennett, DC, Hearing, VJ *et al.* 1994. Identification of a melanosomal matrix protein encoded by the murine si (silver) locus using "organelle scanning". *Proc. Natl. Acad. Sci. U. S A* **91:** 7076-7080.

Zhu, Y and Thomas, P. 1998. Effects of light on plasma somatolactin levels in red drum (Sciaenops ocellatus). *Gen. Comp Endocrinol.* **111:** 76-82.

Ziegler, I. 2003. The Pteridine Pathway in Zebrafish: Regulation and Specification during the Determination of Neural Crest Cell-Fate. *Pigment Cell Res.* **16:** 172-182.

Zsebo, KM, Williams, DA, Geissler, EN, Broudy, VC, Martin, FH *et al.* 1990. Stem cell factor is encoded at the Sl locus of the mouse and is the ligand for the c-kit tyrosine kinase receptor. *Cell* **63:** 213-224.

Zuasti, A, Ferrer, C, Aroca, P, and Solano, F. 1990. Distribution of extracutaneous melanin pigment in Sparus auratus, Mugil cephalus, and Dicertranchus labrax (Pisces, Teleostei). *Pigment Cell Res.* **3:** 126-131.

Zuasti, A, Jara, JR, Ferrer, C, and Solano, F. 1989. Occurrence of melanin granules and melanosynthesis in the kidney of Sparus auratus. *Pigment Cell Res.* **2:** 93-99.

Appendix A

Publications describing data from this thesis

Sequence Characterization of Teleost Fish Melanocortin Receptors

DARREN W. LOGAN, ROBERT J. BRYSON-RICHARDSON, MARTIN S. TAYLOR,[a] PETER CURRIE, AND IAN J. JACKSON

MRC Human Genetics Unit, Western General Hospital, Crewe Road, Edinburgh EH4 2XU, United Kingdom

ABSTRACT: **Zebrafish are an excellent model system for studying the function of melanocortins in developmental and physiological processes, not least because there are a considerable number of mutant lines in which pigment patterns are affected. The behavior of fish melanophores is influenced by α-melanocyte-stimulating hormone (α-MSH) and melanin-concentrating hormone (MCH). We have used a rapid assay for α-MSH and MCH function using melanophores present on single zebrafish scales. By *in silico* analysis, we have identified the full complement of melanocortin receptors in both zebrafish and the pufferfish, *Fugu*. Mammals have five such receptors. Zebrafish have six melanocortin receptors, including two MC5R orthologues, whereas *Fugu*, lacking MC3R, has only four. We have confirmed the sequences of these 10 genes and show the comparison of the amino acid sequences of the encoded proteins with the orthologous receptor in other vertebrates.**

KEYWORDS: **zebrafish; *Fugu*; MC1R; MC2R; MC3R; MC4R; MC5R**

INTRODUCTION

The existence of what we now call melanocortins was first indicated almost 90 years ago with the demonstration that the pituitary played a role in regulation of pigmentation of frogs and tadpoles.[1,2] Much of the early work on melanocyte-stimulating hormone (MSH) was conducted on cold-blooded vertebrates (poikilotherms) and the regulation of pigmentation in amphibia and fish in particular.[3]

In recent years, with the identification by molecular cloning of the family of five melanocortin receptors in mammals, attention has turned to mammalian systems. The realization that melanocortins regulate a wide range of physiological processes, from feeding behavior to sexual function, has greatly increased interest and scientific activity in the area. Poikilotherm melanocortin function has not received a corresponding increase in study. However, the zebrafish, *Danio rerio*, is an excellent model organism for which several powerful genetic tools have been developed that allow the

Address for correspondence: Ian J. Jackson, MRC Human Genetics Unit, Western General Hospital, Crewe Road, Edinburgh, EH4 2XU, United Kingdom. Voice: 44-0-131-567-8409; fax: 44-0-131-343-2620.

ian.jackson@hgu.mrc.ac.uk

[a]Present address: Wellcome Trust Centre for Human Genetics, Oxford University, Oxford, United Kingdom.

Ann. N.Y. Acad. Sci. 994: 319–330 (2003).

identification and study of genes and mutations affecting a range of developmental and physiological processes.[4,5] There is clearly an opportunity to study the genetics of melanocortin function in fish using these resources. What role, if any, melanocortins may play in the behavior of zebrafish is largely unknown. What is known, however, is that the primary effect of MSH on pigment cells, melanophores, is different from that seen in mammals and birds. Genetic and cell biology studies on a range of mammals show that α-MSH acts through the melanocortin receptor-1 (MC1R) on melanocytes and causes the cells to produce dark eumelanin. Lack of signaling through MC1R results in the synthesis of pheomelanin, which is a red or yellow pigment depending on the species and genetic background (reviewed in Jackson[6]). In contrast, action of MSH on the melanophores of fish and amphibia causes a rapid redistribution of melanin granules in the cell, so that intracellular pigment changes from being concentrated around the nucleus to being dispersed throughout the cell.[7] This movement gives the appearance of the cell itself rapidly changing shape and expanding. In poikilotherms, yellow and red pigments are generated in separate cell types (termed xanthophores and erythrophores). There is some evidence that α-MSH can promote a similar cellular redistribution of these pigments in some species, although these are more difficult to study than melanophores. It will be interesting to elucidate the basis for the difference in response of these homologous cell types in cold-blooded versus warm-blooded vertebrates.

Availability of large-scale DNA sequence information from two fish species, zebrafish and the pufferfish *Fugu rubripes*, has facilitated gene identification in these animals.[8] We have used these sequence resources to identify what we believe to be the entire repertoire of melanocortin receptors in the two species.

A SINGLE CELL ASSAY FOR MSH FUNCTION IN ZEBRAFISH

The dark melanophores of zebrafish scales can be readily visualized under bright-field optics. The effect of addition of factors to the medium on melanin dispersion and aggregation can be seen by the apparent shape change of the cells. Sequential collection of digital images over a period of several minutes can generate a movie of the pigment movement within the cell. Use of appropriate image intensity thresholds allows the area occupied by the pigment granules to be rapidly calculated for each time point. Addition of α-MSH, or analogues such as NDP-MSH, to the medium causes a rapid dispersion of pigment (in FIG. 1, 50% maximal dispersion is seen in 215 s). The reverse effect is seen by addition of the peptide hormone melanin concentrating hormone (MCH) (in this example, 50% maximal aggregation in 165 s). Although MCH is a functional antagonist of MSH, it probably signals through a different receptor and inhibits MSH action downstream.[20] The regulation of pigment distribution by MSH/MCH is augmented in some poikilotherms by other control mechanisms. For example, melatonin, a hormone produced in the pineal gland in response to photoperiod, can also aggregate pigment in zebrafish melanophores as can the neurotransmitter noradrenaline.

FIGURE 1 illustrates a single cell assay for NDP-MSH and MCH. More reliable data can be obtained by averaging the intensity across the whole field. This is of course analogous to the frog melanophore assay that has been widely used to assay MSH receptor agonist and antagonist activity but one in which individual cell behavior can be observed and recorded.[9,10]

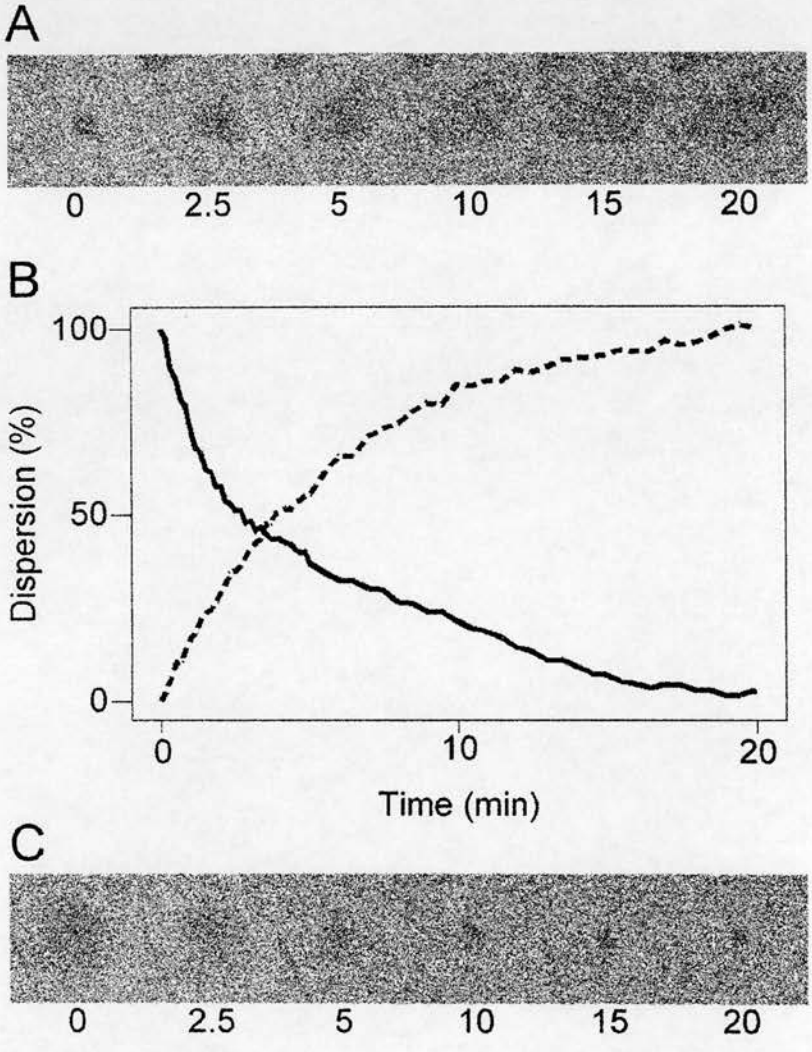

FIGURE 1. Zebrafish melanophore dispersion assay. (**A**) A single dorsal fin scale melanophore after addition of 10 μM NDP-MSH. Noradrenaline (10 μM) was added before the assay to aggregate the melanophores. Images were collected at the times indicated in minutes. (**B**) Percentage dispersion or aggregation over time after addition of 10 μM NDP-MSH (*broken line*) or 10 μM MCH (*solid line*), as in **A** and **C**. Sixty-one images of a field containing several melanophores were collected automatically at 10-s intervals for the first 5 min and 30-s intervals thereafter. Image intensity threshold was set to permit automatic measurement of the area occupied by melanin granules. (**C**) A single dorsal fin scale melanophore after addition of 10 μM MCH. Images were collected at the times indicated in minutes.

IDENTIFICATION OF THE FISH MELANOCORTIN RECEPTOR GENE FAMILY

Extensive DNA sequence data are available for zebrafish and for two pufferfish species, *Fugu rubripes* and *Tetraodon nigroviridis*.[8] (Resources at: www.sanger.ac.uk/Projects/D_rerio/, http://genome.jgi-psf.org/fugu6/fugu6.home.html and www.genoscope.cns.fr/externe/tetraodon/). We used TBLASTN analysis of whole genome shotgun databases of each species using the chicken MC1R amino acid sequence (accession number D78272). Positive sequence reads were assembled using Phred/Phrap[11] and then extended by iterated BLAST searching and assembly. The assembled DNA sequences were confirmed by PCR and resequencing. The process was facilitated by the fact that all previously described melanocortin receptor genes lacked introns in the coding region, and indeed we found that most of the fish orthologues also had only a single coding exon. However, we identified two exceptions. The pufferfish (but not the zebrafish) orthologues of *MC2R* and *MC5R* contained one and three introns, respectively. The single intron of *MC2R* is in the same position (same codon and phase) as the second intron of *MC5R* .[20]

Orthologues of each of the mammalian melanocortin receptor gene family members were clearly identified in fish. We found that MC1R, MC2R, and MC4R have single orthologues in both zebrafish and pufferfish. We identified an orthologue of MC3R in zebrafish but could not find MC3R in pufferfish.

The *Fugu* genome sequence is not yet complete. However, the coverage afforded by the available sequence data is estimated to be 5.6-fold,[8] giving a greater than 95% chance of a read containing the desired sequence. Furthermore, an extensive data set consisting of 6-fold coverage of DNA sequence from the closely related pufferfish *Tetraodon nigroviridis* also lacks sequence corresponding to an *MC3R* orthologue. The probability that these combined databases lack the *MC3R* gene by chance is less than 0.002, and it is highly likely that MC3R is absent from the pufferfish lineage. The pufferfish genome sequence databases contain a single *MC5R* gene. In contrast, and as has been reported previously, zebrafish have two MC5R orthologues.[12]

PROTEIN SEQUENCE COMPARISONS

FIGURES 2 to 6 show the protein sequences of the five melanocortin receptor family members from human, mouse, chicken, *Fugu*, and zebrafish. We examined the sequences for significant differences between the fish receptor sequences and those of other vertebrates.

A good deal of information is known about the effects of both natural and site-directed mutations in MC1R.[13–16] Almost all the amino acid residues known to be important from these mutations are conserved in the fish MC1R. One major difference is in the third intracellular loop. Replacement of certain residues in this loop, between amino acids 226 and 238, by alanine result in loss of coupling of the human

FIGURE 2. Alignment of the amino acid sequences of MC1R from human (Hs), mouse (Mm), chicken (Gg), *Fugu* (Fr), and zebrafish (Dr). Amino acids identical in all sequences are shaded *black*, those different in one species are *dark gray*, and those different in two species are *light gray*.

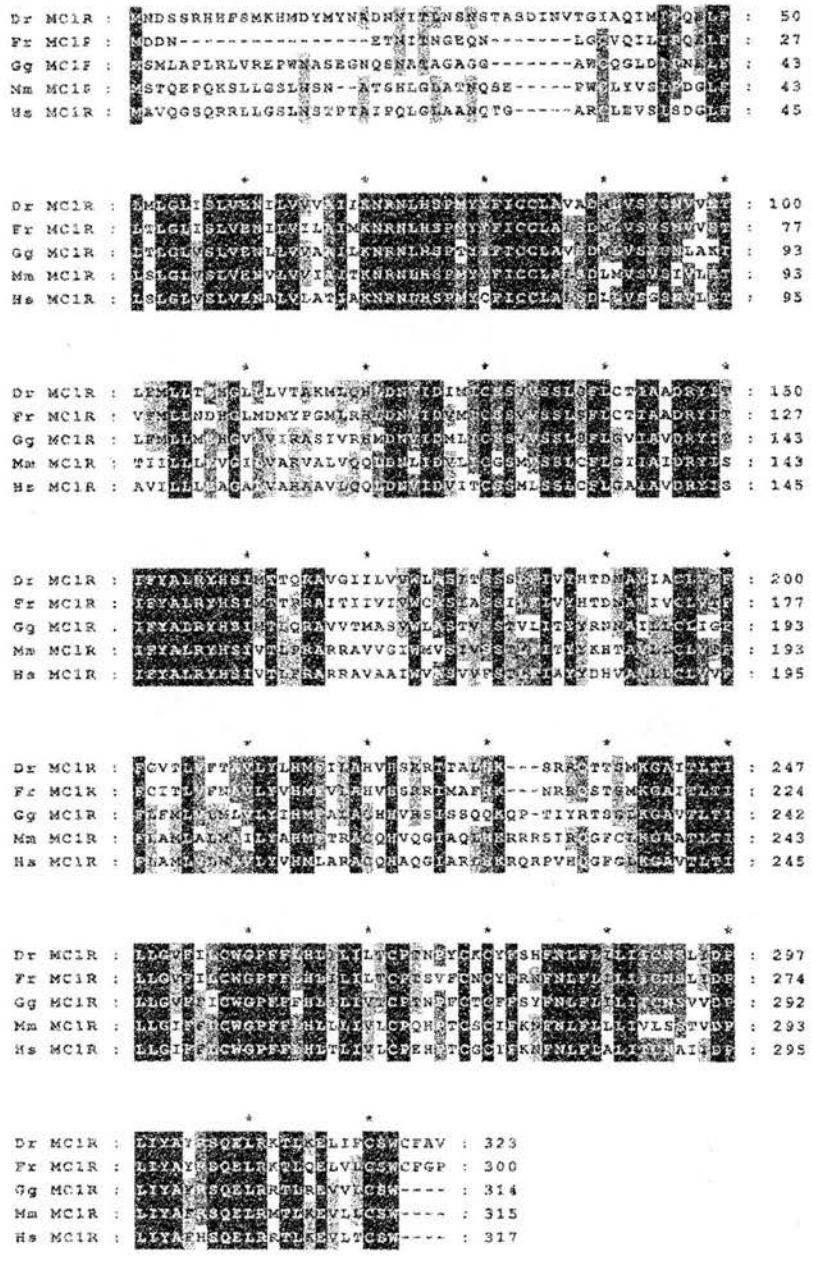

FIGURE 2. *See previous page for legend.*

receptor to G proteins.[16] The region containing these important residues is not well conserved in fish. It is three amino acids shorter than the mammalian receptor, and although K226 and K238 flanking the domain are conserved in the fish MC1R, the intervening amino acids are quite different. The sequence is, however, very basic in charge, similar to the region in humans (and the poorly conserved mouse region). It will be informative to determine whether specific amino acid residues are required for coupling, or whether it is the basic nature that is important.

Another difference between the fish and most other MC1R proteins is at the C terminus. Most G protein–coupled receptors have a cysteine residue in the intracellular, C-terminal tail. This has been shown to be modified by palmitoylation and to be essential for function in some receptors.[17] Previously described MC1R proteins contain the C-terminal tripeptide motif CSW, and truncation of the C-terminal 12 amino acids of MC1R appears to cause loss of receptor function.[18] Although both fish MC1R proteins have the CSW motif, it is not directly at the end of the protein. Both have an additional four residues, including another cysteine residue, which may be an alternative target for palmitoylation.

Human MC3R and MC4R have differential affinity for α–MSH, MC3R having approximately 30-fold higher affinity. Domain swapping between the two receptors indicates that the third extracellular loop is responsible for the difference.[19] Mutation of individual amino acids shows that residues 267 and 268 of MC4R are particularly important, especially Y268. Where MC4R has Phe-Tyr at these positions, MC3R has Leu-Ile. Substitution of the MC4R residues with those found in MC3R at these positions makes the affinity for α-MSH of the resulting receptor similar to that of MC3R. The equivalent positions in fish MC4R are Leu-Met, much more like MC3R. In particular, the bulky Tyr268 is thought to impair binding of α-MSH. In fish MC4R, this is a more compact Met. We suggest based on these comparisons that fish MC4R has a higher affinity for α-MSH than their mammalian and bird counterparts. This may have removed selective pressure to retain MC3R and thus may have allowed loss of *Fugu MC3R*.

The predicted protein sequences of the receptors can be placed in a phylogenetic tree that indicates their likely evolutionary relationship to each other. FIGURE 7 is such a tree in which the branch lengths are an indication of the divergence. Almost all the branch points have a high degree of statistical support, based on bootstrap replicates from 1,000 repetitions. The two exceptions are the branch points where MC1R splits from the rest of the gene family and where MC5R and MC3R split after separating from MC4R. If these nodes are discounted, then it appears that the original melanocortin receptor gene may have split into three members initially, causing the ancestors of MC1R, MC2R, and a single ancestor for the rest of the family. This single ancestor may then have split into three, which became MC3R, MC4R, and MC5R. However, all five family members must have been established before the teleost fish lineage separated from the rest of the vertebrate lineage. Because the melanocortin receptor family is not found in any invertebrate genome, including the urochordate *Ciona intestinalis* (data not shown), it is likely that the family emerged soon after vertebrate evolution and there were several rounds of gene duplication and divergence early on in vertebrate evolution.

The tree indicates that the pair of *MC5R* genes of zebrafish probably duplicated before the separation of the zebrafish and *Fugu* lineages, and the second *MC5R* was subsequently lost from *Fugu*. It is possible, however, that the duplication occurred

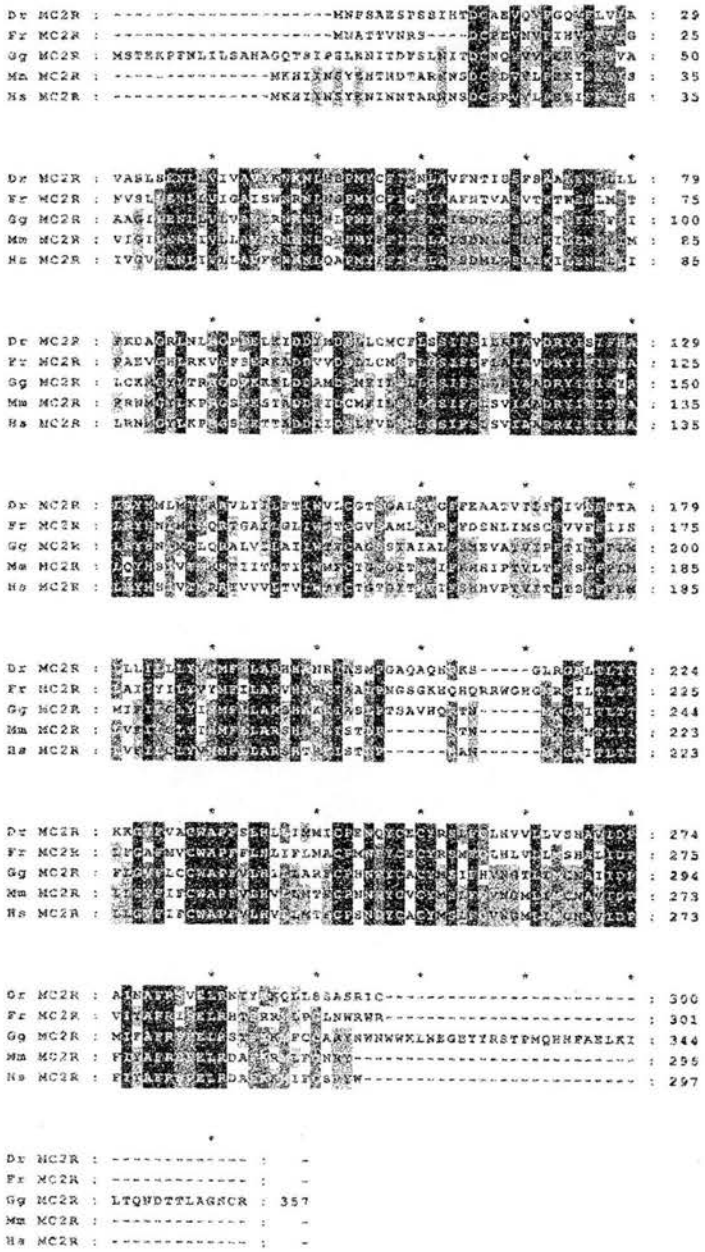

FIGURE 3. Alignment of the amino acid sequences of MC2R. Species and shading are as in FIGURE 2.

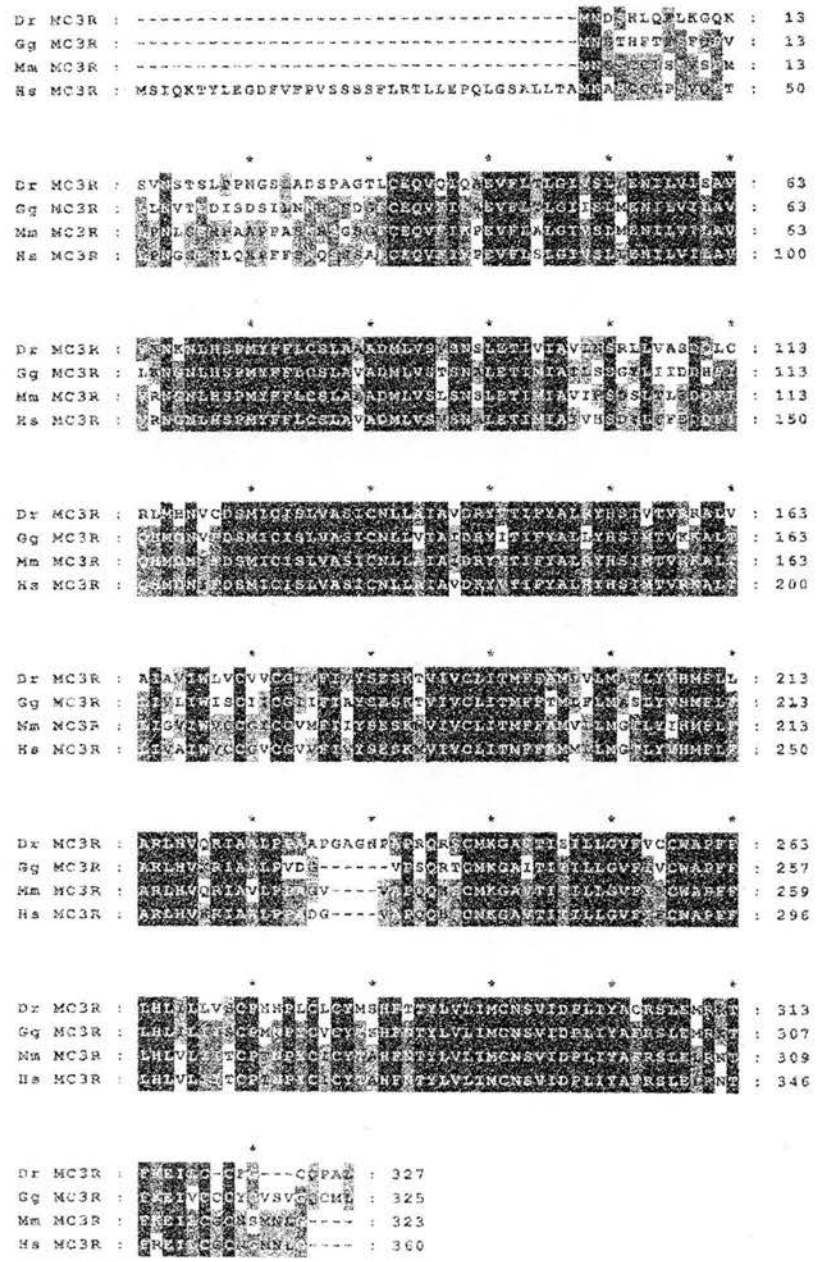

FIGURE 4. Alignment of the amino acid sequences of MC3R. Species and shading are as in FIGURE 2, except that *Fugu* is absent.

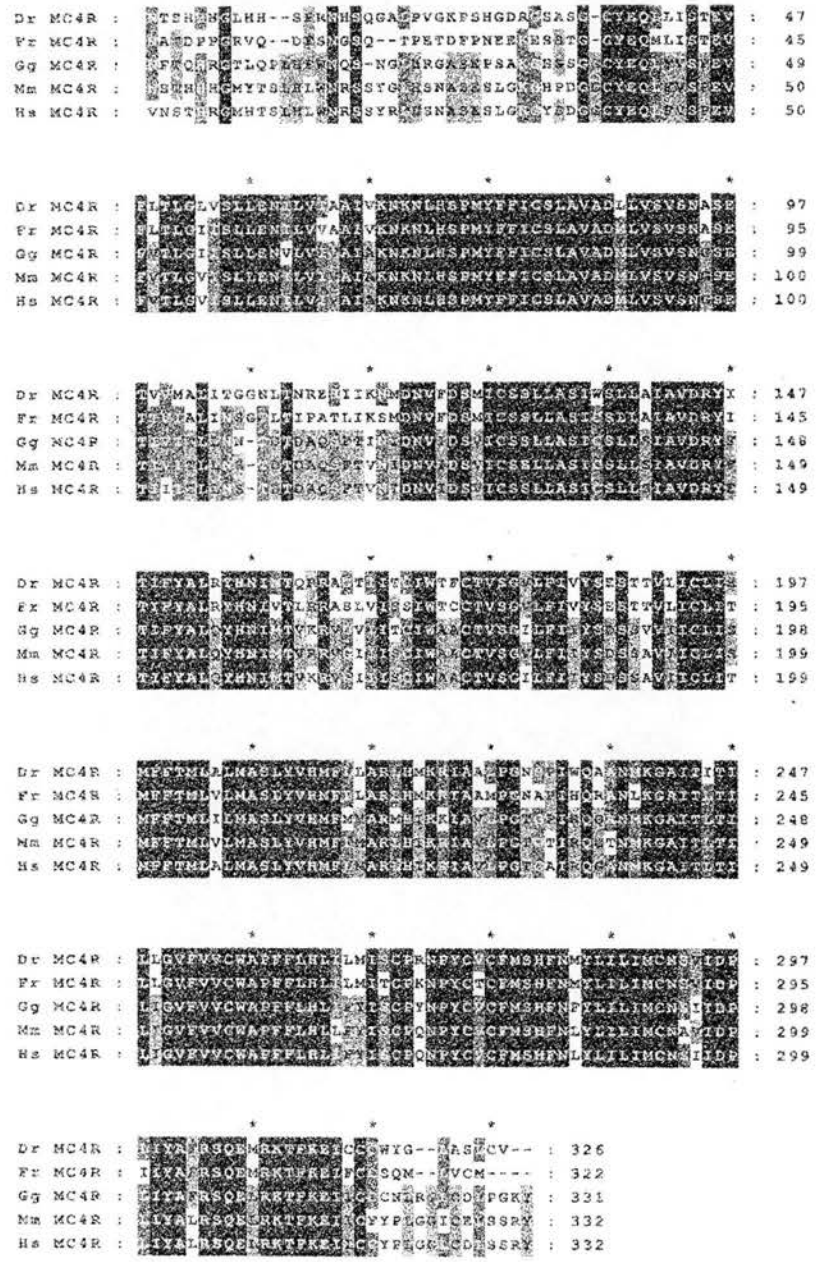

FIGURE 5. Alignment of the amino acid sequences of MC4R. Species and shading are as in FIGURE 2.

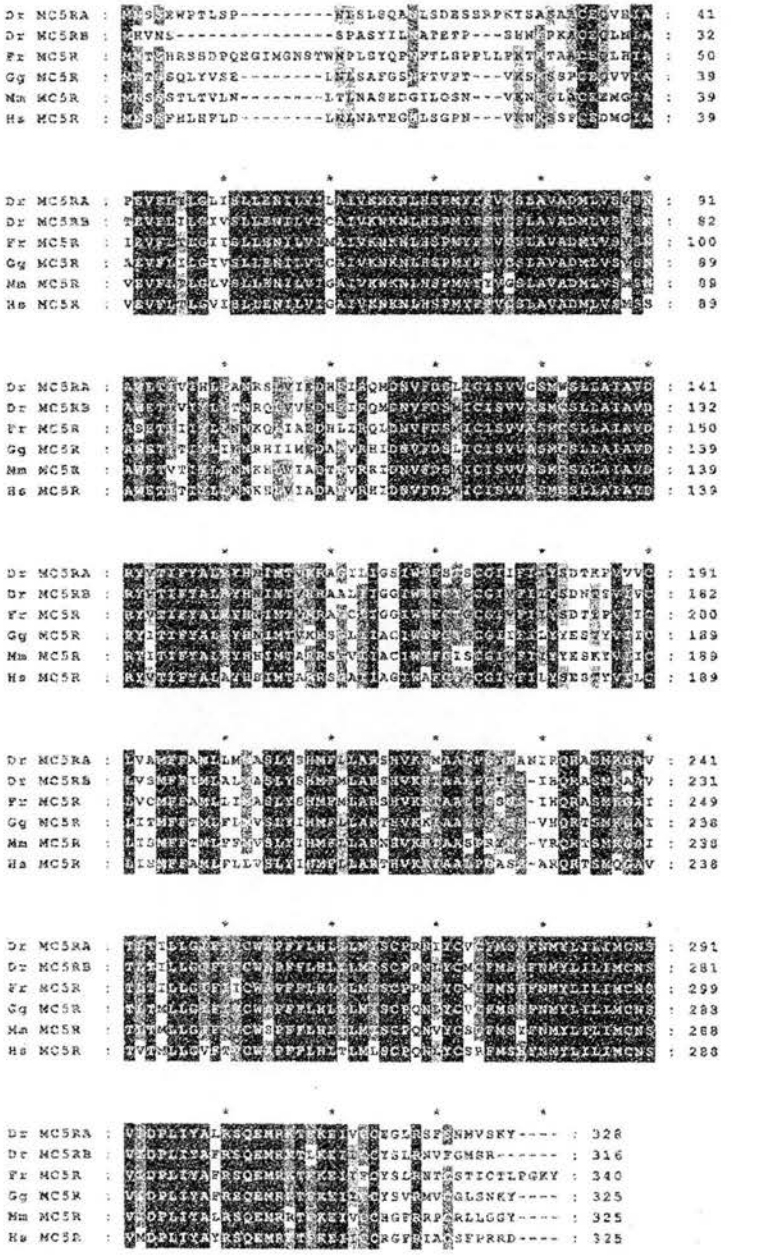

FIGURE 6. Alignment of the amino acid sequences of MC5R. Species and shading are as in FIGURE 2. Note that zebrafish has two MC5R orthologues.

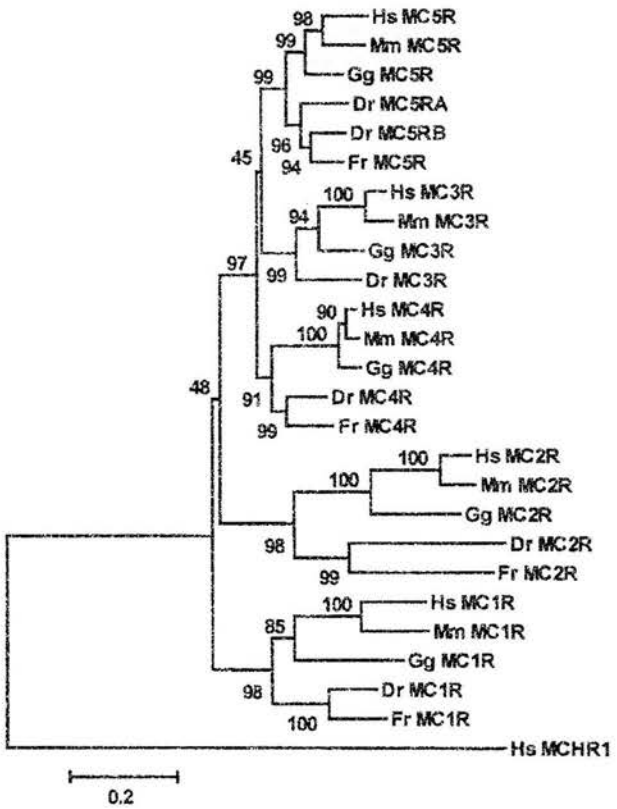

FIGURE 7. Neighbor-joining tree of melanocortin receptor protein sequences as in FIGURES 2 to 6. The tree uses a Poisson correction distance between two sequences where the proportion of amino acid sites at which the two differ is corrected for multiple substitutions at the same site. Thus, the distance is equal to $-\ln(1 - p)$, where p is the proportion of sites that differ. The number at each node is the percentage of bootstrap replicates of the node from 1,000 repetitions.

specifically in the zebrafish lineage, and that *MC5RA* has been freed of evolutionary constraint and thus has evolved more rapidly.

SUMMARY

In summary, the extensive sequence data now available for zebrafish and *Fugu* have allowed us to identify *in silico* the entire family of melanocortin receptors for these species. We have confirmed the sequences of these 10 genes. These are a good foundation for the investigation of melanocortin function in cold-blooded vertebrates.

REFERENCES

1. ALLEN, B.M. 1916. Extirpation of the hypophysis and thyroid glands of *Rana pipiens*. Science **44:** 755–757.
2. SMITH, P.E. 1916. Experimental ablation of the hypophysis in the frog embryo. Science **44:** 280–282.
3. BAGNARA, J.T. 1998. Comparative anatomy and physiology of pigment cells in non-mammalian tissues. *In* The Pigmentary System: Physiology and Pathophysiology. J.J. Nordlund, R.E. Boissy, V.J. Hearing, R.A. King, and J-P. Ortonne, Eds.: 9–40. Oxford University Press. New York.
4. KELSH, R.N., M. BRAND, Y.J. JIANG, *et al.* 1996. Zebrafish pigmentation mutations and the processes of neural crest development. Development **123:** 369–389.
5. ODENTHAL, J., K. ROSSNAGEL, P. HAFFTER, *et al.* 1996. Mutations affecting xanthophore pigmentation in the zebrafish, *Danio rerio*. Development **123:** 391–398.
6. JACKSON, I.J. 1997. Homologous pigmentation mutations in human, mouse and other model organisms. Hum. Mol. Genet. **6:** 1613–1624.
7. FUJII, R. 2000. The regulation of motile activity in fish chromatophores. Pigm. Cell Res. **13:** 300–319.
8. APARICIO, S., J. CHAPMAN, E. STUPKA, *et al.* 2002. Whole-genome shotgun assembly and analysis of the genome of *Fugu rubripes*. Science **297:** 1301–1310.
9. POTENZA, M.N. & M.R. LERNER. 1992. A rapid quantitative bioassay for evaluating the effects of ligands upon receptors that modulate cAMP levels in a melanophore cell line. Pigm. Cell Res. **5:** 372–378.
10. JAYAWICKREME, C.K., J.M. QUILLAN, G.F. GRAMINSKI, *et al.* 1994. Discovery and structure-function analysis of alpha-melanocyte-stimulating hormone antagonists. J. Biol. Chem. **269:** 29846–29854.
11. EWING, B. & P. GREEN. 1998. Base-calling of automated sequencer traces using phred. II. Error probabilities. Genome Res. **8:** 186–194.
12. RINGHOLM, A., R. FREDRIKSSON, N. POLIAKOVA, *et al.* 2002. One melanocortin 4 and two melanocortin 5 receptors from zebrafish show remarkable conservation in structure and pharmacology. J. Neurochem. **82:** 6–18.
13. VALVERDE, P., E. HEALY, I.J. JACKSON, *et al.* 1995. Variants of the melanocyte-stimulating hormone receptor gene are associated with red hair and fair skin in humans. Nat. Genet. **11:** 328–330.
14. STURM R.A., R.D. TEASDALE & N.F. BOX. 2001. Human pigmentation genes: identification, structure and consequences of polymorphic variation. Gene **277:** 49–62.
15. HEALY, E., S.A. JORDAN, P.S. BUDD, *et al.* 2001. Functional variation of MC1R alleles from red-haired individuals. Hum. Mol. Genet. **10:** 2397–2402.
16. FRANDBERG, P.A., M. DOUFEXIS, S. KAPAS, *et al.* 1998. Amino acid residues in third intracellular loop of melanocortin 1 receptor are involved in G-protein coupling. Biochem. Mol. Biol. Int. **46:** 913–922.
17. MORELLO, J.P. & M. BOUVIER. 1996. Palmitoylation: a post-translational modification that regulates signalling from G-protein coupled receptors. Biochem. Cell Biol. **74:** 449–457.
18. NEWTON, J.E., A.L. WILKIE, L. HE, *et al.* 2000. Melanocortin 1 receptor variation in the domestic dog. Mamm. Genome **11:** 24–30.
19. OOSTEROM, J., W.A. NIJENHUIS, W.M. SCHAAPER, *et al.* 1999. Conformation of the core sequence in melanocortin peptides directs selectivity for the melanocortin MC3 and MC4 receptors J. Biol. Chem. **274:** 16853–16860.
20. LOGAN, D.W., R.J. BRYSON-RICHARDSON, K.E. PAGAN, *et al.* 2003. The structure and evolution of the melanocortin and MCH receptors in fish and mammals. Genomics **81:** 184–191.

Available online at www.sciencedirect.com
SCIENCE DIRECT®
ACADEMIC PRESS
GENOMICS
Genomics 81 (2003) 184–191
www.elsevier.com/locate/ygeno

The structure and evolution of the melanocortin and MCH receptors in fish and mammals

Darren W. Logan,[a] Robert J. Bryson-Richardson,[a] Kayleene E. Pagán,[a,b] Martin S. Taylor,[a,1] Peter D. Currie,[a] and Ian J. Jackson[a,*]

[a] *MRC Human Genetics Unit, Western General Hospital, Edinburgh, EH4 2XU, UK*
[b] *University of Puerto Rico, Department of Biochemistry, PO Box 365067, San Juan, Puerto Rico*

Abstract

Zebrafish are an excellent genetic model system for studying developmental and physiological processes. Pigment patterns in zebrafish are affected by mutations in three types of chromatophores. The behavior of these cells is influenced by alpha-melanocyte-stimulating hormone (αMSH) and melanin-concentrating hormone (MCH). Mammals have five αMSH receptors (melanocortin receptors) and one or two MCH receptors. We have identified the full complement of melanocortin and MCH receptors in both zebrafish and the pufferfish, *Fugu*. Zebrafish have six melanocortin receptors, including two MC5R orthologues, while *Fugu*, lacking MC3R, has only four. We also demonstrate that *Fugu* and zebrafish have two and three MCHR genes, respectively. MC2R and MC5R are physically linked in all species examined. Unlike other species, we find the *Fugu* genes contain introns, one of which is in a conserved location and is probably ancestral. We also detail the differential expression of the zebrafish genes throughout development.

Keywords: Zebrafish; *Danio rerio*; *Fugu rubripes*; Melanocortin receptor; Melanin-concentrating hormone receptor; Molecular evolution; Pigmentation

Introduction

The melanocortin receptors are a family of G-protein coupled, 7-transmembrane receptors that respond to small peptide hormones derived from pre-opiomelanocortin (POMC). Humans and mice have five such receptors, MC1R to MC5R [1–4], that have diverse functions in a range of tissues, as shown by analysis of mutant phenotypes [5–14]. Members of the melanocortin receptor family share between 39% and 61% amino acid identity within a species and it appears that MC3, MC4, and MC5 receptors are more similar to each other than they are to MC1R or MC2R (reviewed in [4]).

MC1R is expressed on the surface of mammalian melanocytes and, signalling through this receptor by α-melanocyte-simulating hormone (αMSH), regulates the synthesis of dark eumelanin. Lack of signalling by inactivation of the ligand or receptor or by binding of an inverse agonist, agouti signalling protein (ASP), results in synthesis of red or yellow phaeomelanin [5–7,14,15]. MC2R is the receptor for adrenocorticotrophic hormone (ACTH), another derivative of POMC, and is essential for normal adrenal function [8,16]. Two receptors, MC3R and MC4R, are expressed in a number of different locations in the brain, including the hypothalamus where activation by αMSH and other POMC peptides regulates feeding behavior, energy metabolism, and the partitioning of fuel stores into fat [9,10,17]. The agouti-related protein, AGRP, can antagonize activation of these receptors in the brain in an analogous fashion to the action of ASP on MC1R [18]. The fifth member of the family, MC5R, is expressed in a range of tissues including the skin, where it is required for the synthesis of sebum by the sebaceous glands [13].

The role of αMSH on pigmentation was first identified in lower vertebrates [19,20], although the cellular response to the hormone is different from the response by mammalian melanocytes. Other physiological functions of melanocort-

* Corresponding author. Fax: +44-0-131-467-8456.
E-mail address: ian.jackson@hgu.mrc.ac.uk (I.J. Jackson).
[1] Present address: Wellcome Trust Centre for Human Genetics, Oxford University, Oxford, OX3 7BN, UK.

0888-7543/03/$ – see front matter © 2003 Elsevier Science (USA). All rights reserved.
doi:10.1016/S0888-7543(02)00037-X

ins in these animals are largely unexplored, and differences or similarities with mammals will be instructive. The zebrafish, *Danio rerio*, is an excellent vertebrate model organism in which many mutations have been identified in developmental and physiological systems [21,22]. In particular, there are a large number of mutations affecting zebrafish pigmentation [23,24]. Besides being an important model in biological research, a smaller genome and extensive regions of conserved synteny with the human genome mean it is a useful system for comparative genomics [25].

In contrast to mammals, most fish, reptiles, and amphibia have a highly complex and sophisticated pigmentary system. There are at least six distinct pigment cell types identified in fish, although zebrafish have only three: iridophores, xanthophores, and melanophores. It is now known that αMSH exerts an influence on each of these cell types, but its role in melanophore function has been best characterized. Fish melanophores respond to αMSH by rapidly dispersing aggregated, peri-nuclear localized melanin pigment throughout the cell body and into the dendritic extensions (reviewed in [26]).

The reverse function, by which dispersed pigment is induced to aggregate, is due to the action of a second peptide hormone, a melanin-concentrating hormone (MCH), on melanophores [27,28]. The rapid redistribution of pigment allows the zebrafish to adapt its color to the general tone of its background. This dynamic response to αMSH and MCH is quite different from that of mammalian melanocytes. When administered in vivo to mice, αMSH produces a change in melanin biosynthesis while MCH appears to have no effect, because mice lacking MCH or its receptor are normally pigmented [29–31]. However, recent work has shown that a MCH receptor is expressed on human melanocytes and MCH can antagonize the action of αMSH on these cells in culture [32]. Therefore, in humans at least, MCH may have a role in melanogenic regulation. MCH has been observed in the brains of lampreys, elasmobranches, amphibians, mammals, and birds where it appears to have a neuromodulatory role without melanin-aggregating activity (reviewed in [33]). The hormone has a single receptor in mice (which we will term MCHR1, but has been identified as GPR24 previously) expressed in the hypothalamus and the mutation of which results in mice that are lean yet hyperphagic. The lean phenotype is due to a combination of hyperactivity and increased metabolic rate [31]. Humans have two MCH receptors, which we will term MCHR1 and MCHR2 [34–37]. Other mammals also have two MCH receptors, although rats have only one. Whether rodents have lost one of the receptors or other mammals have duplicated their is not known, although the presence of a pseudogene in rabbits and guinea pigs may suggest that the rodent lineage has lost one functional copy [38]. It is not known if MCH plays a role in feeding and metabolism of fish, but a full comprehension of fish melanocortin function will require an understanding of MCH function both on melanophores and in the brain.

Recently three melanocortin receptors have been identified in zebrafish, one of which appears to be orthologous to MC4R, and two orthologues of MC5R [39]. We wanted to analyze zebrafish melanocortin receptors, not only to gain an understanding of the evolution of this receptor family, but also to provide the foundation for work on the genetics of a variety of physiological systems.

A second fish model organism, the pufferfish, *Fugu rubripes*, has been well studied as a genomic model. It has a genome approximately eight-fold smaller than mammals, but has been shown to encode a similar gene repertoire to other vertebrates [40]. The compact nature of the *Fugu* genome is reflected by a dearth of interspersed repetitive elements, and small intronic and intergenic distances relative to other vertebrates. The teleost lineage that includes both *Fugu* and zebrafish diverged from the mammalian lineage approximately 450 million years ago. Analysis of the melanocortin receptors in *Fugu* provides an additional, well diverged set of sequences for evolutionary comparison. The compact genome may also permit identification of genomic relationships more readily than other larger genomes.

We have identified the full repetoire of melanocortin and MCH receptor genes from both zebrafish and *Fugu*, which will provide a basis for further studies. Additionally, the sequences provide useful information about the evolution of these gene families.

Results and discussion

Sequence analysis of the melanocortin receptor gene family

Extensive DNA sequence data are available for both zebrafish and *Fugu*. We screened shotgun sequence databases of both genomes using iterated BLAST analysis and assembly. The assembled DNA sequences were confirmed by PCR and resequencing.

We identified six melanocortin receptors in zebrafish and four in *Fugu*. Table 1 shows the degree of amino acid identity between the fish and human receptors. To examine the evolutionary relationship of the receptors, the phylogeny of the proteins was examined. A tree summarizing the phylogenetic relationship of zebrafish and *Fugu* receptors, along with the five receptors from human, mouse, and chicken, is shown in Fig. 1. The tree shows that the two zebrafish sequences identified previously as two MC5R sequences indeed appear to be a recently duplicated pair of receptors in the fish lineage. It is interesting that the duplication seems to have occurred before zebrafish and *Fugu* diverged, yet we identify only one *MC5R* sequence in *Fugu*. The *Fugu* genome sequence is not yet complete. However, the coverage afforded by the available sequence data is estimated to be 5.6× [40], giving a >95% chance of a read containing the sequence. Furthermore, an extensive dataset

Table 1
Protein sequence identities of melanocortin receptors

	Hs MC1R	Hs MC2R	Hs MC3R	Hs MC4R	Hs MC5R
Dr MC1R	53.7	40.3	43.9	50.4	50.1
Dr MC2R	36.9	45.5	36.9	41.4	39.1
Dr MC3R	48.6	42.5	63.5	58.1	61.8
Dr MC4R	48.2	44.4	55.1	68.7	62.8
Dr MC5RA	45.2	43.3	55.4	62.8	69.0
Dr MC5RB	45.4	44.3	54.1	61.9	69.5
Fr MC1R	53.0	39.9	42.5	47.7	46.5
Fr MC2R	38.0	46.6	35.3	42.0	38.8
Fr MC4R	49.5	46.0	57.7	65.2	62.2
Fr MC5R	44.3	42.4	52.4	62.9	67.7

Note. Human (Hs) full-length sequences are compared with zebrafish (Dr) and *Fugu* (Fr) sequences. The best human match to each fish gene is indicated by a shaded box. The values are percent identity.

consisting of a 6× coverage of DNA sequence from a closely related pufferfish, *Tetraodon nigroviridis*, also contains a sequence from only a single *MC5R* gene. The probability that these combined databases lack the second *MC5R* gene by chance is less than 0.002, and it is highly probable that MC5RB is absent from the *Fugu* lineage. The phylogenetic relationship of the zebrafish and pufferfish MC5R proteins suggests that the genes duplicated early in fish evolution, and that one of them (orthologous to zebrafish *mc5ra*) was lost in the pufferfish lineage. However, it is possible that the duplication occurred after the zebrafish/pufferfish lineages separated, and selective constraints on one of the pair may have relaxed, allowing it to diverge rapidly.

Both zebrafish and *Fugu* contain single orthologues of *MC1R, MC2R*, and *MC4R, MC3R*, however, appears to be absent from *Fugu*. Again, consideration must be given to the depth of sequence coverage of the *Fugu* data, but we also do not identify *MC3R* gene sequences in the *Tetraodon* sequence trace dataset. It is probable that the pufferfish has lost the *MC3R* gene, which must be considered when the role of MC3R in fish and other vertebrates is studied.

We believe that we have identified the complete melanocortin receptor family from both euteleost (pufferfish) and otocephela (zebrafish) lineages of teleost fish. These will provide the underpinning for further work on the physiological function of these genes in zebrafish.

Genome structure and chromosomal location of melanocortin receptors

The chromosomal location of the six zebrafish genes was determined by analysis of radiation hybrids. Each gene was successfully mapped in duplicate with a LOD score >11 and a net LOD difference >6, indicating significant linkage. The six genes localize to five linkage groups (Table 2). In most cases the zebrafish orthologues were located in regions that showed conserved synteny with both their mouse and human counterparts. For example, zebrafish *mc1r* maps to linkage group (LG) 18, very close to cytochrome oxidase subunit 4 (*cox4*), and distal of tyrosine aminotransferase (*tat*). Orthologous genes are found in the same order within a 15 Mb region on human chromosome 16 and mouse chromosome 8.

The duplicated *mc5r* genes, as has been previously reported, are both linked to genes that are also duplicated in the zebrafish genome, which have themselves a single orthologue in both the mouse and humans, but none of these genes are synthenic with *MC5R* in the mouse, and human genomes [39]. However, radiation hybrid mapping of zebrafish *mc2r* places it within 5 cR (approx. 740 kb) of *mc5ra*. This gene pair has also been closely linked by genetic mapping in the mouse to chromosome 18 and by cytogenetic analysis on human chromosomes to 18p11.2. It appears that the duplicated chromosomal segment that contains the zebrafish *mc5r* paralogue has subsequently lost *mc2r*.

We examined the genome sequence assemblies for both the mouse and human, and found that the *MC2R* and *MC5R* genes are very closely linked, and are convergently transcribed from opposite DNA strands (Fig. 2). They are separated by approximately 40 kb (human) and 67 kb (mouse). We made an assembly of *Fugu* genomic sequence around *MC5R* and *MC2R* and found that in this organism they were also convergently transcribed, and the termination codons of the two coding regions were separated by only a few

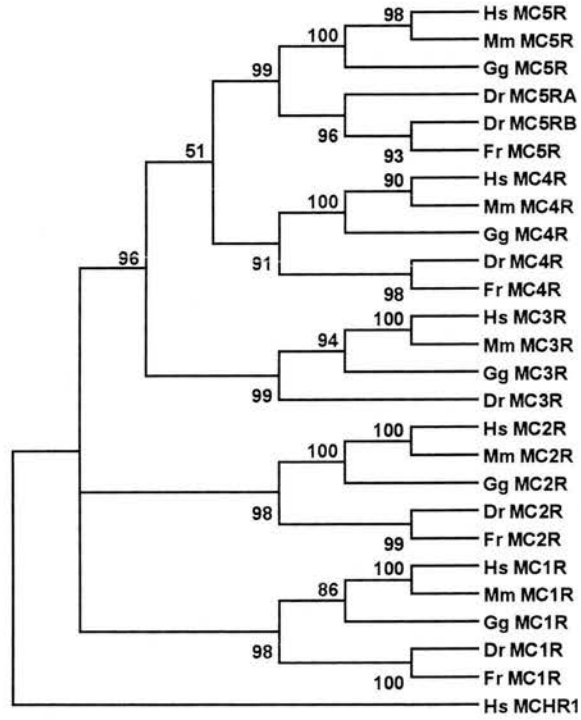

Fig. 1. Phylogenetic analysis of the melanocortin receptor protein family by neighbor-joining. The receptor sequences from human (Hs), mouse (Mm), chicken (Gg), zebrafish (Dr), and *Fugu* (Fr) are shown. The numbers at the nodes indicate percentage of 1000 bootstrap replicates. The human melanin-concentrating hormone receptor was used to root the tree.

Table 2
Chromosomal position of melanocortin and MCH receptors

Gene	Mouse map	Human map	Zebrafish map
MC1R	8, 123.5 Mb	16q24.3, 91.8 Mb	18, 318.1 cR
MC2R	18, 68.7 Mb	18p11.2, 14.0 Mb	16, 313.0 cR
MC3R	2, 173.5 Mb	20q13.2, 54.6 Mb	8, 320.4 cR
MC4R	18, 67.2 Mb	18q22, 57.9 Mb	2, 365.8 cR
MC5RA	18, 68.7 Mb	18p11.2, 13.9 Mb	16, 308.0 cR
MC5RB	—	—	19, 174.2 cR
MCHR1A	15, 82 Mb	22q13.3, 37.7 Mb	6, 291.5 cR
MCHR1B	—	—	3, 184.4 cR
MCHR2	—	6q16.3, 100.2 Mb	20, 340.0 cR

Note. Human cytogenetic locations are shown for each gene followed by position on the Ensembl genomic assembly. Mouse gene locations are shown as chromosome number followed by position on genomic assembly. Zebrafish locations are represented by linkage group followed by position in centiRays (cR). Mammals have only a single orthologue of MC5R and MCHR1; the table does not imply a closer relationship to either zebrafish homologue.

kilobases. The intergenic distance between this gene pair has thus been compressed by 20–30 fold relative to mammals (Fig. 2).

None of the full-length melanocortin receptor genes thus far reported, of which there are more than 40, have introns in the coding region, with the possible exception of a spliced variant of human *MC1R* that is of unknown significance. However, when we examined the assembled sequences from *Fugu*, we find that two of the melanocortin receptor genes, *MC2R* and *MC5R*, do contain introns. The *Fugu MC5R* gene contains three introns in the coding region (situated 156, 263, and 452 nucleotides downstream from the ATG initiator). *Fugu MC2R* contains only one intron (after nucleotide 353), but is in an identical position and phase relative to coding sequence as *MC5R* intron 3 (Fig. 2). There have been previous reports of intronless genes the *Fugu* orthologues of which contain introns, and of additional introns present in *Fugu* [40,41]. This example, however, gives a useful insight into the evolution of the melanocortin receptor genes. *MC2R* and *MC5R* are among the most diverged in the gene family, and yet share a common intron in *Fugu* that is absent from the other family members in this species and from all family members currently identified in other species. It seems probable that this is an ancient intron that has been lost from virtually all members of the gene family, but has been retained in two in *Fugu*. Extensive examination of other GPCR genes in several species, including invertebrates, reveals an intron in the same phase in the equivalent codon in a small but phyogenetically diverse number of these genes, which suggests that the intron is very ancient, but has been lost in the majority of GPCR genes (manuscript in preparation).

Expression of melanocortin receptor genes in zebrafish

In order to assess whether all the zebrafish genes we have identified are transcribed, we performed a reverse-transcription-PCR on mRNA from different stages of zebrafish development and from adults. Fig. 3 shows that all of the genes are transcribed. Transcripts from all genes except *mc2r* can be detected at the earliest time point of two days, although *mc4r* has a particularly weak signal.

Throughout larval development *mc1r* is expressed. It is during this period that fish melanophores differentiate and develop. In adult fish this gene has a lower apparent signal from head RNA than body. This observation is consistent with the smaller number of melanophores found in the head, although quantitative RT-PCR would be required to confirm this difference. The pair of *mc5r* genes do not have the same pattern of expression as each other. It appears that *mc5ra* is largely embryo-specific; no transcript can be detected from the adult head and the adult body gives a relatively weak signal. By contrast, *mc5rb* has a robust signal in both embryonic and adult RNA.

MC3R and MC4R in mammals have exclusively postnatal functions. However, the level of transcription of their orthologues in zebrafish appears much higher in embryonic RNA than in adults. Nevertheless, transcription of both genes in adult fish appears to be higher in the head than the body tissues, which is consistent with these receptors having a role similar to their mammalian function in the hypothalamus.

A more restricted pattern of transcription is shown in *mc2r*. In mammals the gene expression is found only in the adrenals, and we see in zebrafish that the gene is expressed only from the fifth day of development, and is found only in the torso and not the head of adults.

All six zebrafish melanocortin receptor genes are transcribed during embryonic development. Zebrafish offer a

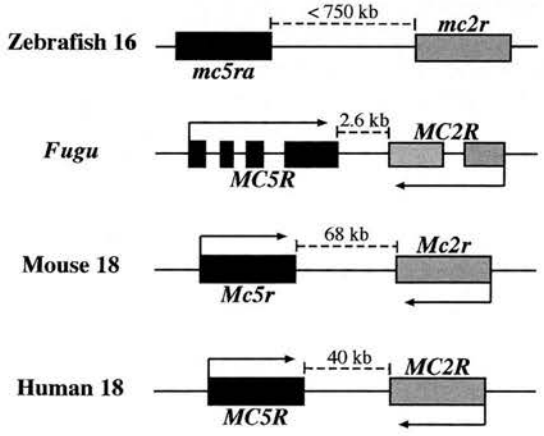

Fig. 2. The conserved linkage relationship between *MC5R* and *MC2R* throughout vertebrate evolution. Species are indicated along with chromosome number where they are known. The direction of *MC5R* (black boxes) and *MC2R* (grey boxes) transcription is indicated by arrows. Each box represents a single exon and the lines between boxes of the same color indicate introns. The single intron in *Fugu MC2R* is in an identical position and phase to the third intron in *Fugu MC5R*. Intergenic distances (dashed lines) are calculated from assembly of genomic sequence, except in zebrafish where it is estimated from centiRay distance by radiation hybrid mapping.

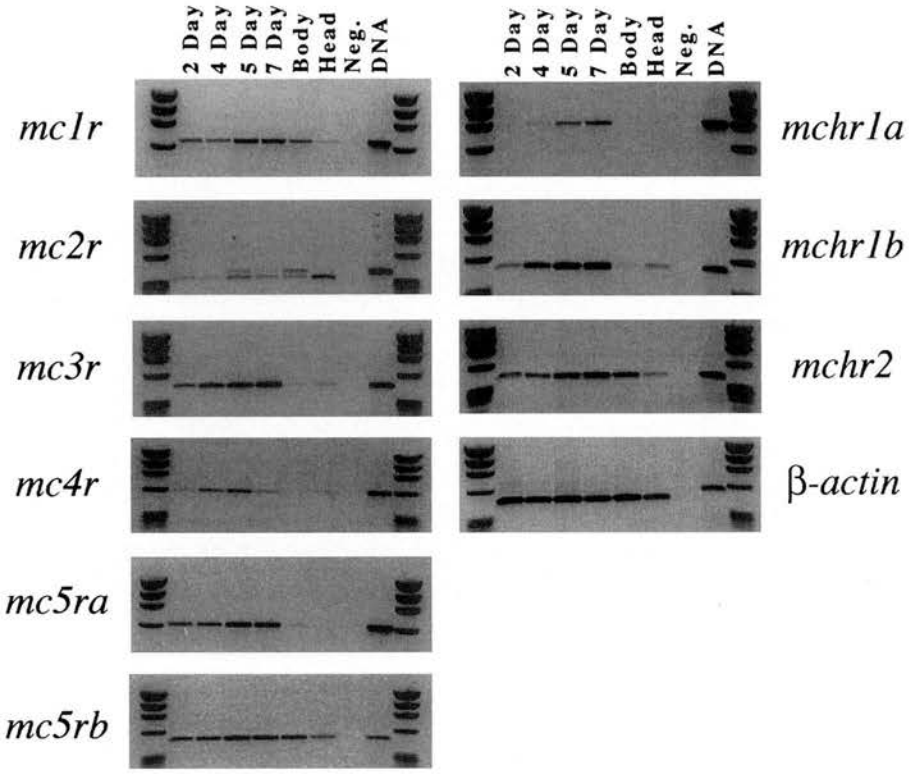

Fig. 3. RT-PCR-assayed expression of MC and MCH receptors in zebrafish embryos and adult tissue. The embryo ages, tissue origin, and controls (neg. = negative control, DNA = positive control) are indicated at the top of the figure with the genes denoted at either side. Zebrafish *b-actin* was used as a control for RNA quality. Zebrafish *mc2r* amplification shows a second, smaller, PCR fragment in all RNA samples. Sequencing indicates that this is a PCR artifact unrelated to *mc2r* sequence.

valuable and relatively simple method to establish gene function. Injection of chemically modified oligonucleotides (termed "morpholinos" after the morpholine moeity that replaces ribose), complementary to the translation initiation codon and upstream sequence of an mRNA into fertilized zebrafish eggs, prevents translation of the targeted mRNA [42]. Morpholino inhibition may be a useful method of determining melanocortin receptor function during embryonic development.

Identification of melanin-concentrating hormone receptor genes in fish

The pigmentary function of αMSH in teleost fish, presumably mediated by MC1R, is functionally antagonized by the action of MCH (reviewed in [26]). It is also possible, by analogy with the mammalian energy homeostasis pathways, that the function of MC3R and MC4R may be balanced by action of MCH in the central nervous system. We therefore identified MCHR sequences from zebrafish and *Fugu* in the whole genome shotgun datasets. *Fugu* contains two *MCHR* genes and zebrafish has three.

A neighbor-joining tree showing the relationship between the fish sequences and representative mammalian MCHR protein sequences is in Fig. 4. It is evident from this analysis that an initial duplication of the *MCHR* gene occurred before the divergence of the vertebrate lineage, and both zebrafish and *Fugu* have clear *MCHR1* and *MCHR2* orthologues. The presence of a single MCH-receptor gene in rodents must be due to the loss of one of these genes (*MCHR2*) after the separation of rodents from the other mammals. The third *MCHR* gene in zebrafish is a late duplication in fish evolution. It appears that a duplication of *MCHR1* has taken place after the divergence of euteleosts

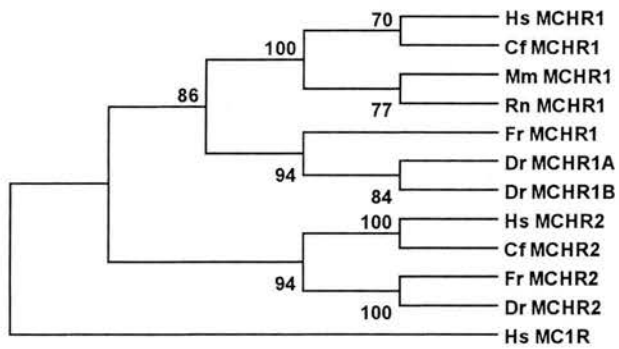

Fig. 4. Phylogenetic analysis of the melanin-concentrating hormone receptor protein family by neighbor-joining. The receptor family from human (Hs), mouse (Mm), domestic dog (Cf), rat (Rn), zebrafish (Dr), and *Fugu* (Fr) are shown. The numbers at the nodes indicate the percentage of 1000 bootstrap replicates. The human melanocortin 1 receptor was used to root the tree.

from the zebrafish lineage, although a loss from the former lineage is possible.

We determined the map location of the three zebrafish genes by an analysis of a radiation hybrid panel (Table 2). Zebrafish *mchr1b* maps to LG3, which is near to the zebrafish orthologues of human ribosomal protein L3 (*RPL3*), mini-chromosome maintenance deficient 5 (*MCM5*), and eukaryotic translation initiation factor 3 subunit 7 (*EIF3S7*). These genes, and human *MCHR1*, are all located within a 5.2 Mb region of human chromosome 22. We identified no synteny between human *MCHR* and zebrafish *mchr1a*. However, we did find other similarly duplicated genes: *mchr1a* maps slightly distal of netrin 1a (*ntn1a*) on LG6, while *mchr1b* maps slightly distal of netrin 1 (*ntn1*). We searched the *Fugu* genome assembly for netrin 1 orthologues and could identify only one, providing further evidence that this particular genomic segment may have duplicated after the divergence of the *Fugu* and zebrafish. Fig. 3 shows the expression of the zebrafish *mchr* genes. It appears that *mchr1a* is embryo specific. No transcripts are detected in adult tissues, and only weak expression can be found in embryos younger than five days. Expression of *mchr1b* appears stronger than *mchr1a*, can be detected in adults and young embryos, and is strongest between days four and seven of development. The expression of *mchr2* seems to parallel that of *mc1r*; it can be detected from the earliest time point, throughout the period of larval melanophore function, and appears to be expressed at higher levels in the adult torso compared to the head. Therefore, based solely on RT-PCR-determined expression patterns, we would suggest that either MCHR1B or MCHR2 is likely to be the receptor that acts to regulate pigmentation.

The presence and possible functional overlap of three MCH receptor genes in zebrafish may make the analysis of their function by mutagenesis or by morpholino-inhibition problematic. The role of a single mouse melanin-concentrating hormone receptor in feeding behavior is well established [31]. In humans, however, the action of MCHR2 remains to be elucidated and there is some evidence that MCHR1 can regulate pigmentation in addition to its neuromodulatory role [32]. We believe further characterization of the spatial expression of the zebrafish receptors may provide an insight into the full extent of MCH function in both humans and fish.

Summary

Our data suggest that the entire MC and MCH receptor families were present before the divergence of the ray-finned fish from the tetrapod lineage approximately 450 million years ago. Using the same search methods in the genomes of the invertebrates *Anopheles gambiae, Drosophila melanogaster, Caenorhabditis elegans*, and *Ciona intestinalis*, we have failed to find MC/MCH receptors, suggesting that this subfamily of seven transmembrane GPCRs may be vertebrate specific. However, the remarkable conservation of amino acid sequence in many of these receptors throughout more than 400 million years of vertebrate evolution implicate an important role in normal physiological function.

The duplication, and potential functional complementation, of *mc5r* in the zebrafish is consistent with a hypothesis of tetraploidization in the teleost lineage [43]. However, an independent duplication in the zebrafish lineage could also explain the existence of two *mchr1* orthologues in zebrafish but only one in *Fugu*. The identification of a common intron in *mc2r* and *mc5r* in *Fugu*, combined with the linkage of both genes in both mammals and teleosts, suggests that an ancestral melanocortin receptor may not have been intronless. Indeed, this intron may have been present even earlier, because the conserved intron is seen in other G-protein-coupled receptors, including human, zebrafish, and *Fugu* MCHR2 (manuscript in preparation).

In conclusion, we have identified, mapped, and characterized the expression of the melanocortin receptor and melanin-concentrating hormone receptor families in teleost fish. These receptors are good candidates for involvement in a range of processes, including background adaptation and feeding regulation. Their identification in zebrafish provides an excellent system in which to investigate their function further.

Materials and methods

Identification of gene sequences

TBLASTN analysis of the *Danio rerio, Fugu rubripes*, and *Tetraodon nigroviridis* whole genome shotgun databases was carried out using the chicken MC1R amino acid sequence (accession number D78272) and the mouse MCHR1 sequence (NM_145132). Matching reads were assembled using Phred/Phrap [44] and extended by repeated BLAST searching and assembly.

The predicted coding sequence of each gene was amplified by PCR using oligonucleotide primers designed using Primer3 [45]. These primer sequences are available on request. PCR products were purified using a QIAquick PCR purification kit (Qiagen, Crawley, UK) and sequenced.

Sequencing

Sequencing reactions were performed using the ABI PRISM BigDye Terminator cycle sequencing kit according to the manufacturer's instructions and analyzed on a ABI-377 automated sequencer (Applied Biosystems, Warrington, UK). The sequences were aligned and compared with the database assemblies using Sequencher v.4.0.5 (Gene Codes, Ann Arbor, MI, USA).

Genetic mapping

Mapping was performed by PCR on the LN54 radiation hybrid panel [46]. Using the following primers, orientated 5′ to 3′: MC1Rf, TCAAAAGGACTGTGGAAGGG; MC1Rr, AAAGTCACGAGACAGGCGAT; MC2Rf, CACCAGCTGGAACTCTCTGA; MC2Rr, GCCACAATCACCAAGAGGTT; MC3Rf, GCTGCAACATCTGACTCTGC; MC3Rr, CAAACGCACAAATTGGTCAC; MC4Rf, TCTGCCTCATCAGCATGTTC; MC4Rr, CACCCTAAAACAGCACGTCA; MC5Raf, TCATCGCCTCTTACCAGACC; MC5Rar, CAGGCTGTGTGTCCGAGTAG; MC5Rbf, GCTTGTGGTGGAAGACCATT; MC5Rbr, GGGACAGGAAATCATGAGGA; MCHR1af, GGTGTGGGCACTCTCTCTTA; MCHR1ar, CAGGGGTACCTCAGGTTGAGT; MCHR1bf, TGACTTTGGACCGATACTTGG; MCHR1br, CGTGCTCATTACGGACACAA; MCHR2f, TTGCAATCGTCCATCCTACA; MCHR2r CTGGTGGGATGCTGGATACT. Each assay was performed twice and discordance between duplicate assays was less than 5%. Map placement was calculated using RHMAPPER (World Wide Web URL: http://mgchd1.nichd.nih.gov:8000/zfrh/beta.cgi).

Comparative mapping

Genes neighboring zebrafish melanocortin and melanin-concentrating hormone receptors were identified from the Zebrafish Information Network (ZFIN), (World Wide Web URL: http://zfin.org/). They were used in a TBLASTX search against the human and mouse whole genome assembly using Ensembl [47] (World Wide Web URL: http://www.ensembl.org/). The best hit was then used in a reciprocal TBLASTN search against the zebrafish assembly. If this identified the original zebrafish sequence as the best hit, the genes were designated as orthologues. Syntenic relationships were established by cross referencing neighboring genes on ZFIN, with the position of their mammalian orthologues using Ensembl. All data from Ensembl were from the most current data assembly on 2 October 2002.

Sequence alignment and phylogenetic analysis

The *Fugu* and zebrafish melanocortin receptor full-length amino acid sequences were aligned with their mouse, human, and chicken orthologues using ClustalW [48]. Melanin-concentrating hormone receptor sequences were aligned with their human, mouse, rat, and dog orthologues. These sequences were obtained from Genbank. Melanocortin receptor accession numbers: NM_002386, NM_000529, XM_009545, NM_005912, XM_008685, NM_008559, NM_008560, NM_008561, AF201662, NM_013596, D78272, AB009605, AB017137, AB012211, AB012868.

Melanin-concentrating hormone receptor accession numbers: NM_005297, NM_032503, AY112658, AY112659, AY049011, NM_031758.

Phylogenetic trees were built by MEGA v.2.2 [49] using a neighbor-joining method. Phylogeny was tested using a bootstrap resampling strategy with 1000 replicates. The human MCHR1 sequence was used to root the melanocortin receptor tree and the human MC1R sequence was used to root the melanin-concentrating hormone receptor tree.

RT-PCR analysis

One male and one female AB strain zebrafish was decapitated and total RNA isolated from the pooled head tissues and body tissues using the RNAgents system (Promega, Southampton, UK). Zebrafish embryos from AB strain matings were raised at 28.5°C and total RNA isolated at defined days after fertilization. The RNA was then RNase-Free DNase treated at 37°C for 15 minutes and purified according to the manufacturer's instructions. The quantity of RNA was controlled using a GeneQuant spectrophotometer (Amersham, Little Chalfont, UK). RNA was reverse transcribed using a First Strand cDNA Synthesis kit (Roche, Lewes, UK) and the product used as a template for PCR. The specific primers for each gene were identical to those used for genetic mapping, with the following exceptions: MC2Rf, CTCTGCTCCTGATCCTCCTG; MC2Rr, CCTGGTTCTCATTCAAGCAC; MC3Rf, TGCATCTCTCTTGTGGCATC; MC3Rr, GGTGAGGACAGGACACCAGT; MCHR1af, AAATGCCAGGCTAAACAAACA; MCHR1ar, AAGACGAAGGGACACAGTGG; MCHR1bf, TGGTGTGGATCCTCTCACTG; MCHR1br, CCGGATGGCAACAATAAACT. Primers specific to zebrafish beta-actin (NM_131031) were used as a positive RNA control: B-actf, TCAACACCCCTGCCATGTAT; B-actr, TTGAAGGTGGTCTCGTGGAT. A PCR with total RNA from each sample as a template was used as a negative control. No DNA contamination was detected. The conditions for PCR were 5 minute denaturation, then 60 s. at 94°C, 60 s. at 60°C, and 90 s. at 72°C for 35 cycles, then a final 10 minutes at 72°C. The PCR products were analyzed on an ethidium bromide-stained, 1.2% agarose gel, and reverse images recorded. Each PCR was carried out at least twice, with the same result achieved each time.

Acknowledgments

We thank Marc Ekker (Ottawa Health Research Institute) for providing radiation hybrid DNA and are grateful to Sally Cross, Ian Smyth and Tom Van Agtmael for energetic discussions. K.E.P. is the recipient of a Minority International Research Training Grant from the John E. Fogarty International Center, NIH.

References

[1] K.G. Mountjoy, L.S. Robbins, M.T. Mortrud, R.D. Cone, The cloning of a family of genes that encode the melanocortin receptors, Science 257 (1992) 1248–1251.

[2] I. Gantz, et al., Molecular cloning of a novel melanocortin receptor, J. Biol. Chem. 268 (1993) 8246–8250.
[3] I. Gantz, et al., Molecular cloning, expression, and gene localization of a fourth melanocortin receptor, J. Biol. Chem. 268 (1993) 15174–15179.
[4] R.D. Cone, et al., The melanocortin receptors: agonists, antagonists, and the hormonal control of pigmentation, Recent Prog. Horm. Res. 51 (1996) 287–317.
[5] L.S. Robbins, et al., Pigmentation phenotypes of variant extension locus alleles result from point mutations that alter MSH receptor function, Cell 72 (1993) 827–834.
[6] P. Valverde, E. Healy, I. Jackson, J.L. Rees, A.J. Thody, Variants of the melanocyte-stimulating hormone receptor gene are associated with red hair and fair skin in humans, Nat. Genet. 11 (1995) 328–330.
[7] E. Healy, et al., Functional variation of MC1R alleles from red-haired individuals, Hum. Mol. Genet. 10 (2001) 2397–402.
[8] A. Weber, A.J. Clark, Mutations of the ACTH receptor gene are only one cause of familial glucocorticoid deficiency, Hum. Mol. Genet. 3 (1994) 585–588.
[9] A.S. Chen, et al., Inactivation of the mouse melanocortin-3 receptor results in increased fat mass and reduced lean body mass, Nat. Genet. 26 (2000) 97–102.
[10] D. Huszar, et al., Targeted disruption of the melanocortin-4 receptor results in obesity in mice, Cell 88 (1997) 131–141.
[11] G.S. Yeo, et al., A frameshift mutation in MC4R associated with dominantly inherited human obesity, Nat. Genet. 20 (1998) 111–2.
[12] C. Vaisse, K. Clement, B. Guy-Grand, P. Froguel, A frameshift mutation in human MC4R is associated with a dominant form of obesity, Nat. Genet. 20 (1998) 113–4.
[13] W. Chen, et al., Exocrine gland dysfunction in MC5-R-deficient mice: evidence for coordinated regulation of exocrine gland function by melanocortin peptides, Cell 91 (1997) 789–798.
[14] H. Krude, et al., Severe early onset obesity, adrenal insufficiency, and red hair pigmentation caused by POMC mutations in humans, Nat. Genet. 19 (1998) 155–7.
[15] D. Lu, et al., Agouti protein is an antagonist of the melanocyte-stimulating-hormone receptor, Nature 371 (1994) 799–802.
[16] H.B. Schioth, V. Chhajlani, R. Muceniece, V. Klusa, J.E. Wikberg, Major pharmacological distinction of the ACTH receptor from other melanocortin receptors, Life Sci. 59 (1996) 797–801.
[17] D.J. Marsh, et al., Response of melanocortin-4 receptor-deficient mice to anorectic and orexigenic peptides, Nat. Genet. 21 (1999) 119–122.
[18] M.M. Ollmann, et al., Antagonism of central melanocortin receptors *in vitro* and *in vivo* by agouti-related protein, Science 278 (1997) 135–138.
[19] B.M. Allen, Extirpation of the hypophysis and thyroid glands of *Rana pipiens*, Science 44 (1916) 755–757.
[20] P.E. Smith, Experimental ablation of the hypophysis in the frog embryo, Science 44 (1916) 280–282.
[21] P. Haffter, et al., The identification of genes with unique and essential functions in the development of the zebrafish, *Danio rerio*, Development 123 (1996) 1–36.
[22] W. Driever, et al., A genetic screen for mutations affecting embryogenesis in zebrafish, Development 123 (1996) 37–46.
[23] R.N. Kelsh, et al., Zebrafish pigmentation mutations and the processes of neural crest development, Development 123 (1996) 369–389.
[24] J. Odenthal, et al., Mutations affecting xanthophore pigmentation in the zebrafish, *Danio rerio*, Development 123 (1996) 391–398.
[25] J.H. Postlethwait, et al., Zebrafish comparative genomics and the origins of vertebrate chromosomes, Genome Res. 10 (2000) 1890–1902.
[26] R. Fujii, The regulation of motile activity in fish chromatophores, Pigment Cell Res. 13 (2000) 300–319.
[27] M. Enami, Melanophore-concentrating hormone (MCH) of possible hypothalamic origin in the catfish *Parasilurus*, Science 121 (1955) 36–37.
[28] H. Kawauchi, I. Kawazoe, M. Tsubokawa, M. Kishida, B.I. Baker, Characterization of melanin-concentrating hormone in chum salmon pituitaries, Nature 305 (1983) 321–323.
[29] I.I. Geschwind, R.A. Huseby, R. Nishioka, The effect of melanocyte-stimulating hormone on the coat color in the mouse, Recent Prog. Hormone Res. 28 (1972) 91–130.
[30] M. Shimada, N.A. Tritos, B.B. Lowell, J.S. Flier, E. Maratos-Flier, Mice lacking melanin-concentrating hormone are hypophagic and lean, Nature 396 (1998) 670–674.
[31] D.J. Marsh, et al., Melanin-concentrating hormone 1 receptor-deficient mice are lean, hyperactive, and hyperphagic and have altered metabolism, Proc. Natl. Acad. Sci. USA 99 (2002) 3240–3245.
[32] M.J. Hoogduijn, J. Ancans, I. Suzuki, S. Estdale, A.J. Thody, Melanin-concentrating hormone and its receptor are expressed and functional in human skin, Biochem. Biophys. Res. Commun. 296 (2002) 698–701.
[33] B.I. Baker, The role of melanin-concentrating hormone in color change, Ann. N.Y. Acad. Sci. 680 (1993) 279–289.
[34] J. Chambers, et al., Melanin-concentrating hormone is the cognate ligand for the orphan G- protein-coupled receptor SLC-1, Nature 400 (1999) 261–265.
[35] Y. Saito, et al., Molecular characterization of the melanin-concentrating-hormone receptor, Nature 400 (1999) 265–269.
[36] S. An, et al., Identification and characterization of a melanin-concentrating hormone receptor, Proc. Natl. Acad. Sci. USA 98 (2001) 7576–7581.
[37] A.W. Sailer, et al., Identification and characterization of a second melanin-concentrating hormone receptor, MCH-2R, Proc. Natl. Acad. Sci. USA 98 (2001) 7564–7569.
[38] C.P. Tan, et al., Melanin-concentrating hormone receptor subtypes 1 and 2: species-specific gene expression, Genomics 79 (2002) 785–792, doi:10.1006/geno.2002.6771.
[39] A. Ringholm, et al., One melanocortin 4 and two melanocortin 5 receptors from zebrafish show remarkable conservation in structure and pharmacology, J. Neurochem. 82 (2002) 6–18.
[40] S. Aparicio, et al., Whole-genome shotgun assembly and analysis of the genome of *Fugu rubripes*, Science 297 (2002) 1301–1310.
[41] B. Venkatesh, S. Brenner, Genomic structure and sequence of the pufferfish (*Fugu rubripes*) growth hormone-encoding gene: a comparative analysis of teleost growth hormone genes, Gene 187 (1997) 211–215.
[42] A. Nasevicius, S.C. Ekker, Effective targeted gene "knockdown" in zebrafish, Nat. Genet. 26 (2000) 216–220.
[43] A. Amores, et al., Zebrafish hox clusters and vertebrate genome evolution, Science 282 (1998) 1711–1714.
[44] B. Ewing, P. Green, Base-calling of automated sequencer traces using phred. II. Error probabilities, Genome Res. 8 (1998) 186–194.
[45] S. Rozen, H. Skaletsky, Primer3 on the WWW for general users and for biologist programmers, Methods Mol. Biol. 132 (2000) 365–386.
[46] N.A. Hukriede, et al., Radiation hybrid mapping of the zebrafish genome, Proc. Natl. Acad. Sci. USA 96 (1999) 9745–9750.
[47] T. Hubbard, et al., The Ensembl genome database project, Nucleic Acids Res. 30 (2002) 38–41.
[48] J.D. Thompson, D.G. Higgins, T.J. Gibson, CLUSTAL W: improving the sensitivity of progressive multiple sequence alignment through sequence weighting, position-specific gap penalties, and weight matrix choice, Nucleic Acids Res. 22 (1994) 4673–4680.
[49] S. Kumar, K. Tamura, I.B. Jakobsen, M. Nei, MEGA2: molecular evolutionary genetics analysis software, Bioinformatics 17 (2001) 1244–1245.